Transportation Fuel Cell Power Systems

2000 Annual Progress Report

U.S. Department of Energy

Energy Efficiency and Renewable Energy

Office of Transportation Technologies

ACKNOWLEDGEMENT

We would like to express our sincere appreciation to Argonne National Laboratory and Computer Systems Management, Inc., for their artistic and technical contributions in preparing and publishing this report.

In addition, we would like to thank all our program participants for their contributions to the programs and all the authors who prepared the project abstracts that comprise this report.

U.S. Department of Energy
Office of Advanced Automotive Technologies
1000 Independence Avenue, S.W.
Washington, DC 20585-0121

FY 2000

Progress Report for Fuel Cell Power Systems

Energy Efficiency and Renewable Energy
Office of Transportation Technologies

Approved by Steven Chalk **Energy Conversion Team Leader**

October 2000

CONTENTS

Page

I. INTRODUCTION 1

II. FUEL CELL POWER SYSTEM DEVELOPMENT 9

A. Atmospheric Fuel Cell Power System for Transportation 9
B. Pressurized Fuel Cell Power System for Transportation 12
C. Cost Analyses of Fuel Cell Stack/Systems 16
D. Fuel Cell Systems Analysis 21

III. FUEL PROCESSING SUBSYSTEM 27

A. Advanced Fuel Processor Development for Next Millennium Fuel Processor™ for Transportation Fuel Cell Power Systems 27
B. Multifuel Processor for Fuel Cell Electric-Vehicle Applications 32
C. Fuel-Flexible, UOB™ Fuel Processor System: Development and Status 36
D. Integrated Fuel Processor Development 40
E. Microchannel Fuel Processor Components 44
F. Catalysts for Improved Fuel Processing 49
G. R&D on a Novel Breadboard Device Suitable for Carbon Monoxide Remediation in an Automotive PEM Fuel Cell Power Plant 53
H. CO Clean-up Development 57
I. Evaluation of Partial Oxidation Fuel Cell Reformer Emissions 62
J. Catalytic Autothermal Reforming 65
K. Alternative Water-Gas Shift Catalyst Development 70

IV. FUEL CELL STACK SUBSYSTEM 75

A. R&D on a 50-kW, High-Efficiency, High-Power-Density, CO-Tolerant PEM Fuel Cell Stack System 75
B. Development of Advanced, Low-Cost PEM Fuel Cell Stack and System Design for Operation on Reformate Used in Vehicle Power Systems 79
C. Cold-Start Dynamics of a PEM Fuel Cell Stack 85
D. Efficient Fuel Cell Systems 88
E. Direct Methanol Fuel Cells 91

CONTENTS (Cont.)

Page

V. PEM STACK COMPONENT COST REDUCTION 95

A. High-Performance, Matching PEM Fuel Cell Components and Integrated Pilot Manufacturing Process 95

B. Design and Installation of a Pilot Plant for High-Volume Electrode Production 100

C. Low-Cost, High Temperature, Solid-Polymer Electrolyte Membrane for Fuel Cells 103

D. Development and Optimization of Porous Carbon Papers Suitable for Gas Diffusion Electrodes 108

E. Electrodes for PEM Operation on Reformate/Air 111

F. New Electrocatalysts for Fuel Cells 115

G. Development of a $10/kW Bipolar Separator Plate 119

H. Layered PEM Stack Development 123

VI. AIR MANAGEMENT SUBSYSTEMS 127

A. Turbocompressor for PEM Fuel Cells 127

B. Development of a Scroll Compressor/Expander Module for Pressurization of 50-kW Automotive Fuel Cell Systems 130

C. Variable Delivery Compressor/Expander Development 133

D. Turbocompressor for Vehicular Fuel Cell Service 137

E. Innovative, High-Efficiency Integrated Compressor/Expander Based on TIVM Geometry 143

VII. HYDROGEN STORAGE 147

A. High-Pressure Conformable Hydrogen Storage for Fuel Cell Vehicles 147

B. Advanced Chemical Hydride Hydrogen-Generation/Storage System for PEM Fuel Cell Vehicles 150

APPENDIX A: ACRONYMS, INITIALISMS, AND ABBREVIATIONS 157

APPENDIX B: DOE TECHNICAL TARGETS FOR FUEL CELL SYSTEMS, SUBSYSTEMS, AND COMPONENTS 161

I. INTRODUCTION

Developing Advanced PEM Fuel Cell Technologies for Transportation

Patrick Davis
Program Manager

Donna Lee Ho
Program Manager

JoAnn Milliken
Program Manager

Nancy Garland
Program Manager

On behalf of the Department of Energy's Office of Transportation Technologies (OTT), we are pleased to present the Fiscal Year (FY) 2000 Annual Progress Report for the Transportation Fuel Cell Power Systems Program. In this introduction, we briefly outline the nature, objectives, and progress of the program, examine the technical barriers to commercialization of the technology, and highlight the program's future directions. For additional information on OTT's R&D activities supporting the development of fuel cell technology, the reader is referred to the FY 2000 Annual Progress Reports on Fuels for Advanced CIDI Engines and Fuel Cells, and Automotive Propulsion Materials.

Worldwide interest in fuel cell technology for a wide range of applications remains very strong. The major automotive and fuel cell companies are announcing technology breakthroughs, development vehicles, partnerships, and new initiatives with increasing frequency. Major energy providers have emerged to begin addressing important fuel infrastructure issues. The U.S. Department of Energy (DOE) remains committed to contributing to this progress in a significant way by supporting R&D activities that address the most critical barriers to the introduction of commercially viable polymer-electrolyte-membrane (PEM) fuel cell systems.

The mission of the Transportation Fuel Cell Power Systems Program is to develop highly efficient, low- or zero-emission automotive fuel cell propulsion systems. DOE has selected the PEM fuel cell as its leading technology candidate because of its high power density, quick start-up capability, and simplicity of construction.

The Program supports the Partnership for a New Generation of Vehicles (PNGV), a cooperative research and development partnership between the federal government and the U.S. Council for Automotive Research, which comprises Ford, General Motors, and DaimlerChrysler. One of the major objectives of PNGV is to develop a mid-size passenger vehicle capable of achieving a gasoline-equivalent fuel economy of 80 miles per gallon (mpg) while adhering to anticipated future emissions standards and maintaining such attributes as performance, comfort, and affordability. PNGV has

General Motors' fuel-cell-powered Precept concept vehicle.

targeted PEM fuel cell power systems as one of the promising technologies for achieving this objective.

The Ford FC5 fuel cell concept vehicle.

The primary purpose of this report is to document the progress made by the DOE Transportation Fuel Cell Power Systems R&D Program during FY 2000 against the R&D barriers and tasks identified in the Office of Advanced Automotive Technologies R&D Plan. We would be remiss, however, if we neglected to note the advances in fuel cell technology being made through other private and public initiatives throughout the year. In January 2000, General Motors introduced the Precept, its second fuel-cell-powered concept vehicle. Designed to operate on hydrogen stored aboard the vehicle as a chemical hydride, the Precept has a projected fuel economy in excess of 100 mpg (gasoline equivalent) and a range of 500 miles. In the fall of 1999, Ford unveiled the FC5 fuel cell vehicle, designed — unlike their previously introduced P2000 — to operate on hydrogen extracted from methanol by means of an onboard fuel processor.

The California Fuel Cell Partnership, a program announced last year, is continuing to generate a high level of interest by industry and governments to accelerate the development of fuel cell vehicles. The Partnership plans to put about 70 fuel cell vehicles — cars and buses — on the road between 2000 and 2003. Over the past year, several new members have joined the Partnership, including DOE and the U.S. Department of Transportation (DOT). Membership now includes six auto companies (DaimlerChrysler, Ford, Honda, Hyundai, Nissan, and Volkswagen); two technology developers (Ballard and International Fuel Cells); seven fuel and fuel infrastructure interests (BP, Shell Hydrogen, Texaco, Air Products, Linde AG, Methanex, and Praxair); two transit agencies (AC Transit and SunLine), and five government agencies (California Energy Commission, California Air Resources Board, South Coast Air Quality Management District, DOE, and DOT). A 55,000-square-foot fuel cell vehicle headquarters and hydrogen refueling facility in West Sacramento, California, is expected to open in the fall of 2000. Initially, up to 18 fuel cell vehicles will be regularly driven throughout the Sacramento area to gain "real world" road experience and increase public awareness.

The DOE Transportation Fuel Cell Power Systems Program is implemented through cost-shared contracts with automotive suppliers and fuel cell and component developers. Furthermore, DOE national laboratories and universities throughout the United States conduct R&D activities to increase the knowledge base and develop enabling technologies for PEM fuel cells.

Transportation Fuel Cell Power Systems Program Partners/Participants

Technical and Economic Challenges

The adjacent chart illustrates the shortfall in meeting the year 2000 transportation fuel cell power system technical and cost targets. These ambitious targets were originally established in 1994 to meet the PNGV timeframe for production prototype vehicles in 2004. However, fuel cells are the long-term technology for PNGV, and a great deal has been learned since the original targets were established. Therefore, DOE is currently in the process of revising the targets (including extension of the timeframe) to better reflect the status of the technology and an improved understanding of fuel cell systems, anticipated progress, and future PNGV fuel cell vehicle requirements.

On the technical side are such challenging issues as reducing component and system costs, reducing platinum usage, demonstrating component and system durability, reducing system start-up time, the availability of high-efficiency air management subsystems, and the availability of a suitable fuel infrastructure. On the economic side are the issues of fuel cell manufacturing capitalization, cost of a new fuel infrastructure, and competition from other technologies.

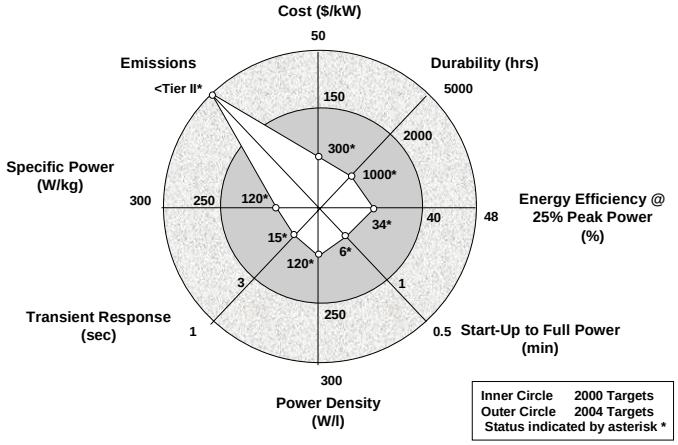

Projected status (pending validation in system deliverables) vs. technical and cost targets for a 50-kw fuel-flexible fuel cell system operating on gasoline.

System and Component Costs. The Arthur D. Little projection of the high-volume manufacturing cost of the fuel cell system based on the current status of the technology ($300 per kW) is six times higher than that needed ($50 per kW) to be competitive with the internal combustion engine. To meet the challenges of lowering system costs, the Transportation Fuel Cell Power Systems Program strives to develop components with lower-cost materials, more advanced manufacturing processes, and higher operating efficiency.

Platinum Cost And Supply. A preliminary analysis done by Arthur D. Little for DOE indicates that the current platinum requirement of a fuel cell system is too high to support market penetration. The platinum alone for a 50-kW system is currently estimated to cost $57/kW, which is higher than the DOE year 2004 cost target for the entire fuel cell system of $50/kW. Even a 10% market penetration at the current system platinum content would exceed current world platinum-production levels. Attainment of the year 2004 goals for platinum use in fuel cell systems will enable large market penetration and ensure adequate world platinum reserves. A more comprehensive study on platinum supply and cost is planned to investigate this critical issue.

Component Durability. The durability of key components, such as membrane/electrode assemblies and fuel processing catalysts, has not been demonstrated to 5,000 hours. Some of these components, including automotive-type sensors and valves, are not even available yet for durability testing. Durability testing of these components in the harsh automotive environment is critically needed. Test fleets, such as those proposed by the California Fuel Cell Partnership, are also needed to identify component failure modes for future development and to help establish vehicle warranties that mitigate the manufacturer's risk.

Start-Up Time. The current start-up time for fuel cell systems, which is controlled by the fuel processor, is in the range of 6 to 20 minutes. This does not compete well with current production vehicles and would be unacceptable to consumers. Lengthy start-up times also have major implications for the fuel cell vehicle's fuel economy and emissions. Batteries could be used with the fuel cell to permit immediate operation of the fuel cell vehicle, but the energy demand on the battery could be large (5 kWh).

Air Management. Fuel cell systems require air to operate, but the current compressors are not very efficient in supplying air to the fuel cell, and the fuel cell is not very efficient in using it. The inefficient use of air results in an oversupply of air delivered to the fuel cell, placing an added burden on the air compressor, lowering the overall system efficiency, and increasing the stack size, weight, and cost. A peer review of the technology determined that no off-the-shelf compressor technology available today comes close to matching the DOE technical requirements for the fuel cell system. Advances in the activity of the cathode catalyst are also needed to effectively reduce the air-supply burden on the air management subsystem.

Fuel Infrastructure. Methanol and hydrogen would be good fuels for the automotive fuel cell, as evidenced by the use of these fuels in the early fuel cell concept cars under test by the automakers. For these and other alternative fuels such as ethanol, significant capital investments in infrastructure will be required. Such investments are unlikely, however, until fuel cell vehicles achieve a market penetration that can support the investment. Petroleum-based fuels, for which an infrastructure already exists, will require the use of a fuel processor, and may require the development of a compatible specialized fuel blend with very low sulfur and reduced aromatics.

R&D Highlights

Researchers supporting the Transportation Fuel Cell Power Systems R&D Program continued to make significant progress in meeting these challenges during FY 2000. Notable advances were achieved in systems development, fuel cell and fuel-processing subsystems technology, air compressor technology, and the development of low-cost, high-volume manufacturing processes for key components. The summaries that follow are selected highlights of the progress made under the program.

Atmospheric Fuel Cell Power System. During FY 2000, International Fuel Cells (IFC) successfully delivered a 50-kW (net) gasoline-fueled power plant configured for system verification testing. The laboratory power plant, designed to operate at near-ambient pressure, consists of a fully tested 50-kW-equivalent fuel-flexible fuel processing system (FPS) and a 50-kW PEM stack assembly. The FPS was tested at steady state throughout the required fuel flow range, as well as during start/stop and transient cycles. Demonstrated fuel conversion was 98%, with overall fuel processor efficiency exceeding 83%. CO levels in the reformate were consistent with required low levels. Separate testing of the 50-kW stack demonstrated a gross power output of ~67 kW dc at a stack voltage of approximately 280 V dc and a current density of ~650 mA/cm^2. Assembly and installation of the integrated power plant in the IFC test stand is complete. Verification testing of the system will be performed once the planned checkout procedure is complete.

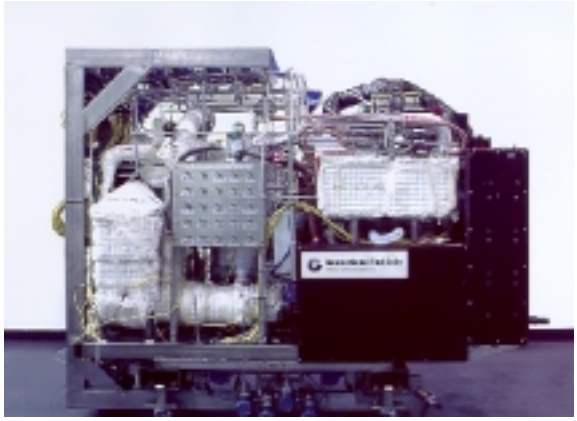

IFC 50-kW gasoline-fueled, PEM fuel cell power plant ready for verification testing.

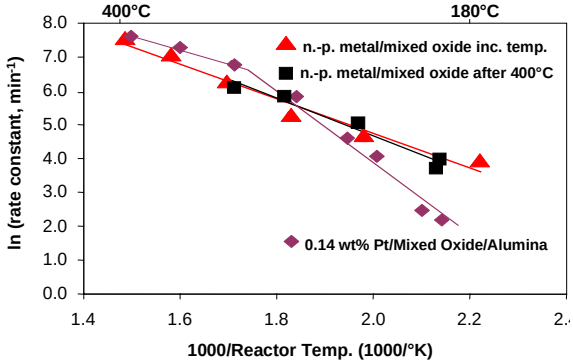

Activity of ANL nonprecious-metal/mixed oxide catalyst compared to that of Pt/mixed oxide/alumina.

Fuel Processor CO Clean-up Catalysts. In a major breakthrough, Argonne National Laboratory (ANL) has identified a nonprecious-metal/mixed oxide water-gas shift (WGS) catalyst that does not lose activity at temperatures up to 400°C and is air-stable. The cost of this catalyst is comparable to the current low temperature WGS catalyst, copper/zinc oxide. Although noble metal catalysts have desirable air and temperature stability, their high cost may limit their acceptability for transportation applications. The nonprecious-metal/mixed oxide catalyst has WGS activity comparable with that of the platinum/mixed oxide at a fraction of the cost. Although the nonprecious metal/mixed oxide catalyst is not as active as copper/zinc oxide, it does not lose its activity after exposure to air at 230°C as does the copper/zinc oxide catalyst.

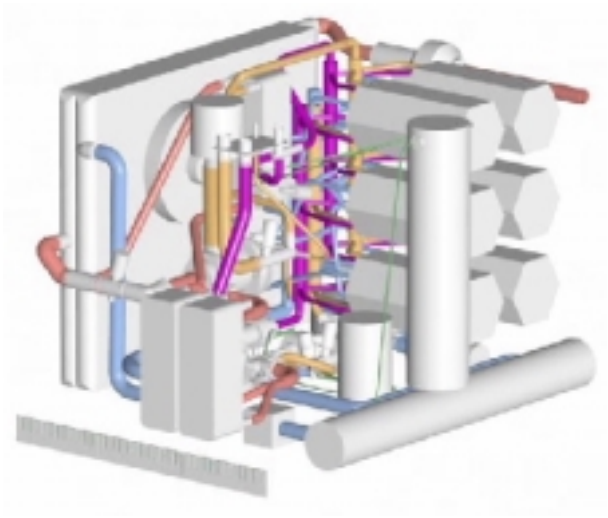

Honeywell 50-kW CO-tolerant PEMFC stack system design.

CO-Tolerant PEM Fuel Cell Stack System. During FY 2000, Honeywell (formerly AlliedSignal) made significant advances in the development of a 50-kW CO-tolerant fuel cell stack system. Design of the 50-kW brassboard system, which includes the PEM stack and the supporting gas-, thermal-, and water-management subsystems, has been completed. The projected nominal efficiency of the brassboard system is 45%. In supporting stack development activities, Honeywell has demonstrated that its cells can tolerate greater than 200-ppm CO contamination in the anode fuel gas without appreciable performance loss; an 82-cell stack

was successfully operated for 250 hours on CO-containing reformate. A subscale stack was also subjected to several freeze-thaw cycles to -40ºC without damage. A 10-kW (112-cell) class stack containing composite bipolar plates with a new flowfield design demonstrated lower stoichiometry capability, a 13% increase in active cell area, and substantial improvements in weight (specific power of 0.87 kW/kg), volume (power density of 1.6 kW/L), and manufacturability.

Optimized Electrodes for Reformate/Air Stacks. Los Alamos National Laboratory (LANL) is working on electrode optimization to achieve maximum performance in PEM fuel cells under conditions appropriate for reformate/air operation. One very important aspect of this work is the identification of new catalysts and operating conditions that improve the tolerance of the PEM fuel cell to CO in reformate fuel from a fuel processor. During FY 2000, a 500-hour life test of a 50-cm^2 cell demonstrated tolerance to 100 ppm CO. Stable cell performance with 500 ppm CO in reformate was also achieved in a 100-hour test with an advanced PtRu catalyst. Significant progress was also made towards the R&D goal of improved performance at high cell voltages. LANL demonstrated that stable performance of 0.4 A/cm^2 at 0.8 V could be achieved with neat hydrogen as a fuel. Although there is still a need to lower the required catalyst loading and operate on the reformate, this does represent a substantial first step on the road to simultaneously achieving acceptable performance and high-voltage efficiency.

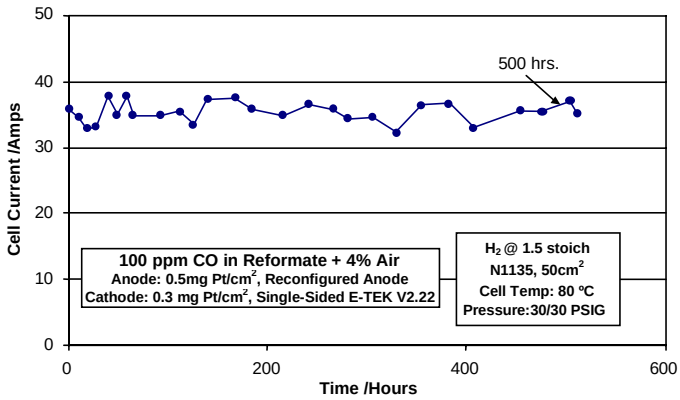

Life test of cell with reconfigured anode exposed to 100 ppm CO in simulated reformate (4% air bleed).

High-Volume Electrode Production. During FY 2000, Southwest Research Institute (SwRI) teamed up with W. L. Gore and Associates, a leading supplier of MEAs for PEM fuel cells, to develop a high-volume pilot manufacturing process for electrode material, a crucial (and currently costly) element in the high-volume production of fuel cell MEAs. The key component of this process is a vacuum coating unit with the capability to produce millions of square feet of high performance, ultra-low-Pt loaded electrodes per year. SwRI is acquiring electrode substrate materials, membranes, and reference MEAs that utilize technology from W.L. Gore and Associates; these items will be used by SwRI for MEA assembly and benchmarking. The objective of the project is to demonstrate the production levels necessary to achieve MEA production costs below $10/kW. Specific power values approaching 5 kW/g of platinum on hydrogen have been achieved by utilizing the new technology, represents progress toward the DOE year 2004 performance target of 5 kW/g of platinum for operation on gasoline reformate. Ultra-low loadings as low as 0.001 mg/cm^2 have been demonstrated in the laboratory with catalyst uniformity within 5% achieved across 15-cm widths of material. Work continues to further

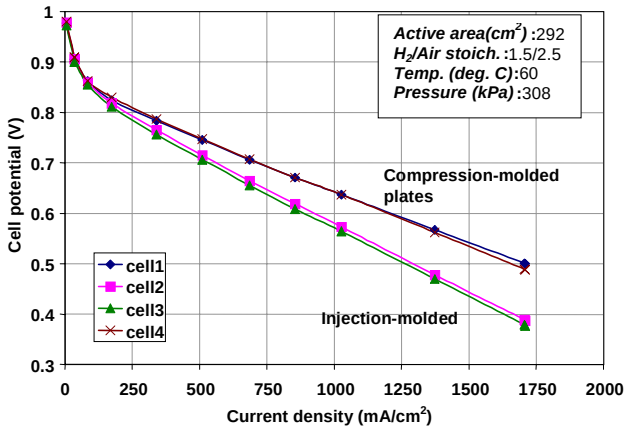

Characteristic cell performance of Energy Partners' injection vs. compression molded plates.

optimize catalyst composition and reduce precious metal content, with a target of less than 0.10 mg/cm^2 thought to be achievable.

Low-Cost Bipolar Plate Development. Research at Energy Partners is contributing to a reduction in stack component costs through the development of a high-speed injection molding process (patents pending) for composite graphite bipolar plates. Composite bipolar plates are currently injection-molded, with cycle times of less than 20 seconds; with proper tool design, the projected cycle time is reduced to about 10 seconds. Energy Partners' thermoplastic technology has the potential to greatly reduce cycle time and processing cost (<$10/kW), improve hydrolytic stability and corrosion resistance, and allow for material recycling. Injection-molded blank plates (500 cm^2) with machined flow fields were evaluated in a fuel cell stack and compared with the performance of cells containing Energy Partners' compression-molded plates (performance similar to that of cells using POCO graphite plates). Although the polarization curves for a four-cell stack were slightly lower for the injection-molded plates than for the compression molded plates (corresponding to the higher conductivity of the compression-molded plates), work in progress at Energy Partners indicates that optimization of the formulation and compounding process will improve the conductivity of the injection-molded plates.

Future Directions

Although substantial progress was made during FY 2000 toward meeting the technical targets for fuel cell systems for light-duty vehicles, significant technical and economic challenges remain before fuel cell vehicles will achieve significant market penetration. As we move forward, we will continue to work with our government and industry partners to address these challenges. We will also increase our cooperation with DOE's PEM Fuel Cells for Buildings and Hydrogen Programs to maximize the synergy with these programs. In developing our future R&D plans, we will put less emphasis on system integration and full-scale stack development because industry has the capability to carry this effort forward. Our future R&D will focus on addressing the most critical issues of cost, durability, and performance of materials, components, and enabling technologies. This is expected to include new work on high-temperature membranes and MEAs with higher activity cathodes and CO-tolerant anodes; advanced fuel processors and water-gas shift catalysts that represent a significant improvement over the state-of-the-art; new compressor/expander technologies; and advanced components including sensors for fuel cell power systems (both chemical and physical), heat exchangers, and devices to enrich the oxygen and hydrogen content in on-board fuel cell feed streams. During FY 2000 we held two workshops to define R&D needs and technical targets: sensor needs for CIDI engines and fuel cells, and basic and applied research needs for PEM fuel cells. The proceedings of these workshops can be found on the World Wide Web at http://www.ott.doe.gov/oaat/library.html.

During FY 2001, researchers at Pacific Northwest National Laboratory will continue to develop microchannel fuel processor technology, which has the potential to substantially reduce the cost, size, and weight of this critical subsystem. Southwest Research Institute and 3M will continue the development of low-cost automated industrial processes for the manufacture of PEM electrode and membrane/electrode assemblies. PEM Plates will continue the development of a bipolar plate compression molding process to substantially reduce cost. Argonne National Laboratory will continue to develop fuel processing and water-gas shift catalysts to improve the performance of fuel-flexible fuel processors. Los Alamos National Laboratory will continue to develop improved electrodes for reformate/air fuel cells, as well as CO cleanup technology for fuel processors. We are also looking forward to the testing of stack subsystems from Energy Partners and AlliedSignal and integrated systems from Plug Power and International Fuel Cells. Through these efforts and other related projects, researchers in the Transportation Fuel Cell Power Systems R&D Program will continue to achieve improvements in cost, durability, efficiency, and overall system performance, allowing us to move closer to the commercial availability of fuel cell vehicles.

The remainder of this report presents project abstracts that highlight progress achieved during FY 2000 under the Transportation Fuel Cell Power Systems Program. The abstracts summarize both industry and national laboratory projects, providing an overview of the work being conducted to overcome the technical barriers associated with the development of fuel cell power systems. Each project abstract identifies the related barriers in the Office of Advanced Automotive Technologies R&D Plan.

Patrick Davis JoAnn Milliken

Donna Lee Ho Nancy J. Garland

Program Managers
Energy Conversion Team
Office of Advanced Automotive Technologies
Office of Transportation Technologies

II. FUEL CELL POWER SYSTEM DEVELOPMENT[1]

A. Atmospheric Fuel Cell Power System for Transportation

Murdo J. Smith
International Fuel Cells
195 Governor's Highway
South Windsor, CT 06074
(860) 727-2269, fax: (860) 727-2399, e-mail: smithmu@ifc.utc.com

DOE Program Manager: Patrick Davis
(202) 586-8061, fax: (202) 586-9811, e-mail: patrick.davis@ee.doe.gov

ANL Technical Advisor: Walter Podolski
(630) 252-7558, fax: (630) 972-4430, e-mail: podolski@cmt.anl.gov

Contractor: International Fuel Cells, South Windsor, Connecticut
Prime Contract No. DE-AC02-99EE50567, October 1999-November 2002

Objective

The objective of this contract is to deliver to the U.S. Department of Energy (DOE) a 50-kW-equivalent gasoline fuel processing system and a fully integrated, gasoline-fueled, 50-kW polymer electrolyte membrane (PEM) power plant for functional demonstration testing. The fuel processing system will utilize fuel-flexible reforming technology that can be modified to accommodate such fuels as methanol, ethanol, and natural gas. Demonstration testing of each of the units will be performed at International Fuel Cells (IFC). After IFC's testing, the PEM power plant will be delivered to Argonne National Laboratory (ANL) for additional operational tests by DOE.

OAAT R&D Plan: Tasks 5, 8, and 11; Barrier J

Approach

- Build and test autothermal fuel processor.
- Build and test an ambient-pressure integrated power plant.

Accomplishments

- Delivered and tested a 50-kW-equivalent gasoline fuel processing system.
- Delivered and tested a 50-kW PEM cell stack assembly for incorporation into the integrated power plant.
- Delivered a 50-kW integrated power plant configured for system verification testing.

Future Directions

- Complete verification testing of the 50-kW PEM power plant at IFC.
- Deliver the power plant to DOE for follow-on testing at ANL.

---

[1] The DOE technical targets for integrated fuel cell power systems can be found in Table 1, Appendix B.

Introduction

International Fuel Cells is committed to the commercialization of PEM fuel cell power plants for transportation applications. We have in place a program that addresses technology development and verification for each of the necessary components and subsystems, and ultimately for the fully integrated power plant itself. The focus of IFC's program is an ambient-pressure PEM power plant system operating on gasoline fuel and delivering 50-kW net direct-current (dc) power to the automotive electrical system.

Project Deliverables

Under the contract, IFC will deliver to DOE a 50-kW-equivalent gasoline fuel processing system (FPS) and a 50-kW PEM power plant.

Planned Approach

Fuel Processing System

Assembly of the gasoline fuel processing system (FPS) deliverable was completed in December 1999. The FPS consists of a fuel desulfurizer, an autothermal fuel reformer, a shift converter, a selective oxidizer, and the balance-of-plant equipment and controls necessary to operate the system. The FPS is sized to provide sufficient hydrogen to meet the requirements of the PEM fuel cell for generating 50 kW of dc electrical power. The objective of the FPS test program was to verify that the operation of the integrated FPS system met the power-plant requirements.

Figures 1 and 2 are photographs of the delivered FPS test article. The locations of the major FPS components are identified.

The FPS was tested against a specific test plan, using gasoline with the characteristics of California reformulated gasoline (RFG) II. The program included steady-state performance demonstrations throughout the required fuel flow range, from idle to rated power conditions, as well as start/stop and transient cycles. Figure 3 illustrates steady-state hydrogen production as a function of gasoline flow. Demonstrated fuel conversion was 98%, with overall fuel processor efficiency exceeding 83%. The FPS efficiency is the ratio of energy delivered by the FPS in the form of hydrogen (LHV 51,574 Btu/lb) to the energy delivered to the FPS in the form of gasoline

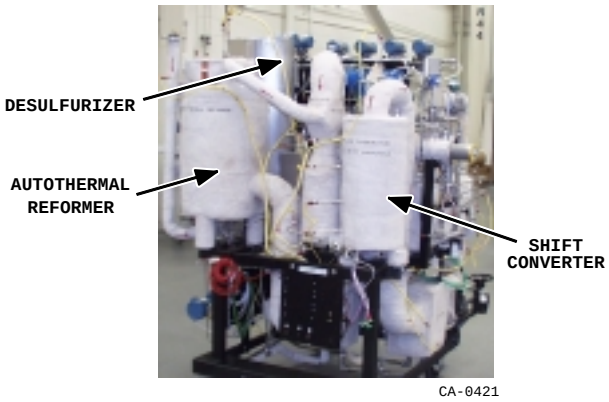

Figure 1. Fuel processing system, showing location of the desulfurizer, autothermal reformer, and shift converter.

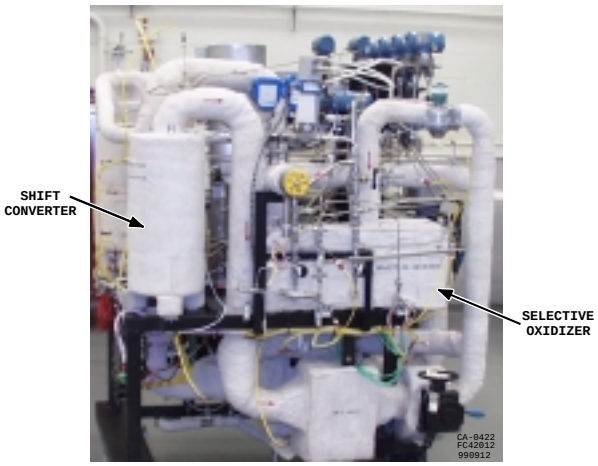

Figure 2. Location of FPS shift converter and selective oxidizer.

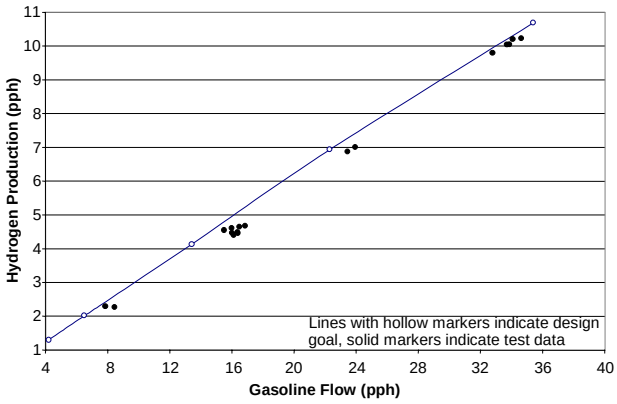

Figure 3. FPS steady-state hydrogen production.

(LHV 18,900 Btu/lb). Exit CO levels were consistent with required levels.

50-kW Power Plant

Figure 4 provides a schematic of the gasoline fuel cell power plant. The major subsystems include the fuel processing subsystem, the power subsystem, and the balance-of-plant. The balance-of-plant includes the thermal management subsystem, the air and water subsystems, and the controller and associated electrical equipment.

The 50-kW power subsystem was assembled and acceptance tested as a separate component. Figure 5 is a photograph of the power subsystem after successful completion of the acceptance test. As shown, the power subsystem comprises two 25-kW PEM ambient-pressure cell stack assemblies.

Stack performance on reformate is presented in Figure 6, which shows stack voltage and power output as a function of current density.

Figure 7 is a photograph of the fully integrated power plant in the process and control (PAC) test configuration. In this configuration, the power-plant system is complete, with the exception of the power subsystem (which is not included). Initial testing is performed without the power subsystem to allow tuning the controls and components without affecting the cell stacks. Assembly of the unit, which weighs 1,550 lb and has a volume of 30 ft^3, was completed in May 2000. It has been installed in the test stand at IFC and is undergoing a planned checkout procedure. When the procedure is completed, the power subsystem will be installed and verification testing of the complete power plant

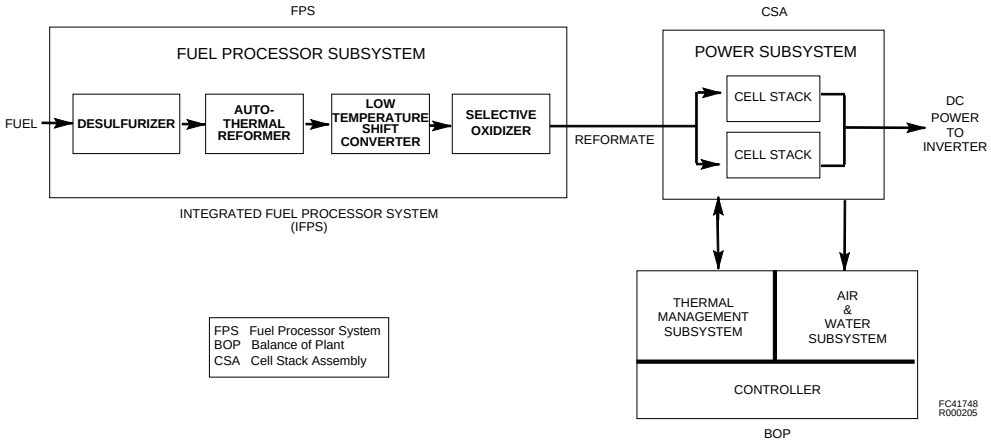

Figure 4. Power-plant schematic.

Figure 5. 50-kW power subsystem.

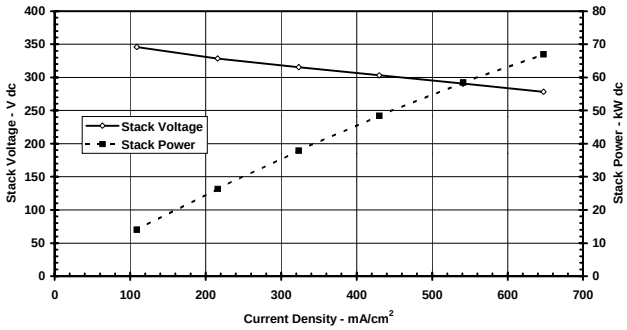

Figure 6. Power subsystem performance.

will be performed. The efficiency of the power plant will be determined during the testing program.

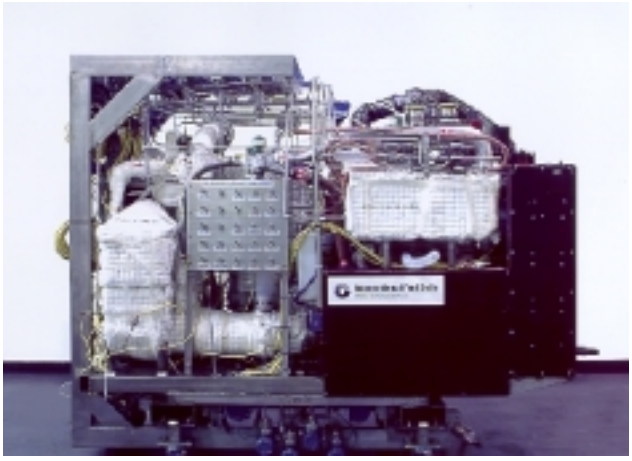

Figure 7. 50-kW gasoline-fueled power plant.

Conclusions

IFC is committed to the commercialization of PEM fuel cell power plants for transportation applications. The focus of IFC's program is an ambient-pressure PEM power plant system operating on gasoline fuel. The assembly and testing of a 50-kW equivalent fuel processing system was completed. The test results confirmed that the operation of the FPS system met the power-plant requirements. A 50-kW power subsystem was also assembled and acceptance tested as a separate component. The fully integrated power plant configured for system verification is now undergoing testing. Following the verification test, the power subsystem will be installed and verification testing of the complete power plant will be performed.

B. Pressurized Fuel Cell Power System for Transportation

William D. Ernst
Plug Power, LLC
Latham, NY 12110
(518) 782-7700, fax: (518) 782-7914, e-mail: William_Ernst@plugpower.com

DOE Program Manager: Donna Lee Ho
(202) 586-8000, fax: (202) 586-9811, e-mail: donna.ho@ee.doe.gov

DOE Program Support: Larry Blair
(202) 586-0626, fax: (202) 586-9811, e-mail: larry.blair@ee.doe.gov

ANL Technical Advisor: Walter Podolski
(630) 252-7558, fax: (630) 972-4430, e-mail: podolski@cmt.anl.gov

Contractor: Plug Power, Inc., Latham, New York 12110
Prime Contract No. DE-FC02-97EE50472, September 30, 1997-December 31, 2000
Major Subcontractor: Nuvera Fuel Cells, Cambridge, Massachusetts 02140

Objectives

- Research and develop a fully integrated fuel cell system that operates on common transportation fuels (gasoline, methanol, ethanol, and natural gas) for automotive applications.
- Deliver a fully integrated, 50-kW_e (net) system consisting of a polymer electrolyte membrane (PEM) fuel cell stack, with balance-of-plant components, and a 50-kW_e (net) fuel-flexible reformer.

OAAT R&D Plan: Tasks 5, 8, and 11; Barriers A-H and J

Approach

The integrated fuel cell system is being pursued in four phases:

- Phase I: Define overall system; build and demonstrate a 10-kW_e system.
- Phase II: Develop components for 50-kW_e system.
- Phase III: Integrate all components into 50-kW_e brassboard system.
- Phase IV: Build and test integrated 50-kW_e power system in a test stand.

Accomplishments

- Built 50-kW_e (net) brassboard fuel cell power subsystem, using commercially available components.
- Achieved functional operation with simulated reformate.
- 50-kW_e (net) fuel cell and fuel processing subsystems are built, characterized, and ready to be integrated with each other.

Fuel Cell Power System

(including fuel processor, stack and auxiliaries; excluding gasoline tank and DC-DC converter)

Characteristic	Status	DOE Technical Target
Net Power (kW_e)	50	50
Energy Efficiency @ 25% Peak Power (%)	40 (predicted)	40
Power Density (W/L)	250 (predicted)	250
Specific Power (W/kg)	250 (predicted)	250
Durability (hours)	2000 (predicted)	2000

Future Directions

- Integrate fuel cell subsystem with fuel processor subsystem.
- During integration, gain experience with compressor/motor/expander unit (CMEU) integration, water balance, system control strategy, and power distribution.
- On the basis of integration experience, develop an integrated system with increased fuel cell and fuel processor efficiency and improve overall system power density.
- Design, build, and test a highly integrated, 50-kW_e gasoline-powered fuel cell system (Phase IV).

Introduction

The goal of Phase I of this program is to develop fundamental knowledge about the individual components in the fuel cell system, culminating in the integration of a 10-kW_e (net) PEM fuel cell stack with a partial oxidation fuel processor. Phase II is the development of components at the 50-kW_e level, followed by brassboard system integration of the various components in Phase III. Phase IV will consist of building a fully integrated, compact 50-kW_e system that incorporates the results of Phase III testing; this system will be used for performance and emissions testing.

Phase I was completed during fiscal year (FY) 1998, and Phase II was completed during FY 1999; Phase III, currently in progress, will conclude with the integration of Plug Power's 50-kW (net) brassboard system with a 50-kW_e (net) fuel processor brassboard system developed and built by Nuvera Fuel Cells (formerly known as ADL/Epyx).

Approach

Components developed during Phases I and II have been integrated into a 50-kW_e brassboard system, but the system has not run in an integrated mode. In Phase III, the fuel cell subsystem and fuel processor subsystem, built on individual skids, will be connected together. The interface points between the fuel cell stack subsystem and the Nuvera fuel processor subsystem have been identified for the integrated system design. At each interface point, the necessary fluid state, flow, and thermal conditions have been defined. The overall system operating strategy has also been established. The key points are that (1) the operating pressure varies from 3.1 atm at maximum power to 2.2 atm at one-fourth power, (2) the closed-loop water management system will be simulated by totaling water generated and water consumed, and (3) fully saturated reformate will be provided to the fuel cell stack. The net effects of these conditions are maintenance of water balance within the system and improved power density.

The philosophy in building the Phase III brassboard system was functionality first, efficiency and emissions second. Size and weight were not as high of a priority in the design. A conservative design approach was taken, and additional hardware (valves, instrumentation, and filtration) was included in the Phase III design to facilitate thorough characterization of the system. The additional items increase the pressure drop of the entire system, leading to a higher parasitic load from the CMEU. (See Figures 1 and 2.)

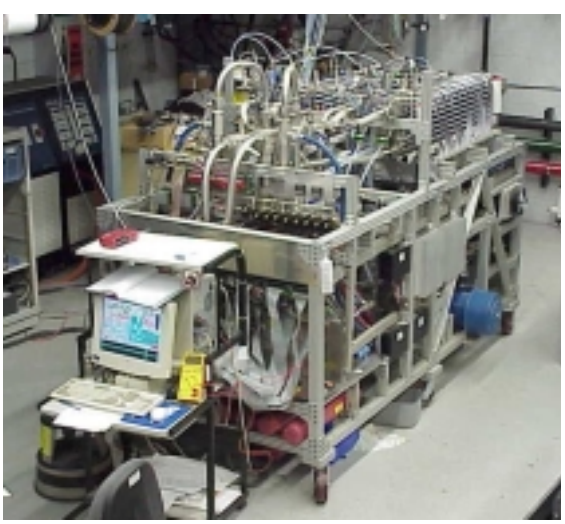

Figure 1. Phase III brassboard fuel cell system, photo.

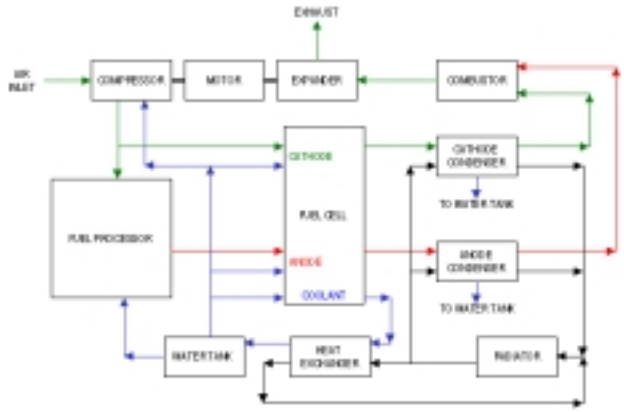

Figure 2. Phase III brassboard fuel cell system, schematic.

Results

Stand-alone operation of the fuel cell brassboard system has been achieved with simulated reformate. (See Figure 3.) Operation of auxiliary systems and components by direct-current (dc) power from the stack has been demonstrated. A battery charging and regulation system is incorporated into the brassboard system to provide independent start-up capability. Due to the power requirements of the CMEU, start-up power for the unit (during fuel processor warm-up) will be provided by a lab power supply.

The control system utilizes a dc-powered, embedded computer to carry out control functions and an integrated, but separable, PC to provide operator interface. Closed-loop flow control is provided by either user-entered flow rates or by system power demand (load following). The fuel processor controls reformate flow on the basis of fuel cell demand. CMEU speed determines air flow

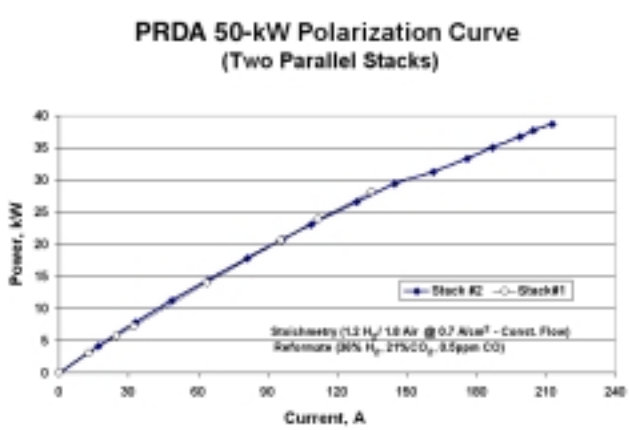

Figure 3. Performance of two Phase III stacks with simulated reformate.

for the entire system. The fuel processor independently controls air flow to its system by taking the air that it needs from the CMEU supply. Stack operating pressure is set by expander operation, in conjunction with back-pressure control valves (used to provide balancing adjustments).

The CMEU has offered its own set of challenges. Foremost, the unit's power consumption is greater than originally planned, primarily because of the increased system pressure drop caused by the addition of filters, control valves, check valves, and instrumentation. To overcome these pressure drops, Plug Power had to retrofit the CMEU with a larger motor and associated controller and power supply. Corrosion of the aluminum components within the CMEU was overcome by choosing different coatings for the internal components.

Improvements to stack hardware were made to better meet the requirements of the PRDA system for Phase IV. Notable improvements include an increase in the active area by 30%, simplification of the endplate and closure mechanism, elimination of contact between the collector plates and the fluid streams, and incorporation of improved alignment features. The net results of these hardware modifications include an increase in power density by 20% at the full power operating point, a 10% increase in plate utilization, a 15-kg reduction in stack weight, shorter stack assembly time, and reduced stack cost.

Conclusions and Future Work

The remainder of this program will focus primarily on systems integration and operation.

During the integrated testing, we plan to quantify the effects of reformate saturation level, pressure, and temperature on system performance. The relationship between water balance and operating pressure will be evaluated. Once an effective operating strategy has been developed, control valves will be eliminated from the system. (We expect to control flows and back pressures entirely with the CMEU, thereby enabling the elimination of valves.) An important goal is to reduce system pressure drop by 50%.

Upon completion of Phase III testing, Phase IV design and development will commence. Test results from Phase III will be used to optimize selection of the components to be used in Phase IV. The Phase IV system will utilize a single design (one set of schematics) and will be built on one compact skid. Upon completion of qualification testing at Plug Power, the Phase IV system will be delivered to Argonne National Laboratory.

References

1. W.D. Ernst, "Plug Power Fuel Cell Development Program," DOE Automotive Technology Development Customers' Coordination Meeting, Dearborn, Mich., Oct. 27-30, 1997.
2. W. Ernst, J. Law, J. Chen, and W. Acker, "PEM Fuel Cell Power Systems for Automotive Applications," Fuel Cell Seminar, Palm Springs, Calif., Nov. 1998.
3. W.D. Ernst, "Reformate-Fueled PEM Fuel Cells," SAE Fuel Cells for Transportation TOPTEC, Cambridge, Mass., March 18-19, 1998.

FY 2000 Publications/Presentations

- W.D. Ernst, J.R. Boyer, D.L. Ho, and W.F. Podolski, "Fuel-Flexible Automotive Fuel Cell Power System," SAE Paper 00FCC-3, presented at Future Car Congress, Washington, D.C., April 3, 2000.

C. Cost Analyses of Fuel Cell Stack/Systems

Eric J. Carlson (primary contact) and Stephen A. Mariano
Arthur D. Little, Inc.
Acorn Park
Cambridge, MA 02140-2390
(617) 498-5903, fax: (617) 498-7012, e-mail: carlson.e@adlittle.com

FY2000 DOE Program Manager: Donna Lee Ho
(202) 586-8000, fax: (202) 586-9811, e-mail: donna.ho@ee.doe.gov

FY2001 DOE Program Manager: Nancy L. Garland
(202) 586-5673, fax: (202) 586-9811, e-mail: nancy.garland@ee.doe.gov

DOE Program Support: Larry S. Blair
(202) 586-0626, fax: (202) 586-9811, e-mail: larry.blair@ee.doe.gov

ANL Technical Advisor: Robert D. Sutton
(630) 252-4321, fax: (630) 252-4176, e-mail: sutton@cmt.anl.gov

Contractor: Nuvera Fuel Cells, Cambridge, Massachusetts
Prime Contract No. DE-FC02-99EE50587, May 1999-March 2004

Objective

To develop an independent cost model for polymer electrolyte membrane (PEM) fuel cell systems for transportation applications and to assess cost reduction strategies for year 2000 to 2004 development programs.

OAAT R&D Plan: Task 8; Barrier J

Approach

- In the first year, develop a baseline system configuration and cost estimate based on best available and projected technology and manufacturing practices.
- In the second year, assess the impact of potential technology developments on system cost reduction.
- In the subsequent four years, update the baseline cost model and system scenarios annually, based on assessments of developments in PEM fuel cell (PEMFC) system technologies and manufacturing processes.

Accomplishments

- Baseline system configuration developed, in conjunction with Argonne National Laboratory.
- Baseline cost model and cost projection of $300/kW at high volume production developed and report prepared for distribution to the fuel cell community.
- Results of study presented to National Research Council (NRC) review committee, Partnership for a New Generation of Vehicles (PNGV) Fuel Cell Technical Committee, and technical conferences, including the Future Car Congress. Constructive feedback on revisions to the model have been obtained through these discussions about basic assumptions and system performance targets.

Future Directions

Develop projections of future system performance and cost on the basis of continued industry feedback and projected technology developments. Projections of future system performance and cost include, at a minimum, the following scenarios:

- An increase in ambient temperature to 120°F resulting in an increase in the size and weight of heat exchangers.
- A stack optimized for high power output (higher current density, but lower cell voltage) resulting in a less efficient but smaller and less costly stack system.
- System hybridization (fuel cell/battery) and the subsequent dependence of system cost ($/kW) on rated power.
- Effect of total pressure on system cost to determine if technical targets can be met at an operating pressure of 2 or 2.5 atm.
- Effect of a high temperature membrane (150°C) on system design and cost.

Introduction

A baseline cost estimate for a 50-kW PEM fuel cell system for passenger vehicles was developed on the basis of technology available in the year 2000, but using a high production volume scenario (i.e., 500,000 units per year). The baseline system cost estimate presented here is the first step in a multiyear program to assess the impact of technology advances on system cost and to monitor progress over the next four years. In 2000, we will be soliciting feedback from system developers and original equipment manufacturers (OEMs), as well as identifying cost reduction opportunities.

Approach

The first step in the construction of the baseline cost analysis was to conduct a technology assessment to define a plausible configuration and realistic operating parameters. Table 1 shows how the various components were allocated to the fuel processing and fuel cell subsystems, as well as miscellaneous components. To meet the PNGV goals, an overall system efficiency above 35% and water self-sufficiency were required; these conditions strongly influenced the design and specification of the system, as shown in Figure 1. System efficiency was the major driver in specifying and developing the system parameters shown in Table 2.

Table 1. Allocation of components between subsystems.

Fuel Processor Subsystem		Fuel Cell Subsystem	Balance-of-Plant
Reformate Generator • Autothermal Reformer (ATR) • High-Temperature Shift (HTS) • Sulfur Removal • Low-Temperature Shift (LTS) • Steam Generator • Air Preheater • Steam Superheater • Reformate Humidifer **Reformate Conditioner** • NH_3, Removal • PROX • Anode Gas Cooler • Economizers (2) • Anode Inlet Knockout Drum	**Fuel Supply** • Fuel Pump • Fuel Vaporizer **Water Supply** • Water Separators (2) • Heat Exchanger • Steam Drum • Process Water Reservoir	• Fuel Cell Stack (Unit Cells) • Stack Hardware • Fuel Cell Heat Exchanger • Compressor/Expander • Anode Tailgas Burner • Sensors and Control Valves	• Start-up Battery • System Controller • System Packaging • Electrical • Safety
• Sensors and Control Valves for each section			

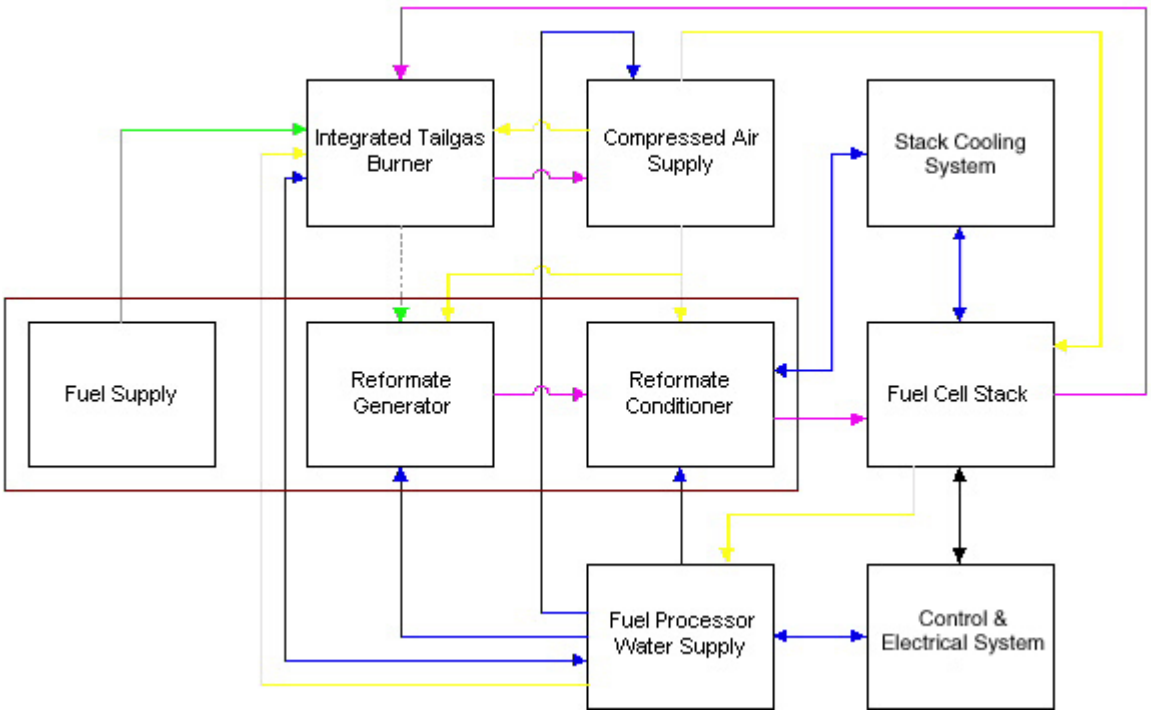

Figure 1. Block diagram of overall system.

Table 2. Important system parameters and design goals.

System Requirements	***Fuel Cell Module***	***Fuel Cell Stack***
• Fuel Flexible (gasoline) • System Efficiency >35% • Water self-sufficiency • 3-atm operation • Turbocompressor/Expander	• 50-kW (net) ❑ 300 V @ full power • 80°C • Reformate fuel	• 0.8 V per cell ❑ 310 mA/cm^2 current density ❑ One cooling plate per cell ❑ Total power, 56 kW$_e$ • 85% H_2, utilization
• *Specified by DOE*	❑ *Established during technology assessment*	

The factory cost estimate of the fuel cell system and components presented in this paper includes fixed and variable manufacturing costs, but it excludes corporate expenses (e.g., research and development, sales, marketing, general and administrative) and profits. A bottom-up manufacturing model, identifying critical manufacturing operations, was used to estimate the cost of major fuel processor and fuel cell components. The cost of the balance of the system components (e.g. heat exchangers, control valves, sensors) is based on discussions with potential suppliers. However, many of the components needed in the system (such as valves and sensors) are not readily available and will have to be developed. Others are available but will likely require redesign for high-volume manufacturing. In those cases, the costs in the model are based on Arthur D. Little's best estimates.

Results

The model results indicate that the overall system cost for the baseline year 2000 is $14,700 (or $294/kW). As shown in Table 3, the cost of the fuel cell subsystem represents 60% of the overall system cost; the fuel processor subsystem, about 30%; and the balance-of-plant and assembly, the remaining 10%.

The fuel cell stack represents approximately 80% of the fuel cell subsystem cost, while the integrated tailgas burner ($460), compressed air supply ($860), and stack cooling system

Table 3. Breakdown of cost by major subsystems (50-kW_e net, 500,000 units/year).

Subsystem	Factory Cost ($)	Percent Total (%)	Cost ($/kW)		
			Baseline Model	PNGV Goals	
				Year 2000	Year 2004
Fuel Cell	8,850	60	177	100	35
Fuel Processor	4,310	29	86	30	10
Balance-of-Plant	500	3	10	Not listed separately in PNGV goals	
Assembly	1,040	8	21		
Total	14,700		294	150	50

($480) make up the balance. Within the fuel cell stack (Table 4), the precious metal content in the membrane electrode assemblies (anode – Ru/Pt 0.2/0.4 mg/cm^2; cathode – Pt 0.4 mg/cm^2; total of 180 grams of Pt per stack) makes up 35% of the stack cost.

Most of the fuel processor costs are in the reformate generator (which includes the reformer/shift reactor and associated heat exchanger), the reformate conditioning system (preferential oxidizer, or PROX, reactor), and steam generator, as indicated in Table 5. In the fuel processing system, thermal, water, and steam management, controls, and packaging contribute 70% to the overall cost of this subsystem. Consequently, in addition to advances in catalyst technology needed to reduce bed size and improve catalyst life, improved system design and engineering will be required to reduce the cost of peripheral systems in the fuel processor.

In the high production volumes assumed for the cost modeling, materials and purchased components make up approximately 80% of the total factory cost.

The estimated power density for the baseline system is approximately 80 W/kg. Table 6 provides a breakdown by major subsystem. The total weight includes 110 kg for components included in the balance-of-plant.

Conclusions

Specification of high-efficiency operation (i.e. 0.8 volts per unit cell) and the resulting modest power density, 250 mW/cm^2, are major factors in the high fuel cell stack cost. If the stack were optimized for high power output instead, the stack cost would be significantly reduced (perhaps by as much as half). Operation at high power lowers the unit cell voltage but increases the current density, resulting in a net decrease in fuel cell materials. The active volume is approximately inversely proportional to the power density. Revisions to the design guidelines are now being considered and will be incorporated into the model as appropriate. Calculations based on a drive cycle will lessen the impact on estimated system efficiency of a lower unit cell voltage at rated power.

Thermal and water management components contribute approximately 20% to the baseline system weight of 600 kg. Design of heat exchangers for higher ambient temperatures (e.g., 120°F) and lower fuel cell unit voltages will further increase this percentage and the weight of the heat exchangers. Consideration of higher fuel cell operating temperatures (e.g., through membranes operating at 150°C) will reduce heat exchanger weight and volume.

In our development of costs for many of the purchased components, such as heat exchangers, sensors, valves, controllers, the compressor/expander, pumps, and motors, we found that these components are in need of technology development to satisfy performance requirements and need to be made cost-effectively in high volumes. These components presently contribute approximately 20% to the total system cost. Simplifications in design, alternative technologies, and economies of scale in high-volume production have the potential to lower these component costs.

Table 4. Breakdown of fuel cell stack costs (50-kW_e net, 500,000 units per year).

Component		Cost		
		%	$	$/kW
MEA	Anode and Cathode Layers	50	3,625	75
	Electrolyte	20	1,310	25
	Gas Diffusion Layers	5	420	5
	Bipolar Plates	15	1,035	20
	Gaskets	5	380	10
	Other	5	280	5
	Total	100	7,050	140

Table 5. Breakdown of fuel processor costs (50-kW_e net, 500,000 units per year).

Component	Cost		
	%	$	$/kW
Fuel Supply	2	100	2
Reformate Generation	47	2,035	40
Reformate Conditioning	24	1,015	20
Water Supply	27	1,160	24
Total	100	4,310	86

Table 6. Increased power density of individual subsystems needed to meet PNGV performance targets (50-kW_e net)

Subsystem	Weight (kg)	Specific Power, Year 2000 (W/kg)	
		Baseline System Estimate	PNGV Target
Fuel Cell	295	169	350
Fuel Processor	215	233	600
Total*	620	80	250
*Total includes 110 kg for balance-of-plant components.			

D. Fuel Cell Systems Analysis

Romesh Kumar (primary contact), E. Danial Doss, Rajesh Ahluwalia, Howard Geyer, and Michael Krumpelt
Argonne National Laboratory
9700 South Cass Avenue
Argonne, IL 60439-4837
(630) 252-4342, fax: (630) 252-4176; e-mail: kumar@cmt.anl.gov

DOE Program Manager: JoAnn Milliken
(202) 586-2480, fax: (202) 586-9811, e-mail: joann.milliken@ee.doe.gov

---

Objectives

- Identify key design parameters and operating efficiencies.
- Assess design, part-load, and dynamic performance.
- Support U.S. Department of Energy (DOE)/Partnership for a New Generation of Vehicles (PNGV) developmental efforts.

OAAT R&D Plan: Task 8; Barrier J

Approach

- Develop, document, and make available an efficient, versatile system design and analysis code.
- Develop models of different fidelity (mechanistic detail).
- Apply models and modeling to issues of current interest as they evolve.

Accomplishments

- Defined a base-case system for the detailed manufacturing cost study being undertaken by Arthur D. Little, Inc., including system configuration, operating conditions, and state points.
- Completed a detailed analysis of a generic autothermal gasoline fuel processor, including effects of reforming temperature, steam-to-carbon ratio, and operating pressure.
- Analyzed fuel cell vehicles on drive cycles to assess fuel cell performance parameters that are needed to meet PNGV Goal 3, fuel economy up to 80 miles per gallon (mpg).

Future Directions

- Influence of vehicle weight and other parameters on onboard fuel storage requirements.
- Effects of revised performance targets for the compressor-expander module.
- Design/configuration issues for high ambient temperatures.
- Component weight and volume trade-offs vs. system parameters and efficiency.
- Additional trade-offs with respect to cost.

Introduction

While individual developers are addressing improvements in fuel cells and stacks, fuel processors, compressor/expander modules, and other fuel cell system components, in this work we use modeling and analysis to address issues of system integration, thermal management, design point and part-load operation, and component, system, and vehicle-level efficiencies and fuel economies. We provide modeling results and analytical support to DOE program managers, fuel cell developers, the relevant PNGV technical teams, and other researchers in the field.

Approach

For this work, we use the GCtool software package developed at Argonne National Laboratory[1] to devise and analyze system configurations and operation. We have adapted this software to the PC platform with the Windows-95/98/NT operating systems, and we have made GCtool available for licensing by research and development organizations, universities, etc. In response to comments by fuel cell developers and program reviewers, we are now using typical cell performance data, recently obtained from Los Alamos National Laboratory (see Figure 1). These data replace the rather high-performance Energy Partners "super cell" data used in our earlier analyses.

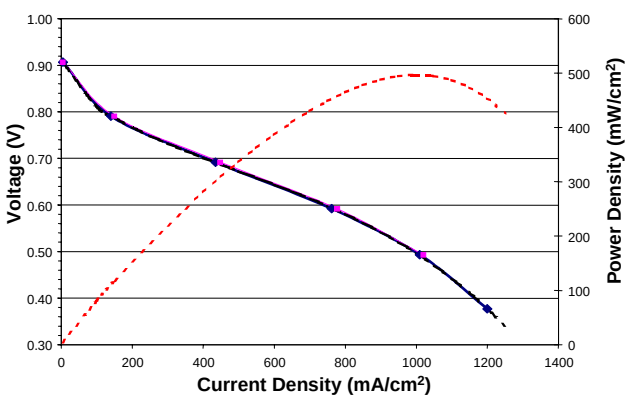

Figure 1. Cell polarization curve used in the fuel cell system simulation. Pressurized (3 atm) operation on gasoline reformate. (Courtesy of Tom Zawodzinski, Los Alamos National Laboratory.)

Results

During fiscal year (FY) 2000, we used systems analysis to address three major tasks:

1. Base-case system definition for the detailed manufacturing cost study by Arthur D. Little.
2. Detailed analysis of the authothermal fuel processor operation and performance.
3. Vehicle-level simulations and analyses of design and operating parameters needed to achieve PNGV Goal 3, fuel economy up to 80 miles per gallon of gasoline.

ANL/ADLittle Base-Case System Definition for the Manufacturing Cost Study

Arthur D. Little is conducting a DOE-sponsored study to assess the manufacturing costs of gasoline-fueled automotive fuel cell systems (see report 2.C). We have worked with them to define the operating envelope (ambient temperature, design point system power and cell voltage, etc.), system configuration (e.g., placement of the water recovery condenser), and other design and operating parameters. This base-case system design is shown in Figure 2. In continuing work, we will examine the effects of varying some of the design parameters (e.g., designs for higher ambient temperatures).

Gasoline Autothermal Fuel Processor Analysis

We have analyzed in detail the operation and performance of the fuel processor part of the fuel cell system shown in Figure 2. These analyses were helpful in quantifying the effects on efficiency of varying the autothermal reforming conditions (temperatures, water-to-carbon ratios), operating pressure, and the use of thermal energy from the anode exhaust burner in the fuel processor.

Figures 3 and 4 show the total system efficiencies for an atmospheric pressure system and a pressurized (3-atm) system. Subject to the assumptions used in the analysis (e.g., 85% electrochemical fuel utilization in the fuel cell stack, fixed air and steam preheat temperatures), the system efficiency increases with decreasing reforming temperatures in both cases. In addition, at the higher reforming temperatures, the fuel

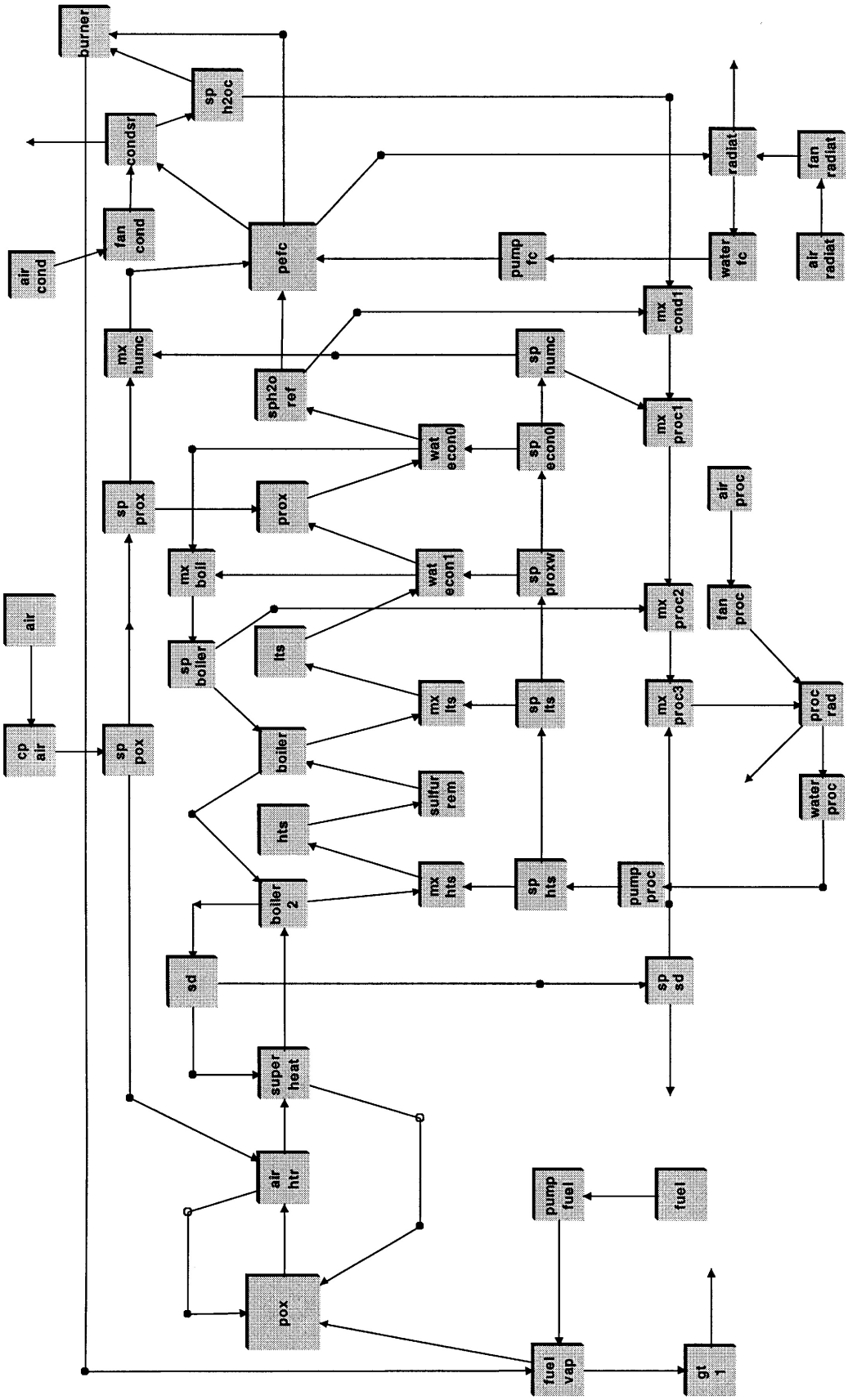

Figure 2. Reference system design and configuration for the autothermal-reformed, gasoline-fueled, automotive polymer electrolyte fuel cell system.

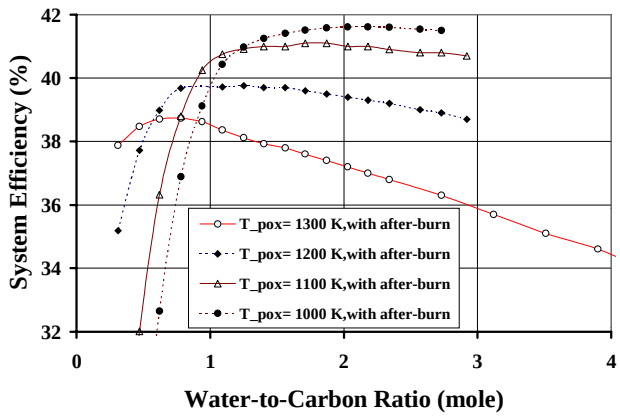

Figure 3. The overall system efficiency as a function of the water-to-carbon ratio and reforming temperature for an atmospheric pressure system.

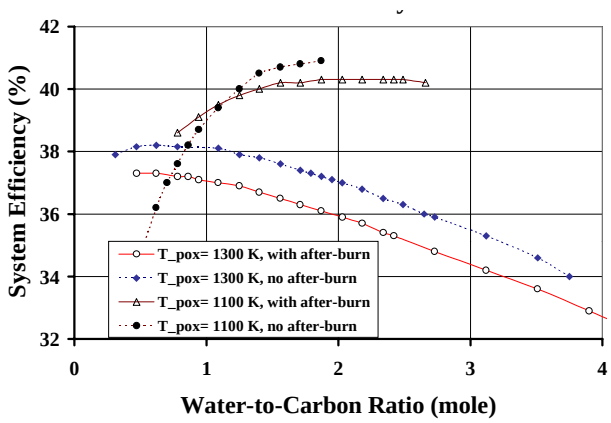

Figure 4. Total system efficiency as a function of the water-to-carbon ratio and reforming temperature for a pressurized system.

processor efficiency decreases with increasing amounts of water used in the fuel processor. For a pressurized fuel cell system, Figure 4 shows that the system efficiency actually increases if the thermal energy at the anode exhaust burner is *not* used in the fuel processor (but is recovered more effectively in the expander). Thus, these results show that the optimum fuel processor design and configuration would be different for pressurized and nonpressurized fuel cell systems.

Achieving PNGV Goal 3

Our earlier modeling results had shown that to achieve the target efficiencies of 38.4% at rated power and 48% at one-fourth of rated power, average operating cell voltages of 0.772 V and 0.896 V would be needed at the respective power levels. At these rather high cell voltages, the corresponding current and power densities in today's fuel cells are low, requiring a large active area and a concomitantly high-cost fuel cell stack. We reanalyzed the gasoline-fueled systems, using the more conservative fuel cell performance curve shown in Figure 1. Vehicle-level analyses were then conducted for three different vehicles, a lightweight vehicle, a heavier but more aerodynamic vehicle, and a lightweight and aerodynamic vehicle. For these vehicles, the fuel economies on the Federal Urban Driving Schedule (FUDS) and highway cycles, as well as the combined fuel economies, were determined. The key vehicle parameters used in the analyses are given in Table 1. This table also shows that the maximum and average power requirements for the three vehicles on the two driving schedules are approximately 22–35 kW and 3–8 kW, respectively.

We first analyzed an 80-kW (net) fuel cell system, with 0.7 V/cell at the rated power (rather than the 0.772 V/cell used in the earlier analyses). Figure 5 shows the cell voltage and the corresponding current density for part-load operation between 0 and 80 kW, as would be needed on the prescribed driving schedules. At the maximum required power output of 35 kW or less, the current densities are less than ~150 mA/cm^2. At the average power requirement of $\leq$8 kW, the current densities are less than ~35 mA/cm^2. The combined fuel economy for the three vehicles is shown in Figure 6. The effect of using a smaller fuel cell system (40 kW instead of 80 kW), as well as the effect of a lower design-point cell voltage (0.65 V instead of 0.7 V) is shown in Figure 7.

Table 1. Vehicle parameters used in the PNGV Goal 3 analyses and the vehicle power requirements over the FUDS and Highway cycles.

Parameter	Vehicle		
	Lightweight	Aerodynamic	Lightweight & Aerodynamic
Test weight, kg	1043	1379	1043
Frontal area, m^2	2.18	2.18	2.18
Drag coefficient	0.25	0.163	0.163
Rolling resistance coefficient	0.0064	0.0064	0.0064
Wheel radius, mm	326	326	326
Auxiliary power, kW	0.5	0.5	0.5
Max (avg) power FUDS, kW	27.7 (3.97)	35.2 (4.54)	27.3 (3.77)
Max (avg) power Highway, kW	22.9 (8.17)	28.7 (7.68)	22.4 (6.75)

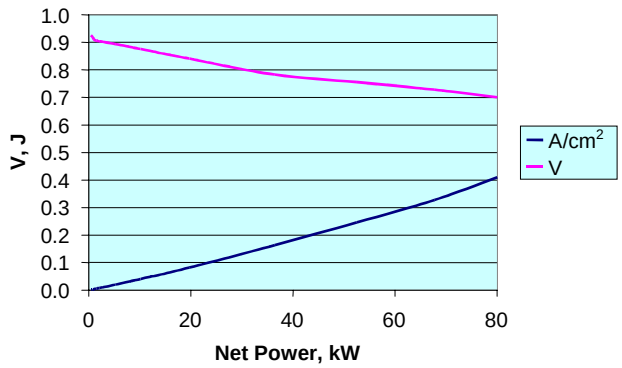

Figure 5. Cell voltage and current density at part-load for an 80-kW (net) fuel cell system.

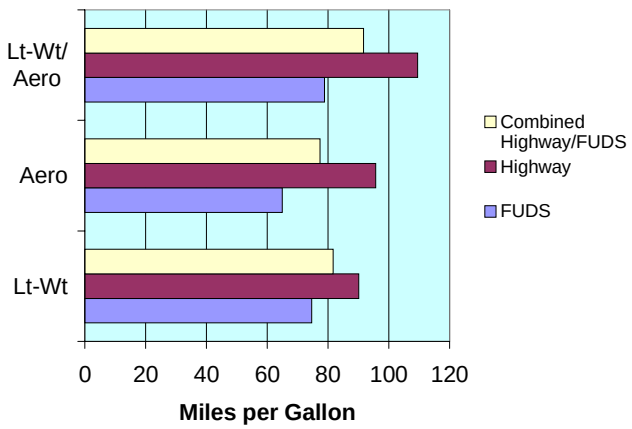

Figure 6. Fuel economy of the three vehicles with an 80-kW system, 0.7 V/cell at the rated power.

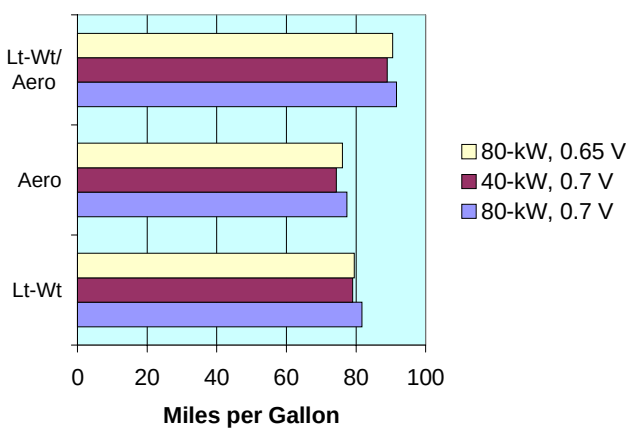

Figure 7. Effect of fuel cell system size and the design-point cell voltage on the combined FUDS/Highway fuel economy for the three vehicles.

Conclusions

- To achieve PNGV Goal 3, up to 80 mpg fuel economy, a gasoline-fueled, 80-kW fuel cell vehicle will need to be extremely lightweight and reasonably to highly aerodynamic.
- The 40-kW (or smaller) fuel cell system can meet FUDS and Highway cycle power requirements for all of these vehicles (but it may not be adequate to provide acceptable acceleration performance).
- The fuel cell system is never operated at the rated power on these drive cycles; average power draw is ~10% of rated power, with short bursts to ~35% of rated power.
- Operating current densities are low, <35 mA/cm^2 on average, with a maximum of ~150 mA/cm^2 (for the 80-kW system) for short periods.
- The effect of lowering the design point cell voltage may be minor on fuel economy, but it may reduce the fuel cell stack size significantly. The sizes of the fuel processor and the heat exchangers would increase, however, because of the lower efficiency at the design point.
- Using a smaller fuel cell system would decrease system weight, volume, and cost, with a relatively small decrease in fuel economy (but an appropriate battery would be required to provide adequate acceleration and passing performance).

References

1. H. K. Geyer and R.K. Ahluwalia, *GCtool for Fuel Cell Systems Design and Analysis: User Documentation*, Argonne National Laboratory Report ANL-98/8, March 1998.

FY 2000 Publications/Presentations

- R. Kumar, E. Doss, R. Ahluwalia, H. Geyer, and M. Krumpelt, "Fuel Cell Systems Air Management Overview," presented at the Compressor/Expander Module Review Meeting, held at USCAR, Southfield, Mich., Oct. 12, 1999.
- R. Kumar, E. Doss, R. Ahluwalia, H. Geyer, and M. Krumpelt, "Design Considerations for Developing Efficient Fuel Cell Systems," presented at the IEA PEFC Annex XI Meeting, Argonne, Ill., Oct. 21-22, 1999.

- R. Kumar, "Fuel Processing Considerations: Cold Start, Transients, Coking, and Related Issues," presented at the NRC/Fuel Cell Review Meeting, held at USCAR, Southfield, Mich., Jan. 12, 2000.
- E. Doss, R. Ahluwalia, R. Kumar, and M. Krumpelt, "Automotive Fuel Cell System Design Points, Efficiency Targets, and Tradeoffs to Achieve PNGV Goal 3," presented at the Fuel Cell Targets Workshop, held in conjunction with the 2000 Future Car Congress and Exposition, Arlington, Va., April 2-6, 2000.
- E. Doss, R. Ahluwalia, H. Geyer, R. Kumar, and M. Krumpelt, "Transportation Fuel Cell Systems Modeling and Analysis," presented at the 2000 Annual National Laboratory R&D Meeting, Fuel Cells for Transportation Program, held at Pacific Northwest National Laboratory, Richland, Wash., June 7-8, 2000.

III. FUEL PROCESSING SUBSYSTEM[1]

A. Advanced Fuel Processor Development for Next Millennium Fuel Processor™ for Transportation Fuel Cell Power Systems

William L. Mitchell, P.E. (primary contact), Prashant Chintawar, Srinivasa Prabhu, and James Cross
Nuvera Fuel Cells/Arthur D. Little, Inc., 35 Acorn Park, Cambridge, MA 02140
(617) 498-6149, fax: (617) 498-6655, e-mail: mitchell.william@adlittle.com

DOE Program Manager: Patrick Davis
(202) 586-8061, fax: (202) 586-9811, e-mail: patrick.davis@ee.doe.gov

ANL Technical Advisor: Walter Podolski
(630) 252-7558, fax: (630) 972-4430, e-mail: podolski@cmt.anl.gov

Contractor: Nuvera Fuel Cells/Arthur D. Little, Inc., Cambridge, Massachusetts
Prime Contract Nos. DE-RA02-97EE50443 (PRDA) and DE-FC02-99EE50580 (SFAA)
Subcontractors/Partners: Modine Manufacturing, Energy Partners, Illinois Department of Commerce and Community Affairs, United Catalysts, Inc., Corning, Inc., and STC Catalysts, Inc.

Objectives

- Under our Department of Energy (DOE) PRDA program for advanced fuel processor development, Nuvera Fuel Cells/Arthur D. Little, Inc. (Nuvera), is:
  - Developing a 50-kW_e fuel reformer capable of processing gasoline and alternative fuels, such as ethanol.
  - Developing and testing an advanced 50-kW_e preferential oxidation (PROX) device based on proprietary catalyst technology, with a major focus on gas purity when reforming gasoline and ethanol.
  - Supporting Plug Power in the development of a 50-kW fuel cell power system.
- Under our DOE SFAA project to develop a Next Millennium Fuel Processor™ for transportation fuel cell power systems, we are utilizing our current in-depth understanding of fuel processing and fuel cell systems in a three-part R&D program that will yield a fully optimized fuel processing subsystem:
  - In Phase I, Nuvera will work with Energy Partners to integrate existing hardware into a 10-kW_e multifuel power system, to identify key system-level trade-offs in the design of a fuel processing subsystem, and to allow validation of computer models developed both internally and by Argonne National Laboratory (ANL).
  - In Phase II, Nuvera will utilize existing integrated and modular fuel processors to perform endurance testing to identify and address material and catalyst degradation mechanisms.
  - In Phase III, Nuvera will conduct an in-depth core technology R&D program designed to identify high-activity, low-cost catalysts; develop and design compact adsorbents, catalysts, and heat exchangers to enhance power density and specific power and reduce start-up time; develop fuel purification (sulfur removal) and reformate clean-up technologies to address the issue of system durability; integrate the new catalysts and supports into a fuel processor package specifically suited to the optimized catalyst suite; and deliver a fully integrated fuel processing subsystem to the DOE that meets or exceeds 2004 Partnership for a New Generation of Vehicles (PNGV) targets.

---

[1] The DOE technical targets for fuel-flexible fuel processors can be found in Table 2a, 2b, and 2c, Appendix B.

OAAT R&D Plan: Tasks 5 and 6; Barriers E, F, G, and H

Approach

- PRDA:
  - Build and test a brassboard 10-kW_e system based on existing reformer design, existing stack hardware, and other available components as a proof of concept (3-atm pressure).
  - Investigate multiple steady-state CO clean-up options at 10-kW_e level.
  - Integrate complete 10-kW_e system and test it at Nuvera using a 10-kW_e system test facility.
  - Assist Plug Power in the development of a test facility for full-scale (50-kW_e) system testing.
  - Design and build an advanced 50-kW_e fuel processor based on Phase I and Phase II testing.
  - Continue catalyst refinement from Phase I.
  - Test 50-kW_e fuel processor/PROX combination at Nuvera/ADL labs, including transients.
  - Provide integration assistance for testing 50-kW_e brassboard (Phase III) system demonstration at Plug Power.
  - Aid Plug Power in the mechanical design and packaging of the 50-kW_e Phase III system, focusing on system functionality and efficiency of operation.
  - Work with Plug Power to perform transient tests of the integrated Phase III system.
  - Build and deliver a Phase IV 50-kW_e fuel processor subsystem to Plug Power for final system integration. The Phase IV system will meet PNGV weight and volume targets for the year 2000.
- SFAA:
  - Perform automotive system analysis and identify strategies to meet PNGV targets.
  - Evaluate the control strategies on a 10-kW_e fully automated system.
  - Set targets (weight, volume, performance, efficiency) for key technologies and components based on the system analysis.
  - Work closely with Nuvera partners to develop advanced catalyst, substrate, and heat-exchanger technologies.
  - Develop conceptual design of a fuel processor based on new technologies and draft control and fuel cell integration strategies.
  - Design, fabricate, and test the fuel processor on all fuels and investigate efficiency, emissions, steady-state and transient performance, and reformate purity.
  - Integrate the fuel processor and fuel cell and investigate the performance of the power system. Identify system-level integration issues (Phase I).
  - Continue technology development and refinement in Phase II, based on Phase I results.
  - Test fuel processor, integrated power system, and obtain test data (Phase II). Phase II system will meet PNGV targets for specific power and power density, transient response, and reformate purity.

Accomplishments

- PRDA:
  - Designed, built, and integrated a fully automated 50-kW_e Phase III fuel processor subsystem that exceeded all Phase III targets.
  - Demonstrated fuel processing efficiencies with California Phase II gasoline in excess of 85%.
  - Demonstrated PROX exit efficiencies of 83% and exit CO concentrations lower than 10 ppm.
- SFAA:
  - Designed 10-kW_e fuel cell power system in conjunction with Energy Partners.
  - Built a 15-kW_e (gross) automated fuel processing subsystem for integration with the fuel cell.
  - Identified “system level” strategies for weight and volume reduction of fuel cell power system.
  - Developed transportation-specific substrate (monolith, foam) -based adsorbents, catalysts, and compact heat exchangers for all reaction zones of multifuel processor.
  - Investigated specialized heat exchanger in a test rig under simulated fuel processor conditions, with results suggesting that novel heat exchangers are capable of obtaining ≥ 5 times improvement in heat-transfer coefficient over conventional types.

- Developed a compact gasoline desulfurizer, designed for 5,000 miles at change-out.
- Performed catalyst studies in disintegrated fuel processor at 130-kW_{th} firing rate. Results show that the new catalysts have about an order of magnitude lower thermal mass and pressure drop, and need about an order of magnitude lower contact time, than the conventional catalysts.
- Established that with advanced technologies, ≥ 750 W/L power density and ≤ 2 min start-up time should be attainable for the fuel cell power system, and other PNGV targets can be met or exceeded.

Future Directions

- PRDA:
  - Integrate Phase III unit with 60-kW_e stack from Plug Power and evaluate system efficiency and thermal and water balance issues.
  - Develop Phase IV fuel processing system, based on performance of the Phase III integrated system.
- SFAA:
  - Integrate 15-kW_e fuel processing system with Energy Partners' stack.
  - Conduct detailed system trade-off and control strategy evaluation.
  - Commence conceptual and detailed design of 50-kW_e fuel cell power system.
  - Improve core technology and system models to fully exploit the benefits of lightweight and low-thermal-mass media.

Introduction

Nuvera Fuel Cells (NFC) is a leading supplier of fuel cell power systems in the stationary and transportation markets. Widespread implementation of fuel cell systems requires significant improvements in many aspects of the technology, including power density, specific power, response, efficiency, and cost. In addition, the ability to operate on a number of hydrocarbon fuels that are available through the existing infrastructure is a key enabler for commercializing fuel cell systems. NFC is working with the DOE to develop efficient, low-emission multifuel processors for transportation applications. The fuels include gasoline, methanol, ethanol, and natural gas.

In the PRDA program, NFC is developing reformer subsystems (fuel processor, CO clean-up, and exhaust clean-up) and integrating them with fuel cells for system-level evaluation of issues like efficiency, water balance, transient response, thermal integration, and parasitic power. The results of this program will identify and quantify the key technology challenges that need to be addressed in developing fuel processing systems for automotive applications. The deliverable of the program is an integrated power system that meets PNGV targets for year 2000.

In the SFAA program, the challenges identified in the PRDA program will be addressed through an intensive technology development program. Catalysis, novel heat-exchange media, and their integration will be developed through internal efforts and partnerships with leading companies in this field. Two generations of fuel processors will be developed and tested with fuel cells. The deliverable of this program is an integrated fuel processing system that exceeds PNGV targets for year 2004.

PRDA Phase III Results

The performance targets for the Nuvera Phase III fuel processor are shown in Table 1. The measured performance of the Phase III fuel processing system is shown in Figures 1 and 2. The overall efficiency of the fuel processor is defined as the LHV of hydrogen output of the fuel processor divided by the LHV of fuel input.

Table 1. PRDA Phase III fuel processor system targets.

Fuel Processor (kW)	175	40	18
Overall Fuel Processor Efficiency, %	68	68	55
Exit Hydrogen Flow Concentration, %	35	35	28
Exit Hydrogen Flow Rate, kg/hr	3.65	0.81	0.3
Pressure Drop, psi	5	2	1
Emissions	< Tier II	< Tier II	< Tier II
Parasitics, kW	0.5	0.2	0.2

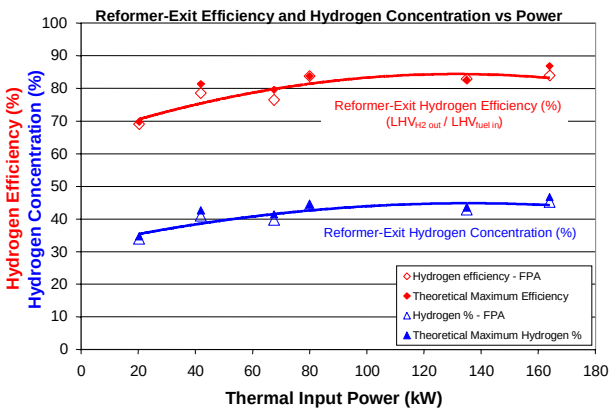

Figure 1. PRDA Phase III reformer efficiency and hydrogen concentration.

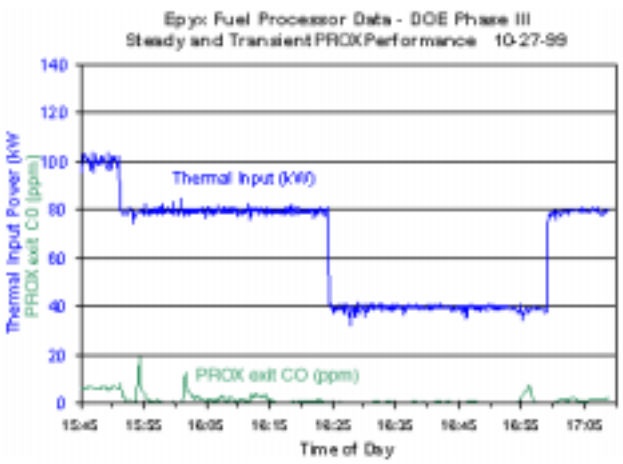

Figure 2. PRDA Phase III PROX performance.

The efficiency of the Nuvera fuel processing system is about 85% at the higher powers and ~70% at a turndown of 8:1. At these conditions, the dry gas hydrogen concentration is in excess of 40%. Also shown in Figure 1 are the maximum achievable efficiencies and hydrogen concentrations at the operating conditions of our system. The fuel processing system exit (PROX exit) carbon monoxide (CO) gas concentrations during steady-state and mild transients are shown in Figure 2. The Nuvera PROX technology is able to maintain CO concentrations below 20 ppm over these transients.

SFAA for Next Millennium Fuel Processor™

Because automotive fuel processor catalysts are subjected to rapid start-up and transient conditions (e.g., ATR catalyst temperature rises from 25°C to ~800°C in less than 60 s), Nuvera has installed and operated transient reactors (Figure 3) to evaluate catalysts under those conditions. The results are providing data under real-world conditions.

To improve the power density and specific power of our system, Nuvera is developing advanced substrate-based heat-transfer technology. Figure 4 shows the test rig to evaluate new heat-exchanger designs. We have identified compact and moderate pressure drop heat-exchanger configurations capable of providing 4-6 times improvement in the heat-transfer coefficient over that of the conventional shell and tube designs. Currently, we are investigating durability, cost reduction, and manufacturability issues of these novel designs.

Figure 3. Transient catalytic reactor capable of simulating automotive transients. It can change the gas composition and flow rate instantaneously and can raise the catalyst temperature to 1100°C in < 30 s.

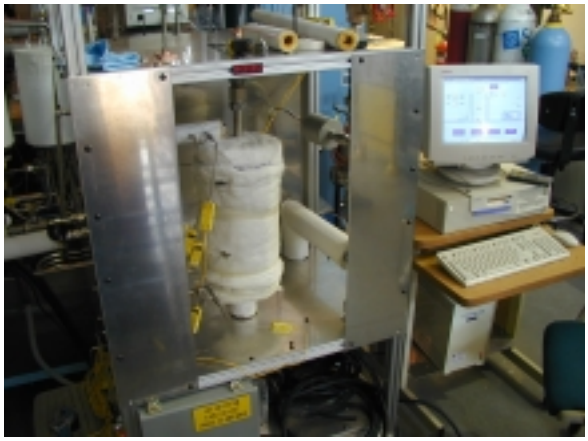

Figure 4. Heat exchanger test rig simulates the fuel processor atmosphere.

Water-gas-shift catalysts (WGSCs) account for a large share of the volume and weight of autothermal-reforming-based automotive fuel processors. Conventional WGSCs, based on Fe/Cr and Cu/Zn oxides, are not suitable for the intermittent operation of the automotive fuel cell power system. By working closely with its partners, Nuvera has developed a new generation of substrate-based catalysts (Figure 5). Data obtained in the modular pressurized reformer at 130 kW_{th} suggest that these new media need about six times lower contact time than the conventional media. We are conducting short-term and long-term durability testing of these media.

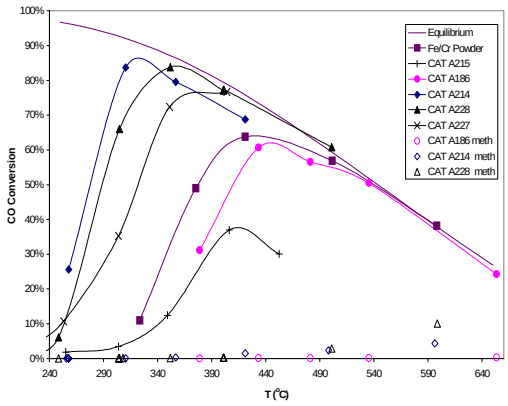

Figure 5. Monolith-based water-gas-shift catalysts exhibit higher activity than conventional pelleted catalysts.

System modeling plays a significant role in predicting the performance (conversion, temperature, and concentration profile) of catalytic reactors and heat-exchanger assemblies. This is particularly true for PROX reactors, where high temperatures can lead to runaway situations. On the basis of single-component data, Nuvera has developed and utilized computational fluid dynamics (CFD) codes for improving reactor design (Figure 6).

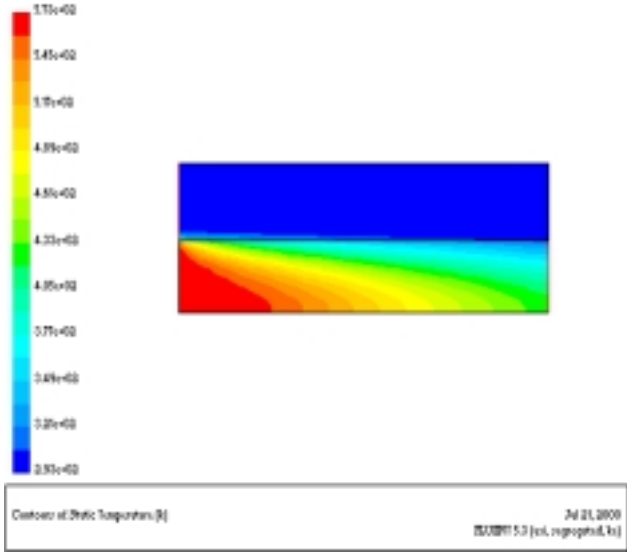

Figure 6. Computational fluid dynamics is used to predict the behavior of compact heat exchangers.

B. Multifuel Processor for Fuel Cell Electric-Vehicle Applications

Tom Flynn (primary contact)
McDermott Technology, Inc.
1562 Beeson Street
Alliance, OH 44601-2196
(330) 829-7622, fax: (330) 829-7283, e-mail:tom.j.flynn@mcdermott.com

Brian Engleman (subcontractor)
Catalytica Advanced Technologies
430 Ferguson Drive
Mountain View, CA 94043-5272
(650) 940-6391, fax: (650) 968-7129, e-mail: bde@mv.catalytica-inc.com

DOE Program Manager: Nancy Garland
(202) 586-5673, fax: (202) 586-9811, e-mail: nancy.garland@ee.doe.gov

ANL Technical Advisor: Walter Podolski
(630) 252-7558, fax: (630) 972-4430, e-mail: podolski@cmt.anl.gov

Contractor: McDermott Technology, Inc., Alliance, Ohio
Prime Contract No. DE-FC02-99EE50586, June 1999-September 2001

Objectives

Design, build, and demonstrate a fully integrated, 50-kW_e catalytic fuel processor system. The fuel processor will produce a hydrogen-rich gas for direct use in polymer electrolyte membrane (PEM) fuel cell systems for electric-vehicle applications.

OAAT R&D Plan: Task 5; Barriers E, F, G, and H

Approach

- Develop preliminary design of 50-kW_e fuel processor system, as well as performance goals for individual components.
- Evaluate alternative approaches for the major catalytic components (e.g., desulfurizer, reformer, shift reactor, and selective oxidation reactor).
- Conduct subsystem testing of major components, utilizing best catalyst approach.
- Develop final design of overall system and design specifications for individual components.
- Assemble 50-kW_e fuel processor system.
- Perform demonstration testing, using gasoline and methanol as fuels.
- Ship fuel processor system to Argonne National Laboratory (ANL).

Accomplishments

- Developed process flow models for single-catalyst bed autothermal reformer (ATR) and plate reformer designs.
- Demonstrated liquid-phase gasoline desulfurizer that uses specifically tailored zeolitic adsorbents.
- Performed screening tests for candidate ATR catalysts and plate reforming catalysts.

- Evaluated three low-temperature shift catalysts.
- Assessed NexTech CARAT program medium-temperature shift catalyst.
- Established development agreements with Los Alamos National Laboratory and Battelle/Pacific Northwest National Laboratory for selective oxidation reactor and microchannel heat exchangers.

Future Directions

- Proceed with detailed design and subsystem testing for plate-based 50-kW_e fuel processor.
- Develop dynamic simulation model.
- Perform subsystem catalyst evaluation.
- Investigate options for fuel preconversion.

Deliverables

A 50-kW_e fully integrated fuel processor.

Introduction

Development of a compact, efficient, and low-cost processor for converting carbon-based fuels to hydrogen is an important aspect of the successful implementation of fuel cells for transportation applications. Current approaches based on noncatalytic partial oxidation technology provide the advantages of fast start-up and transient response, but these approaches have not been fully demonstrated on sulfur-bearing gasoline. A catalyst-based reforming approach for fuel processing can provide fast start-up and transient response, high efficiency, and compactness. When coupled with a liquid-fuel desulfurizer, the multifuel processor under development by McDermott/Catalytica promises to approach the Partnership for a New Generation of Vehicles (PNGV) targets.

Approach

The fuel processor will consist of a liquid-fuel desulfurizer, a catalytic reformer, high- and low-temperature water-gas shift units, a selective oxidizing unit, and ancillary components (including pumps, compressor/expander, heat exchangers, and controls). A conceptual drawing of the fuel processor system is shown in Figure 1. The design has been described previously [1].

The liquid-fuel desulfurizer will reduce the sulfur in gasoline to less than 3 ppm. The reformer unit, operating at an average temperature of 800°C, will produce a hydrogen-rich gas from the fuel feed. Two approaches will be evaluated during the

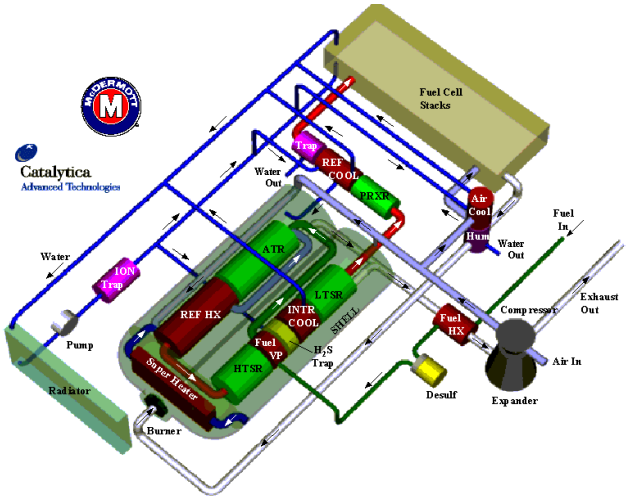

Figure 1. Process flow diagram.

program: (1) a packed bed that uses a single catalyst and (2) a plate-based catalyst system. A shift reactor, consisting of either a single catalyst bed or individual high-temperature and low- temperature catalyst beds, will reduce the CO concentration in the reformate gas to approximately 2000 ppm. Final reduction of CO in the reformate gas will be achieved in a selective oxidation reactor.

McDermott Technology, Inc., will develop the overall system design, including heat integration, mechanical design, ancillary equipment, and instrumentation/controls. Catalytica Advanced Technologies will develop the catalytic components, including improved catalysts. NexTech, as a subcontractor on the project, will contribute its

expertise and technology in the area of shift catalysts. The program consists of five major tasks: preliminary design, catalyst development, subsystem testing, final design, and prototype assembly and demonstration.

Results

During this reporting period, the first two tasks were completed.

Preliminary Design

Steady-state ASPEN process simulation models were generated for the catalyst-bed and plate-reformer concepts. The system using the catalyst-bed concept had a predicted efficiency of 87% at 25% load, assuming 70% hydrogen utilization in the fuel cell and 50% fuel-cell efficiency. Actual performance data for the fuel pump, humidifier, compressor/expander, and fuel cell were incorporated into the simulation model. The system power density and specific power are 564 W/L and 316 W/kg, respectively. The compressor/expander, humidification system, and start-up burner are included in the fuel processor scope.

The plate concept showed a comparable system efficiency. The plate approach yields a smaller-size system with comparable weight.

For both systems, the heat-exchanger types and sizes have been selected. A control system vendor has also been selected.

Catalyst Development

Desulfurizer

We demonstrated removal of thiophenes and methyl-substituted thiophenes from aromatic solvents by using zeolitic adsorbents. The thiophenes are most difficult to remove because of steric hindrance around sulfur and competitive adsorption by aromatics. A typical adsorption profile, illustrating the adsorption of thiophene with a low-aluminum ZSM5 zeolite, is shown in Figure 2. Proprietary modifications of zeolites provided the best performance. We obtained promising results with California CARB Phase 2 gasoline (30 ppm sulfur reduced to < 3 ppm sulfur).

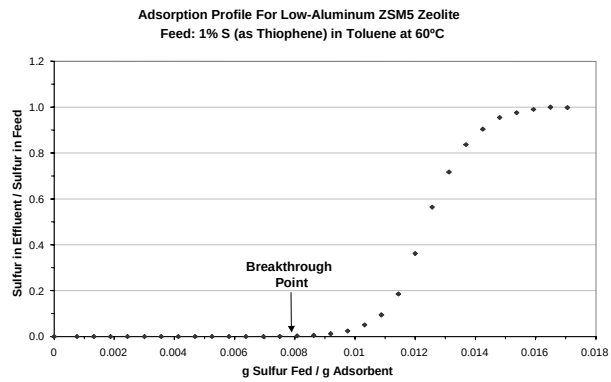

Figure 2. Typical adsorption profile.

Reforming Catalyst

We completed a successful 100-hour test with California CARB gasoline. The catalyst demonstrated a capacity of approximately 5 kW_e/kg. Equilibrium conversions were maintained throughout the run (Figure 3.)

We also demonstrated the feasibility of using Catalytica's Xonon™ combustion catalyst, in combination with a reforming catalyst, in the plate arrangement.

An evaluation of the advantages and disadvantages of the two approaches was made. The results are summarized in Table 1.

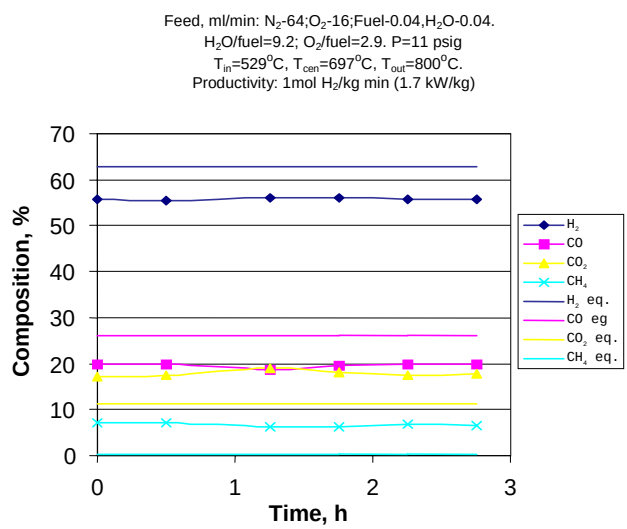

Figure 3. Approach to equilibrium for Catalytica ATR-10 catalyst.

Table 1. Advantages and disadvantages of plate vs. bed concepts.

Plate Concept	**Bed Concept**
Advantages	*Advantages*
Rapid start-up and response	Rapid start-up and response
No dilution – smaller downstream components	
Higher H_2 partial pressure for enhanced fuel cell performance	
Availability of existing proprietary combustion catalyst and washcoat technology	
Disadvantages	*Disadvantages*
Preprocessor required	Difficult thermal balance within bed
	Nitrogen dilution
Difficult thermal balance across plate	Lower H_2 partial pressure results in poorer fuel cell performance
Neutral	*Neutral*
Safety issues: manifolding, leakage	Safety issues: combustible mixtures
Catalyst formulation work required	Catalyst development required – no available commercial catalyst

Shift Catalysts

High-temperature shift (HTS) and low-temperature shift (LTS) catalysts are traditionally sensitive to oxygen, condensed moisture, and sulfur poisoning. Commercial HTS catalysts tend to be more rugged than LTS catalysts. For this reason, the team focused on LTS catalyst development.

We completed benchmark tests of commercially available catalysts. We assessed alternative LTS catalysts, including high-activity supported Cu catalysts, nanoscale Cu/Zn/Al mixed oxide catalysts, and NexTech's noble metal/ceria catalyst, which is being developed under the CARAT program [2]. The best results were obtained with a proprietary third-party catalyst. The relative reaction and deactivation rate constants are summarized in Table 2. (Catalyst C is a widely used commercial LTS catalyst.)

The NexTech catalyst is a medium-temperature shift (MTS) catalyst; as such, it is not intended to operate in the same temperature range as low-temperature shift catalysts, so direct comparison is not possible.

Table 2. Catalyst properties.

Catalyst	Relative Reaction Rate Constant	Relative Deactivation Rate Constant	Post-/Pre-Activity Moisture
A	1.31	0.095	1.00
B	1.05	0.514	0.56
C	1.0	1.0	----

However, NexTech's catalyst possesses some important properties that warrant continued consideration for the prototype design. The NexTech catalyst remains active in the oxidized or reduced state. It is less sensitive to condensed moisture. Noble metal washcoating on a monolith catalyst substrate is a proven technology. Finally, because it operates at a higher temperature, it is less sensitive to sulfur poisoning, the minimum achievable CO concentration is limited by equilibrium. As a result, the selective oxidation reactor must be designed to handle a higher inlet CO concentration. Therefore, its use must be assessed in the context of the entire system design.

Conclusions

Significant progress has been made toward meeting the PNGV targets. The size target is less formidable than the weight target. On the basis of first-year project results, the following major decisions have been made:

- Proceed with subsystem testing of catalyst formulations.
- Proceed with plate-based catalytic reforming system design.
- Include MTS catalyst in determination of best combination of HTS/MTS/LTS/selective oxidation for CO clean-up.

References/Publications

1. T.J. Flynn, R.M. Privette, M.A. Perna, K.E. Kneidel, D.L. King, and M. Cooper, "Compact Fuel Processor for Fuel Cell-Powered Vehicles," International Congress and Exposition, Detroit, Mich., March 1-4, 1999, SP-1425, pp. 47-53.
2. S.L. Swartz, "Nanoscale Water-Gas-Shift Catalysts," *Snapshots of CARAT Projects,*

Phase 2, published by Argonne National Laboratory, Transportation Technology R&D Center, March 2000, pp. 11-12.

C. Fuel-Flexible, UOB™ Fuel Processor System: Development and Status

Richard Woods (primary contact), John Cuzens, and Josh Mauzey
Hydrogen Burner Technology, Inc.
3925 Vernon Street
Long Beach, CA 90815
(562) 597-2442, fax: (562) 597-8780, e-mail: Rwoods@HydrogenBurner.com

DOE Program Manager: Patrick Davis
(202) 586-8061, fax: (202) 586-9811, e-mail: patrick.davis@ee.doe.gov

ANL Technical Advisor: William Swift
(630) 252-5964, fax: (630) 252-4176, e-mail: swift@cmt.anl.gov

Contractor: Hydrogen Burner Technology, Long Beach, California
Prime Contract No. DE-FC02-97EE50482, October 1997-December 1999

Objectives

- Research, develop, assemble, and test a 50-kW_e net (12-kW_e nominal), fuel-flexible fuel-processing (F^3P) subsystem.
- Conduct performance mapping of the subsystem on various fuels, including natural gas, gasoline, ethanol, and methanol.
- Verify the humidified low-temperature shift (HLTS) concept and assess its applicability.
- Coordinate with fuel cell system developers in preparation for system-level integration activities.

OAAT R&D Plan: Task 5; Barriers E, F, G, and H

Approach

This program includes process and hardware design for a F^3P subsystem, assessment of alternative materials and catalysts, fabrication of integrated hardware assemblies, and evaluation of alternative carbon monoxide (CO) polishing approaches.

- The hardware design approach selected for the prototype F^3P subsystem includes three assemblies – the F^3P assembly, fuel vaporizer assembly, and CO polishing assembly. A breadboard control package is also included to allow automatic control of the subsystem.
- The F^3P assembly integrates the primary systems/functions required for a fuel processor – reformer reactor, thermal management, shift reactors, and integrated steam generation.
- The fuel vaporizer assembly integrates the functions of fuel vaporization and anode off-gas combustion.
- The CO polishing concepts being evaluated include methanation and preferential oxidation (PROX) of CO.

The program also includes verification of the HLTS reactor concept, which encompasses the evaluation of alternative hardware configurations and development of advanced low-temperature shift (LTS) catalysts with improved activity at lower temperatures and higher humidity.

Accomplishments

- F^3P subsystem hardware was successfully adapted from noncatalytic partial oxidation (POX) design to autothermal reformer (ATR) design.
- A total of eight F^3P systems have been fabricated, and seven have been tested. Under parallel programs, four prototypes have been delivered to an automotive manufacturer, a fuel cell integrator, and a national laboratory.
- A total of almost 800 combined hours of operation have been achieved on these units.
- "Push Button Start" automated control logic was completed for natural gas, propane, and gasoline operation.
- Packaged hardware design of a diesel fuel processing subsystem was completed. Successful initial operation was achieved.
- Concept verification testing of HLTS hardware was completed.
- PROX hardware was integrated into the F^3P system.
- The technology foundation for fuel processing subsystems, which has been applied to both vehicular and stationary applications, was established.

Future Directions

Submit final report to DOE.

Introduction

Fuel cells are considered to be a viable alternative to the internal combustion engine for automotive applications. The direct use of hydrogen (H_2) permits the easiest, smallest fuel cell system, but "on-board storage" of H_2 raises many concerns, as does the absence of any H_2 refueling infrastructure. An alternative approach would be to use existing liquid fuels, such as gasoline, or evolving fuels, such as ethanol, methanol, or synthetic liquids. Any of these fuels would require an "on-board reformer" to convert the liquid fuel into H_2 gas on demand. Hydrogen Burner Technology, Inc. (HBT), has entered into a cooperative agreement with the U.S. Department of Energy through the Office of Transportation Technologies. This agreement is focused on development and testing of a F^3P subsystem for automotive applications.

Program Overview

The greater share of the work involves the design, construction, and testing of a prototype F^3P subsystem. A second effort is related to verification of the HLTS concept.

Activities during FY00 have included the following: conversion of F^3P hardware from the POX design to the ATR design; completion of controller software for natural gas, propane, and gasoline operation; concept verification testing of HLTS hardware; integration of PROX hardware into the F^3P subsystem; and completion of a packaged hardware design.

F^3P Subsystem Design and Hardware

The basis of the F^3P subsystem has changed from a noncatalytic POX reactor to a catalytic ATR reactor. The improvements this change offers are threefold: (1) increased efficiency, (2) lower operating temperatures, and (3) simplification of process control.

The hardware approach taken in more recently built packaged systems utilizes four separate hardware assemblies to allow for evaluation testing of alternative components. The four assemblies are the fuel vaporizer/anode gas oxidizer assembly, the F^3P assembly, the CO polishing assembly, and the economizer. The overall process is shown in Figure 1.

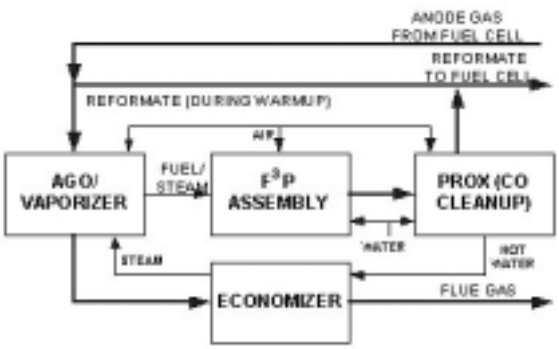

Figure 1. Fuel reformer subsystem.

The seven most critical chemical processes of the F^3P subsystem are thermally and physically integrated into the F^3P assembly hardware (see Figure 2). The F^3P assembly provides close thermal interaction between the ATR reaction zone, which operates at 760 to 870°C (1400 to 1600°F), and the lower-temperature zones of the process air preheater and high-temperature shift zones, which operate at 300 to 650°C (600 to 1200°F). This configuration minimizes heat loss while maximizing reaction temperature.

All of the processes identified in Figure 2 are physically integrated into the hardware illustrated in Figure 3. The prototype F^3P assembly, with conventional, commercially available catalysts, weighs about 104 kg (230 lb), approximately 25% more than its target weight of 83 kg (183 lb). Most of this excess mass is due to high-density commercial catalyst and flange structures used for easy disassembly and inspection. The volume of the F^3P assembly is approximately 85 L (3 ft^3).

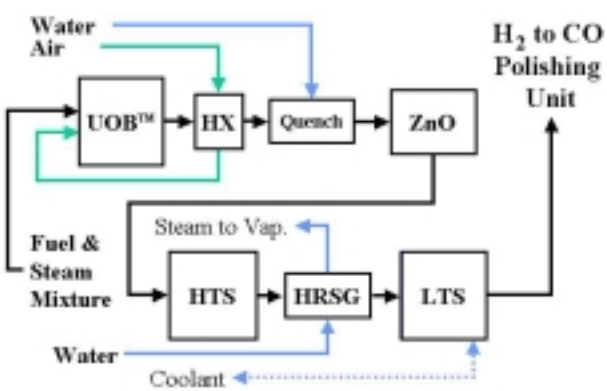

Figure 2. Integrated F^3P assembly.

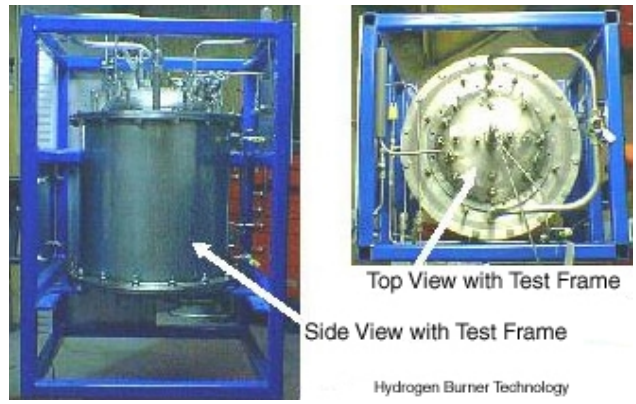

Figure 3. Prototype F^3P assembly configuration.

Increasing this size by the volume needed for the vaporizer, CO polishing, and economizer assemblies indicates that the prototype hardware is approximately twice as great as its target volume.

A complete subsystem, including all four required assemblies, is shown in Figure 4. The fuel vaporizer/anode gas oxidizer provides a fully vaporized fuel/steam mixture to the F^3P assembly. This fuel/steam mixture mixes with preheated air within the F^3P before entering the ATR reactor.

The reformate gas exits the F^3P assembly and enters the PROX for CO polishing. Once fuel cell operation begins, the remaining energy in the anode off-gas is recovered in the fuel vaporizer/anode gas oxidizer. Any remaining unburned hydrocarbons or hydrogen will be oxidized in the economizer, where any additional heat recovered contributes to steam generation.

Results

To date, HBT has accumulated almost 800 hours of operational experience on the F^3P subsystems fabricated. This experience includes 268 start-stop

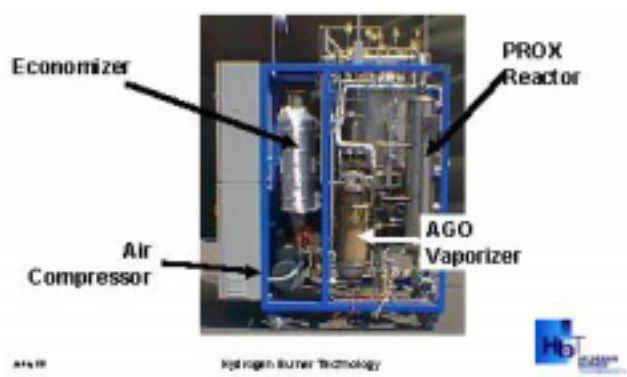

Figure 4. HBT-023 unit, right side.

cycles, and operation on five fuels: gasoline, methanol, natural gas, propane, and diesel.

Table 1 provides a summary of operating experience achieved to date. The summary represents testing performed with both manual and automatic controls.

This operating experience has partially mapped the performance characteristics of the F^3P subsystem on five fuels. A summary of achievements to date is given in Table 2. Results shown are from tests in which the ATR configuration of the F^3P was used for all fuels except methanol, which has only been tested with the noncatalytic POX configuration.

Figure 5 shows example test data taken over the course of six tests. The F^3P subsystem used was S/N 001. California reformulated gasoline was used as the fuel.

Table 1. Operating experience on F^3P summary.

	S/N 001	S/N 002	S/N 003	S/N 004
Customer	HBT/DOE	Auto Mfg'er	LANL	FC Devel
Fabrication	12/30/98	2/20/99	3/9/99	7/1/99
Delivered	1/1/99	3/5/99	5/28/99	9/13/99
Runs	90	14	43	45
Hours	175	20	102	150
Fuels	NG, Gasoline	NG, Gasoline	NG, Gasoline Methanol	NG
	S/N 005	S/N 006	S/N 007	S/N 008
Customer	FC Devel	FC Devel	CeCert	SMUD
Fabrication	9/20/99	1/20/00	3/31/00	TBD
Delivered	10/19/99	TBD	4/10/00	TBD
Runs	40	25	11	N/A
Hours	250	58	33	N/A
Fuels	NG, Propane	NG, Diesel	NG, Diesel	Diesel

Table 2. Performance of F^3P subsystem for five fuels.

Item	Nat. Gas	LPG	Gasoline	Diesel	Methanol
Efficiency[1]	81%	75%	75-80%	73%	76%
Max H_2, % dry	49.5%	44.0%	41-42%	42-42%	40%
Min. CO LTS Out	0.8%	0.2%	0.5-0.6%	1%	0.1-0.3%
Capacity kW_e[2,3]	35	3.5	35	15	38

[1] Efficiency = (LHV H_2 out)/(LHV Fuel into Reformer)

[2] Estimated power based on fuel cell operational assumptions.

[3] These are maximum capacities tested thus far. Max. subsystem capacity is probably in the range of 40-50 kW_e.

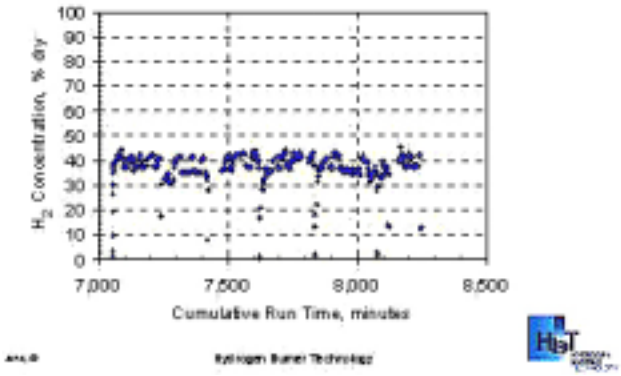

Figure 5. H_2 concentration on gasoline.

Conclusions

To date, the F^3P subsystem has successfully demonstrated operation and fuel flexibility, and it has approached its performance targets. These efforts have provided the technology foundation for advanced fuel processing subsystems being fabricated at HBT; testing is due to begin in June 2000. This hardware represents the next leap forward with respect to efficiency, size, and weight performance targets.

D. Integrated Fuel Processor Development

S. Ahmed, S.H.D. Lee, E. Doss, C. Pereira, D. Colombo, and M. Krumpelt
Argonne National Laboratory, 9700 S. Cass Ave., Argonne, IL 60439
(630) 252-4553; fax: (630) 972-4553, e-mail: ahmed@cmt.anl.gov

DOE Program Manager: JoAnn Milliken
(202) 586-2480, fax: (202) 586-9811, e-mail: joann.milliken@ee.doe.gov

---

Objectives

Determine the design and operating conditions for an integrated fuel processor that can meet the targets of the Partnership for a New Generation of Vehicles (PNGV):

- With a microreactor process train (100 W).
- With an engineering-scale integrated reactor (5-10 kW_e)

OAAT R&D Plan: Task 3; Barriers F and G

Approach

- Study fuel processing steps individually in microreactors to determine suitable catalysts, their kinetic parameters, and desirable operating conditions.
- Verify component performance in the integrated reactor, validate the reactor model, and identify concepts that could improve fuel processor performance.

Accomplishments

- Demonstrated fuel processor functions in the microreactor process train:
  - Demonstrated conversion of hydrocarbon fuel to produce reformate containing 1% (dry basis) carbon monoxide.
  - Evaluated preferential oxidation catalysts for use in the integrated reactor.
- Developed algorithm to determine the optimal temperature profile for the shift reactor.
- Demonstrated operation of an integrated reactor with methanol at the 7-kW_e level, with reformate containing 46% hydrogen.
- Demonstrated operation of an integrated reactor with hydrocarbon fuel at the 4-kW_e level, 75% efficiency, with reformate containing 40% hydrogen.

Future Directions

- Study fuel processing steps in the microreactor to evaluate catalysts and determine kinetics and favorable operating conditions.
- Integrate a preferential oxidation unit into the engineering scale reactor.
- Transfer technology to industrial partners.

Introduction

The objective of this work is to determine the fuel processor layout, design, and operating parameters needed to meet PNGV targets (efficiency, size, weight, cost, response, etc.) for the automotive fuel cell system.

Approach

To achieve this objective, the fuel processor is being studied at two levels. First, a microreactor process train has been established, with a series of reactors set up to represent the various unit processes. Each microreactor is enclosed in an electric furnace for accurate temperature control. The feed stream to each unit can be a simulated reformate gas metered in from a cylinder, or from the previous unit process in the fuel processing train. The feed and product streams can be sampled and analyzed by using an on-line gas chromatography/ mass spectrometry (GC/MS) system or with infrared analyzers.

Results

The effectiveness of two water-gas-shift (WGS) reaction catalysts was evaluated in the process train. The first microreactor was loaded with a commercial high-temperature-shift (HTS) catalyst (Fe/Cr oxide) and maintained at 300°C. This was followed by a second microreactor, which was loaded with Argonne National Laboratory's (ANL's) shift catalyst to represent the low-temperature-shift (LTS) reactor and was maintained at 215°C. A synthetic reformate gas, with the composition shown in Figure 1, was passed through the reactors.

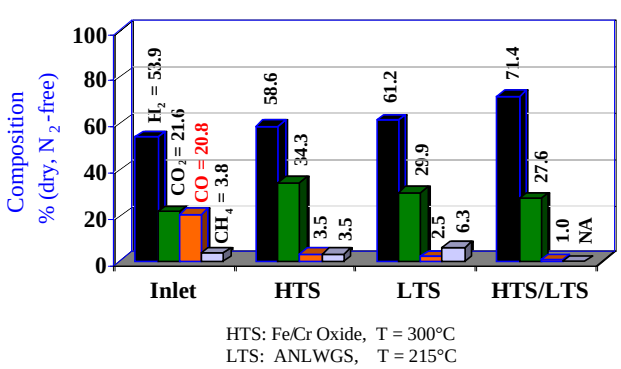

Figure 1. The combination of a commercial HTS catalyst and Argonne's shift catalyst lowered the CO level to 1%.

The product from the HTS unit reduced the CO level from 21.6% to 3.5%. With the inlet gas fed directly into the LTS, the CO level was reduced from 21.6% to 2.5%, and some methanation activity was also seen, as shown by the increase in the CH_4 levels. With the two reactors operating in series, the product gas emerging from the LTS unit contained 1% CO and undetected levels of CH_4.

The rate of reaction for the conversion of carbon monoxide in the shift reactor can be maximized by maintaining temperatures high enough to favor fast kinetics and yet cool enough that a large driving force toward equilibrium CO concentrations can be maintained. This is typically achieved by maintaining a progressively declining temperature profile within the shift reactor. An algorithm to calculate this optimal temperature profile has been developed; it calculates the smallest catalyst volume necessary for the conversion of a given inlet gas mixture to the desired outlet CO concentration, given the specifications for the H_2O/CO ratio and the rate expression for the catalyst. Figure 2 shows an optimal temperature profile and the resulting CO profile for conversion of 85% of the inlet CO, using Argonne's shift catalyst and a H_2O/CO ratio of 3. It is noteworthy that ~50% of the catalyst volume is needed to lower the CO level from 1.5% to the desired 1%, due to the lower temperatures (slower reaction rate) at the tail end of the reactor.

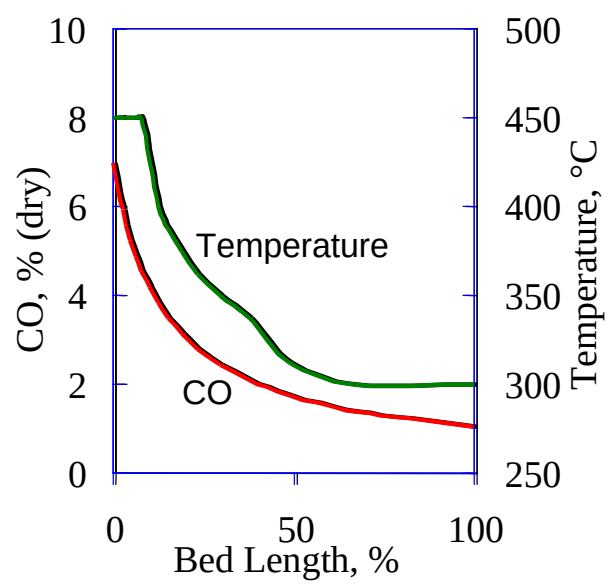

Figure 2. Calculated optimal temperature and CO concentration profile in a shift reactor using ANL's catalyst (CO_{in} = 7%, CO_{out} = 1%, H_2O/CO = 3).

Two preferential oxidation catalysts were evaluated in the microreactor. The commercial catalyst was able to reduce 1% CO (Figure 3) to under 500 parts per million (ppm) at a gas hourly space velocity (GHSV) of 5000/hr at 150°C, with O_2/CO = 2. At higher space velocities, methanation activity was observed. A Mn-based catalyst developed at ANL showed the ability to reduce the CO, but at a much lower GHSV of 500/hr (Figure 4). This type of material needs further development before it can be considered as a practical alternative.

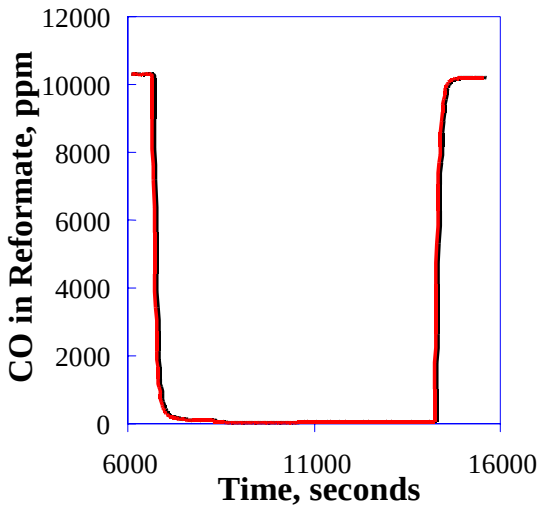

Figure 3. CO preferentially oxidized with a commercial catalyst (GHSV = 5000/hr, 150°C, O_2/CO = 2).

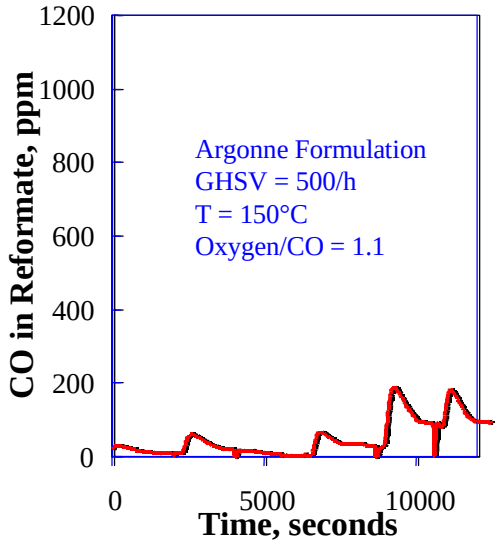

Figure 4. CO preferentially oxidized with a Mn-based catalyst (GHSV = 500/hr, 150°C, O_2/CO = 1.1).

Figure 5 shows a picture of the integrated engineering-scale reactor. With a volume of 7 L, the hardware includes the autothermal reformer, the sulfur trap, and the shift reactor, together with thermal integration.

The fuel processor was operated with methanol (7 kW_e) to yield a reformate that contained 46% (dry basis) hydrogen but also 5% carbon monoxide.

With a synthetic hydrocarbon blend resembling gasoline, the reactor was operated at 4 kW_e. The reformate contained 40% hydrogen and 2% CO, and it operated at an efficiency of 75%. Figure 6 shows the product gas compositions obtained during the experiment.

Figure 5. Picture of the engineering-scale integrated fuel processor.

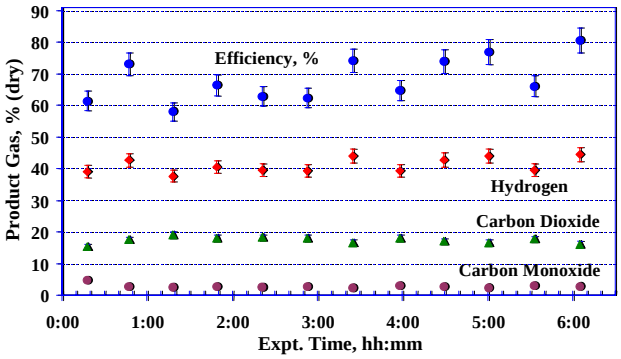

Figure 6. Product gas compositions obtained from the conversion of a synthetic gasoline blend.

Conclusions

Fuel processors are being studied with reactors at the 100-W and 10-kW levels. The microreactor has been used to study the kinetics and effectiveness of WGS catalysts. An algorithm has been developed for determining the optimal temperature profile in the shift reactor, and this has been approximated with two reactors in series. Commercial preferential oxidation catalysts have also been evaluated in the microreactor.

The engineering-scale integrated fuel processor has been tested with methanol, iso-octane, and a hydrocarbon blend resembling gasoline. The unit was operated with hydrocarbon fuels at over 75% efficiency, where the reformate contained >40% hydrogen and ~2% carbon monoxide. This engineering-scale integrated hardware currently lacks the preferential oxidation unit and the spent anode gas burner. A collaborative effort with Los Alamos National Laboratory is under way to incorporate the preferential oxidizer into the ANL fuel processor.

Publications

1. S. Ahmed, B. Bergin, T. Krause, J.D. Carter, J-M. Bae, L. Ruscic, D. Applegate, J. Kopasz, D. Myers, J. Krebs, C. Pereira, S.H.D. Lee, and M. Krumpelt, "Fuel Processor Development at Argonne National Laboratory," presented at the Army Research Office Workshop, Detroit, Mich., June 19-21, 2000.
2. S. Ahmed, J.P. Kopasz, B.J. Russell, and H.L. Tomlinson, "Gas-to-Liquids Synthetic Fuels for Use in Fuel Cells: Reformability, Energy Density, and Infrastructure Compatibility," to be published in the Proceedings of the 3rd International Fuel Cell Conference, Nagoya, Japan, held Nov. 30–Dec. 3, 1999.
3. M. Krumpelt, S. Ahmed, R. Kumar, S. Chalk, and J. Milliken, "Partial Oxidation Fuel Reforming for Automotive Power Systems," to be published in the Proceedings of the 3rd International Fuel Cell Conference, Nagoya, Japan, held Nov. 30–Dec. 3, 1999.
4. S. Ahmed, R. Kumar, and M. Krumpelt, "Fuel Processing for Fuel Cell Power Systems," Fuel Cells Bulletin, Elsevier Press, London, U.K., Sept. 1999.
5. S. Ahmed, J. Kopasz, B.J. Russell, and H.L. Tomlinson (Syntroleum Corp.), "Cobalt-Based Fischer-Tropsch Paraffin Fuels for Fuel Cell Power," poster paper presented at the Sixth Grove Fuel Cell Symposium, London, U.K., Sept. 13-16, 1999.
6. S. Ahmed, S.H.D. Lee, R. Kumar, J.D. Carter, R. Wilkenhoener, and M. Krumpelt, "The Argonne Catalytic Fuel Processor for Automotive and Small Fuel Cell Power Systems," poster paper presented at the Sixth Grove Fuel Cell Symposium, London, U.K., Sept. 13-16, 1999.
7. J. Kopasz, R. Wilkenhoener, S. Ahmed, J.D. Carter, and M. Krumpelt, "Fuel Flexible Partial Oxidation Reforming of Hydrocarbons for Automotive Applications," preprints of the Symposium on Hydrogen Production, Storage, and Utilization, 218th ACS National Meeting, Vol. 44, No. 4, pp. 899-904, New Orleans, La., Aug. 22-26, 1999.

Patents Issued

1. S. Ahmed, R. Kumar, and M. Krumpelt, "Methanol Partial Oxidation Reformer," Patent No. 5,942,346, issued on Aug. 24, 1999.
2. S. Ahmed, R. Kumar, and M. Krumpelt, "Methanol Partial Oxidation Reformer," Patent No. 5,939,025, issued on Aug. 17, 1999.
3. M. Krumpelt, S. Ahmed, R. Kumar, and R. Doshi, "Method for Making Hydrogen-Rich Gas from Hydrocarbon Fuel," Patent No. 5,929,286, issued on July 27, 1999.

Awards/Recognitions

1. Best Poster Award at the Grove Symposium, London, U.K., September 1999.
2. Annual National Laboratory R&D Award from DOE/OTT/OAAT, Richland, Wash., June 2000.

E. Microchannel Fuel Processor Components

Greg A. Whyatt, Ward E. TeGrotenhuis, Robert S. Wegeng, Victoria S. Stencamp, James M. Davis, John G.H. Geeting, and Larry R. Pederson (primary contact)
Pacific Northwest National Laboratory, P.O. Box 999, Richland, WA 99352
(509) 375-2731, fax: (509) 375-2167, e-mail: larry.pederson@pnl.gov

DOE Program Manager: JoAnn Milliken
(202) 586-2480, fax: (202) 586-9811, e-mail: joann.milliken@ee.doe.gov

---

Objectives

Develop compact reactors, separators, and heat exchangers for the onboard automotive production of hydrogen from liquid hydrocarbons.

OAAT R&D Plan: Task 3; Barriers F, G, and H

Approach

Utilize unique heat and mass transport advantages available in engineered microstructures to develop and demonstrate an integrated steam reforming subsystem. The integrated subsystem consists of multiple microchannel reactors, combustors, multistream recuperative heat exchangers, fuel and water vaporizers, and vapor/liquid separators.

Accomplishments

- High hydrogen selectivity and low methane slip were achieved for steam reforming of iso-octane in a microchannel reactor at a rate sufficient to support a 0.5- to 1.0-kW_e fuel cell.
- An integrated microchannel steam reformer subsystem consisting of a four-cell reactor, multistream recuperative heat exchangers, and water/fuel vaporizers was designed and fabricated. Conservatively designed to reform iso-octane to supply a 10-kW_e fuel cell, the steam reforming subsystem incorporates an innovative combustion gas reinjection approach that allows it to operate in an energy-efficient manner, a significant improvement over previous designs.
- Integrated, multistream recuperative heat exchangers were developed to support operation of an energy-efficient steam reformer. The exchangers recover heat from either the reformate or the combustion streams to preheat reactants and combustion air and to vaporize fuel and water. Except for a low-temperature air preheater, these heat exchangers provide all of the recuperator and vaporizer functions needed for the steam reforming subsystem.
- A microchannel vapor-liquid separation concept was demonstrated in a single-microchannel device. Capillary and surface forces were utilized to achieve qualitatively complete phase separation. Heat-exchange channels were also incorporated in the single-channel phase separator, resulting in technology capable of performing condensation and phase separation in a single compact device. The technology is projected to be substantially smaller, with a lower pressure drop, than competing technologies.

Future Directions

- Demonstrate highly efficient operation of the steam reforming subsystem at 10 kW_e and higher.
- Design and demonstrate steam generators and vapor/liquid separators to be incorporated into the integrated steam reforming subsystem, or other systems, with target pressure drops of <0.1 psi.
- Evaluate long-term reactor, heat exchanger, and catalyst performance.

- Continue industrial interactions to evaluate microchannel reactors, recuperative heat exchangers, and fuel and water vaporizers.
- Advance to the reforming of transportation fuels.
- Investigate means to lower manufacturing costs and improve manufacturability.

Heat Exchangers and Vaporizers

A recuperator demonstrated in late FY 1999 successfully confirmed the ability to accurately predict microchannel recuperator performance. The test unit, shown in Figure 1, had a volume of 37 cm^3. Performance results for this recuperator operated with balanced nitrogen flows are given in Figure 2. At the design conditions, the unit is expected to achieve 89% effectiveness, with a duty of 897 watts and a heat-transfer intensity in the core of 56 W/cm^3.

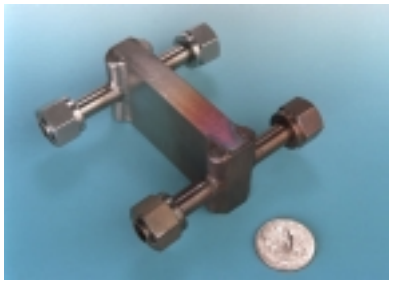

Figure 1. Microchannel reformate recuperator test unit.

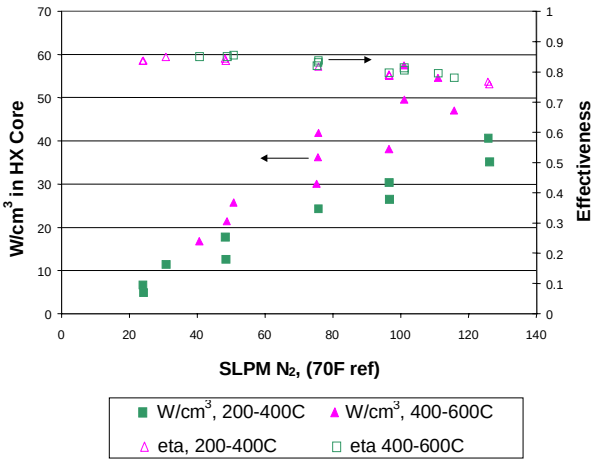

Figure 2. Microchannel recuperator test unit performance on balanced nitrogen flows.

On the basis of the successful demonstration of the recuperator test unit, the microchannel heat exchanger concept was extended to design and fabricate multistream heat exchangers to support the operation of an energy-efficient 10-kW_e steam reforming system. Two multistream exchangers (shown in Figure 3) were designed so that, following a successful demonstration, they can be integrated into a single compact, multistream microchannel heat exchanger that will, with the exception of a low-temperature air preheater, contain all the recuperators and vaporizers needed for the steam reforming subsystem.

The microchannel design enables the water vaporizer to efficiently extract heat from the combustion exhaust, cooling it to just above 100°C while still maintaining significant superheat in the generated steam (see Figure 4).

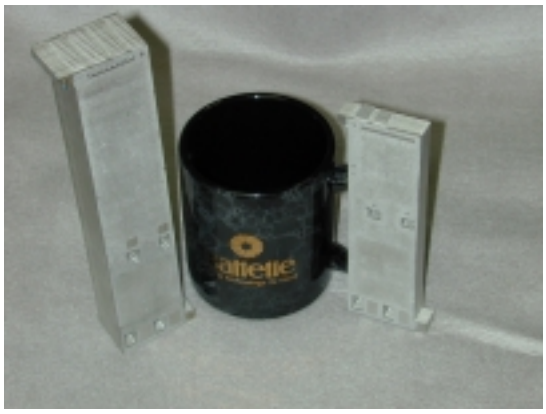

Figure 3. Integrated multistream microchannel heat exchangers prior to header attachment. Unit on left contains a combustion gas recuperator and water vaporizer. Unit on right contains a 90%-effective reformate recuperator, a fuel vaporizer, and a water preheater. These two units are designed to support up to a maximum of a 5-kW_e steam reformer operating a 3:1 steam-to-carbon ratio.

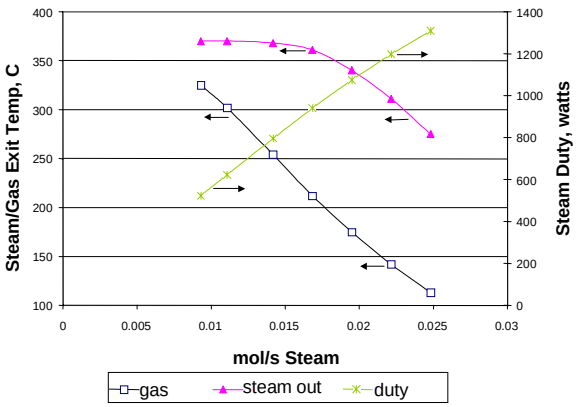

Figure 4. Performance data on water vaporizer section of integrated exchanger.

Steam Reformer Reactor Testing

The microchannel steam reforming reactor that was designed, fabricated, and operated in FY 1999 was tested over a range of operating conditions. The objective was to collect performance data for design of the next-generation steam reformer at the 10-kW_e scale. The data demonstrated the reforming capacity of the first-generation reactor design to validate projections for power density, and it was used to develop predictive models for microchannel reforming for incorporation into models of the steam reforming fuel processor.

The statistically designed experiment employed a four-factor, full-factorial design using iso-octane flow, water flow, combustor temperature, and combustion air flow as variables. These variables translate into the design parameters, reactant residence time, steam-to-carbon ratio, reactor operating temperature, and heat-transfer efficiency. The steam-to-carbon ratio was varied between 3:1 and 12:1. Figure 5 shows a summary of selectivity data over the range of conditions tested. Iso-octane conversion ranged from about 50% to slightly over 90%. The equivalent power output ranged from 500 to 975 We (assuming 90% conversion and 100% selectivity in the low-temperature-shift reactor, and 48% fuel cell stack efficiency), which translates to a productivity sufficient to supply 16 to 32 kW_e of fuel cell capacity per liter of reactor core. Statistical analysis of the data indicated that for iso-octane conversion, the order of importance of the variables is (1) fuel flow rate, (2) operating temperature, (3) water flow rate, and (4) combustion air flow rate.

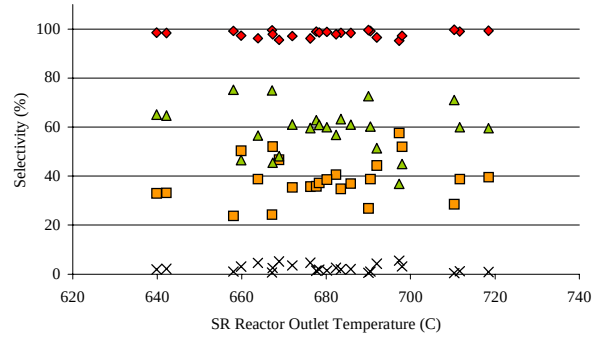

Figure 5. Summary of selectivity data for the statistically designed experiment operated using the first-generation microchannel steam reforming reactor. Data reflect a range of operating conditions for reactant flows and temperatures.

10-kW_e Steam Reforming Subsystem

The 10-kW_e steam reforming subsystem was designed on the basis of data discussed in the previous sections. The objectives of the 10-kW_e steam reforming system are to substantially scale up the earlier steam reformer and, through an integrated heat exchanger network and a redesign of the reactor, produce a system that is energy-efficient. This system has been designed and fabricated, and will be tested in late FY 2000. It is designed to operate at pressures up to 5 bar on the reaction side. The 10-kW_e system hardware is shown in Figure 6.

The 10-kW_e reactor contains four independent cells, each with 2.5-kW_e capacity. The reactants and products are processed through these four cells in parallel, while the combustion gases providing the heat to drive the reaction pass through the cells in series. As the combustion gases pass from one cell to the next, a small amount of additional fuel is injected and burned to restore the temperature to the desired level prior to entering the next cell. This approach increases the product of (mass flow) × (heat capacity) of the combustion gases passing through a single cell, which reduces the temperature drop across the reactor and dramatically reduces the incoming temperature required to sustain a given reaction rate. It also reduces the overall amount of combustion air used, thereby reducing the amount of heat lost to the combustion exhaust. This approach also allows test units to be manufactured and

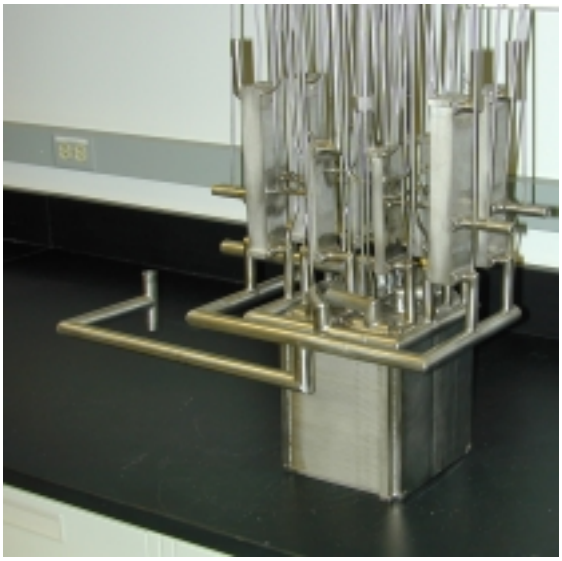

Figure 6. Integrated 10-kW_e steam reforming subsystem. Reactor containing four cells is located on the bottom, with one pair of integrated exchangers provided for each cell of the reactor. All reactor connections are made on one face of the reactor for ease of insulation and to reduce overall heat loss. The many vertical tubes are for thermocouples and pressure sensors for the experimental system, and would not be part of a final commercial system.

operated using 316L stainless steel. The optimal operating temperature involves a trade-off between reactor cost, productivity, efficiency, and operating lifetime; this trade-off has not yet been resolved. However, it is expected that the series use of combustion gases will allow lower-cost alloys to be used, compared to those required if 1,000°C combustion temperatures were utilized.

Microchannel Condenser with Vapor/Liquid Separation

Pacific Northwest National Laboratory (PNNL) expanded efforts toward size and weight reduction of balance-of-plant items by developing and demonstrating a concept for combining partial condensation with vapor/liquid phase separation within a single compact microchannel device. This approach would surpass conventional phase separation technologies, such as centrifugal separators, in capacity per unit hardware mass and volume. The result is increased power density and specific power for the overall fuel processor/fuel cell system, regardless of the choice of reforming technology.

This PNNL study demonstrated the concept of, and collected performance data for, vapor/liquid separation in a *single*-channel microchannel device. Subsequently, heat-exchange channels were incorporated to accomplish the combined functions of partial condensation and phase separation. Future work will include scale-up to multichannel devices.

Figure 7 shows flow capacity curves for two configurations of the single-channel phase separation device, indicating the maximum gas and liquid flow rates that can be processed within the device while achieving qualitatively complete phase separation. Performance was compared to that of a conventional centrifugal separator. A separation achieved in 0.08 s residence time in the microchannel device is projected to require 0.4 s in the centrifugal separator. This corresponds to a volume of 0.5 L for a full-scale device capable of treating reformate stream from a steam reformer, compared to a volume of > 2 L for a centrifugal separator. Channel pressure drop was calculated to be 0.08 in. of water, based on slit flow, while the centrifugal separator is rated at 1.4 in. of water.

Microchannel Fuel Processing System Implications

The current steam reforming subsystem is projected to meet the Department of Energy's (DOE's) targets for power density and fuel processor efficiency, but improvements are needed to meet specific power and cost targets.

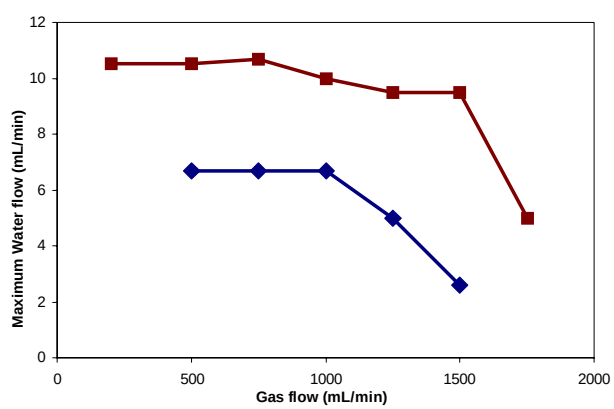

Figure 7. Flow capacities for 100%-efficient phase separation of a dispersed gas and liquid feed stream for two configurations of the single-channel microchannel phase separator.

Performance targets, current status, and short- and long-term project goals are summarized in Table 1.

The overall system efficiency, including the current fuel processor and PEM fuel cell, is projected to be 39-41%. High system efficiency is usually equated with high hydrogen utilization but with relatively low stack current density. However, because unused hydrogen from the fuel cell is recycled to the fuel processor to provide heat for reforming, system studies have shown the overall efficiency to be relatively insensitive to hydrogen utilization in the stack. Thus, it is expected that a compact, microchannel steam reforming system coupled with a fuel cell can ultimately provide both high efficiency and high power density.

Table 1. Comparison of DOE-OAAT targets for an automotive fuel processor.

Technical Target	DOE 2004 Target	PNNL Status	PNNL FY 2001 Goals	PNNL Long-Term Goals
Power Density (We/L)	750	1500	3000	>6000[a]
Specific Power (We/kg)	750	280	600	>1500[a]
Cost ($/kW)	10	60[b]	30[b]	<4[a,b]
Fuel Processor Efficiency	80%	83-85%	83-85%	83-85%

[a] Requires improvements to catalyst performance and/or manufacturing costs.
[b] Based on cost of bonded unit only (no catalyst costs).

Publications and Presentations

- R.S. Wegeng, "Microchannel Fuel Processor Hardware Development Status," F-CELLS 2000, Palm Springs, Calif., May 22-26, 2000.
- R.S. Wegeng, "Reducing the Size of Automotive Fuel Reformers," Fuel Cells Infrastructure Workshop, Chicago, Ill., Dec. 6-7, 1999.
- J.L. Zilka-Marco, A.Y. Tonkovich, M.J. Lamont, S.P. Fitzgerald, D.P. VanderWiel, Y. Wang, and R.S. Wegeng, "Compact Microchannel Fuel Vaporizer for Automotive Applications," 4th International Conference on Microreaction Technology, AICHE/DECHEMA, Atlanta, Ga., March 2000.
- M.K. Drost, R.S. Wegeng, P.M. Martin, K.P. Brooks, J.L. Martin, and C. Call, "MicroHeater," 4th International Conference on Microreaction Technology, AICHE/DECHEMA, Atlanta, Ga., March 2000.
- D.L. Brenchley, R.S. Wegeng, and M.K. Drost, "Development of Micro-Chemical and Thermal Systems," 4th International Conference on Microreaction Technology, AICHE/DECHEMA, Atlanta, Ga., March 2000.
- S.P. Fitzgerald, R.S. Wegeng, A.Y. Tonkovich, Y. Wang, H.D. Freeman, J.L. Marco, G.L. Roberts, and D.P. VanderWeil, "A Compact Steam Reforming Reactor for Use in an Automotive Fuel Processor," 4th International Conference on Microreaction Technology, AICHE/DECHEMA, Atlanta, Ga., March 2000.
- E.A. Daymo, D.P. VanderWiel, S.P. Fitzgerald, Y. Wang, R.T. Rozmiarek, M.J. Lamont, and A.Y. Tonkovich, "Microchannel Fuel Processing for Man Portable Power," 4th International Conference on Microreaction Technology, AICHE/DECHEMA, Atlanta, Ga., March 2000.
- T.M. Werner, S.C. Schmitt, E.A. Daymo, and R.S. Wegeng, "Microchannel Gasoline Vaporizer Unit Manufacturing Cost Study," PNNL-12226, June 1999.

F. Catalysts for Improved Fuel Processing

Rod Borup (primary contact), Michael Inbody, Byron Morton, JinKi Hong, and José Tafoya
ESA-EPE, MS J580
P.O. Box 1663
Los Alamos National Laboratory, Los Alamos, NM 87545
(505) 667-2823, fax: (505) 665-6173; e-mail: Borup@lanl.gov

DOE Program Manager: JoAnn Milliken
(202) 586-2480, e-mail: joann.milliken@ee.doe.gov

Objectives

- Understand fuel processor catalyst durability and causes for catalyst degradation.
  - Examine fuel effects on fuel processor catalyst performance and durability. Of interest are effects on catalyst activity associated with fuel composition, component, and impurities.
  - Evaluate short-residence-time reaction events, leading to unique fuel processor designs and concepts.
  - Evaluate catalysts to determine variation in rates and reaction mechanisms during use.
  - Delineate catalyst degradation mechanisms.

OAAT R&D Plan: Task 3; Barrier E

Approach

- Understand and document catalyst performance over a range of relevant conditions.
  - Measure adiabatic reforming performance under real operating conditions.
  - Determine activity, kinetic rates, durability, and performance under isothermal conditions.
  - Study the effects of varying fuel constituents and contaminants within candidate fuels.
  - Examine combinations of catalyst and catalyst supports to understand catalyst component degradation.
- Utilize catalyst characterization and surface analytical techniques to help delineate catalyst degradation mechanisms.
  - Characterize catalyst's elemental composition, particle size, and surface area before and after testing.
  - Evaluate catalyst structural changes.

Accomplishments

- Tested and characterized catalysts with various fuel components.
  - Nickel and rhodium catalysts (commercial and in-house).
  - With individual fuel components.
  - With fuel impurity (sulfur).
- Utilized catalyst characterization and surface analytical techniques to delineate catalyst degradation mechanisms.
  - Characterized catalysts and quantified surface area.
  - Evaluated kinetic vs. equilibrium data for candidate catalysts for partial oxidation.

Future Directions

- Study fuel processor catalyst operation with petroleum-based fuels to evaluate effects of fuel constituents.
  - Measure fuel processor catalyst activity and durability with individual fuel constituents and fuel blends, as well as with fuel impurities.

- Monitor carbon formation *in situ* in adiabatic reactor with laser-scattering extinction apparatus. Map carbon tendencies of individual catalysts, catalyst supports, and fuels constituents, and examine commercial catalysts to observe carbon formation tendencies.

- Automate microscale test equipment, reactant mixtures, and sample injection system.
  - Initiate long-term, unattended and automated catalyst testing for durability measurements.
  - Evaluate fuel processing catalysts in both microscale and macroscale reactors to compare molecular-level degradation mechanisms.

Introduction

This report covers technical progress during fiscal year (FY) 2000 on fuel processing catalyst characterization. These development efforts support U.S. Department of Energy (DOE) activities in the development of compact, transient-capable reformers for on-board hydrogen generation starting from candidate fuels. The long-term objectives include increased durability and lifetime, in addition to smaller volume, improved performance, and other specifications required for meeting fuel processor goals.

The technical barriers to compact fuel processor size, transient capability, and compact, efficient thermal management are all functions of catalyst performance. Significantly, work at Los Alamos National Laboratory (LANL) now involves testing large-scale fuel processors for performance and durability, as influenced by fuels and fuel constituents, and complements that testing with microscale catalyst evaluation, accomplished under well-controlled conditions.

Approach

The fundamental tools for our research on fuel processing catalysts are reactor test beds and catalyst characterization techniques. Catalyst activity and performance are measured in two different types of reactor test beds, which serve complementary roles in our laboratory. An adiabatic reactor exposes catalysts to fuel processing conditions under actual system conditions and relatively high power levels, while an isothermal microscale reactor, in which catalysts are used under extremely well defined and controlled conditions, exposes the catalyst to individual operating conditions. In addition, catalyst characterization techniques are used to define the catalyst structure and structural changes upon exposure to fuel processor conditions in the reactor test beds. These techniques, all available at LANL, include elemental analysis techniques and techniques to quantify surface area and particle size changes, such as X-ray Photoelectron Spectroscopy (XPS), BET/H_2 or CO chemisorption, X-ray Diffraction (XRD), and Scanning Electron Microscopy and Energy Dispersive Spectroscopy (SEM/EDS). Other techniques available at LANL include Transmission Electron Microscopy (TEM), X-ray Fluorescence Spectroscopy (XRF), and temperature-programmed desorption (TPD), which will be used as required to further delineate catalyst degradation mechanisms.

The adiabatic reactor used to evaluate catalysts and fuel components, including the tendency for carbon formation, is shown in Figure 1. This reactor features ease of catalyst replacement, the ability to incorporate catalysts supported on commercially used substrates (such as corderite monoliths or pellet

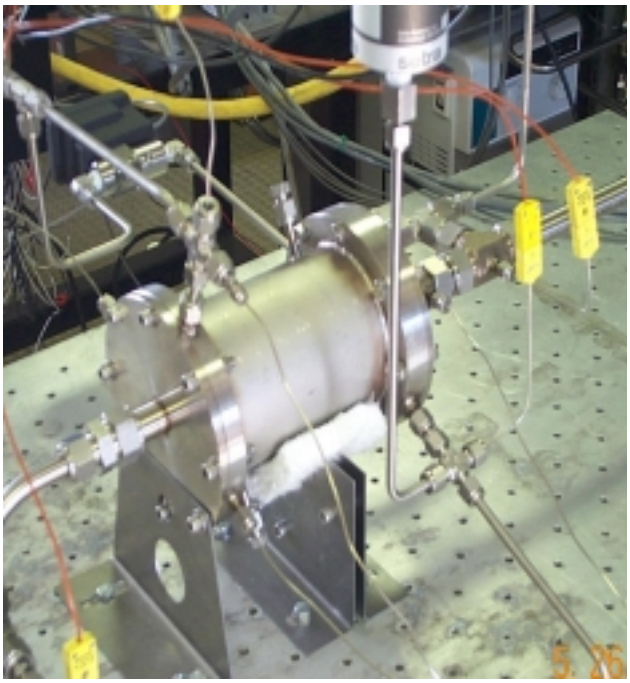

Figure 1. Adiabatic partial oxidation reactor.

and powder catalysts), *in situ* carbon formation monitoring, and gas and temperature measurements with radial and axial profiles. The reactor first became operational in May 2000; the *in situ* carbon formation monitoring will be added in the fourth quarter of FY 2000. For *in situ* carbon formation monitoring, an argon ion laser will be used with extinction monitoring to observe the onset of carbon formation. Scattering will also be utilized to observe relative carbon particle-size distributions and the initial onset of carbon formation, and spectral detection will allow for fluorescence detection of polycyclic aromatic hydrocarbons (PAHs).

The isothermal microscale catalyst reactor for use in fuel and catalyst measurements under well-defined, controlled conditions is shown in Figure 2. This reactor is constructed of a quartz tube and an isothermal oven. Typical catalyst samples are 300–500 milligrams. Vapor or liquid fuels combined with oxidant (air) are mixed and preheated prior to introduction into the catalyst, while the temperature of the catalyst remains essentially constant because of the isothermal furnace, small catalyst quantities, and small reactant volumes.

Results

Results using two different metal catalyst samples, rhodium and nickel, are described in this report. The rhodium catalyst was a commercial 0.5-wt% catalyst supported on alumina; nickel catalysts were prepared at Los Alamos with variable nickel loadings from 0.5 wt% to 5 wt%. Initial tests were conducted to measure catalyst performance with partial oxidation and steam reforming reactions. An example of these measurements is shown in Figure 3 for the isothermal partial oxidation of methane on a nickel catalyst. Methane conversion reached nearly 100 % at 700°C, while the selectivity for hydrogen production was highest at 600°C. The isothermal partial oxidation of methane on a rhodium catalyst is shown in Figure 4. The rhodium catalyst shows slower oxidation kinetics, and therefore less methane conversion, than the nickel catalyst at similar temperatures, and it does not reach 100% methane conversion, even at 750°C. However, the rhodium loading was an order of magnitude less than the nickel, so the TON (turn-over number) for each catalyst site was much higher for the rhodium catalyst than the nickel catalyst; thus, the rhodium has higher intrinsic activity than the nickel. In Figures 3 and 4, X_{CH4} is the fraction of methane converted, S_{H2} is the selectivity for hydrogen production, and S_{CO} is the selectivity for CO production, as defined below.

$$S_{H2} = 0.5\ H_{2,\ out} / (CH_{4,\ in} - CH_{4,out}) \qquad (1)$$

$$S_{CO} = CO,_{\ out} / (CH_{4,in} - CH_{4,\ out}) \qquad (2)$$

Figure 5 shows XRD of nickel catalysts before and after testing with iso-octane and methane. The main nickel diffraction peak occurs at a 2 Theta of 44 degrees. The diffraction of the new nickel catalyst is broad, indicating small dispersed nickel particles, while after testing with methane, the peak has grown sharper, and after testing with iso-octane,

Figure 2. Microscale catalyst test station.

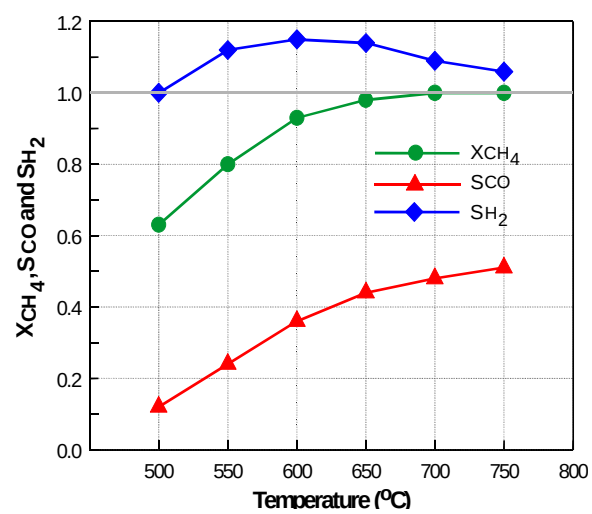

Figure 3. Isothermal POX of CH_4 with temperature on Ni/Al_2O_3 catalyst.

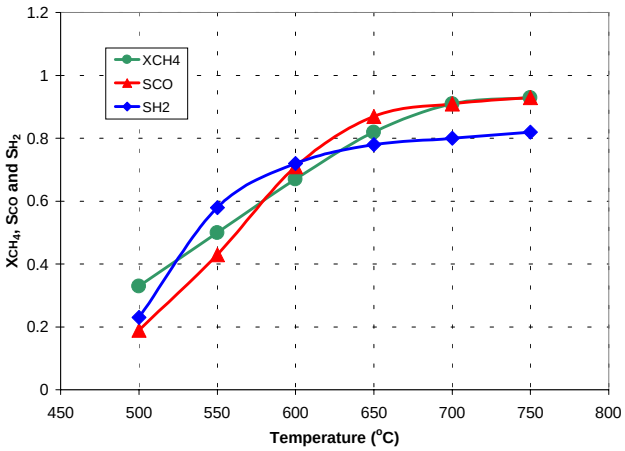

Figure 4. Isothermal POX of CH_4 with Temperature on Rh/Al_2O_3 catalyst.

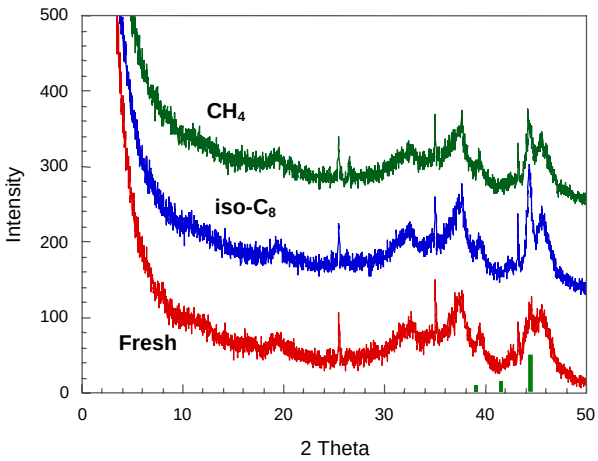

Figure 5. XRD of nickel catalyst after testing.

the peak is still sharper. The sharpening peak indicates nickel catalyst particle growth, either by particle sintering or agglomeration, during the testing with the hydrocarbons. BET surface area analysis by CO chemisorption leads to similar conclusions, and is summarized in Table 1 for various rhodium and nickel catalyst samples. Sample 1, the rhodium catalyst before testing, had arhodium surface area of 0.718 m^2/g catalyst or 143.8 m^2/g rhodium. After testing with methane, the rhodium surface area decreased to 50.8 m^2/g rhodium (sample 2), while after testing with iso-octane, the surface area was negligible (sample 3). The negligible surface area of sample 3 probably indicates a rhodium/alumina formation of a spinel, and thus complete loss of pure rhodium particles – but not loss of the rhodium itself. Nickel catalyst samples show a similar trend toward decreasing surface area. The initial surface area of the nickel is much lower at 28 m^2/g nickel (sample 4); however, this is typical for a catalyst with a much higher metal loading. After testing, a decrease in nickel surface area is observed – 23.6 m^2/g nickel (sample 5) after testing with iso-octane and 4.7 m^2/g nickel after testing with methane (sample 6).

A different fuel processor degradation mechanism is carbon formation during the oxidation and steam reforming of hydrocarbon fuels. Carbon formation has been monitored by the carbon buildup on the catalyst surface over time as a function of different fuel components. Figure 6 shows the XPS

Table 1. Catalyst surface areas by CO chemisorption of rhodium and nickel catalysts.

Sample # (Description)	**CO Chemisorption** (cc_{STP}/g at 55 Torr)	**Dispersion** (%)	**Crystallite Diameter** (nm)	**Metal Surface Area** (m^2/g catalyst)	**Metal Surface Area** (m^2/g metal)
1. (fresh 0.5% Rh/Al_2O_3)	0.4278	39.31	3.4	0.718	143.6
2. (fresh 0.5% Rh/Al_2O_3 with CH_4)	0.1502	13.8	9.6	0.254	50.8
3. (fresh 0.5% Rh/Al_2O_3 with iso-octane)	Negligible	Very Low	Very Large	Negligible	Negligible
4. (fresh 5% Ni/Al_2O_3)	0.97	5.08	24.1	1.4	28
5. (5% Ni/Al_2O_3 with iso-octane)	0.819	4.29	28.5	1.18	23.6
6. (5% Ni/Al_2O_3 with CH_4)	0.164	0.86	143	0.235	4.7

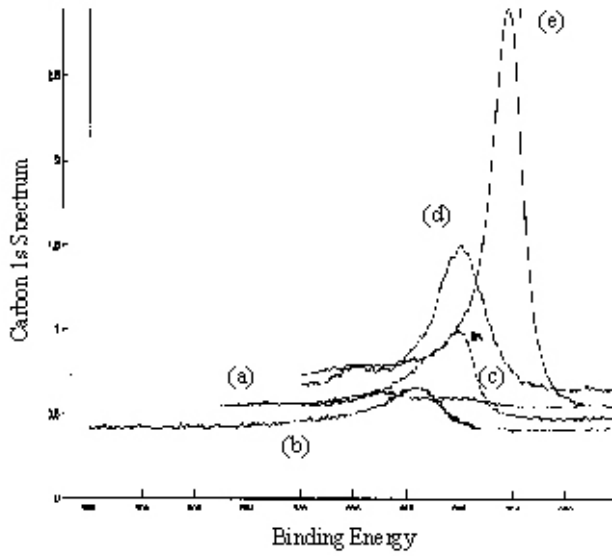

Figure 6. XPS of catalysts, (a) initial carbon signal and after partial oxidation with (b) iso-octane, (c) 1-pentene, (d) methylcyclohexane, and (e) p-xylene.

C1s signal for nickel catalyst samples tested with iso-octane, pentene, methylcyclohexane, and xylene. This shows relative carbon formation to be much higher with the aromatic and unsaturated compounds than with the aliphatic hydrocarbons. All nickel samples after testing showed at least a small amount of carbon present.

Conclusions

Catalyst characterization techniques and different catalyst test beds are employed to understand catalyst durability and degradation mechanisms, leading to the development of fuel processing catalysts with longer durability. Testing of catalysts to observe their degradation under well-defined conditions and actual fuel processing conditions leads to a better understanding of such degradation. The catalysts are examined to determine their relative activity and degradation during fuel processing reactions under different conditions, including different fuel components and fuel impurities.

Both noble metal (rhodium) and base metal (nickel) catalysts have been shown to decrease in surface area during fuel processing reactions. The decrease in surface area is catalyst- and fuel-dependent. The rhodium catalyst, after testing with iso-octane, showed a complete loss of pure rhodium particles.

Carbon formation has also been observed to be a degradation mechanism. The tendency toward carbon formation has been observed to be a function of the fuel component; the general trend is as follows: xylene > methylcyclohexane > pentene > iso-octane.

G. R&D on a Novel Breadboard Device Suitable for Carbon Monoxide Remediation in an Automotive PEM Fuel Cell Power Plant

Nguyen Minh (primary contact) and Stan Simpson (co-principal investigator)
Honeywell Engines and Systems
2525 W. 190th Street, MS-36-1-93140
Torrance, CA 90504-6099
Nguyen Minh: (310) 512-3515, fax: (310) 512-3432, e-mail: nguyen.minh@honeywell.com
Stan Simpson: (310) 512-4604, fax: (310) 512-4128, e-mail: Stan.Simpson@ honeywell.com

Di-Jia Liu (co-principal investigator)
Honeywell Des Plaines Technology Center
50 E. Algonquin Road
Des Plaines, IL 60017-5016

DOE Program Manager: Patrick Davis
(202) 586-8061, fax: (202) 586-9811, e-mail: patrick.davis@ee.doe.gov

ANL Technical Advisor: William Swift
(630) 252-5964, fax: (630) 252-4473, e-mail: swift@cmt.anl.gov

Contractor: Honeywell Engines and Systems, Torrance, California
Prime Contract No. DE-FC02-99EE50578, October 1999-December 2001

Objectives

Develop, implement, and demonstrate a new carbon monoxide removal system for use in polymer electrolyte membrane fuel cell (PEMFC) systems that provides high carbon monoxide (CO) removal efficiency, low parasitic hydrogen consumption, and tolerance to CO input variation in an easily controlled manner. The system will be designed for removal of CO from a continuous reformate flow sized for a 10-kW PEMFC stack with a CO input level of 5000 to 8000 parts per million (ppm).

OAAT R&D Plan: Task 7; Barrier E

Approach

- In a 27-month program, Honeywell will research and develop a novel technology to selectively remove CO from reformate fuel for use in PEMFCs. Two approaches to CO removal will be explored and developed: the adsorption/catalytic oxidation of CO (ACO) and the adsorption/electrocatalytic oxidation of CO (ECO). Following an initial 12-month R&D phase, the two approaches will be evaluated critically for downselection on the basis of efficiency, system compatibility, and cost criteria. A breadboard CO-remediation system sized for a 10-kW PEMFC stack will then be constructed and tested on both synthetic reformate and reformate obtained from an operating fuel processor.
- The program consists of four major tasks:
  - Research and development on two potentially viable approaches to remove CO from reformate.
  - Downselection of the most promising technique, on the basis of performance and cost.
  - Design and fabrication of a brassboard CO-removal device based upon the selected technology of choice.
  - Testing of the CO-removal system.

Accomplishments

- Proof-of-principle experiments for both technologies have been demonstrated.
- CO-removal efficiency for both ACO and ECO has been increased significantly through optimization of catalyst, support, and active adsorption surface.
- Significant progress has been made in preliminary ACO/ECO engineering design.

Future Directions

- Catalyst aging studies (currently in progress).
- Evaluation of parasitic hydrogen consumption and tolerance to CO transients.
- System engineering to reduce pressure drop and volume.

Introduction

The PEMFC continues to benefit from intense development efforts for its potential application in automobiles. PEMFCs offer a number of inherent advantages, including high efficiency, low noise, low chemical emissions, and low operating temperature. Hydrogen is the most energetic fuel for the PEMFC, but the lack of an existing infrastructure for the routine handling and distribution of hydrogen severely limits its utility. Alternatively, such hydrocarbon fuels as gasoline or

methanol can be reformed to a hydrogen-containing fuel mixture, known as reformate, via a fuel processor. Unfortunately, a typical reformate consists of a mixture of gaseous products that includes CO at concentration levels near 1%; the detrimental effect of CO at even the ppm concentration levels on the performance of a PEMFC operating with platinum catalysts is well documented. One approach to the CO problem is to incorporate a pretreatment device or process in the fuel line (between the fuel processor and the fuel cell) to significantly decrease the CO concentration in the reformate. This process can be either by physical removal (as in the case of membrane separation) or by chemical reaction (as in the case of methanation or the use of preferential oxidation, PROX). These techniques suffer from various disadvantages, including high cost and complexity, high parasitic hydrogen consumption, and a lack of tolerance for large CO transients (without complicated and expensive control processes).

Approach

The goal of this program is to develop and demonstrate a novel, easily controlled CO-removal system that provides high CO removal efficiency plus an increased tolerance for CO input variation. This system will be incorporated in a working PEMFC system, between the fuel processor and the PEMFC stack, as shown in Figure 1. The system will be based upon the use of a selective CO removal device that can be regenerated periodically when saturated with CO. Potential advantages of this approach include a high tolerance toward variations in CO input during the change of load dynamics, low parasitic hydrogen consumption, relative simplicity of operation, and an ability to control and operate during the "cold-start" condition.

Two innovative approaches to selective CO removal and regeneration are being investigated in this project. Both approaches make use of multiple, CO-selective adsorption surfaces that can be regenerated quickly, simply, and efficiently with minimal consumption of hydrogen fuel in the reformate stream. The methods, referred to as the adsorption/catalytic oxidation (ACO) technique and the electrocatalytic oxidation (ECO) technique, differ in the manner by which the active adsorption surfaces are regenerated. In ACO, CO is adsorbed over a bifunctional material bed and subsequently oxidized chemically to CO_2. In ECO, the adsorbed CO is removed through electrocatalytic oxidation.

Results

Proof-of-Principle Experiments

Initial proof-of-principle experiments for both ACO and ECO have been successfully demonstrated in laboratory-scale testing. These experiments clearly indicated the potential of both techniques for continuous, efficient removal and treatment of CO in fuel reformate streams. In the case of ACO, continuous CO removal can be achieved through the use of multiple adsorption beds that are alternately cycled between adsorption and regeneration modes. In ECO, the adsorption/regeneration cycle is generated electrically, and continuous CO removal is achieved by changing the frequency of cell operation. Importantly, this approach can be controlled electronically without the need for moving parts.

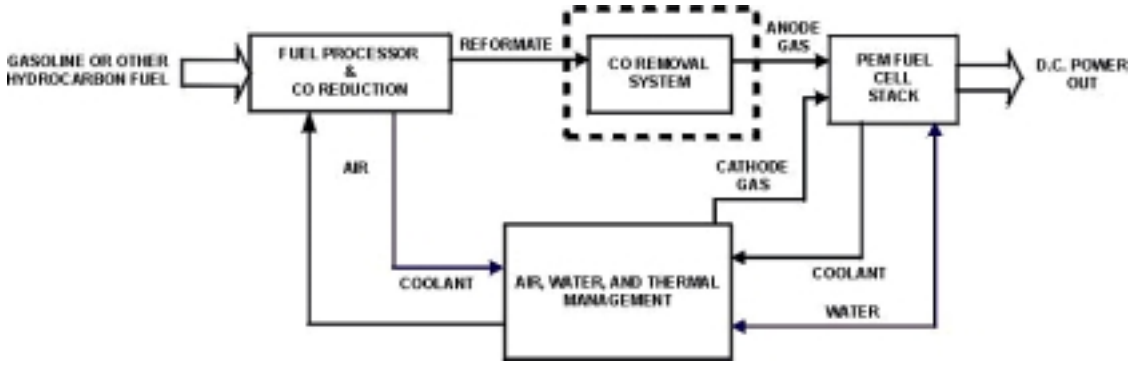

Figure 1. The CO removal system in a reformer-fueled PEMFC power system.

ACO/ECO Material Development

A sorption bed material suitable for ACO application must meet the following basic criteria: it must be capable of selectively adsorbing CO in the presence of high levels of hydrogen, steam, carbon dioxide, etc.; it must be capable of oxidizing the adsorbed CO to CO_2 to regenerate the capacity in a rapid and repeatable manner; and it should possess an extended lifetime for long-term use in the PEMFC application. One of the primary objectives in the initial phase of this R&D effort is to identify low-cost ACO materials that possess these attributes.

Two parallel routes to the development of a robust ACO sorption material that meets the previously described criteria have been explored. The first route focuses on the active component used in ACO. Thus far, a wide range of metals and preparation methods have been evaluated at the laboratory scale. Specific chemical precursors and preparation methods have been selected to emphasize the effective metal utilization and to minimize cost.

The second route focuses on the support material upon which the active adsorption medium is dispersed. Criteria used for support material selection include high surface area, good pore size distribution to ensure effective mass transfer, and stability during the repeated swings in temperature and humidity that accompany the alternate adsorption and catalytic oxidation steps. A variety of support materials and geometries have been evaluated. The catalyst and support development activities are ongoing.

Figure 2 illustrates an experimental demonstration of the tolerance of a developmental ACO metal-substrate combination to a rapid change in reformate CO concentration. In the initial portion of the experiment, a synthetic reformate mixture bypasses the ACO device. A 30-second injection of CO (representing a CO transient) is introduced into the reformate stream, resulting in a 40% increase in the CO concentration in the gas mixture, as shown by the detector trace. To demonstrate the tolerance of the ACO material to CO transients, the gas mixture is directed into the ACO unit prior to a second equivalent injection of CO. An immediate depletion of CO to a near-zero level is observed initially. During the second, identical 30-second injection of CO, virtually no CO leakage is

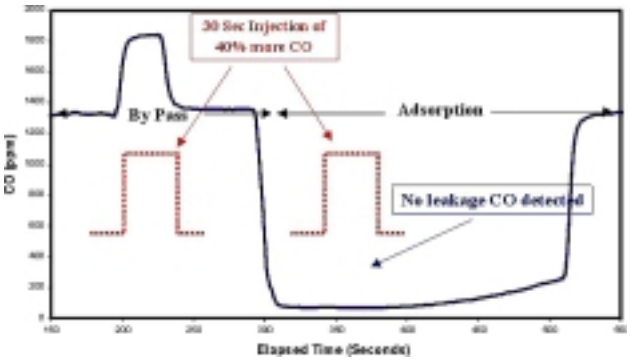

Figure 2. Demonstration of tolerance to CO transient variation in an ACO reactor.

observed. This experiment illustrates clearly the ability of the ACO technique to tolerate CO spikes.

A similar material development effort was performed for the ECO approach, with slightly different development criteria. While the need for high CO adsorption capability and selectivity remains, the ECO material must also demonstrate high catalytic activity toward CO electro-oxidation during the regeneration phase. A wide range of ECO materials have been evaluated on the basis of these criteria. Several have demonstrated the necessary selectivity and regenerability; optimization studies of these materials are under way.

Preliminary Engineering Design and Improvement

Several engineering design studies are under way for both ACO and ECO. As an example, ACO design activities are in progress to optimize CO removal efficiency and minimize the system pressure drop. Additional studies on alternative operating modes will begin soon to further improve efficiency and reduce system volume and cost. For ECO, efforts are under way to optimize both electrode and system performance. As a result of these efforts, CO removal capacity has been improved by a factor of four over that observed at the beginning of the program.

Figure 3 offers an example of CO removal by using a periodically regenerated ECO unit. During the experiment, the CO concentration in a synthetic reformate formulation was monitored by a broad-band infrared spectrometer located at the exit of the ECO device. As shown in Figure 3, over 90% of the

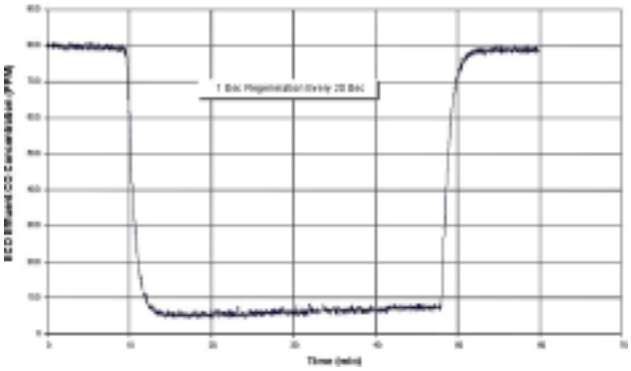

Figure 3. Demonstration of removal of CO by a regenerated ECO unit.

CO in the reformate stream was removed during the continuous period of ECO operation.

Conclusions

Two new technologies for the removal of CO from processed hydrocarbon reformate for the PEMFC application have been introduced. The feasibility of both approaches, adsorption/catalytic oxidation and adsorption/electrocatalytic oxidation, was demonstrated through proof-of-concept experiments. Significant progress has been made in improving CO removal efficiency, capacity, and selectivity for both technologies. Preliminary engineering studies have demonstrated the benefit of both approaches and have identified directions for further improvement.

Publications/Presentations/Patents

- D-J Liu, J. Williams, M. Kaiser, D. Winstead, J. Kudart, S.F. Simpson, and T.J. Rehg, "Two New Approaches for CO Removal from Reformate Fuel for the PEM Fuel Cell Application," Society of Automotive Engineers, Paper No. 2000-01-0379, Detroit, Mich., 2000.
- D-J Liu, D. Winstead, M. Kaiser, and T.J. Rehg, "Removing CO from Reformate for Fuel Cell Application using a Regenerable CO Adsorption/Catalytic Oxidation Bed Device," U.S. Patent Pending.
- T.J. Rehg, D-J Liu, M. Kaiser, and J. Williams, "An Electro-Catalytic Oxidation (ECO) Device to Remove CO from Reformate for Fuel Cell Application," U.S. Patent Pending.

H. CO Clean-Up Development

Michael Inbody (primary contact), Rod Borup, James Hedstrom, Byron Morton, JinKi Hong, and José Tafoya
ESA-EPE, MS J576
Los Alamos National Laboratory, Los Alamos, NM 87545
(505) 665-7853, fax: (505) 665-9507, e-mail: inbody@lanl.gov

DOE Program Manager: JoAnn Milliken
(202) 586-2480, fax: (202) 586-9811, e-mail: joann.milliken@ee.doe.gov

Objectives

Research and develop carbon monoxide clean-up technology for integration into fuel processor systems to enable them to meet the fuel purity requirements for a fuel cell stack by:

- Removing trace contaminants to purity levels required by the fuel cell stack.
- Maintaining system efficiency by minimizing hydrogen consumption.
- Operating effectively through automotive transients – changes in power level, start-up, and shutdown.
- Meeting overall fuel processor targets for energy efficiency, power density, specific power, and cost.

OAAT R&D Plan: Task 3; Barrier E

Approach

- Combine laboratory investigation with industrial collaboration to develop working processes and hardware for fuel processor systems.
- Investigate and develop CO clean-up technology.
  - Investigate catalysts and catalyst performance to improve baseline performance.
  - Use carefully instrumented and controlled experiments at the component level to measure performance.
  - Develop proof-of-concept hardware on a laboratory scale.
  - Develop design tools and models for application to specific design problems.
- Work with fuel processor developers to integrate CO clean-up technology into fuel processor systems.
  - Collaborate on specific designs for automotive hardware and system integration.
  - Fabricate hardware and test performance of integrated CO clean-up technology.

Accomplishments

- Developed a laboratory PROX system for testing PROX concepts and catalysts, based on a multistage reactor approach.
- Conducted catalyst evaluation in a single-stage PROX configuration.
  - Measured temperature and gas composition profiles of catalyst volumes in the baseline PROX configuration.
  - Conducted initial series of tests on catalyzed ceramic foams.
- Conducted transient PROX experiments in the four-stage configuration; measured dynamic response to inlet CO concentration variation.
- Measured kinetic data on precious metal catalysts in a microscale isothermal catalyst test reactor.

Future Directions

- Work on technology transfer through industrial collaborations; integrate PROX technology into developer fuel processor designs.
- Continue testing of catalysts and of multistage PROX hardware.
  - Measure reformate composition effects, hydrogen consumption, and CO conversion.
  - Conduct transient tests, including power transients and start-up transients.
  - Test catalysts and catalyst supports for compact automotive designs.
- Continue development of PROX design methodology to delineate successful understanding of PROX mechanisms.
- Address further challenges to automotive implementation; develop technology to reduce start-up times and enable cold starts.

Introduction

This report describes research conducted during fiscal year (FY) 2000 on the development of carbon monoxide clean-up technologies as a subset of reformate clean-up technology for integration into automotive fuel processor systems. Reformate clean-up typically is the last unit operation in the fuel processor process stream in most fuel processor-fuel cell system architectures. Its function is to remove the trace contaminants from the fuel processor outlet stream to meet the fuel purity requirements of the fuel cell stack. The research objective then is to develop reformate clean-up technology that not only removes the trace contaminants, but does so with minimal hydrogen consumption to maintain system efficiency. Automotive applications require that the technology enable the fuel processor to meet the fuel

purity requirements of the fuel cell stack through automotive transients and lead to commercially viable fuel processor systems that meet automotive requirements for cost, volume, weight, and durability.

The primary focus of reformate clean-up has been removal of CO to levels less than 10 ppm under steady-state conditions and less than 100 ppm in transients. The program at Los Alamos National Laboratory (LANL) has researched preferential oxidation (PROX) as a method to remove CO to these levels. Work in prior years (FY 1996-FY 1999) focused on developing laboratory and demonstration PROX reactor hardware for gasoline fuel processing systems.

Work this year (FY 2000) focused on expanding fundamental knowledge of CO removal processes and then codifying that knowledge for technology transfer. Also, work was done to address automotive requirements for the reformate clean-up system by investigating catalysts and catalyst supports that reduce system size and are rugged, and by investigating transient control requirements to reduce the number of sensors and actuators in the systems.

Approach

Our approach combines laboratory investigations to research and develop the fundamentals of reformate clean-up technology with industrial collaborations to apply that technology. We first develop laboratory PROX reactor hardware for carefully instrumented and controlled experiments at the component level to measure performance. These experiments allow us to investigate catalysts and quantify catalyst performance in working hardware under simulated reformate conditions. We also conduct transient experiments on multistage hardware to identify the transient response and control requirements. Measured profiles of temperature and gas composition through the catalyst volume and the measured temperature and pressure response of the reactor components in transients provide the basis for developing detailed models of PROX reactor performance. The understanding developed in the proof-of-concept hardware is applied to design PROX hardware for integration into specific fuel processor systems, in collaboration with fuel processor developers.

Results

The reformate clean-up method is based on preferential oxidation of CO in an adiabatic reactor. A multistage reactor has been implemented to obtain a low CO output while minimizing hydrogen consumption. A schematic of the reactor (Figure 1) shows a four-stage configuration for reducing 2% CO at the inlet to less than 10 ppm CO at the outlet. The reactor operates as a series of short-residence-time reactor stages, each having thermal management, air injection and mixing, and catalyst volume. The catalysts in each stage are selected to work together to improve the transient performance and minimize the control requirements. Temperature and air injection are controlled so that CO is removed primarily by oxidation, with some additional removal by methanation and water-gas-shift reactions. Temperature control is critical to preventing the reverse water-gas-shift reaction and runaway methanation reactions.

The laboratory reactor shown in Figure 2 implements this reactor schematic. The performance of the reactor in removing CO from 2% CO to less than 10 ppm CO has been verified in operation on natural gas reformate (reported in FY 1999) and on simulated gasoline reformate (during testing conducted in the last quarter of FY 1999 through FY 2000). The modular laboratory design is flexible for testing catalysts, reactor configurations, and control schemes. The design of the reactor and use of lightweight internal components enhance transient performance. The design has been verified to give uniform air distribution and mixing into the catalyst volume and to provide the desired control of the inlet temperature to the stages.

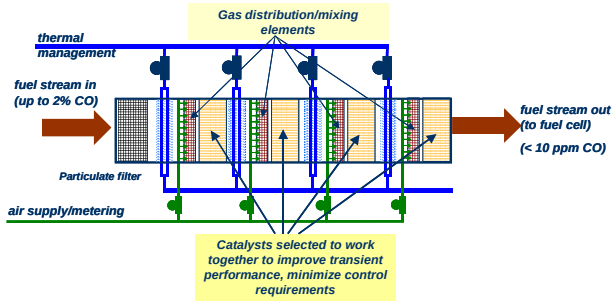

Figure 1. Schematic of the four-stage PROX reactor.

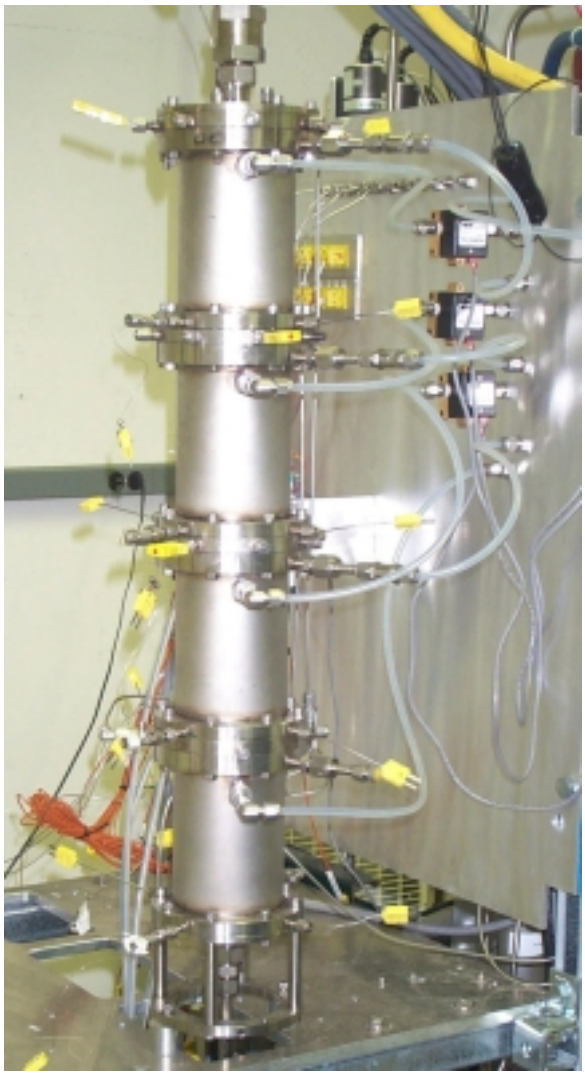

Figure 2. Four-stage configuration of the laboratory PROX reactor.

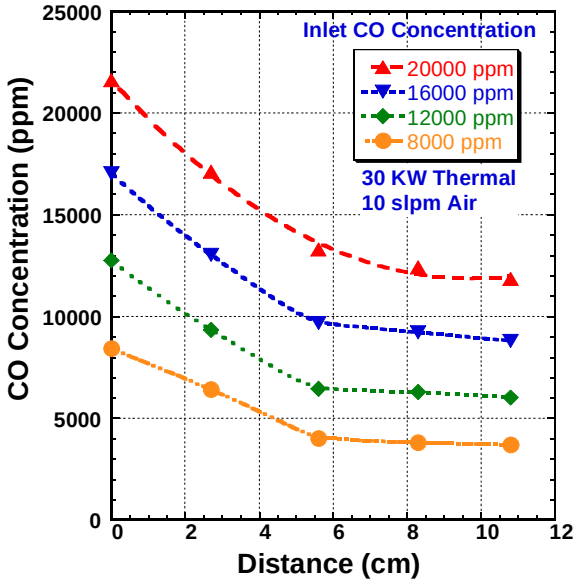

Figure 3. CO concentration profile of the PROX reactor inlet stage.

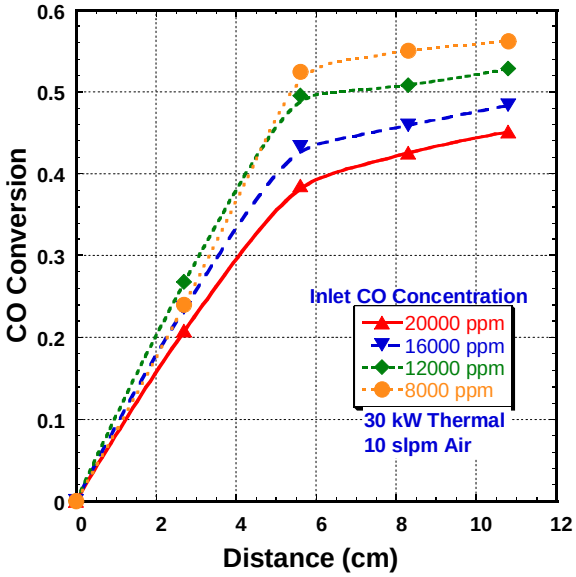

Figure 4. CO conversion as a function of depth in the PROX reactor inlet stage.

A single-stage PROX reactor setup was used for measuring temperature and gas composition profiles of catalyst volumes and for testing catalysts on automotive supports. The measured profiles provide data for detailed modeling of the reactor stages. The initial focus of our catalyst testing was on characterizing the performance of the PROX inlet stages because they use a new catalyst that we had not characterized before. We also think that a greater understanding of these stages will lead to a further reduction in the parasitic hydrogen loss.

Figures 3 and 4 show some examples of measured profiles of CO concentration and CO conversion, respectively, as a function of depth within the catalyst volume. Four inlet CO concentrations are shown, at a constant overall flow rate and air injection rate. Flow rates and air injection rates were varied to map the catalyst volume over its expected range of operation. These data were compiled to develop curves such as the one shown in Figure 5, which shows the CO conversion as a function of oxygen stoichiometry at a single flow rate for four different inlet CO concentrations. The solid line on the graph shows the ideal curve for no parasitic hydrogen consumption. Points lying further to the right from

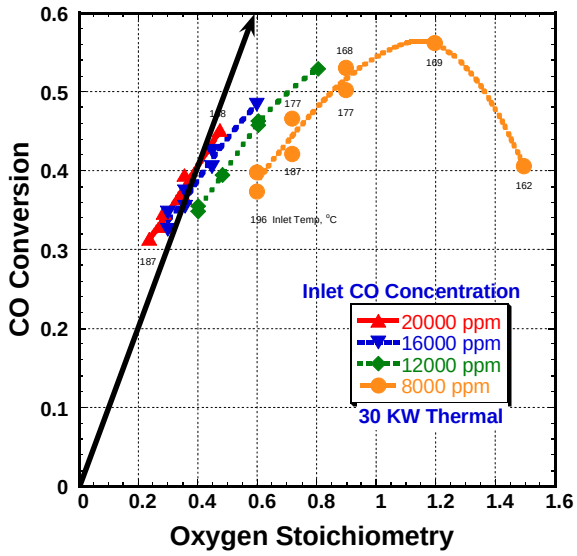

Figure 5. CO conversion as a function of oxygen stoichiometry for the PROX inlet stage.

the curve have increased hydrogen consumption. Thus, the curves show the relationship between increasing CO conversion and increasing hydrogen consumption, and they indicate our rationale for using staging to minimize hydrogen consumption. The data also provide the input to our models for optimizing the PROX staging and operating conditions.

Figures 6 and 7 show an example of the use of the model to optimize the PROX for an operating condition. The Stage 1 oxygen stoichiometry is varied for a constant inlet CO concentration and total flow rate. Figure 6 shows the CO concentration at the stage outlets as a function of the Stage 1 oxygen stoichiometry. The Stage 2 and 3 oxygen stoichiometries are held constant, and the fourth stage is set to achieve 10 ppm CO at its outlet in this model. Figure 7 shows the hydrogen produced (as a percent of the hydrogen inlet flow) as a function of stoichiometry. The H_2 total curve shows a peak at an oxygen stoichiometry of about 0.25, suggesting an optimal operating point for Stage 1.

Other catalyst testing this year included testing of catalyzed ceramic foams in the single-stage PROX reactor setup. We are investigating catalyzed ceramic foams as a possible rugged catalyst support for automotive use that may also reduce the size by increasing turbulent mixing and combining gas mixing and distribution elements with the catalyst supports. Initial tests showed no improvement over monoliths; we are iterating to optimize pore size and

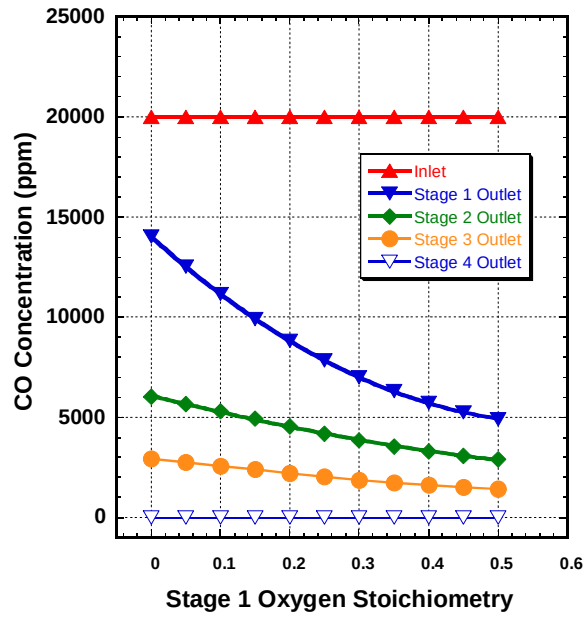

Figure 6. Model predictions of the outlet CO concentrations from each stage as a function of the Stage 1 oxygen stoichiometry.

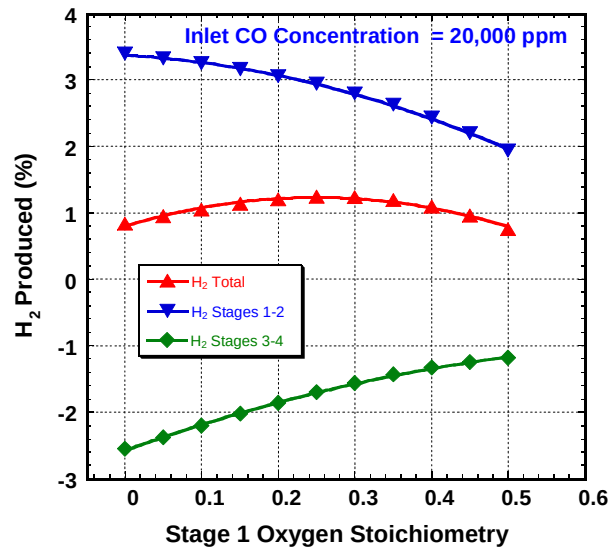

Figure 7. Net hydrogen produced as a percent of total hydrogen flow as a function of the Stage 1 oxygen stoichiometry.

catalyst. We are also investigating higher-density cpsi (>600 cpsi) monoliths and a catalyzed particle filter for use as PROX catalyst substrates.

The four-stage PROX reactor setup is being used for investigating the transient response of the reactor components. Initial tests have been conducted to identify the PROX response to a sine-wave-modulated CO input at an overall steady flow.

These tests measure the sensitivity of the PROX to changes in inlet CO concentration. These data are critical to the development of control strategies and to determining the requirements for a CO sensor. Both power transient testing and start-up transient testing will be conducted in the fourth quarter of FY 2000. These tests will be used to quantify the limiting factors on the transient response of the PROX to changes in the total flow rate, corresponding to changes in power demand, and on the start-up time.

Industrial collaborations have been initiated to apply and develop the CO clean-up technology for specific fuel processor designs. An industrial collaboration has been started with McDermott Technology to integrate a PROX system with their multifuel fuel processor. A second collaboration has started with Argonne National Laboratory to integrate a PROX with their integrated fuel processor.

Conclusions

A working laboratory reactor has been developed to investigate the fundamentals of CO clean-up technology. The multistage reactor has demonstrated CO removal from a 2% CO inlet to less than 10 ppm CO at the outlet. Detailed measurements of the catalyst and reactor performance of the inlet stages were used to determine optimal operating points. Transient experiments on the multistage configuration are being used to measure the limits of the dynamic response and the requirements for controls. Industrial collaborations were begun to apply the technology to specific fuel processors and to transfer the technology. Remaining work this fiscal year includes continuation of catalyst testing to lead to more compact designs, testing of transient response to changes in power level and start-up, and work on industrial collaborations.

I. Evaluation of Partial Oxidation Fuel Cell Reformer Emissions

Stefan Unnasch (primary contact)
Arthur D. Little, Inc.
Acurex Environmental
10061 Bubb Road
Cupertino, CA 95014
(408) 517-1550, fax: (408) 517-1553, e-mail: unnasch.stefan@adlittle.com

DOE Program Manager: Nancy Garland
(202) 586-5673, fax: (202) 586-9811, e-mail: nancy.garland@ee.doe.gov

ANL Technical Advisor: Walter Podolski
(630) 252-7558, fax: (630) 972-4430, e-mail: podolski@cmt.anl.gov

Contractor: Arthur D. Little, Inc., Cupertino, California
Prime Contract No. DE-FC02-99EE50585, September 1999-June 2001
Subcontractors: Nuvera Corporation, Hydrogen Burner Technology

---

Objectives

- Measure the emissions from partial oxidation/autothermal fuel processors for polymer electrolyte membrane fuel cell (PEMFC) systems under both cold-start and normal operating conditions.
- Assess the feasibility of meeting emissions standards for automobiles and light-duty trucks through the use of a fuel cell vehicle with a multifuel reformer.

OAAT R&D Plan: Task 5; Barriers F and G

Approach

- Define a representative test cycle consisting of both cold-start and normal operating conditions.
- Use the established test cycle to quantify emissions from a partial oxidation (POX) reformer before and after anode-gas-burner treatment.
- Perform the test procedure using four different feed fuels in the reformer (gasoline, methanol, ethanol, and natural gas), as well as different catalyst formulations for the anode gas burner.
- Perform the test procedure on both Nuvera (formerly Epyx) and Hydrogen Burner Technology (HBT) fuel processors to quantify the emissions impact of fuel reformer design.
- Use reasonable approximations and estimates to convert emissions data from a gram-per-unit fuel basis to a predicted gram-per-mile basis.

Accomplishments

- Assessed sensitivity of gas chromatograph.
- Identified sampling procedures.

Future Directions

Develop control strategies to minimize emissions.

Introduction

The operation of fuel reformers is generally divided into two operating modes: start-up and normal partial oxidation. During start-up, the fuel processor burns fuel at near-stoichiometric conditions until critical system temperatures and pressures stabilize to target values. Once the target conditions are reached, the reformer operates in the normal mode, in which the fuel processor burns fuel at very rich conditions. Since the two modes encompass considerably different operating conditions, it follows that the emissions associated with each of these modes also differ considerably.

The combustor is typically cold under start-up conditions, so the emissions produced during this brief period (target times are under 30 seconds) can be substantially higher than those produced during the remaining, much longer portion of the driving cycle. The pollutant emissions produced in this operating mode include NO_x, CO, formaldehyde, and organic compounds. These organic compounds, which include hydrocarbons, alcohols, and aldehydes, are referred to in California and are regulated as nonmethane organic gases (NMOG).

Under normal operating conditions, in which the combustor is sufficiently warm and operated under fuel-rich conditions, virtually no NO_x is formed (although the formation of ammonia is possible). Most hydrocarbons are converted to carbon dioxide (or methane, if the reaction is incomplete); however, trace levels of hydrocarbons can pass through the fuel processor and fuel cell. The shift reactors and the preferential oxidation (PROX) reactor reduce CO in the product gas, resulting in a feed concentration to the fuel cell that can be less than 20 ppm. The fuel cell may also convert CO to CO_2, thereby further reducing exhaust CO levels. Thus, of the criteria pollutants (NO_x, CO, and hydrocarbons [NMOG]), NO_x and CO levels are generally well below the most aggressive standards. NMOG concentrations, however, can exceed emission goals unless these compounds are efficiently eliminated in the catalytic burner.

Figure 1 shows estimated NMOG emissions from partial oxidation (POX) systems fueled by compressed natural gas (CNG) and gasoline [1]. The figure clearly indicates the trend described above with respect to the relative contribution of start-up emissions and the emissions levels over the total driving cycle. Furthermore, the figure also indicates the importance of catalyst performance in reducing NMOG emissions. For example, if the catalyst

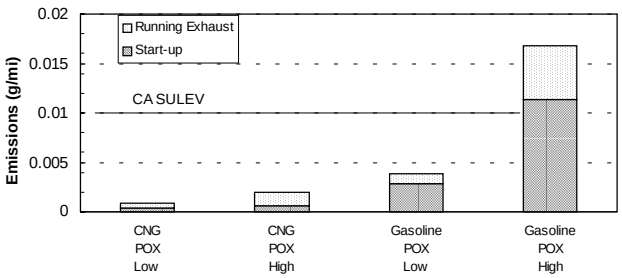

Figure 1. Estimated NMOG exhaust emissions for POX/PEMFC systems with varying anode gas combustor efficiencies.

efficiency is reduced from 85% (low emissions) to 20% (high emissions), a gasoline-fueled POX reformer/PEMFC can no longer meet the California super ultra-low emissions vehicle (SULEV) standard for NMOG emissions.

Approach

In this study, POX fuel reformers will be operated under conditions simulating both cold-start and normal operation. Emissions will be measured before and after treatment by an anode gas burner in order to quantify the effectiveness of the burner catalyst in controlling start-up emissions. The emissions sampling system will comprise continuous emissions monitors (CEMs) for O_2, CO_2, CO, NO_x, and total hydrocarbons (THC). Also, integrated gas samples will be collected in Tedlar bags for hydrocarbon speciation analysis via gas chromatography (GC). This analysis will yield the concentrations of the hydrocarbon species required for the California NMOG calculation. In addition, the particulate concentration in the anode burner exhaust will be measured through either isokinetic sampling or the placement of a filter in the exhaust stream.

Concentrations of the aforementioned species will be obtained by using an emissions sampling system similar to the one shown schematically in Figure 2. Because emissions from a POX system vary significantly between start-up and normal operation (see Figure 1), a wide range of analyzer capabilities will be required. Specifically, NO_x, CO, and hydrocarbon levels will each be between 10 and 1000 ppm during start-up and will fall below 10 ppm during normal operation.

This study will explore the sensitivity of reformer emissions to several variations in the

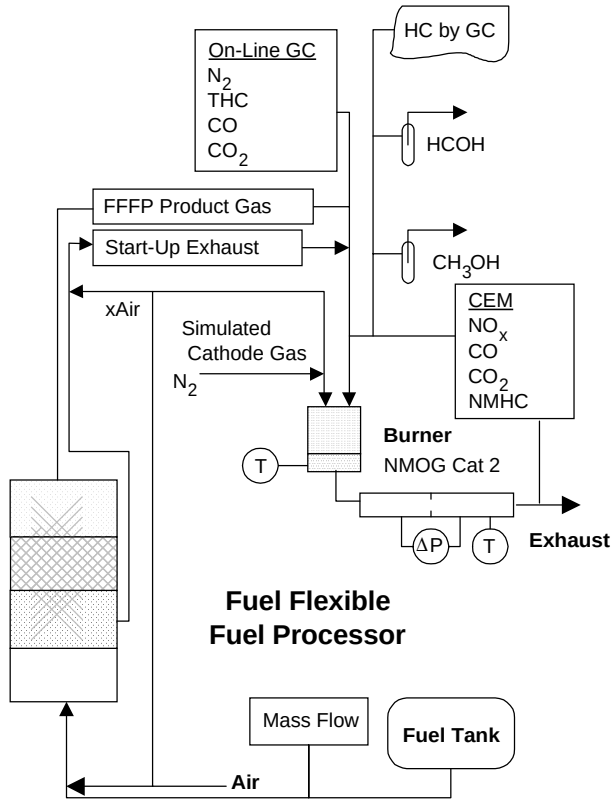

Figure 2. Emission testing setup.

system. In particular, the impact of fuel reformer design will be assessed by testing systems from two different manufacturers: Nuvera and HBT. The sensitivity of reformer emissions will also be quantified by repeating identical test procedures for four different fuels: gasoline, methanol, ethanol, and natural gas. Similarly, the sensitivity of emissions to anode burner catalyst formulations will also be quantified. An example test matrix based on the aforementioned variations (assuming the use of two catalyst formulations) is shown in Table 1.

To make quantitative conclusions regarding the impact of fuel composition on reformer emissions, the measured volumetric exhaust concentrations of each pollutant will be converted to a gram-per-unit fuel basis. To make further conclusions regarding the feasibility of meeting California SULEV emissions standards, appropriate assumptions and estimates with respect to the powertrain of a fuel cell vehicle will be used to convert the measured emissions levels to a predicted gram-per-mile basis. These results will be presented in a final report that evaluates the reformer/anode-gas-burner configurations.

Table 1. Example test matrix for testing multifuel reformer emissions.

Test ID	Nuvera	HBT
Test # 1	Gasoline	Gasoline
Test # 2	Gasoline/Control Strategy B	Gasoline/Control Strategy B
Test # 3	Natural Gas	Natural Gas
Test # 4	Natural Gas/Control Strategy B	Natural Gas/Control Strategy B
Test # 5	Methanol	Methanol
Test # 6	Methanol/Control Strategy B	Methanol/Control Strategy B
Test # 7	Ethanol	Ethanol
Test # 8	Ethanol/Control Strategy B	Ethanol/Control Strategy B

Conclusions

The purpose of the proposed project is to assess the emissions from partial oxidation fuel cell reformer systems and to evaluate the performance of catalytic burners in controlling startup emissions. This objective will be achieved by testing the emissions from the HBT and Nuvera fuel-flexible fuel processors.

Reference

1. Unnasch, S., "Evaluation of Fuel Cell Reformer Emissions," Final Report for Contract 95-313, prepared for California Air Resources Board, Sacramento, Calif., Aug. 1999.

J. Catalytic Autothermal Reforming

Michael Krumpelt (primary contact), Rolf Wilkenhoener, David J. Carter, Joong-Myeon Bae, John P. Kopasz, Theodore Krause, and Shabbir Ahmed
Argonne National Laboratory, 9700 S. Cass Ave., Argonne, IL 60439
(630) 252-4553; fax: (630) 972-4553, e-mail: krumpelt@cmt.anl.gov

DOE Program Manager: JoAnn Milliken
(202) 586-2480, fax: (202) 586-9811, e-mail: joann.milliken@ee.doe.gov

---

Objectives

- Improve catalytic activity and reduce cost of autothermal reforming (ATR) catalyst.
- Determine long-term (>1000-h) stability of the catalyst.
- Investigate the effect of catalyst structure (e.g. pellet, monolith, microchannel) on catalyst activity.
- Develop a better understanding of the reaction mechanism.

OAAT R&D Plan: Task 3; Barrier E

Approach

- Measure hydrocarbon conversion and H_2 selectivity vs. temperature and space velocity for new catalyst formulations.
- Conduct life tests to evaluate catalyst stability during >1000-h period.
- Fabricate different catalyst structures, and investigate the relationship between structure and activity.
- Subcontract catalyst characterization studies to academia.

Accomplishments

- Several non-noble metal formulations with excellent activity were identified.
- The importance of oxide ion conductivity in the catalyst substrate was clearly established.
- Catalyst stability during 1,000 h was demonstrated.
- With the catalyst in a microchannel configuration, an H_2 selectivity of >50% (dry, N_2-free basis) was observed at a space velocity of 125,000 h^{-1}.
- Strong metal-support interactions were observed by using x-ray photoelectron spectroscopy (XPS) and extended x-ray absorption fine structure (EXAFS) methods.
- Patent for catalyst formulation was licensed to United Catalysts (now known by SudChemie, Inc.)

Future Directions

- Catalyst cost vs. activity issues will be addressed.
- Work will continue on determining optimal metal(s) and support composition that maximizes catalytic activity, provides long-term stability, and provides tolerance to catalyst poisons.
- Surface area will be increased.
- Surface stability and mechanical properties need more attention.
- Relationship between structure (supported vs. free-standing configurations) and catalytic activity will be evaluated.
- Understanding of the chemical and physical properties of the catalyst and how these properties influence catalytic activity will be increased.

Introduction

In prior years, Argonne National Laboratory has articulated the merits of autothermal reforming for automotive fuel cell systems in terms of reactor volume and weight, as well as for fast transient response and start-up. We have reported good success with a catalyst derived from solid oxide fuel cell technology, where the metal is a transition metal element and the substrate is an oxide ion conductor, such as zirconia, ceria, or lanthanum gallate. We have also shown that a good operating temperature is 700°C, which requires catalytic enhancement of the reaction rates.

Approach

During the past year, we have synthesized new catalyst formulations in which either the metal or the substrate composition was varied. We have evaluated the catalytic activity of these new catalyst formulations by measuring the hydrocarbon conversion and H_2 selectivity as a function of temperature and space velocity in a microreactor system. We have conducted life tests (>1000 h) to evaluate the stability of these catalysts toward deactivation. We have fabricated new structured forms of the catalyst, such as a monolith or a spiral microchannel configuration, to improve catalyst durability and to minimize diffusional resistances. Using characterization techniques, such as inductively coupled plasma (ICP), energy-dispersive x-ray spectroscopy (EDX), XPS/Auger, EXAFS, x-ray absorption near-edge spectroscopy (XANES), and transmission electron microscopy (TEM), a better understanding of the chemical and physical properties of the ATR catalyst and how these properties influence the catalytic activity has begun to develop.

Results

A major focus of the work during this period was to identify potential non-noble transition metals to replace precious metals, such as Pt, in order to reduce the cost of the catalyst. The catalytic activity of various metals supported on a doped ceria substrate was evaluated by measuring the hydrocarbon (2,2,4-trimethylpentane) conversion and H_2 selectivity as a function of temperature and space velocity. The percent conversion of

hydrocarbon in the feed and H_2 selectivity as a function of temperature for the various metals tested are shown in Figures 1 and 2, respectively. These data were obtained by using an O_2/C ratio of 0.46 and a H_2O/C ratio of 1.14 at a space velocity ~3000 h^{-1} in a temperature-controlled microreactor. Although all of these catalysts were prepared in an identical manner, substantial differences exist in the BET surface areas that may account for the differences observed in H_2 selectivity. In general, the BET surface area of the non-noble transition metal catalysts is 50-80% lower than that of Pt catalyst.

Some of the non-noble metals (e.g., nickel, copper, iron, cobalt) are as active as the more expensive platinum or palladium at temperatures as low as 700°C. Considering that the partial oxidation of methane using a Pt/alumina catalyst requires a reaction temperature of 1000°C to achieve high conversion [1], it appears that an oxide-ion-conducting substrate may play a significant role in the reaction sequence. To better understand the role of this substrate, three different oxide-ion-conducting substrates (ceria, zirconia, and lanthanum gallate) were tested. As shown in Figure 3, the H_2 yield ranged from 34% to 60% (dry, N_2-free basis) for these different oxide-ion-conducting substrates. In comparison, the H_2 yield was less than 30% using a Pt/alumina catalyst under similar reaction conditions. Work is continuing to find the optimal metal/oxide formulation in terms of activity, stability, and cost.

Long-term (>1000-h) life cycle studies were conducted to evaluate the stability of the ATR catalyst toward deactivation. As shown in Figure 4, the H_2 concentration in the product gas was relatively constant at ~35% (dry basis) over a 47-day life test. For this test, a benchmark fuel was used, and the catalyst was Pt supported on a doped ceria substrate. In view of the fact that this catalyst was far from being optimized, particularly with respect to maximizing the surface area, it proved remarkably stable. (See the report by Kopasz et al. for the stability of the catalyst in the presence of sulfur [2].)

From an engineering perspective, a structured form of the ATR catalyst, such as a monolith or a microchannel configuration, is preferred over a pellet form to minimize such potential problems as back-pressure buildup. Furthermore, if the reaction is severely mass-transfer-limited, a structured form of the ATR catalyst that minimizes diffusional

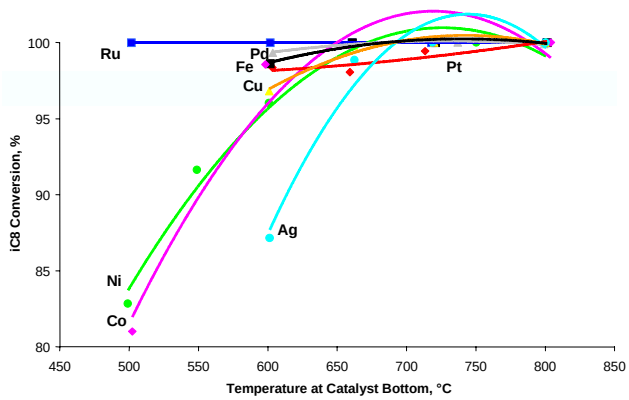

Figure 1. Hydrocarbon conversion for autothermal reforming of iso-octane (2,2,4-trimethylpentane) as a function of temperature for various transition metals supported on a doped ceria substrate.

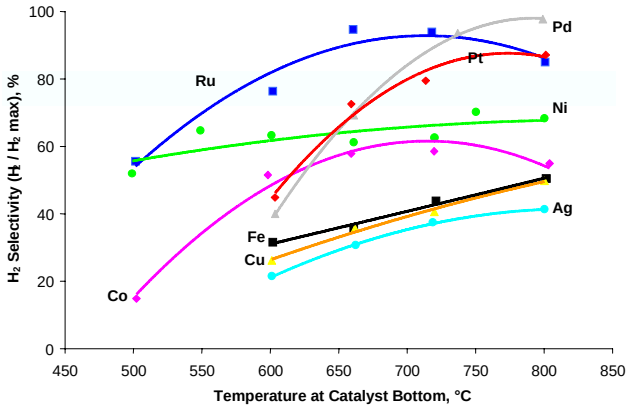

Figure 2. H_2 selectivity for autothermal reforming of iso-octane (2,2,4-trimethylpentane) as a function of temperature for various transition metals supported on a doped ceria substrate.

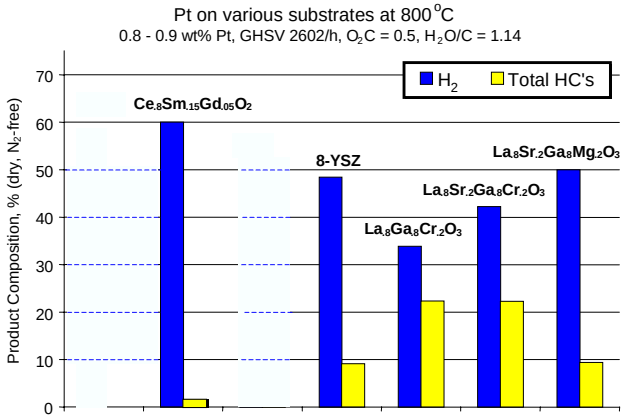

Figure 3. H_2 selectivity for autothermal reforming of iso-octane (2,2,4-trimethylpentane) for Pt supported on various oxide ion substrates.

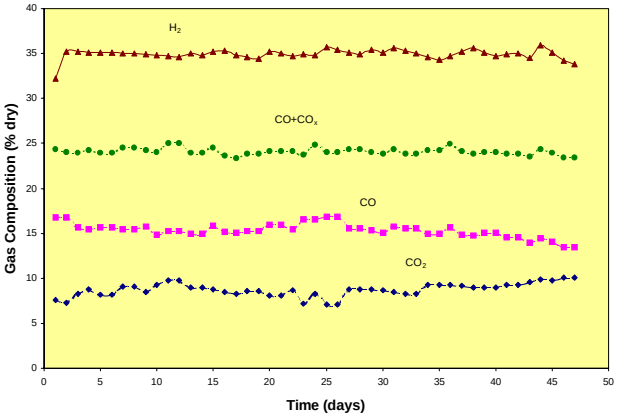

Figure 4. H_2 selectivity for autothermal reforming of iso-octane (2,2,4-trimethylpentane) for Pt supported on a doped ceria substrate over a 47-day test.

resistances will have a higher activity per unit volume than a pellet form. The higher activity of the structured form of the catalyst will allow for higher processing rates (space velocities), which means that a reactor designed for use with a structured form of the catalyst will be smaller and require less catalyst than a reactor designed for use with pellets. For these reasons, we have developed a microchannel form of the catalyst, as shown in Figure 5. With the ATR catalyst in a spiral microchannel configuration, a reformate having a H_2 concentration of >50% (dry, N_2-free basis) is produced at space velocities as high as 125,000 h^{-1} (Figure 6).

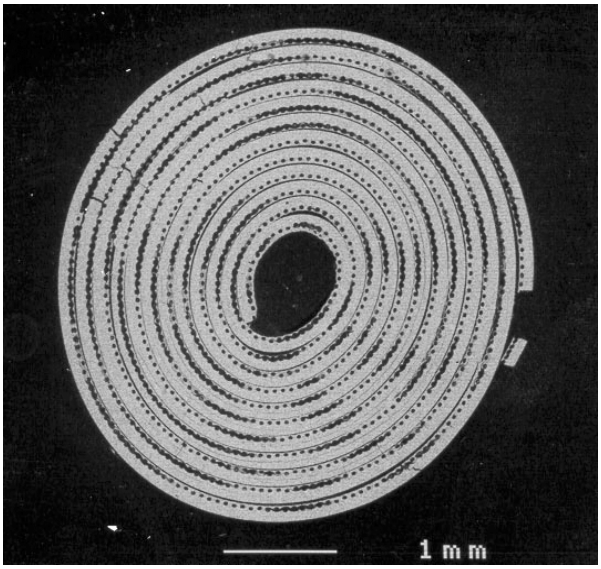

Figure 5. Spiral microchannel configuration of ATR catalyst.

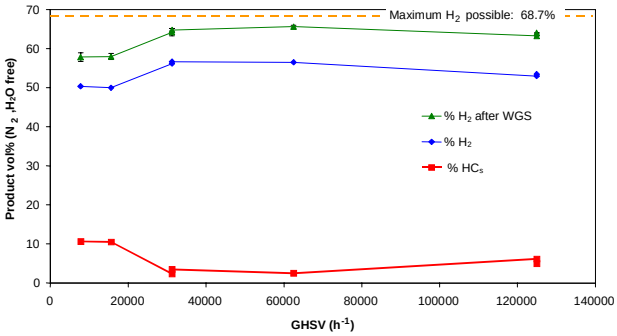

Figure 6. H_2 selectivity for autothermal reforming of iso-octane (2,2,4-trimethylpentane) as a function of space velocity for a spiral microchannel configuration.

To optimize the catalytic activity, an understanding of how the chemical and structural properties (e.g. metal particle size and size distribution, oxidation state of the metal, surface composition, and interaction between the metal and the oxide) of the catalyst influence the reaction rate is required. Catalyst characterization studies, using such techniques as ICP, EDX, XPS/Auger, EXAFS, and XANES to measure and investigate these properties, have been initiated. Argonne National Laboratory (ANL) is working with the University of Alabama to investigate the nature of the interaction between the metal and the oxide by using ICP, EDX, and XPS/Auger, and the metal particle size and size distribution by using TEM. Results from this work will be disclosed in detail at a later date. In an EXAFS study conducted at ANL by Christopher Marshall, small Pt clusters (Pt_4) are present on Pt supported on an undoped ceria substrate, whereas there is no evidence of Pt clusters (no Pt-Pt bonding) on Pt supported on a doped (Sm or Gd) ceria substrate (see Table 1). This suggests that the metal-

Table 1. Particle size determination and Pt nearest neighbor for Pt supported on doped and undoped ceria, as determined by EXAFS.

	Composition	Particle sizes	Reduction Stability	Comments
TARK-44	Pt/CeO_2	>10Å	High	Pt_4 No Pt-O
TARK-13	Pt/CSAO (prep 1)	<5 Å	High	No Pt-Pt Pt-O-(Ce)
TARK-19	Pt/CSAO (prep 1)	<5 Å	Med.	No Pt-Pt Pt-O-(Ce)
TARK-34	Pt/CGO	<5 Å	Low	No Pt-Pt Pt-O-(Ce)

support interaction is stronger between Pt on doped ceria than Pt on undoped ceria [3]. Experimental work is continuing to explore how the metal-support interaction influences the reaction mechanism as well as the reaction rate.

Conclusions

We have demonstrated that high hydrocarbon conversions and H_2 selectivity, comparable with those observed with Pt, can be achieved with certain less costly, non-noble metals supported on oxide ion conductors. Long-term reactor tests demonstrated that the Pt catalyst is stable, with little evidence for deactivation. The Pt catalyst does not appear to be poisoned by sulfur at concentrations in the fuel comparable to fiscal year (FY) 2004 sulfur targets [2].

We have developed structured forms of the catalyst, including a monolith and a spiral microchannel configuration, and demonstrated that a reformate containing >50% H_2 (dry, N_2-free basis) can be produced at a space velocity of 125,000 h^{-1} using the microchannel configuration. We have observed that the addition of a dopant, such as Sm or Gd, to ceria results in a strong metal-support interaction that minimizes the formation of Pt clusters and strongly influences the reaction rate.

Future work will focus on developing a nonprecious-metal catalyst to reduce the cost. New formulations of these nonprecious-metal catalysts and oxide ion conductors will be investigated to maximize catalytic activity, provide long-term stability, and minimize the effects of sulfur poisoning. Characterization and reaction mechanism studies will continue to determine which chemical and physical properties of the catalyst should be optimized. Work will continue on optimizing the catalytic activity and improving the mechanical properties of new structured forms of the catalyst.

References

1. P.M. Torniainen, X. Chu, and L.D. Schmidt, *J. Catal.* **146**:1-10 (1994).
2. J.P. Kopasz, D. Applegate, L. Ruscic, S. Ahmed, and M. Krumpelt, "Effects of Fuels/Contaminants on Reforming Catalyst Performance and Durability," presented at the Annual National Laboratory R&D Meeting of the DOE Fuel Cells for Transportation Program, Richland, Wash., June 7-8, 2000 [to be published in *Advanced Petroleum-Based and Alternative Fuels – 2000, Annual Progress Report, Energy Conversion Team*, U.S. Department of Energy, Office of Advanced Automotive Technologies, Washington, D.C., 2000].
3. S. Bernal, J.J. Calvino, M.A. Cauqui, J.M. Gatica, C. Larses, J.A. Perez Omil, and J.M. Pintado, *Catal. Today* **50**:175-206 (1999).

Publications

1. S. Ahmed, B. Bergin, T. Krause, J.D. Carter, J-M. Bae, L. Ruscic, D. Applegate, J. Kopasz, D. Myers, J. Krebs, C. Pereira, S.H.D. Lee, and M. Krumpelt, "Fuel Processor Development at Argonne National Laboratory," presented at the Army Research Office Workshop, Detroit, Mich., June 19-21, 2000.
2. M. Krumpelt, S. Ahmed, R. Kumar, S. Chalk, and J. Milliken, "Partial oxidation fuel reforming for automotive power systems," to be published in *Proceedings of the 3rd International Fuel Cell Conference*, Nagoya, Japan, Nov. 30-Dec. 3, 1999.
3. S. Ahmed, J. Kopasz, B.J. Russell, and H.L. Tomlinson (Syntroleum Corporation), "Cobalt-based Fischer-Tropsch Paraffin Fuels for Fuel Cell Power," poster paper presented at the Sixth Grove Fuel Cell Symposium, London, U.K., Sept. 13-16, 1999.
4. S. Ahmed, S.H.D. Lee, R. Kumar, J.D. Carter, R. Wilkenhoener, and M. Krumpelt, "The Argonne Catalytic Fuel Processor for Automotive and Small Fuel Cell Power Systems," poster paper presented at the Sixth Grove Fuel Cell Symposium, London, U.K., Sept. 13-16, 1999.
5. J. Kopasz, R. Wilkenhoener, S. Ahmed, J.D. Carter, and M. Krumpelt, "Fuel flexible partial oxidation reforming of hydrocarbons for automotive applications," preprints of the Symposium on Hydrogen Production, Storage, and Utilization, 218th ACS National Meeting, **44**(4):899-904, New Orleans, La., Aug. 22-26, 1999.

Patents Issued

1. M. Krumpelt, S. Ahmed, R. Kumar, and R. Doshi, "Method for making hydrogen-rich gas from hydrocarbon fuel," Patent No. 5,929,286, issued on July 27, 1999.
2. M. Krumpelt, S. Ahmed, R. Kumar, and R. Doshi, "Partial Oxidation Catalyst," patent application pending.

Awards/Recognitions

1. Best Poster Award at the Grove Symposium, London, U.K., Sept. 1999.
2. Annual National Laboratory R&D Award from DOE/OTT/OAAT, Richland, Wash., June 2000.

K. Alternative Water-Gas Shift Catalyst Development

Deborah J. Myers, John F. Krebs, Theodore R. Krause, and Michael Krumpelt
Argonne National Laboratory, Argonne, IL 60439-4837
(630) 252-4261, fax: (630) 252-4176, e-mail: myers@cmt.anl.gov

DOE Program Manager: JoAnn Milliken
(202) 586-2480, fax: (202) 586-9811, e-mail: joann.milliken@ee.doe.gov

---

Objectives

- Develop alternative water-gas shift (WGS) catalysts to:
  - Eliminate the need to sequester catalyst during system shutdown.
  - Eliminate the need to activate catalyst *in situ.*
  - Increase tolerance to temperature excursions.
  - Reduce size and weight of the shift reactor(s).
  - Extend lifetime of the catalyst.

OAAT R&D Plan: Task 3; Barriers E and G

Approach

- Develop metal-support combinations to promote bifunctional mechanism of catalyst action:
  - One component to adsorb CO (e.g., metal with intermediate CO adsorption strength).
  - Second component to adsorb and dissociate H_2O (e.g., mixed-valence oxides with redox properties under reformate conditions).
- Develop bimetallic or polymetallic oxide mixtures to perform the regenerative WGS mechanism:
  - Each metal oxide catalyzes one-half of the WGS reaction.
  - Metals need to be in intimate contact for efficient electron transfer.

Accomplishments

- Demonstrated <1% CO at 230-300°C from diesel and 1.1% CO from simulated reformate (Nov. 1999 milestone).
- ANL Pt/mixed oxide shift catalyst reduces WGS catalyst volume to 68% of Fe/Cr - Cu/ZnO combination and does not lose activity with exposure to air (not pyrophoric).

- Platinum loading reduced by a factor of three while maintaining catalyst's WGS activity.
- A nonprecious-metal/mixed oxide catalyst was identified that reduces cost of catalyst to <1% that of Pt/mixed oxide.
- Binary oxides show promise as inexpensive, air- and thermally-stable WGS catalysts.

Future Directions

- Increase low-temperature activity of nonprecious-metal catalysts.
- Explore other metal/oxide and oxide/oxide combinations.
- Determine durability and stability of metal/mixed oxide catalysts under reformate conditions, including tolerance to sulfur.
- Set up catalyst fabrication equipment to supply industry with evaluation-scale quantities.

Introduction

The water-gas shift (WGS) reaction,

$$CO + H_2O \rightarrow CO_2 + H_2$$

is used to convert the bulk of CO in raw reformate to CO_2 and additional H_2. In the chemical process industry (e.g., in the manufacture of ammonia), the shift reaction is conducted at two distinct temperatures. The high-temperature shift (HTS) is carried out at 350–450°C, using an Fe-Cr catalyst. The low-temperature shift (LTS) is carried out at 160–250°C with the aid of a Cu-Zn catalyst.

The commercial HTS and LTS catalysts require activation by careful pre-reduction *in situ* and, once activated, lose their activity very rapidly if they are exposed to air. Moreover, the HTS catalyst is inactive at temperatures below 300°C, while the LTS catalyst degrades if heated to temperatures above 250°C. For the automotive application, with its highly intermittent duty cycle, it is important to develop alternative WGS catalysts that (1) eliminate the need to sequester the catalyst during system shutdown; (2) eliminate the need to activate the catalyst *in situ*; (3) increase tolerance to temperature excursions; and (4) reduce the size and weight of the shift reactors.

Approach

No single metal, with the exception of copper, has high activity for both the water dissociation and carbon monoxide oxidation steps of the WGS reaction. Therefore, we are investigating bifunctional catalysts, where one component of the catalyst adsorbs or oxidizes CO and the other component dissociates the water. Our present research is focused on metal-support and bimetallic/polymetallic oxide combinations to promote this bifunctional mechanism.

For the metal-support bifunctional catalysts, the metallic component is chosen to adsorb CO at intermediate adsorption strengths (Pt, Ru, Pd, PtRu, PtCu, Co, Ag, Fe, Cu, Mo). The support, chosen to adsorb and dissociate water, is typically a mixed-valence oxide with redox properties (such as lanthanide oxides, manganese oxide, vanadium oxide) under the highly reducing conditions of the reformate.

For the bimetallic/polymetallic oxide catalysts, one metal oxide is raised to a higher oxidation state while reducing water to form hydrogen; another metal oxide donates electrons to this first oxide and oxidizes carbon monoxide to complete the cycle. A structural requirement for this mechanism is that the two metal centers be in intimate contact for efficient electron transfer. The metal oxides are chosen on the basis of the two halves of the reaction being thermodynamically favored (in particular, materials with solid-state structures). An example of this type of catalyst is vanadium-cobalt oxide.

Results

Early in this project, a platinum/mixed oxide catalyst was identified as a potential WGS catalyst with several desirable properties. As opposed to copper/zinc oxide, this catalyst does not have to be reduced *in situ*, it does not lose activity upon exposure to air at 21°C to 550°C, and it is active over a 180-400°C temperature range. Over the first two years of the project, the WGS activity of the platinum/mixed oxide catalyst was quadrupled, while the platinum loading was reduced from 1 wt% to 0.42 wt%. The catalyst was also supported on an

alumina extrudate. This past year, we developed a new synthesis method for the alumina-supported catalyst to further reduce the platinum loading. As shown in Figure 1, the new method allowed a reduction in platinum loading from 0.42 wt% to 0.14 wt%, with no loss of WGS activity.

Argonne's platinum/mixed oxide/alumina catalyst can reduce shift reactor volumes significantly. Figure 2 shows a comparison of the calculated shift reactor volumes for the commercial HTS and LTS catalysts and for the Argonne catalyst used at 300°C and 400°C. The calculated reactor volumes were based on the measured intrinsic reaction rates and activation energies for the Argonne catalyst, and on the published kinetic data for the commercial catalysts. The HTS and LTS stages were assumed to operate adiabatically. The calculated amount of catalyst is that needed to reduce the exit CO concentration to 1% (dry basis) from an inlet reformate gas consisting of 10% CO, 10% CO_2, 34% H_2, 33% N_2, and 13% H_2O (wet basis). As shown in Figure 2A, for the commercial HTS and LTS catalysts operated at 400°C and 200°C, respectively, a total catalyst volume of 19.2 L is needed for a 50-kW_e fuel cell system. In comparison, with the Argonne catalyst operated at 400°C and 300°C, respectively, the total required catalyst volume is 13.5 L, a 30% reduction. Also shown in Figure 2 are the improvements in the activity of the platinum/mixed oxide catalyst throughout the duration of this project, as reflected in the estimated reactor size, and the reduction in the

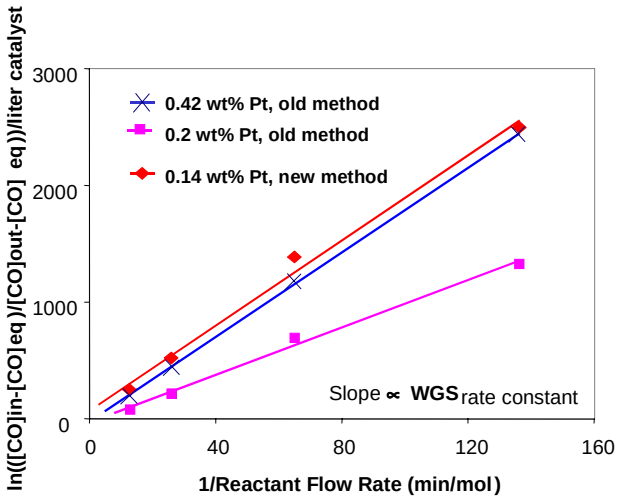

Figure 1. New synthesis method reduced the platinum loading of the catalyst while maintaining high activity.

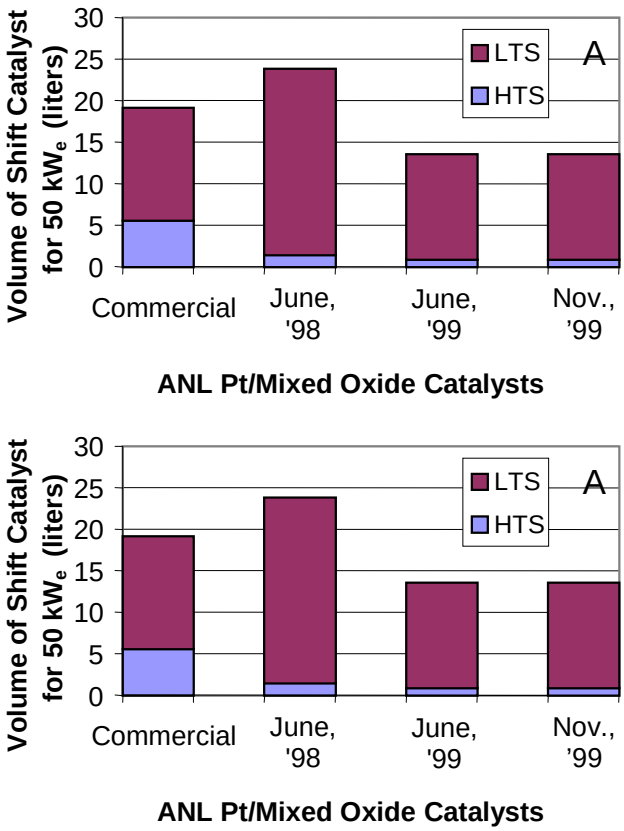

Figure 2. The Argonne catalyst can reduce shift reactor volumes significantly. Projected size (A) and cost (B) of the Argonne shift reactors are being reduced.

amount of platinum needed. The platinum loading has been reduced from 1 wt% to 0.14 wt%, for an overall platinum weight of 32 grams for a 50-kW_e system.

Although the noble metals have desirable air stability and temperature stability, their high cost may limit their acceptability for transportation applications. This past year, we developed a nonprecious-metal/mixed oxide alternative to the platinum/mixed oxide catalyst. As shown in Figure 3, the nonprecious-metal/mixed oxide catalyst has WGS activity comparable to that of platinum/mixed oxide and does not lose activity at temperatures up to 400°C. The nonprecious-metal/mixed oxide catalyst is not initially as active as commercial copper/zinc oxide (United Catalyst Incorporated's C18-7), but the Argonne catalyst does not lose its activity after exposure to air at 230°C (Figure 4).

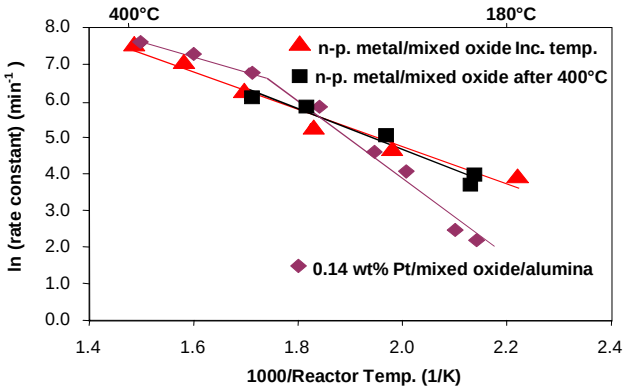

Figure 3. Nonprecious-metal/mixed oxide catalyst shows activity comparable with that of platinum/mixed oxide/alumina.

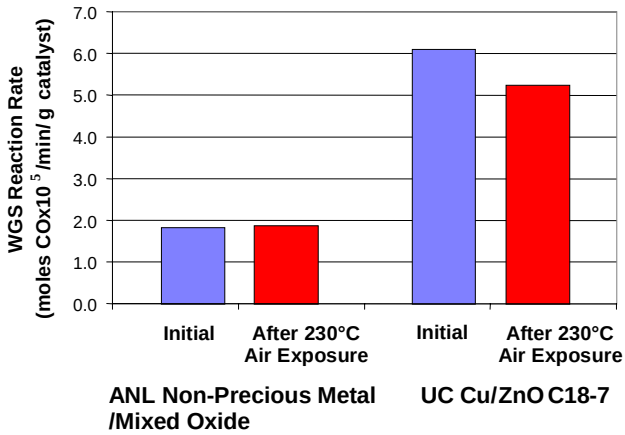

Figure 4. Nonprecious-metal/mixed oxide catalyst retains activity after exposure to air at 230°C.

Another promising nonprecious-metal WGS catalyst, developed using the bimetallic/ polymetallic oxide approach, is vanadium-cobalt oxide. This material has been prepared by two different routes: glycine-nitrate combustion and solid state synthesis. As shown in Figures 5 and 6, vanadium-cobalt oxides prepared by the glycine-nitrate process have activities (normalized to catalyst surface area) that are comparable with those of copper/zinc oxide; the activities (normalized to catalyst surface area) are higher than those of copper/zinc oxide when prepared by the solid-state synthesis route. In addition, these materials can be operated at temperatures up to 400°C and can be oxidized and re-reduced without loss of activity. They have low surface areas, and thus low overall conversions of carbon monoxide. We are currently attempting to prepare these materials in high-surface-area forms.

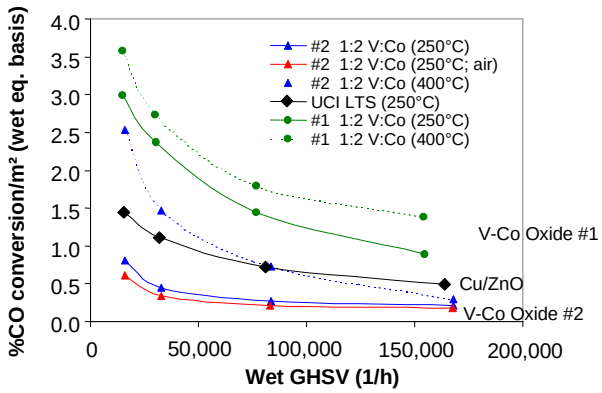

Figure 5. Vanadium-cobalt oxides prepared by combustion technique have activities (per m^2) comparable with that of Cu/ZnO.

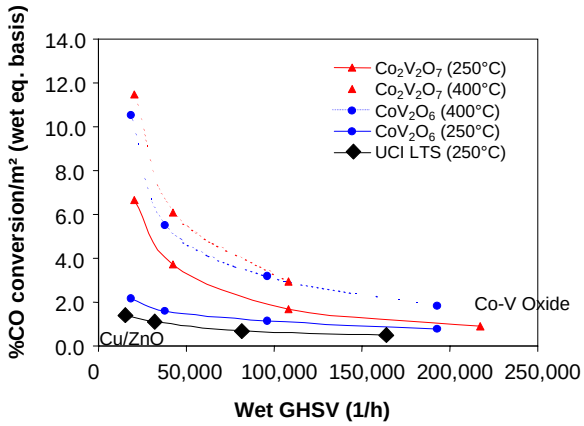

Figure 6. Vanadium-cobalt oxides prepared by solid-state technique have higher WGS activity (per m^2) than Cu/ZnO.

Conclusions

In the past year, we have demonstrated the operation of a single-stage adiabatic reactor using ANL's platinum/mixed oxide/alumina catalyst. The reactor was shown to reduce the carbon monoxide level in simulated reformate from 10.5% (dry) to 1.1% (wet) and to <1% in actual diesel reformate. During the past year, the platinum loading on this catalyst has been reduced from 0.42 wt% to 0.14 wt% while maintaining the WGS activity. Estimates based on isothermal kinetic data show that the platinum/mixed oxide catalyst has the potential to reduce WGS catalyst volume to 70% that of the commercial Fe/Cr-Cu/ZnO combination. In addition, the Argonne catalyst does not lose activity after exposure to air.

A nonprecious-metal/mixed oxide catalyst was identified that has activity comparable with that of

the platinum/mixed oxide/alumina catalyst in the 180-400°C temperature range. This material does not lose activity upon exposure to air and re-reduction at 230°C. Another alternative to the platinum catalyst, a binary oxide of cobalt and vanadium, shows promise as an inexpensive, air- and thermally-stable WGS catalyst.

IV. FUEL CELL STACK SUBSYSTEM[1]

A. R&D on a 50-kW, High-Efficiency, High-Power-Density, CO-Tolerant PEM Fuel Cell Stack System

Tim Rehg (primary contract) and Nguyen Minh
Honeywell Engines & Systems
2525 W. 190th Street, MS-36-1-93193
Torrance, CA 90504-6099
Rehg, (310) 512-2281, fax: (310) 512-3432, e-mail: Tim.Rehg@Honeywell.com
Minh, (310) 512-3515, fax: (310) 512-3432, e-mail: Nguyen.Minh@Honeywell.com

DOE Program Manager: Patrick Davis
(202) 586-8061, fax: (202) 586-9811, e-mail: patrick.davis@ee.doe.gov

ANL Technical Advisor: William Swift
(630) 252-5964, fax: (630) 272-4473, e-mail: swift@cmt.anl.gov

Contractor: Honeywell Engines & Systems, Torrance, California
Prime Contract No. DE-FC02-97EE50470, October 1997-September 2000

Objectives

Research, develop, assemble, and test a 50-kW net polymer electrolyte membrane (PEM) fuel cell stack system composed of a PEM fuel cell stack and the supporting gas, thermal, and water management subsystems. The PEM fuel cell stack system will be capable of integration with at least one of the fuel processors currently under development by Hydrogen Burner Technology (HBT) and Arthur D. Little, Inc.

OAAT R&D Plan: Task 11; Barriers A, B, C, D, and E

Approach

This phased program includes the fabrication and testing of three 10-kW subscale PEM fuel cell stacks, leading up to the final 50-kW system. Stack technology development and system analysis are conducted iteratively to identify pertinent technology advances to be incorporated into successive subscale stack builds. The final system analysis will define the 50-kW stack and system configuration.

- Phase I:
  - PEM stack R&D to demonstrate multifuel capability and carbon monoxide (CO) tolerance.
  - PEM stack R&D to advance technologies toward U.S. Department of Energy (DOE) targets.
- Phase II:
  - Subscale integration, electronic control system development, transient characteristics and durability testing.
- Phase III:
  - Testing of the 50-kW PEM fuel cell stack system.
  - Hardware delivery of 50-kW PEM fuel cell stack system.

---

[1] The DOE technical targets for fuel cell stack systems running on hydrogen-rich fuel from a fuel-flexible fuel processor can be found in Table 3, Appendix B.

Accomplishments

- A >200-ppm CO tolerance was demonstrated in single-fuel-cell tests.
- The second 10-kW-class stack containing conducting composite bipolar plates has been built and tested. This 112-cell stack showed significant improvements in cell-to-cell uniformity and attained a specific power of 0.87 kW/kg and a power density of 1.6 kW/L.
- An 82-cell stack was subjected to a 250-hour life test, running on CO-containing reformate.
- A subscale (15-cell) stack was subjected to several freeze-thaw cycles to –40°C without damage, as judged by subsequent performance testing.
- The 50-kW brassboard system design was completed. Component performances have been specified, and balance of plant component procurement is scheduled to be completed in 3Q 2000.
- Most of the balance of 50-kW brassboard plant hardware assembly (minus fuel cell stacks) will be completed in 3Q 2000.
- Controls and interfaces for real-time operation of the 50-kW brassboard are being designed, and the Hardware/ Software Interface definition is nearly complete.
- The stack engineering design has been completed for the third 10-kW subscale PEM fuel cell stack. Component procurement is in process.

Future Directions

- Build and test the third 10-kW-class PEM stack (scheduled for November 2000).
- Deliver 50-kW net PEM fuel cell stack system brassboard to Argonne National Laboratory (ANL) at the conclusion of the project (March 2001).
- Continue collaboration with ANL and fuel processor contractors on system integration issues.
- Continue to drive development toward DOE 2000 technical targets for high-volume production costs ($100/kW for 5,000,000 units/year).

Introduction

Fuel cell power plants will become viable substitutes for the internal combustion engine (ICE) in automotive applications only when their benefits of increased fuel efficiency and reduced emissions are accompanied by performance and cost comparable to those of the ICE. Meeting these requirements is a significant technical challenge that calls for an integrated systems approach. This effort encompasses the technical and developmental activities required to incorporate innovations necessary to develop a 50-kW fuel cell stack system to meet the requirements set forth by the DOE. During this reporting period, Honeywell is in Phase II of the program.

Approach and Results

The PEM fuel cell stack system consists of the fuel cell stack and supporting gas, thermal, and water management systems, as shown in Figure 1. Overall system performance depends on the careful integration of these subsystems.

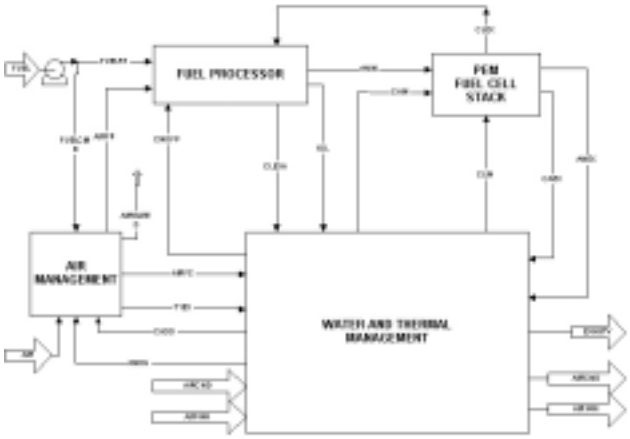

Figure 1. Performance of second 10-kW stack.

The brassboard system design for the 50-kW fuel cell stack has been completed. Six hexagonally shaped stacks are pictured in Figure 2. Component performances have been specified, and procurement of major components is nearly completed. The brassboard has been designed for 50-kW electric power output, operating at high efficiency on gasoline reformate. It incorporates full integration and management of on-board thermal, water, and air subsystems, and it makes use of off-the-shelf components to minimize cost and assembly time. Controls are being designed on the assumption of full dynamic control capability, but provisions are being made for a variety of actuation schemes. Supervisory controls and built-in tests have been partially completed. The Hardware/Software Interface definition, which is nearly complete, will be finalized once the remaining actuated control valves have been selected.

In the area of membrane electrode assembly (MEA) technology development, Honeywell has demonstrated that our cells can tolerate >200 ppm CO contamination without appreciable performance loss. Honeywell plans to use these MEAs, along with molded conducting composite bipolar plates, in the upcoming third 10-kW stack and the final 50-kW brassboard system build. The designs have been completed for these builds and the procurement is in process.

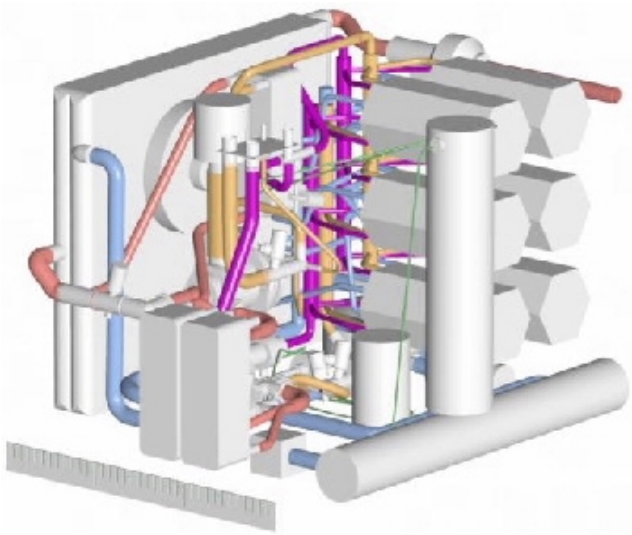

Figure 2. 50-kW brassboard system design.

The second 10-kW-class stack containing conducting composite bipolar plates has been built and tested. A comparison of the first and second stack designs is given in Figure 3, and a photo of the second stack is shown in Figure 4. This 112-cell stack showed significant improvements in cell-to-cell uniformity over the first stack (compare Figures 5 and 6). Improvements for the second stack included a new flow field with lower stoichiometry capability, conducting composite bipolar plates, 13% increase in active cell area, and substantial improvements in stack weight, volume, and manufacturability. The performance data for the second stack are presented in Table 1, and 250-hour life testing data (run on gasoline reformate/air) are indicated in Figure 7.

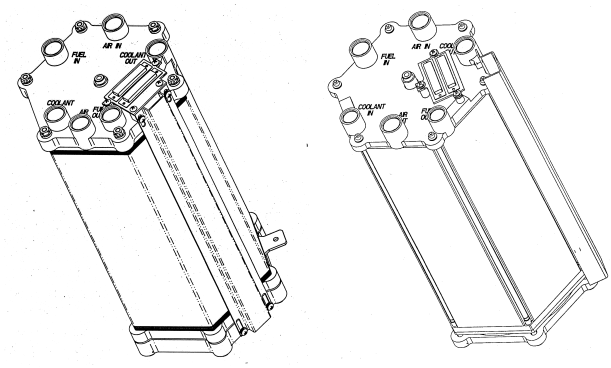

Figure 3. 10-kW stack designs. Comparison of stack I (left) and stack II (right) designs.

Figure 4. Photo of second 10-kW-class stack.

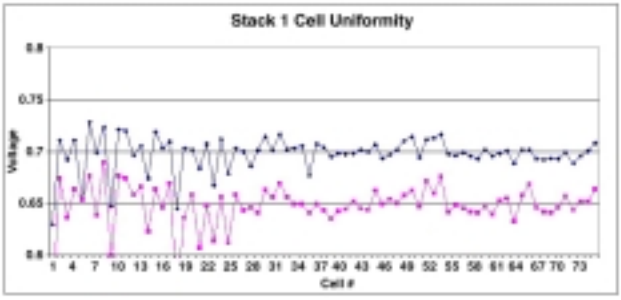

Figure 5. Stack I cell uniformity.

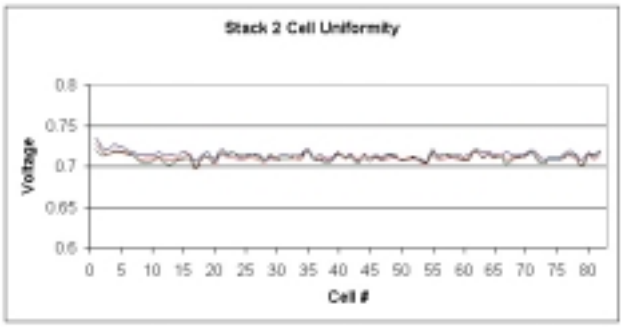

Figure 6. Stack II cell uniformity.

Table 1. Performance of second 10-kW stack.

Item	Second Stack
Number of Cells	112
Stack Weight (lb)	38
Absolute Peak Power (kW)	15
Specific Power at Peak (kW/kg)	0.87
Power Density at Peak (kW/L)	1.6
H_2 Stoichiometry at Nominal	1.25x

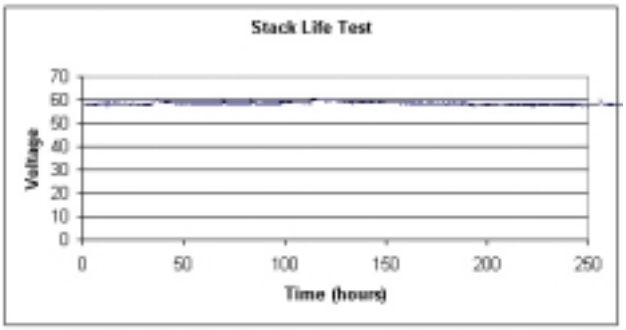

Figure 7. Stack II life test data.

Conclusions

In this reporting period, Honeywell has made the transition to Phase II of the program. The focus is now on the design and construction of the 50-kW brassboard final deliverable, incorporating our third stack design and molded composite bipolar plates. The current projected brassboard system nominal efficiency is 45% and the projected power densities are ~0.2 kW/kg and ~0.15 kW/L, versus the PNGV/DOE targets of 55%, 0.35 kW/kg, and 0.35 kW/L. It should be noted that the above numbers include contributions from off-the-shelf components for the brassboard, i.e., oversized heat exchangers and valves.

FY 2000 Publications/Presentations

- R. Loda, "Development of PEM Fuel Cells at Honeywell," presented at Long Beach 2000, Annual Battery Conference on Applications and Advances, California State University, Long Beach, Calif., Jan. 11, 2000.
- J. Ferrall, T. Rehg, and P. Sokolov, "Design and Development of an Air-Reformate PEM Fuel Cell Stack System for Light-Duty Vehicles," Paper No. 00FCC-6 presented at 2000 Future Car Congress, Arlington, Va., April 2000.
- J. Ferrall, "Automotive PEM Fuel Cell Development at AlliedSignal," presented at the Joint Fuel Cell Technology Review Conference, Chicago, Ill., Aug. 3-5, 1999.

B. Development of Advanced, Low-Cost PEM Fuel Cell Stack and System Design for Operation on Reformate Used in Vehicle Power Systems

Michel Fuchs (primary contact) and Frano Barbir
Energy Partners, L.C.
1501 Northpoint Parkway, #102
West Palm Beach, FL 33407
(561) 688-0500, fax: (561) 688-9610, e-mail: mfuchs@energypartners.org

DOE Program Manager: Donna Ho
(202) 586-8000, fax: (202) 586-9811, e-mail: donna.ho@ee.doe.gov

DOE Program Support: Larry Blair
(202) 586-0626, fax: (202) 586-9811, e-mail: larry.blair@ee.doe.gov

ANL Technical Advisor: William Swift
(630) 252-5964, fax: (630) 972-4473, e-mail: swift@cmt.anl.gov

Contractor: Energy Partners, L.C., West Palm Beach, Florida
Prime Contract No. DE-FC02-97EE50476, September 30, 1997-June 30, 2001

Objectives

- Develop low-cost bipolar collector plates through improvements in materials and processes.
- Evaluate and optimize membrane-electrode assembly (MEA) configurations with enhanced carbon monoxide (CO) tolerance and low platinum loading:
  - Stable, usable performance with steady-state CO levels of 10 ppm and transient levels of 100 ppm.
  - Platinum loading less than 0.5 mg/cm^2 per MEA.
- Design and demonstrate a reformate-capable fuel cell stack with a 50-kW$_{net}$ power output.
- Design, integrate, and demonstrate a reformate-capable 50-kW$_{net}$ automotive fuel cell power system.

OAAT R&D Plan: Task 11; Barriers A, B, C, and D

Approach

- Phase I: Demonstration and delivery of a polymer electrolyte membrane (PEM) 10-cell stack with reformate capability and 10 additional bipolar plates manufactured by the compression molding process.
- Phase II: Demonstration and delivery of a high-efficiency, reformate-tolerant 50-kW$_{net}$ fuel cell stack and power system utilizing injection-molded bipolar plates (with compression molded plates as an alternative), excluding power conditioning and fuel processor, to Argonne National Laboratory (ANL) for independent testing and verification.

Accomplishments

- Bipolar plates:
  - Completed compression molding development for high performance.
  - New injection molding of advanced molded composite bipolar plates results in high performance, low cost (<$10/kW), and 100% recyclability, with less than 20 seconds cycle time per part per machine on 232-cm^2 plates.
  - Tested injection-molded plates in a Model NG2000™ stack.

- Demonstration of hydrogen and reformate fuel cell performance:
  - Scale-up of 50-kW_{net} automotive reformate design Model NG3000™ comparable to previous 20-kW_{gross} Model NG2000™.
  - Built and tested 10-cell Model NG3000™ on H_2/air.
  - Achieved target performance with 10-cell Model NG3000™ on reformate/air.
  - Completed nearly 2000 hours of endurance testing.
  - Performed freeze-tolerance testing with coolant temperature down to −10°C.
  - Performed cold start-up testing from −40°C, with stack in an environmental chamber.
  - "Field" tested an 8-kW_{gross} Model NG2000™ (hydrogen fuel cell stack) in a Deere & Co. Gator™ industrial vehicle.
- Packaged 50-kW_{net} system components into an automotive test stand.
- System optimization and analysis:
  - Performed trade-off studies to increase efficiency to perform at temperature extremes.
  - Reduced componentry with thermally integrated system approach.
  - Water balance achievable.
  - Tested Arthur D. Little compressor-expander under simulated system conditions.
  - Enhanced 50-kW_{net} system model using actual component performance data.

Future Directions

- Continue evaluations of new MEA materials for reformate performance.
- Optimize bipolar material compounding process and increase conductivity.
- Injection-mold net-shaped bipolar plates with all features (500 cm^2).
- Injection-mold large-scale blank bipolar plates (1000 cm^2).
- Deliver reformate-tolerant 10-cell stack.
- Finish fabrication, assembly, controls, and testing of the 50-kW_{net} system and prepare it for delivery.

Introduction

Energy Partners' program objective is to develop a state-of-the-art, reformate-tolerant PEM fuel cell stack and integrate it into a reformate-capable operating system that meets automotive design requirements. The development effort, focused on a systems approach, is broken down into three discrete areas: bipolar collector plates, PEM fuel cell stack, and integrated system.

Results

Composite Bipolar Collector Plate Development

An optimal bipolar collector plate should be low-cost, impermeable, highly conductive, chemically inert, lightweight, and easily manufactured. The available choices for PEM fuel cells are metals, graphite, and graphite-composite materials. Energy Partners has used compression-molded graphite composite plates in all of its fuel cell stacks since 1992. With the advances made in fillers, binders, and processes, these plates have properties comparable to those of pure graphite. However, compression molding is not suitable for automotive-style mass production because of its long processing time and high energy consumption.

Energy Partners is developing materials and processes suitable for high-speed injection molding (patents pending). Graphite materials are initially compounded with thermoplastic polymers and formed into pellets in a continuous process. We have demonstrated a production rate of over 60 kg/h, with much higher rates possible on larger machines.

Composite bipolar plates are currently injection-molded with cycle times under 20 seconds. With proper tool design, cycle time can be reduced to about 10 seconds. This is more than 8 times faster than injection-molded processes for conductive thermoset materials. By comparison, Energy Partners' thermoplastic technology offers greatly

reduced cycle time and processing cost, improved hydrolytic stability and corrosion resistance, and potential for recycling. Table 1 compares properties of Energy Partners' compression- and injection-molding technologies to specified DOE requirements.

Recently, 500-cm^2 injection-molded blank plates were machined to include fluid flow fields and evaluated in a fuel cell stack. For comparison, cells containing Energy Partners' compression-molded plates (performance similar to that of cells using POCO graphite plates) were assembled in the stack adjacent to the injection-molded plates. The polarization curves for a 4-cell stack are shown in Figure 1. The difference in performance corresponds to higher conductivity for compression-molded plates. Work in progress indicates that optimization of the formulation and compounding process will provide injection-molded plates with improved conductivity. Figure 2 shows some of the current collector plates molded at Energy Partners.

PEM Fuel Cell Stack

For the past year, work has been focused on testing short fuel cell stacks of both the NG2000™ (~300 cm^2) and NG3000™ (~600 cm^2) designs. The program baseline is the advanced hydrogen PEM fuel cell stack NG2000™ rated at 20 kW_{gross}, which also has a reformate-tolerant equivalent (NG2000R™). The new NG3000™ was designed specifically for reformate, with automotive design criteria as specified by the program (50 kW_{net}). Testing has shown comparable performance of both the NG2000™ and NG3000™ designs (Figure 3). A 10-cell version of the NG3000™ (Figure 4) was also assembled and tested to obtain information related to scaling up the design. The 10-cell version exhibited very good cell-to-cell consistency (i.e., there was very low variation in voltage between the individual cells, even at high current densities). Figure 5 shows cell-to-cell voltage variation at different current densities.

The configuration of both the NG2000™ and NG3000™ is flexible, ranging from 2 to 250 cells.

Table 1. Bipolar plate status and properties.

Plate Property	Compression (complete)	Injection (in progress)	DOE Specs.
Bulk conductivity	>320 S/cm	>110 S/cm	> 100 S/cm
	4-point probe method		
Surface resistance	<30 mΩ-cm^2	<50 mΩ-cm^2	None
	<20 mΩ-cm^2 (POCO)		
Corrosion rate	< 16 μA/cm^2	< 16 μA/cm^2	< 16 μA/cm^2
H_2 permeability	<<2 x 10^{-6} cm^3/cm^2-s	<< 2 x 10^{-6} cm^3/cm^2-s	< 2 x 10^{-6} cm^3/cm^2-s
Crush strength	~14,000 psi	~14,000 psi	None
Flexibility (modulus)	1.35 x 10^6 psi	>1 x 10^6 psi	None
Flexural strength	6,000-6,500 psi	6,500-9,000 psi	None
Material cost	~$7.5/kW	~$7.5/kW	None
Manufactured cost estimate	$146/kW	<$10/kW	$10/kW
Production cycle time	< 40 min	< 20 s	None
Recyclability	None	100%	None
Durability @ 60°C	>5,000 h	>5,000 h	None
Dimensions:	In Production	Development	None
Total plate	1,045 cm^2	500 cm^2	
Active area	600 cm^2	300 cm^2	
Thickness	<3.0 mm	<3.0 mm	
Weight	~ 450 g	< 200 g	
Material density	2.0-2.2 g/cm^3	~2.0 g/cm^3	None

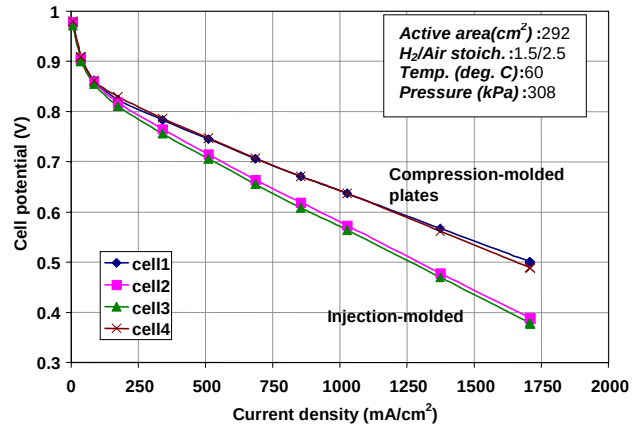

Figure 1. Injection- vs. compression-molded plates.

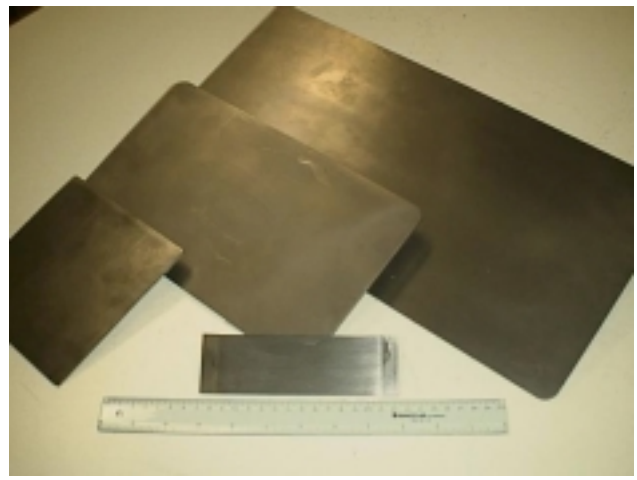

Figure 2. Compression- and injection-molded bipolar plates.

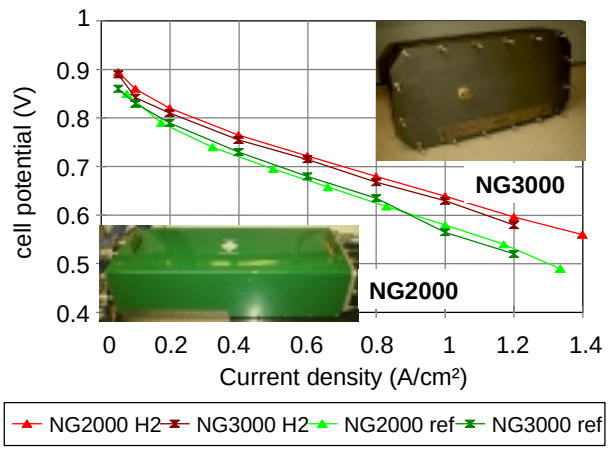

Figure 3. Comparison of NG2000™ and NG3000™ stacks on hydrogen and on reformate.

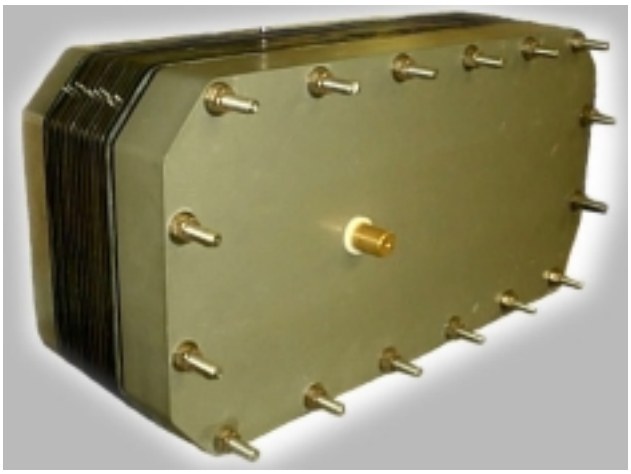

Figure 4. NG3000™ 10-cell stack.

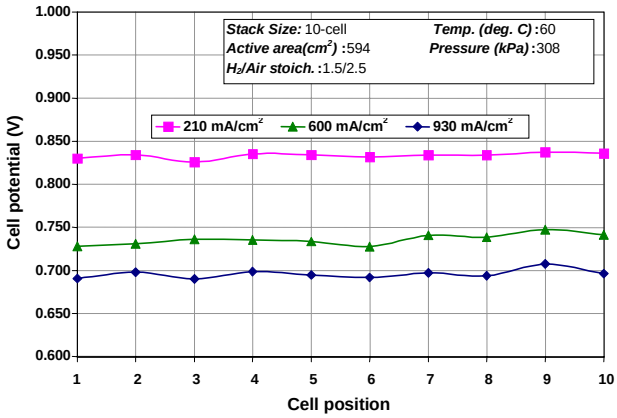

Figure 5. NG3000™ 10-cell stack, cell voltage variation on H_2/air.

They operate at between 0.2 and 3 atm pressure with reformate (40% H_2, 40%N_2, 20%CO_2) and are CO-tolerant to 100 ppm (steady state). Testing has shown durability of nearly 2000 hours on a NG2000™ 4-cell stack running on hydrogen. Figure 6 shows that after nearly 2000 hours, performance still remains relatively constant.

To prove automotive design concepts on actual hardware, freeze-tolerance testing was performed with the stack coolant temperature as low as –10°C. Figure 7 shows performance of the stack when held for one hour at negative 10°C and 15 minutes at all other temperatures. In addition, Los Alamos National Laboratory has been able to successfully start up an NG2000™ 12-cell stack from –40°C, with the use of an environmental chamber.

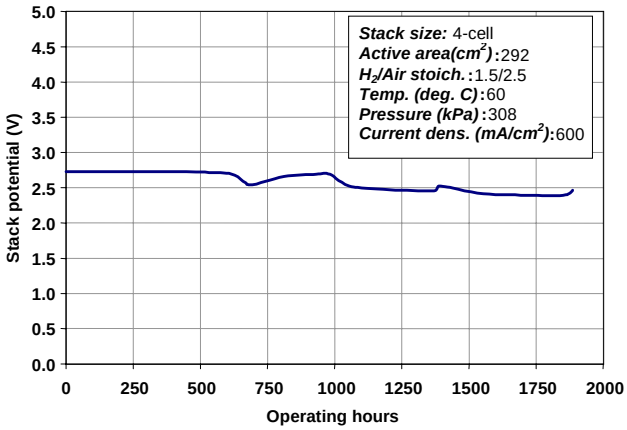

Figure 6. Durability of a 4-cell stack @0.60 A/cm^2 at 100% humidification on H_2/air.

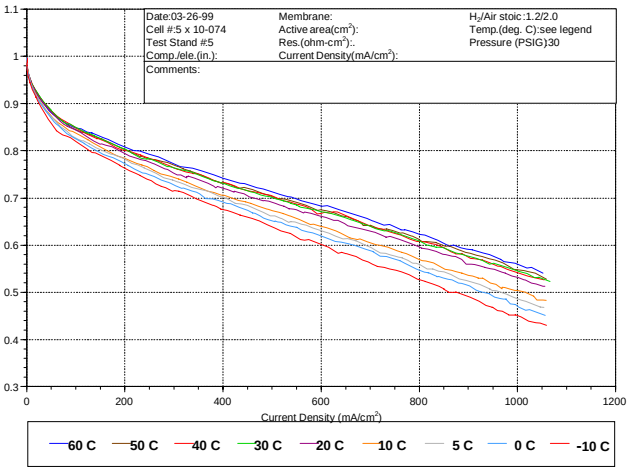

Figure 7. Freeze-tolerance performance on H_2/air at 1.2/2.0 stoich.

Since the introduction of the Model NG2000™, two in-vehicle evaluations of the stack have taken place. The first was in Virginia Tech's hybrid vehicle, which took second place in the 1999 FutureCar Challenge. The second was in a Deere & Co. Gator™ industrial vehicle, which used an 8-kW_{gross} version of the stack (Figure 8). Both vehicles provided extensive information on our fuel cell in an actual vehicle application.

Integrated System Analysis

The system simulations that were previously performed were enhanced by incorporating actual system component performance data. All of the major system components [i.e., radiator fan motor, compressor/expander system (Figure 9), and coolant pump] were tested individually under the integrated system operating envelope. This enabled the integrated system model to provide more realistic performance information (Table 2).

Operating conditions were optimized to permit the smallest heat-exchanger equipment size while maintaining water balance. The resulting system is shown in Figures 10 and 11. A control strategy was developed to maintain neutral water balance over the entire system operating range (kW) and under different ambient conditions (patent pending). Simplified humidification techniques were investigated, which led to the design and certification of an air humidifier able to meet the necessary requirements.

Rapid start-up from an extreme ambient temperature of –40°C is possible with Energy Partners' system design. Experimental results from freeze-tolerance tests (explained earlier) were used in the simulations. The quick start-up feature is the result of optimal utilization of feed gas thermal energy and fuel cell stack thermal dissipation (patent pending). Currently, the integrated system's impact on the start-up process, from –40°C, is being investigated at Los Alamos National Laboratory (LANL).

Figure 8. NG2000™, 8 kW, installed in Deere & Co. Gator™ industrial vehicle.

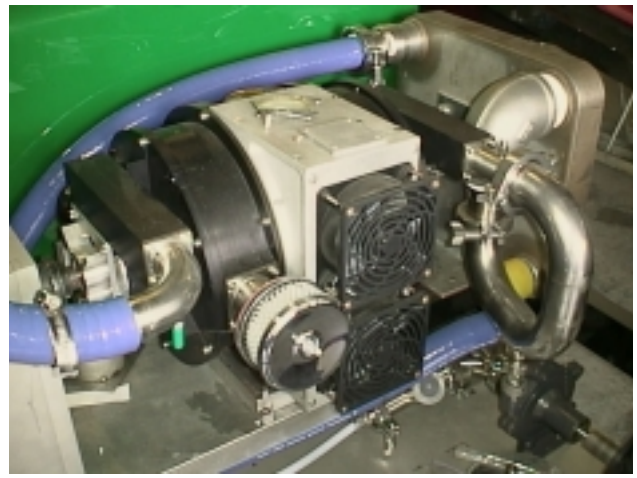

Figure 9. Picture of Arthur D. Little compressor/ expander machine.

Table 2. Energy Partners' status vs. DOE goals.

Characteristic	EP Status (7/00)	DOE Goals
System efficiency @50 kW_{net} (wo/FP) @12.5 kW_{net} (wo/FP)	 42-44% 50-51%	 ≥44% ≥55%
Net power density (W/L)	163 W/L	350 W/L
Net specific power (W/kg)	116 W/kg	350 W/kg
Cost/kW	<100 (est.)	100/kW
Durability	>1880 h	2000 h
Emissions	<<Tier 2	<<Tier 2
Transient performance (10% to 90%)	~0 s	3 s
Precious metal (anode + cathode)	0.6 mg/cm^2, 1.17 g/kW	0.5 mg/cm^2, 0.9 g/kW
Cold start-up to full power –40°C 20°C	 <5 min 97% in ~0 s	 5 min 1 min
CO tolerance (<20 mV loss at 0.7 V) (steady state)	~0 mV with 2% air bleed	>10 ppm
CO tolerance (<20 mV loss at 0.7 V) (3-s transient)	~0 mV with 2% air bleed	>100 ppm

Conclusion

Energy Partners is developing an automotive fuel cell power system to meet DOE performance goals. Significant progress has been made in

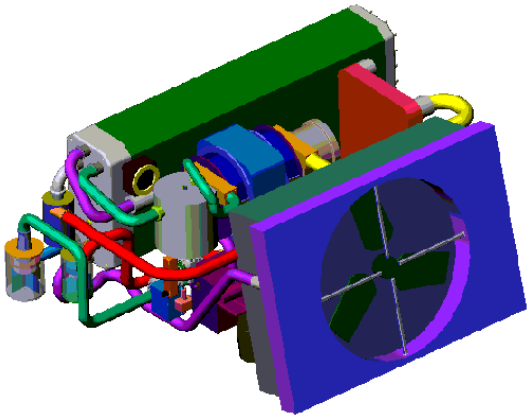

Figure 10. Resulting 50-kW_{net} automotive system.

Figure 11. Picture of 50-kW_{net} automotive system.

development of mass-producible bipolar plates, in stack and system design, and in development of a control strategy that will result in neutral water balance over the entire system operating range and under different ambient conditions.

Presentations/Publications:

- M. Fuchs, F. Barbir, and M. Nadal, "Fuel Cell Powered Utility Vehicle with Metal Hydride Fuel Storage," submitted to the GlobeEx 2000 Conference, Las Vegas, Nev., July 2000.
- F. Barbir, "Recent Progress and Remaining Technical Issues in PEM Fuel Cell Development," submitted to the World Hydrogen Energy Conference, WHEC XIII, Beijing, China, June 2000.
- F. Barbir, "Air, Water and Heat Management in Automotive Fuel Cell Systems," presented at the Intertech Conference on Commercializing Fuel Cell Vehicles 2000, Berlin, Germany, April 2000.
- M. Fuchs, F. Barbir, A. Husar, J. Neutzler, D. Nelson, and M. Ogburn, "Performance of Automotive Fuel Cell Stack," presented at the 2000 Future Car Congress, Arlington, Va., April 2000.
- F. Barbir, "Bi-polar Plates, Flow Fields and Stack Design Criteria," presented at the American Physical Society Meeting, Minneapolis, Minn., March 2000.
- F. Barbir, M. Fuchs, A. Husar, and J. Neutzler, "Design and Operational Characteristics of Automotive PEM Fuel Cell Stacks," Fuel Cell Power for Transportation, SAE SP-1505, Proc. SAE International Congress & Exhibition, Detroit, Mich., March 2000, pp. 63-69, SAE, Warrendale, Pa., 2000.
- V. Gurau, F. Barbir, and H. Liu, "An Analytical Solution of a Half-cell Model for PEM Fuel Cells," *Journal of Electrochemical Society*, Vol. 147(7), 2000.
- F. Barbir, M. Nadal, and J. Neutzler, "Development of PEM Fuel Cell Power Systems for Transportation Applications," presented at the IQPC Conference, Fuel Cell Technology Asia 99, Tokyo, Japan, Dec. 1999.
- F. Barbir, B. Balasubramanian, and J. Neutzler, "Trade-off Design Study of Operating Pressure and Temperature in PEM Fuel Cell Systems," Proc. ASME Advanced Energy Systems Division – 1999 ASME International Mechanical Engineering Congress & Exposition, AES Vol. 39, pp. 305-315, ASME, 1999.
- F. Barbir, B. Balasubramanian, and J. Neutzler, "Optimal Operating Temperature and Pressure in PEM Fuel Cell Systems in Automotive Applications," Proc. 218th ACS National Meeting, Vol. 44, No. 4, pp. 977-981, American Chemical Society, 1999.
- F. Barbir, J. Braun, and J.Neutzler, "Properties of Molded Graphite Bi-Polar Plates for PEM Fuel Cells," *International Journal on New Materials for Electrochemical Systems*, No. 2, pp. 197-200, 1999.

C. Cold-Start Dynamics of a PEM Fuel Cell Stack

Kirk Weisbrod (primary contact), Jim Hedstrom, José Tafoya, Rod Borup, and Mike Inbody
Los Alamos National Laboratory
MS J576, Los Alamos, NM 87545
(505) 665-7847, fax: (505) 667-0600, e-mail: weisbrod@lanl.gov

DOE Program Manager: JoAnn Milliken
(202) 586-2480, fax: (202) 586-9811, e-mail: joann.milliken@ee.doe.gov

---

Objective

Develop cold-start strategies for stacks through the use of models, verified by experiments.

OAAT R&D Plan: Task 11; Barriers B and C

Approach

- Develop a global model of heat requirements and water transients associated with start-up from subfreezing temperatures.
- Experimentally verify two cases:
  - Autothermal start-up, applicable with stored hydrogen.
  - Start-up with coolant heated by fuel processor waste heat.

Accomplishments

- Developed two transient models for stack/system start-up.
- Completed test apparatus in an environmental chamber that operates down to –40°C.
- Performed initial cold start-up tests with 12-cell stack from Energy Partners.

Future Directions

Complete autothermal and coolant-heated cold-start tests, using electrochemical impedance diagnostic tools to characterize stack and individual cell performance.

Introduction

Rapid fuel cell system start-up to full power is an automotive requirement. Quantification of limiting parameters on cold-start stack response starting from –40°C is the primary objective of this study. Start-up of the stack on reformate at low temperature is hindered by high sensitivity of the anode catalyst to CO poisoning, low ionomer conductivity, potential blocking of the catalyst layer through ice accumulation in the backing layer, and ice plugging of feed channels. Through measurements and generic model predictions, fuel cell subsystem and component requirements will be defined.

Approach

Two models were developed. An autothermal model represented start-up on stored hydrogen gas. An overall heat and mass balance was defined around the stack. Assumptions for the autothermal model include the following:

- No interaction with a coolant system takes place.
- Measured polarization curves are available down to –10°C. Below –10°C, the curves are estimated.
- Dry air is available from a compressor at 78°C (isentropic compression from –40°C).

- Vent gases leave the stack at 100% relative humidity.
- Bipolar plates are thermally isolated from the end plates.

The second model included an external heat source that simulated waste heat from a fuel processor. Equations were solved by the Applied Engineering Equation Solver (EES) software from F-Chart Software.

All stack hardware, including the stack cooling loop, was installed in an environmental chamber that operated down to – 40°C. A 12-cell stack specifically designed by Energy Partners for cold-start tests was used. A schematic of the flow loop, given in Figure 1, includes a reservoir containing a 60% ethylene glycol/water mixture and a heating element. Coolant is pumped through the fuel cell stack cooling channels and returns to the reservoir until the stack reaches operating temperature. Subsequently, coolant may be circulated through the heat exchanger, which removes waste heat to the environmental chamber. Figure 2 shows the equipment layout.

Results and Discussion

Autothermal modeling results predicted both the temperature rise and the accumulation of water in the backing layer. It was assumed in the simulation that 0.5 A/cm^2 was produced until the stack reached 0°C. After that point, a constant current of 1 A/cm^2 was produced by the stack. Figure 3 indicates that approximately 6.5 minutes would be required to reach an operating temperature of 60°C.

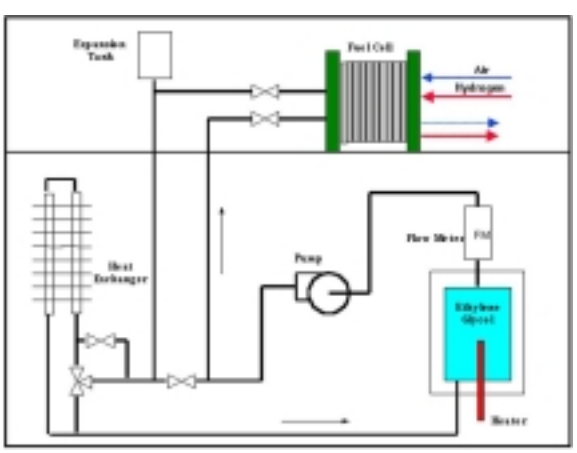

Figure 1. Schematic of the cold-start system with external heat source.

Figure 2. Environmental chamber and apparatus for cold-start measurements.

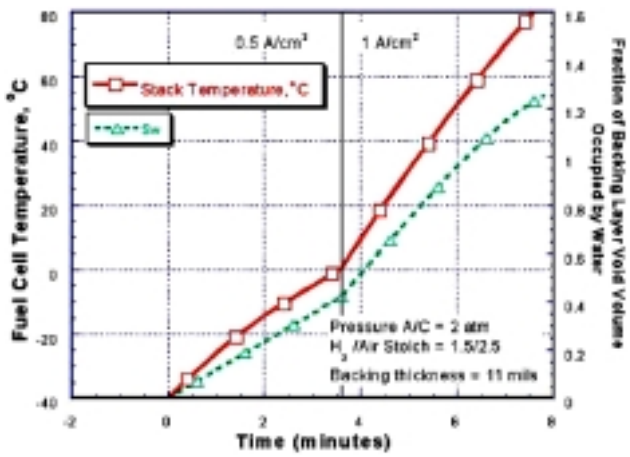

Figure 3. Autothermal cold-start predictions of cell temperature and water saturation.

The fraction of the pore volume, within an 11-mil-thick backing layer, that would be occupied by ice was also calculated. To reach 0°C, approximately 40% of the void volume of the cathode backing layer would be occupied. The impact of ice upon gas diffusion into the active catalyst layer, though it is uncertain at this time, will be evaluated in future experiments.

Figure 4 illustrates the impact of constant voltage control instead of constant current. Under a constant average cell voltage of 0.3 V, the stack reached operating temperature 1.5 minutes earlier. Greater chemical energy was converted to heat at current densities up to 2 A/cm^2.

Multiple start-up tests were conducted with the Energy Partners stack and cooling loop, starting from –40°C. Start-up with simulated waste heat from the fuel processor involved use of 2 kW heat input up to 0°C, followed by full power draw at 1 A/cm^2 with feed gas humidification. Figure 5

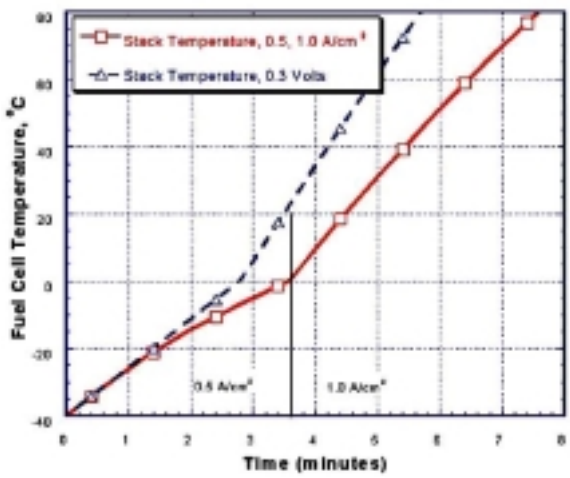

Figure 4. Autothermal cold-start model results for current vs. voltage control.

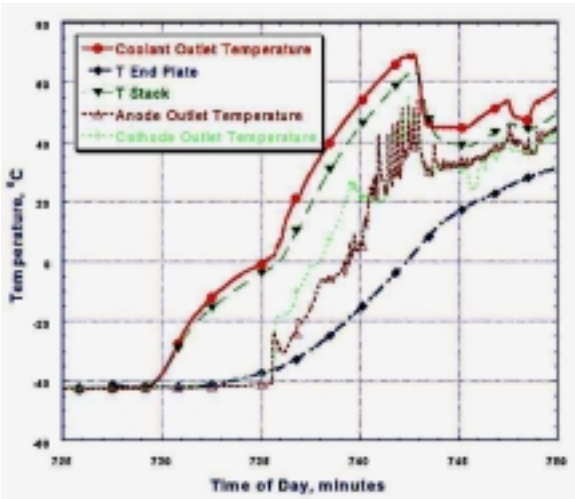

Figure 5. Temperature history during cold start of the Energy Partners' stack.

traces heating transients. The outlet gas temperatures rose when gas flow began at 0°C. Stack end plates lagged in temperature.

System transients were modeled as described above. A match between system performance and model results is given in Figure 6. On the basis of the validated model, predictions were made of heat-up rate. Figure 7 indicates that with no external heat input, 20 minutes is required to bring the stack to operating temperature (60°C). With 5 kW of input, 5 minutes is required. To attain the FY2004 goal of 0.5 minute for stack heat-up, approximately 50 kW of heat would be required for this specific system. Thus, coolant system thermal mass will have to be minimized.

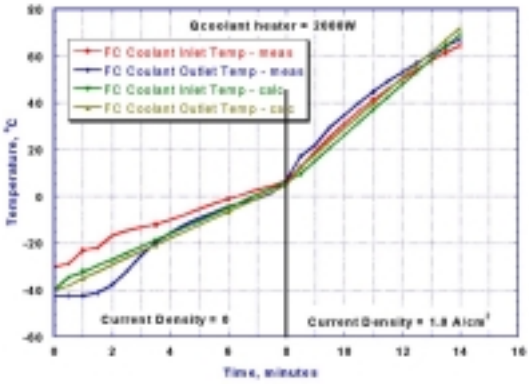

Figure 6. Validation of fuel cell/system model.

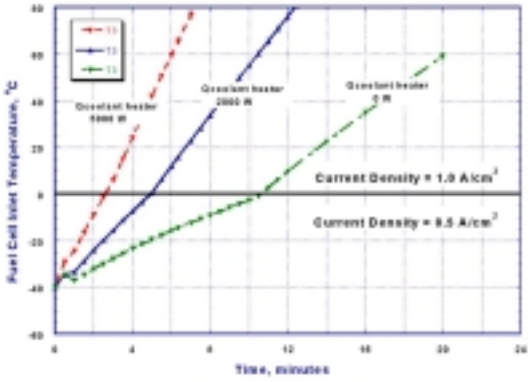

Figure 7. Model predictions for fuel cell/coolant system.

Conclusions

The following operation and design guidelines are recommended to minimize start-up times. For autothermal start-up:

- Reduce the thermal load of end plates on the stack by thermal isolation or by lowering their heat capacity or thermal conductivity.
- If feasible, operate the stack at a constant low stack voltage to maximize stack heat production.
- Use dry feed gases up to 0°C to eliminate plugging of feed lines and internal stack components with ice.

Additional issues connected with start-up when an external heat source is available include the following:

- The thermal mass of the coolant flow loop should be minimized.
- A large external heat source is required to obtain start-up times approaching 0.5 minutes.

D. Efficient Fuel Cell Systems

Mahlon S. Wilson (primary contact), Steffen Moeller-Holst, and Christine Zawodzinski
Los Alamos National Laboratory
Materials Science and Technology Division, MST-11, MS D429
Los Alamos, NM 87545
(505) 667-6832, fax: (505) 665-4292, e-mail: mahlon@lanl.gov

DOE Program Manager: JoAnn Milliken
(202) 586-2480, fax: (202) 586-9811, e-mail: joann.milliken@ee.doe.gov

---

Objective

Develop a simple, low-parasitic-power, low-cost fuel cell system with high net power densities and efficiencies.

OAAT R&D Plan: Task 13; Barriers B and C

Approach

- Utilize direct liquid water hydration of the membrane/electrode assemblies (MEAs).
- Operate the cathodes at near-ambient pressures to attain minimal parasitic power losses.
- Operate the stack in an "adiabatic" configuration.

Accomplishments

- Demonstrated a surplus water balance with <2% parasitic power at nominal power (and high-altitude conditions).
- Demonstrated system efficiencies on neat hydrogen that exceed 55% (low heat value, LHV, of hydrogen) at nominal power.
- Attained *net* stack volumetric power densities of 350 W/L (based on the graphite bipolar plate area) or 450 W/L (based on active area) at nominal power.
- Simplified system to require a single water pump to handle both water makeup and recirculation.

Future Directions

- Further simplify system (e.g., by eliminating the hydrogen recirculation pump).
- Simplify stack design and decrease unit cell thickness by introducing new design approaches.
- Improve stack performance and reliability.

Introduction

Of all the potential fuel cell markets, transportation is probably the most demanding and competitive. The challenge for fuel cells becomes more severe if the overall systems are highly complex and intrinsically expensive. Therefore, the basic thrust of this effort is to develop a fuel cell system that is as simple as possible but still provides competitive net power densities and efficiencies.

The primary benefits of simplicity are low costs and reliability, both critical factors in the competitive transportation market. As systems become simpler, the parasitic power requirements of the peripherals are inherently lower. It is possible to attain overall high efficiencies and power densities by minimizing parasitic power losses instead of maximizing stack performance (i.e., pressurized systems).

Approach

The key to simplifying our fuel cell system is to directly humidify the fuel cell membrane/electrode assemblies (MEAs) with liquid water, as previously developed in this program. The humidification is accomplished by the introduction of an anode wicking backing, which conveys liquid water in the anode flow-field plenum through the nominally hydrophobic gas diffusion layer directly to the membrane throughout the active area.

A second critical element is the operation of the air-side of the fuel cell stack at very near ambient pressure; even relatively modest pressures can result in surprisingly high power requirements. For this reason, inlet air pressures of less than six inches of water are targeted. With the use of the membrane hydration scheme described above, the higher pressure drops associated with humidification modules, internal manifolding, and two-phase flows in the cathode channels are eliminated, which allows the use of low air pressures in our system.

The result of operating a well-humidified fuel cell stack with a dry, ambient-temperature cathode air inlet is that the airstream becomes heated and water-vapor-saturated as it passes through the cells. This configuration then provides *in situ* evaporative cooling of the stack, which eliminates the need for a separate cooling system or cooling plates within the stack. Since evaporation is a very effective heat-transfer mechanism, the waste heat is transferred to the air as generated and where generated. The air inlet is at room temperature and the effluent is at 60–70°C, so a large temperature gradient develops across the stack. This differs from most fuel cell stack designs, which typically strive to attain isothermal conditions. In our case, the stack is designed to encourage a monotonically increasing temperature as the air passes through it, to discourage any condensation from occurring within the flow-field channels. This general scheme of nonisothermal operation with *in situ* evaporative cooling results in an "adiabatic" stack.

Since the system relies on evaporative cooling instead of conventional stack cooling plates and radiator, the ability to maintain a net positive water balance under standard and more severe ambient conditions is among the issues addressed this year.

Results

Over the past year, the adiabatic stack system has been further simplified. A current schematic of our roughly 1.5-kW system is depicted in Figure 1. Water recirculation through the stack (for the direct liquid hydration) and makeup from the ambient-pressure main water reservoir are now accomplished by using a single water pump in conjunction with a pressure switch and float valve. With this scheme, a second pump, liquid level controller, and motor controller are eliminated or replaced by lower-cost, nonpowered components.

One of the primary issues with utilizing evaporative cooling in the adiabatic stack system was the ability to operate with a net positive water balance. A plastic flat-plate condenser with a roughly 1/6-ft^3 exchange volume and a 12-W cooling fan was used for water recovery from the cathode effluent. In the water balance tests, the thermally isolated end plates were heated to minimize passive cooling that would skew the water recovery results. In a typical run at 24°C ambient temperature, the 26-cell, 300-cm^2-active-area stack was operated at a voltage of 17.5 V (0.673 V/cell, or a voltage efficiency of 57% based on LHV of hydrogen) and a current of 83 A, for 1.45 kW gross power. The blower provided roughly three times stoichiometric air flow at a 5.5-in. H_2O inlet pressure. The total power draw for the various components (blower, hydrogen and water pumps, and condenser fan) was 26.1 W, or 1.8% of the stack power. Net power is then 1.43 kW at a 56% overall efficiency. Surplus water was recovered at a rate of 2.5 g/min.

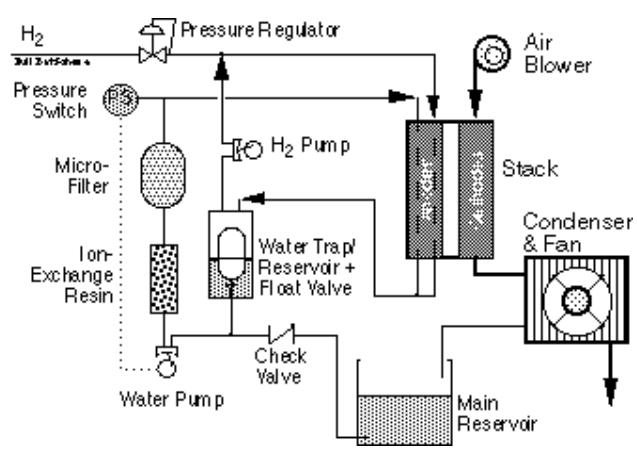

Figure 1. Schematic of the adiabatic stack fuel cell system.

While surplus water was easily recovered under the high desert conditions (0.76 ambient pressure, 24°C, low humidity) in the experiment described above, a parametric study using a system heat and mass balance model was used to anticipate water recovery under other scenarios (e.g., Florida). Whereas the effect of humidity is relatively insignificant, much more critical factors are the ambient temperature and pressure, because the condenser inlet temperatures increase strongly with both. In addition, the heat-transfer coefficients are proportional to ambient pressure. The net result is that, for equivalent condensers and cooling air mass flow rates, operating at a 25°C ambient temperature in Los Alamos (0.76-atm ambient pressure) is akin to operating at a 40°C ambient temperature at sea level. For this and other reasons, it may be that evaporative cooling plus water recovery is actually a superior alternative to the conventional radiator plus coolant approaches.

The less than 2% parasitic power level is of critical importance to allow the modest performance of the adiabatic stack to compete favorably with pressurized fuel cell stacks in terms of *net* power density and efficiency. The parasitic power significance is illustrated in Figure 2. Here, a

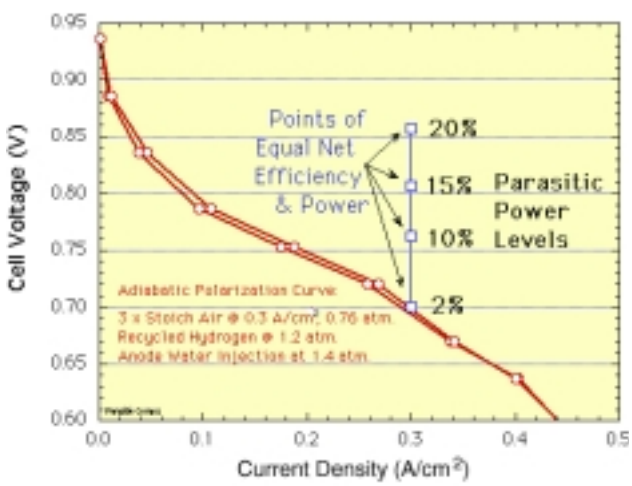

Figure 2. Effect of parasitic power requirements on net efficiencies.

polarization curve depicting the rather modest performance of the adiabatic stack is depicted. However, for a higher parasitic power (e.g., pressurized) system to match the net efficiency of the adiabatic stack, it must operate at a higher cell voltage. For example, if a system has a 15% parasitic power level (probably optimistic for a 30-psig stack), then it must operate at about 0.81 V/cell to attain the same net efficiency. The unit cells will actually need to be thinner to achieve the same *net* power density, because the pressurized stack must also accommodate cooling plates etc.

Conclusions

A complete and simple version of an adiabatic stack system has been developed and demonstrated. Water self-sufficiency has been shown to be readily achievable. System modeling indicates that the experimental results attained at high altitude are equivalent to those for sea-level conditions (i.e., 40°C ambient temperature). Parasitic power levels of less than 2% have been demonstrated. Because of such low losses, *net* power efficiencies and power densities of the adiabatic stack are comparable with those for pressurized stacks. All else being equal, it would appear that the adiabatic system's intrinsic simplicity and low cost would give it a competitive edge over pressurized systems for transportation applications.

Patents Issued/Pending

1. M. S. Wilson, "Fuel Cell Membrane Humidification," U.S. Patent No. 5,952,111.
2. M. S. Wilson, "Ambient Pressure Fuel Cell System," U.S. Patent Pending.

E. Direct Methanol Fuel Cells

Xiaoming Ren, Piotr Zelenay, Huyen Dinh, John Davey, and Shimshon Gottesfeld (primary contact)
Los Alamos National Laboratory, Los Alamos, NM 87545
(505) 667-6853, fax: (505) 665-4292, e-mail: gottesfeld@lanl.gov

DOE Program Manager: JoAnn Milliken
(202) 586-2480, fax: (202) 586-9811, e-mail: joann.milliken@ee.doe.gov

---

Objectives

Develop materials, components, and operation conditions for direct methanol fuel cells (DMFCs) so as to prove the potential of DMFCs for transportation applications in terms of power density, energy-conversion efficiency, and cost. *Specifically,*

- Continue to optimize anode and cathode catalyst layers to enhance cell performance;
- Prove that low fuel utilization can be resolved through a combination of ionomeric membranes of good protonic conductivity and optimized stack structure and operation conditions; and
- Prove the stability of all cell components – primarily anode catalyst – in longer-term operation subject to these combined requirements.

OAAT R&D Plan: Task 14; Barriers B, F, H, and I

Approach

- Operate DMFCs and stacks near 100°C with a variety of membrane/electrode assemblies (MEAs), using optimized catalyst layers to demonstrate performance and stability.
- Optimize other cell components, including backing layers and bipolar plate/flow fields, to maximize demonstrated performance in DMFC small stacks operating near 100°C.

Accomplishments

- *Small DMFC Stack Development*: 30-cell, 45-cm^2 active area, methanol/air stack fabricated, employing Los Alamos National Laboratory (LANL) hardware; 80 W generated by stack in initial testing near ambient conditions (200 W expected near 90^oC).
- *Lowered Pt Loading*: Low-Pt DMFCs (50 cm^2) demonstrated: 5 g Pt/kW, with peak power of 0.15 W cm^{-2}; 2 g Pt/kW with peak power of 0.12 W cm^{-2}.

Future Directions

- Further lowering of precious catalyst loading.
- Possible scale-up of stack to the 1.0-kW level (budget permitting).

Introduction

The objective of the direct methanol fuel cell effort at LANL, sponsored by the U.S. Department of Energy's Office of Advanced Automotive Technologies (DOE/OAAT), has been to develop materials, components, and operation conditions for such cells and small stacks, to prove their potential for transportation applications in terms of power density, energy conversion efficiency, and cost. Introduction of a DMFC as a primary power source for transportation could provide the combined attractive properties of a liquid fuel of good potential availability, high system simplicity (liquid fuel + air *in*, DC power *out*), good potential for packaging as required to achieve 350-mile range in a passenger

vehicle, and good potential for achieving zero-emission-vehicle (ZEV) characteristics.

Results

Our DMFC work in fiscal year (FY) 2000 included advances in DMFC stack component development, stack assembly, and stack testing. In addition, we made significant headway in demonstrating DMFCs with catalyst loadings that were lower by a factor of 10 compared with the loading used in military applications of the technology, at a cost in peak power of only about 30%. The demonstration of operation on such lower-Pt loadings has provided hope for bringing precious-metal catalyst levels in DMFCs to within a factor of two of the precious metal level per kilowatt used today in fuel cell systems, based on on-board reforming. Figure 1 shows a comparison at 100°C and 110°C of DMFC (single-cell) performance on >10 mg Pt/cm^2 and on <1 mg Pt/cm^2. It is clear that the lowering in peak power, observed as a result of lowering the Pt loading by an order of magnitude, is rather modest. The trade-off between DMFC Pt loading per kilowatt and cell peak power is summarized in Table 1. For comparison, fuel cell power systems based on reforming-on-board use at present attain near 2 g Pt/kW, while generating stack peak power near 0.5 W cm^{-2}.

We extended our DMFC work to the level of a 30-cell stack of 50-cm^2 cells, shown in Figure 2. Novel stack hardware has been developed in-house. We have demonstrated initial power output of 80 W under close-to-ambient conditions, and by the end of this calendar year we expect to be able to demonstrate 200 W from the same stack under the higher temperature and pressure applicable for transportation applications. We showed that very effective packaging could be achieved with our stack structure, which has a pitch per cell of 2 mm, or 5 cells/cm. This corresponds to a power density of 1 W/cm^3, or 1 kW/L of active volume of the stack when operated at a higher temperature, around 90°C, and at 30-psig air. We see the success in building the small stack as a substantial basis for scale-up to the 1-kW level.

Another important demonstration this year was the applicability of "factory-grade" methanol to DMFC operation, without any further purification. Analytic-grade methanol and methanol from the factory gate yielded the same cell performance and performance stability. Significantly, no special "fuel cell grade" methanol will apparently be required for DMFCs.

An important development this year has been the interest expressed by Motorola in working with LANL on DMFC technology for a variety of

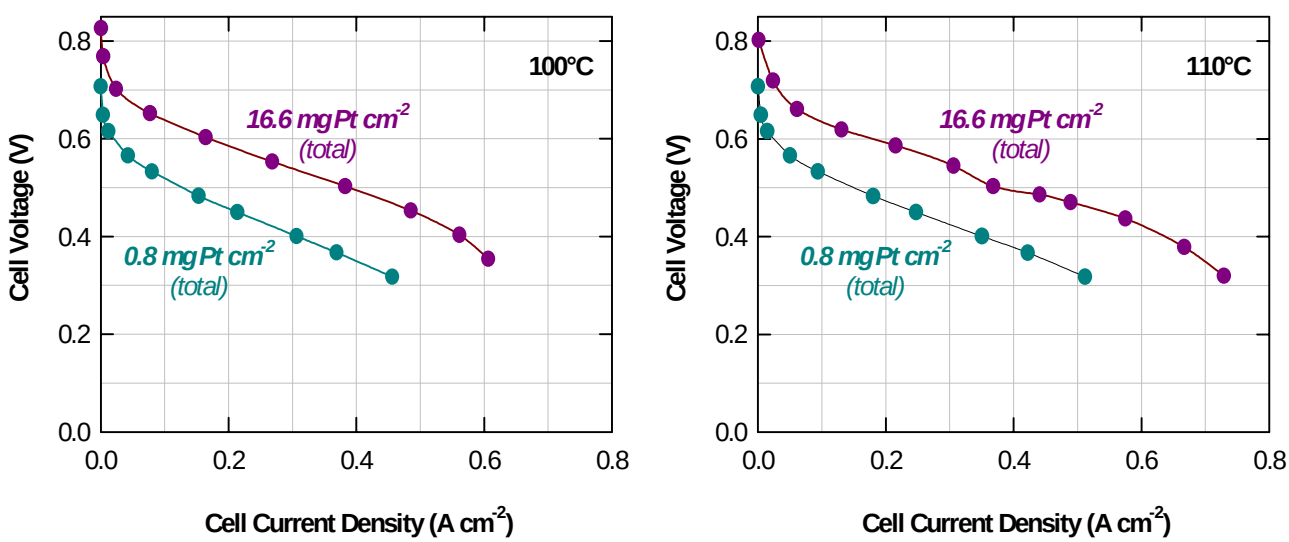

Figure 1. DMFC polarization curves for ultra-high and low Pt loadings at 100 and 100°C (45-cm^2 cell).

Table 1. Trade-off between peak power density and catalyst requirement per kilowatt with lower overall Pt loading.

Total Pt Loading (mg cm^{-2})	g/kW (*peak*)	Peak Power (W cm^{-2})
16.6	66.0	0.250
1.9	10.0	0.190
1.1	6.1	0.185
0.8	4.9	0.170
0.4	2.7	0.140
0.2	1.4	0.130
Milestone of 5 g Pt/kW achieved with 45-cm^2 cell at peak power of 0.17 W cm^{-2} (at 2 g Pt/kW, peak power is still ~0.14 W cm^{-2}).		

Figure 2. LANL 30-cell 45-cm^2 DMFC stack.

applications. The first application chosen, leading to a cooperative research and development agreement (CRADA) with Motorola, has been a power system for cellular phones, based on a hybrid DMFC/battery system (see Figure 3).

Conclusions

As a result of the DOE/OAAT-sponsored efforts at LANL targeting potential transportation applications of DMFCs, the technical status reached is significant. In terms of power density and energy-conversion efficiency, the DMFC (based on short stack results) is today comparable with an on-board methanol reforming system. There is a remaining (although smaller than perceived) gap in precious-metal catalyst requirements, with the DMFC requiring 5 g Pt kW^{-1} vs. about 2 g Pt kW^{-1} required today for an on-board reforming system. We plan (budget permitting) to extend our DMFC work in FY 2001 to fabrication and testing of stacks in the range of 1 kW, operating near 100°C.

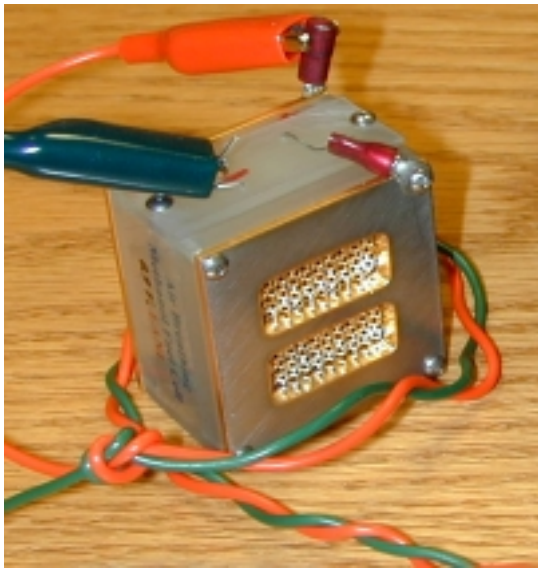

Figure 3. DMFC application: portable power for cellular phones.

V. PEM STACK COMPONENT COST REDUCTION[1]

A. High-Performance, Matching PEM Fuel Cell Components and Integrated Pilot Manufacturing Processes

Mark K. Debe and Judith B. Hartmann (primary contact)
3M Company
3M Center, Building 201-1C-30
St. Paul, MN 55144-1000
(651) 736-1772, fax: (651) 575-1187, e-mail: jbhartmann@mmm.com

DOE Program Manager: JoAnn Milliken
(202) 586-2480, fax: (202) 586-9811, e-mail: joann.milliken@ee.doe.gov

ANL Technical Advisor: James Miller
(630) 252-4537, fax: (630) 972-4537, e-mail: millerj@cmt.anl.gov

Contractor: 3M Company, St. Paul, Minnesota
Subcontractor: Energy Partners, Inc., West Palm Beach, FL
Prime Contract Nos. DE-FC02-97EE50473, September 1997-March 31, 2000
DE-FC02-99EE50582, September 1999-December 2001

Objectives

- Conclusion of Contract #1, Phase 2: Demonstrate scale-up potential for fabricating CO-tolerant anode catalysts and targeted performances of prototype manufactured membrane electrode assemblies (MEAs) in a subcontractor-provided fuel cell stack.
- Contract #2: Develop a set of high-performance, matched polymer electrolyte membrane (PEM) fuel cell components and pilot manufacturing processes to facilitate high-volume, high-yield stack production, and demonstrate the matched component performance in a subcontractor-provided 10-kW fuel cell stack.

OAAT R&D Plan: Task 13; Barriers A and B

Approach

- Contract #1, Phase 2:
  - Transfer anode catalyst fabrication from laboratory- to pilot-scale facility.
  - Conduct single-cell tests at subcontractor facility to define flow field design; prepare MEAs for evaluation in their short stack design at subcontractor facilities.
- Contract #2, Phase 1:
  - Develop anode catalyst compositions and structures with higher reformate tolerance, based on a proprietary catalyst support system.
  - Investigate catalyst compositions and structures to produce higher-activity cathodes, based on a proprietary catalyst support system.
  - Carry out pilot manufacturing scale-up of the process for fabrication of catalyst-coated membrane (CCM) assemblies.

---

[1] The DOE draft technical targets for fuel cell system and fuel cell stack components, sensors, and catalysts can be found in Tables 3, 4a, and 4b, Appendix B.

- Develop carbon electrode backing (EB) media, optimized for performance with the catalyst system.
- Optimize the fuel cell flow field, with the stack manufacturing subcontractor, for water management and air bleed utilization with the catalyst system.

- Contract #2, Phase 2:
  - Evaluate matched component system's performance in subcontractor stack tests.
  - Fabricate and deliver a 10-kW stack.

Accomplishments

- Successfully scaled up anode catalyst, completed large-area short stack testing at Energy Partners, and prepared final report on Contract #1.
- Defined and implemented development of methods for fast screening of new anode and cathode catalyst compositions and structures, which have direct correlation with fuel cell performance.
- Implemented and refined multiple *in-situ* techniques for characterizing MEA properties relevant to fuel cell performance.
- Systematically evaluated multiple PEMs and gas diffusion layer media in MEAs to select the optimal set for catalyst screening experiments.
- Developed a quantitative understanding of optimal water management and operating conditions for the nanostructured MEAs.
- Identified critical factors in MEA components and fuel cell break-in conditioning, leading to significant improvements in performance.
- Identified and implemented improvements in pilot-scale CCM fabrication, which resulted in improved fuel cell performance.
- Achieved improved definition of process windows for catalyst and CCM fabrication; identified key process parameters for statistically designed scale-up and quality improvement studies in the next stage of the effort.
- Completed the greater portion of the work needed to establish test stations, in-line process equipment, and monitoring equipment to support the laboratory- and pilot-scale studies.
- Completed fuel cell evaluations and characterization studies of ~50 different electrode backings, which fall under four different media categories. Identified key EB characteristics related to fuel cell performance and developed increased understanding of differences among the types of media that influence how to optimize their use.
- Evaluated the effects of EB coating properties on fuel cell performance for the different types of EB media.
- Implemented three-dimensional flow field model for simulation of down-channel and cross-channel distributions of oxygen, temperature, current density, and water saturation levels.

Future Directions

- Continue development and evaluation of anode and cathode catalysts, emphasizing scaleable process methods that yield higher specific surface area activities for oxygen reduction.
- Continue EB materials and process development to optimize water management with a high-volume manufacturing process.
- Continue development of the CCM pilot-scale process to improve on-line process control methods, yields, quality, and performance.
- Continue flow field optimization modeling and verification.

Introduction

The membrane electrode assembly is the core component set of a PEM fuel cell stack. An MEA consists of five basic components: anode and cathode catalysts, ion exchange polymer membrane, and anode and cathode gas diffusion layers. The functions of these basic components are intimately related, and the interfaces between them are critical for optimal performance. For large-scale volume fabrication at the costs and quality targets required by transportation applications, very high yields and in-line process control of integrated processes based on cost-effective materials are required. This contract is directed toward demonstrating high-performance, matching PEM fuel cell components manufacturable by integrated pilot processes, utilizing a proprietary nanostructured thin-film catalyst support system.

In fiscal year (FY) 2000, the initial contract (DOE-1) to demonstrate the feasibility for such an approach was concluded, and a follow-on, expanded contract was initiated (DOE-2). In this report, we summarize the progress in Phase 2 of the initial contract and in the current contract to date. Phase 2 of DOE-1 focused on evaluating full-size MEAs, based on a nanostructured support system and fabricated by feasibility process methods, in a short stack at the subcontractor facilities. The objective of DOE-2 is to build on the feasibility of the first contract, further optimizing the component performances, their integration, and development of high-volume pilot manufacturing processes for continuous fabrication of the catalyzed membranes and gas diffusion layers used to form five-layer MEAs. In the second phase of DOE-2, the performance of the matched component system will be demonstrated in a 10-kW fuel cell stack.

Approach

The objectives and approaches of DOE-1 are described in the FY 1999 edition of this report. In completing Phase 2 of DOE-1, the proprietary nanostructured anode catalysts developed in Phase 1 were scaled up and used to fabricate 150- and 300-cm^2 MEAs for single-cell and, finally, short stack testing. Evaluation of single-cell MEAs with different catalysts, membranes, and gas diffusion layers was performed using different subcontractor flow field designs to determine a likely best component set for the short stack. New short stack bipolar plates were fabricated for the short stack tests and combined with the best MEA component set fabricated by the feasibility pilot process.

The objectives of DOE-2 both extend and add to those of DOE-1, and the approach reflects this as well. In Phase 1 of DOE-2, new cathode catalyst compositions and structures based on nanostructured support films are being developed for higher performance and efficiency on low-pressure air, and development is continuing on improved anode catalysts for operation on reformate with better air bleed utilization. For both areas of catalyst development, the unique nanostructured support and catalyst coating methods are similar and offer many potential combinations of materials and process conditions to obtain higher-performing, more cost-effective electrodes. Because of the large number of potential new multicomponent catalyst structures that can be fabricated by this approach, a fast screening methodology is being developed to permit the electrochemical evaluation of the new catalysts as quickly as possible, to support selection of those that merit more thorough evaluation. In addition, multiple *in-situ* techniques for characterizing MEA properties relevant to fuel cell performance have been defined and implemented on the fuel cell test stations.

Scale-up of the processes for producing the catalyst support structures and CCMs is being done in a pilot-plant facility. Initial work has focused on experiments to better define the process windows and to identify key process parameters. Improvements to the processes and equipment are being made as the need is identified through experiments. On-line monitoring and inspection methods are being defined and implemented, and fuel cell test stations are being installed to support pilot-scale, statistically designed process experiments and quality improvement studies, which will begin when the test station installation is completed.

Electrode backings in four categories of media are being evaluated by fuel cell performance tests and by a variety of characterization studies. Preliminary assessment of relative process feasibility and cost is also part of the selection process. Experiments are being conducted to identify key characteristics and to develop an understanding of the differences among the types of media. Future work will include more detailed

evaluation of the most promising types of substrates, one of which will be selected for scale-up.

Finally, the proprietary nanostructured-catalyst-based MEAs have different water management requirements than MEAs fabricated with conventional carbon-particle-supported catalysts, requiring optimized gas diffusion layers and flow field designs for best performance. An empirical approach was used in DOE-1 for investigation of two types of existing flow fields. In the current contract, modeling via computational fluid dynamics (CFD) is being utilized by the subcontractor to simulate the operating environment within the cell for different flow field design parameters and gas diffusion layer properties.

Results

A six-cell stack was fabricated at Energy Partners, using their bipolar plate technology, and 3M CCMs were fabricated by continuous process methods with anode and cathode catalysts developed under DOE-1. Figure 1 shows a set of three stack polarization curves taken under pure hydrogen, 40% H_2 with 60% N_2, and 40% H_2 with 40% N_2 and 20% CO_2. No H_2 dilution effects or loss in performance from the CO_2 are seen. Performance did not match the single-cell tests, but it was discovered after the tests were completed that the anode flow rates were inadequate because of a test station leak. The stack will be retested for benchmarking under DOE-2.

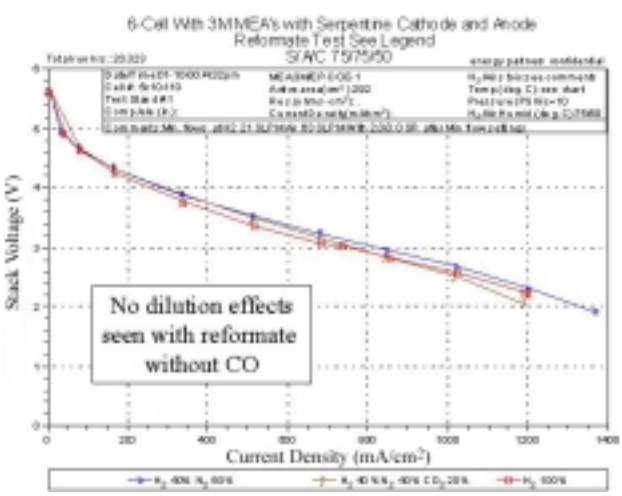

Figure 1. Short stack polarization curves from DOE-1, Phase 2, final tests of 300-cm^2 MEAs fabricated by the pilot continuous process methods.

Significant progress has been made, since the beginning of DOE-2, in determining materials, process, and fabrication factors that give improved performance, but are still based on the anode and cathode catalysts developed in DOE-1. These factors involve water management, the type of PEM and gas diffusion layer, and the conditions for assembling them. Figure 2 illustrates a series of four polarization curves representing the best performance at the date indicated, with constant Pt cathode loadings of ~0.22-0.28 mg/cm^2. All measurements were taken at ambient pressure in a potentiodynamic scanning mode.

The nanostructured catalyst process is very facile, and many new catalyst alloys and composites can be made rapidly for evaluation. A rapid screening technique had to be implemented with a close correlation to fuel cell performance to facilitate the catalyst evaluations, which guide the process development. A 16-segment cell (16 working electrodes) and 16-channel potentiostat now under development will allow AC-impedance characterization of the CCMs made with the new catalyst types, specifically to allow simultaneously measuring and distinguishing the catalyst reaction polarization impedances from membrane, contacts, and interfacial impedances. Figure 3 illustrates AC impedance plots obtained at open circuit voltage

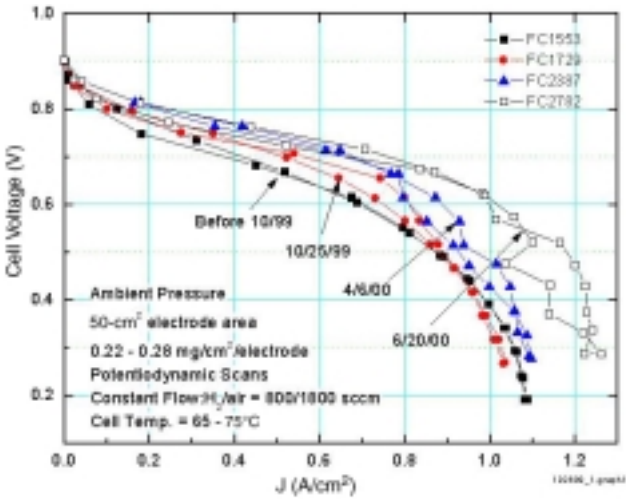

Figure 2. Illustration of the continuing improvement in ambient pressure performance obtained since the start of DOE-2 with the same nanostructured catalysts, by advances in other MEA components, fabrication methods, and testing protocols.

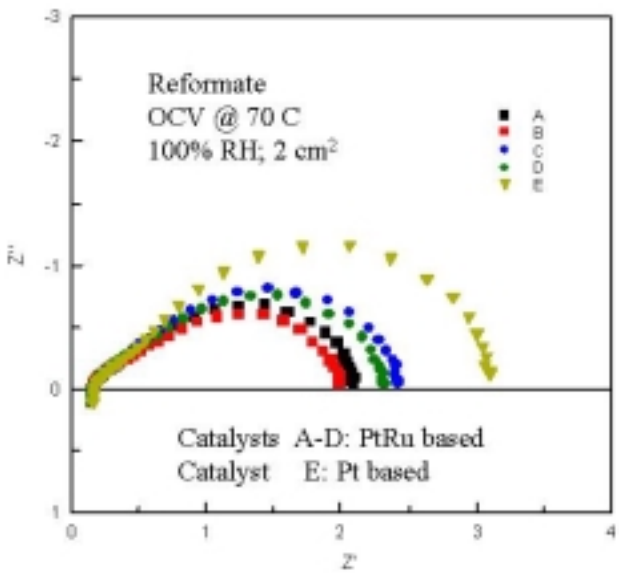

Figure 3. AC impedance plots obtained at open-circuit voltage under reformate with a prototype segmented cell from five different catalyst compositions. The low-frequency intercept is seen to be a strong function of catalyst composition. The final 16-segment cell and potentiostat will be used to rapidly screen new anode and cathode catalysts.

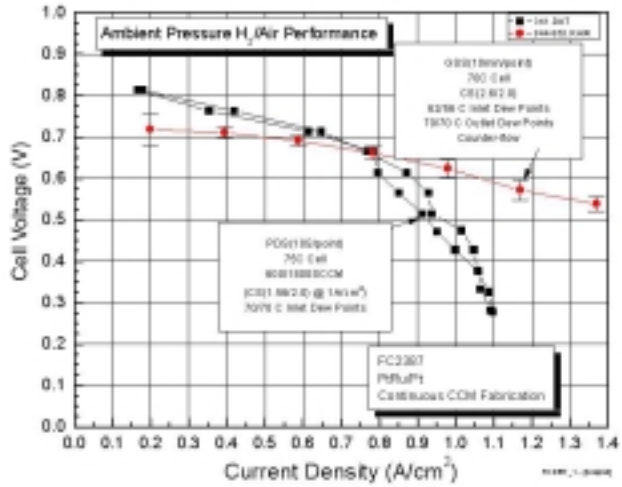

Figure 4. Ambient-pressure polarization curves comparing two scanning protocols for CCMs fabricated by pilot process methods. PDS = potentiodynamic scan, constant flow, 10 sec/point; GSS = galvanostatic scan, constant stoichiometry, 10 min/point.

under reformate, with a prototype segmented cell, from five different catalyst compositions. The low-frequency intercept is seen to be a strong function of catalyst composition.

Improvements to the pilot-plant CCM fabrication process and equipment resulted in material having improved fuel cell performance. Ambient-pressure polarization curves taken in potentiodynamic/constant flow (PDS) and galvanostatic/constant stoichiometry (GSS) scanning modes for this material are shown in Figure 4. The discrepancy at low current densities between the PDS and GSS curves reflects the need for optimized electrode backings and flow fields. Experiments conducted on the catalyst fabrication process resulted in better definition of the process windows and identification of major variables for future, statistically designed experiments. Installation of pilot-plant test equipment to support statistically designed scale-up and process quality improvement studies is nearing completion.

Fuel cell evaluations and characterization studies were completed for ~50 different EBs, which fall under four different media categories. Also, several experiments were completed to evaluate the effects of coating properties on fuel cell performance and identify differences among the different types of media. Key EB characteristics that relate to fuel cell performance were identified, and an increased understanding of differences among the types of media that influence how to optimize their use was developed. Methods for achieving improved performance are being identified and implemented as needed to complete the evaluation and selection process.

The final deliverable of DOE-2 (and the focus of Phase 2) is assembly of a 10-kW stack by the subcontractor. The bipolar-plate flow field design is an important factor affecting MEA performance, particularly with respect to water management and air bleed utilization across the area of an individual cell. A final task of DOE-2 is thus directed at utilizing experience from the DOE-1 short stack testing and the subcontractor's computer modeling and simulation programs to design a flow field that optimizes the performance of the MEAs with the nanostructured-catalyst system in an operating stack.

CFD simulations (single phase with heat transfer) of five different flow field designs have been examined for qualitative implications, and the feature(s) examined that have the most influence on uniformity of current density, temperature, oxygen, and water vapor distributions across and along the

flow field channels. Measurements of critical gas transport properties of the gas diffusion layer are put into the model. Designing for the optimized feature(s) and most effective water removal through the gas diffusion layer will provide guidelines for the initial design of the flow fields.

Conclusions

Significant progress is being made in all aspects of our efforts to develop high-performance, matched PEM fuel cell components and pilot manufacturing processes.

B. Design and Installation of a Pilot Plant for High-Volume Electrode Production

James Arps (primary contact)
Southwest Research Institute (SwRI)
P.O. Drawer 28510
San Antonio, TX 78228-0510
(210) 522-6588, fax: (210) 522-6220, e-mail: jarps@swri.org

DOE Program Manager: JoAnn Milliken
(202) 586-2480, fax: (202) 586-9811, e-mail: joann.milliken@ee.doe.gov

ANL Technical Advisor: James Miller
(630) 252-4537, fax: (630) 972-4537, e-mail: millerj@cmt.anl.gov

Contractor: Southwest Research Institute, San Antonio, Texas
Contract No. DE-FC02-00EE50625, Period of Performance December 1, 2000-May 1, 2002
Subcontractors: General Motors, Warren, MI; W.L. Gore and Associates, Elkton, MD

Objectives

- Demonstrate proofs-of-concept for the large-scale preparation of high-performance electrodes for membrane electrode assemblies (MEAs) and review electrode and MEA architecture against Partnership for a New Generation of Vehicles (PNGV) cost targets.
- Design, build, and install equipment for a high-volume pilot plant capable of catalyzing 100,000 square meters of electrode material per shift per year.
- Complete process development and qualification of the pilot plant.
- Benchmark MEAs fabricated at SwRI against commercially available products.
- Incorporate MEAs into a 50-kW fuel cell stack built by General Motors (GM) and deliver to Argonne National Laboratory (ANL) for testing and evaluation.

OAAT R&D Plan: Task 13; Barrier B

Approach

- Optimize catalyst loading composition, uniformity, and throughput on a pre-pilot scale.
- Prepare MEAs, using ultra-low-load (<0.10 mg/cm^2 Pt) electrodes, and test them under representative operating conditions.

- Finalize system specifications, including detailed requirements for material handling dimensions, throughput, process controls, interfaces, and diagnostics.
- Solicit bids for equipment and construct pilot plant.
- Assess the impact of large-scale catalyzation methods on MEA performance.
- Determine process yields, metal recovery approaches, and methods to optimize them.
- Fabricate sufficient ultra-low-load MEAs from catalyzed electrode material for incorporation into 50-kW stack.

Accomplishments

- Completed MEA test fixtures, fabrication equipment, and facility space for pilot system.
- Took delivery of more than 3,000 linear feet of intermediate electrode substrate material from W.L. Gore and Associates.
- Prepared laboratory quantities (~100 ft^2/batch) of catalyzed electrode material, utilizing various alloy compositions and loadings of from 0.005 to 0.1 mg/cm^2.
- Reviewed MEA preparation methods at Los Alamos National Laboratory (LANL) and produced baseline MEAs at SwRI.
- Fabricated and tested experimental MEAs having a total catalyst loading on the order of 0.10 mg Pt/cm^2.
- Developed robust quality control approaches to characterize catalyzed electrode material.
- Drafted comprehensive requirements list for system, based on pre-pilot trials and discussions with several equipment suppliers.
- Prepared an analysis detailing key manufacturing and ownership costs of the catalyzation process and their contributions to overall MEA costs.

Future Work

- Continue efforts to reduce electrode precious-metal content while maintaining or increasing power density.
- Finalize system design and begin construction.
- Prepare several full-scale MEAs (>500-cm^2 active area) for short stack testing at GM.

Introduction

Commercial acceptance of fuel cell technology for use in the automotive area requires a fuel cell system that meets the PNGV cost target of $50/kW. One of the most critical components affecting overall system performance and economics is the membrane electrode assembly. It is anticipated that the MEA must be available for $10/kW or less in order to meet the overall PNGV cost targets.

The primary objective of this project is the design and installation of a pilot manufacturing process for a crucial (cost-prohibitive) element in the high-volume production of fuel cell MEAs that will address the need for fuel cells in transportation applications. This pilot line will be scaled to catalyze up to 300,000 m^2 of electrode material on a three-shift basis (enough to allow the fabrication of MEAs for more than 50,000 fuel-cell-powered automobiles).

Approach

To support this effort, SwRI will acquire electrode substrate materials, membranes, and reference MEAs (that do not utilize SwRI technology) from W.L. Gore and Associates; these will be used by SwRI for MEA assembly and benchmarking. The products delivered by the end of the project are projected to demonstrate sufficient production levels to achieve MEA production costs below $10/kW. The centerpiece of this effort will be a vacuum coating unit with the capability to produce millions of square feet of high-performance, ultra-low-load electrodes per year. SwRI initially demonstrated the feasibility of this nanoscale, precious-metal technology as part of a DOE-sponsored program on advanced fuel cells for transportation applications. The electrodes produced by the high-volume process will be assembled with available polymer electrolyte membranes (PEMs),

using established assembly technologies, into complete MEAs. Once the pilot quantities of material are produced, General Motors (Global Alternative Propulsion Center), a major participant in the PNGV program, has agreed to design and construct a 50-kW stack utilizing SwRI-supplied MEAs. Upon completion, this system will be delivered to ANL for evaluation.

Results

SwRI has developed novel technologies that provide high-performance electrodes (anode and cathode) that are intimately bonded to the membrane to produce high-performance MEAs. Efforts at SwRI have been aimed at creating electrode layers employing ultra-low levels of precious metals by utilizing vacuum deposition techniques. As shown in Figure 1, superior power density has been demonstrated for MEAs with electrode layers prepared by vacuum deposition, compared to the performance of MEAs with the same or higher levels of precious metals that were prepared by conventional and other electrode-coating techniques.

This superiority can also be expressed in terms of catalyst mass activity (mA/mg Pt) and specific power (mW/mg Pt). For example, specific power values approaching 5 kW per gram of platinum have been achieved with the new technology. Ultra-low loadings as low as 0.001 mg/cm^2 have been demonstrated in the laboratory, with catalyst uniformity within 5% achieved across 15-cm widths of material. To our knowledge, such levels cannot currently be achieved with conventional processes. Work continues to further optimize catalyst composition and reduce precious metal content, with a target of less than 0.10 mg/cm^2 thought to be achievable.

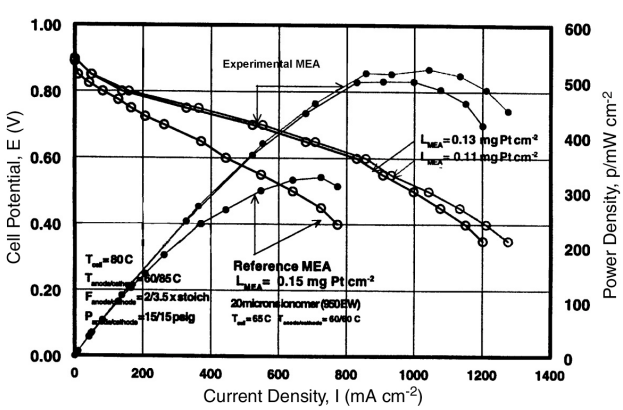

Figure 1. Comparison of SwRI-catalyzed MEAs with baseline sample.

Pre-pilot trials, conducted at SwRI and off-site at a contract facility, have indicated that high feed material rates of 20 m/min and catalyst deposition rates in excess of 0.05 mg/cm^2 · s are possible. To date, W.L. Gore and Associates have provided more than 3,000 linear feet of intermediate electrode substrate material for use in these ongoing trials. A representative roll of this material (~500 ft^2) is shown in Figure 2. Additional large-volume orders will further aid in accelerating MEA material manufacturing capabilities.

Conclusions

The clear potential of SwRI's vacuum deposition methods to manufacture high volumes of electrode material at extremely low cost and with a high degree of uniformity promises to help break the barrier to commercialization of polymer electrolyte fuel cells on a broad scale. Vacuum deposition methods for rolled products, commonly referred to as "web coating," have been applied for more than 15 years in the manufacture of thin-film capacitors, magnetic media, and packaging for food products.

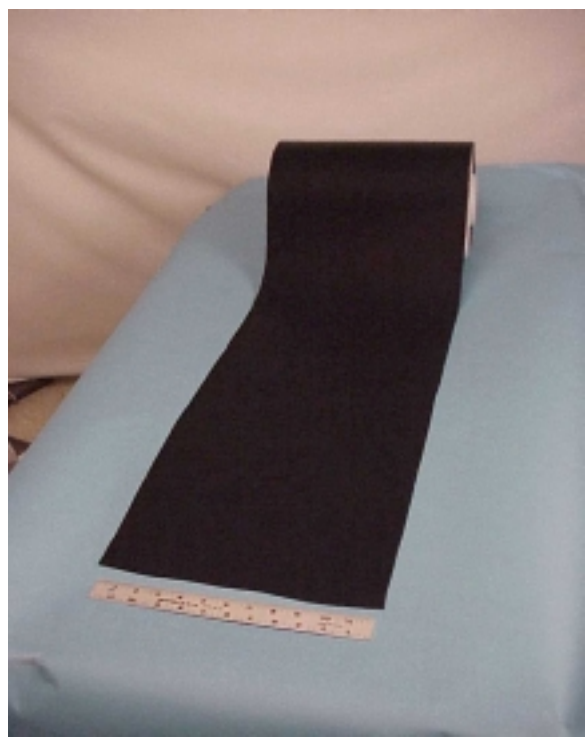

Figure 2. Continuously manufactured intermediate electrode material.

Typical costs for manufacture of metallized plastic are in the range of pennies per square meter of material. Typical production volumes for single industrial web coaters are in the range of 30 million square meters per year. Thus, the work at SwRI points to the tremendous potential cost reductions that are possible with the improved power density, lower loadings of precious metals utilized in the electrode layers of the MEAs, and high volumes of material that can be processed. If this approach is successful, the total projected platinum loading for an automotive stack utilizing this technology could be comparable to the amount found in a modern-day catalytic converter. Efforts in the coming year will focus on final design and installation of the pilot facility, performance assessment of MEAs fabricated with electrodes utilizing this technology, and integration of materials into test stacks for evaluation at GM.

C. Low-Cost, High-Temperature, Solid-Polymer Electrolyte Membrane for Fuel Cells

Robert F. Kovar, Paul Osenar, and Leslie Rubin
Foster-Miller, Inc
195 Bear Hill Avenue
Waltham, MA 02154
(781) 684-4000, fax: (781) 290-0693, e-mail: bkovar@foster-miller.com

DOE Program Manager: Donna Lee Ho
(202) 586-8000, fax: (202) 586-9811, e-mail: donna.ho@ee.doe.gov

ANL Technical Advisor: James Miller
(630) 252-4537, fax: (630) 972-4537, e-mail: millerj@cmt.anl.gov

Contractor: Foster-Miller, Inc., Waltham, Massachusetts
Prime Contract No. DE-FC02-97EE50478, Period of Performance: September 30, 1997-September 29, 2000
Subcontractor: Giner, Inc., Waltham, MA 02154

Objectives

Demonstration of a new class of low-cost, high-temperature solid-polymer electrolyte composite membranes for use in automotive (Partnership for a New Generation of Vehicles) and stationary power applications.

OAAT R&D Plan: Task 13; Barrier B

Approach

The following tasks are required to develop and qualify the composite membrane (and membrane electrode assemblies):

- Identify and develop a qualifying ion-conducting polymer (ICP); the ICPs employed must show less than 10% ionomer degradation in accelerated fuel cell life testing.
- Identify and develop qualifying microporous polymeric substrates; the substrates employed must be dimensionally stable, thin, and pinhole-free structures.

- Develop fabrication methods for high-temperature composite membranes (using the selected ICP and substrate). The ICP and substrate must be combined to form an interpenetrating network.
- Develop appropriate electrode structure and corresponding attachment methods for fabrication of membrane electrode assemblies (MEAs).
- Demonstrate MEA via single-cell testing.

Accomplishments

- Identified, synthesized, and evaluated several aromatic ICPs:
  - Selected most promising system, based on commercially available starting polymers, and completed synthesis and scale-up studies.
  - Identified several ICP systems for advanced development, with the focus on improved stability and lifetime.
- Identified, synthesized, and evaluated selected substrate polymers:
  - Selected poly-p-phenylene benzobisoxazole (PBO) as the most promising polymeric substrate material.
  - Demonstrated fabrication methodology for high-porosity, unoriented substrates for PBO on a batch scale.
  - Identified fabrication methodology for oriented substrates (for increased strength) with improved porosity. Feasibility of extruding 6-wt.% PBO was demonstrated at laboratory scale.
- Developed an imbibition/pressing fabrication method for processing the ICP/substrate combination into composite membranes with good proton conductivity and barrier properties.
- MEAs are being developed by industry and Los Alamos National Laboratory (LANL) with the investigation of electrode structures and corresponding electrode attachment methods.
- Continued single-cell testing of MEAs:
  - Demonstrated performance curves similar to those of state-of-the-art perfluorinated membranes.
  - Began looking at high-temperature performance and long-term stability of composite MEAs operating in a fuel cell.

Future Directions

- Continue development of low-cost, high-temperature aromatic-based ICPs that show long-term fuel cell stability.
- Continue development of improved substrates with microstructure suitable for interpenetrating network formation:
  - Design and build a continuous casting operation to improve substrate quality.
  - Continue development of oriented (higher-strength) substrates.
- Continue development of electrode application method(s) and evaluation of their structure in conjunction with LANL.
- Continue single-cell fuel cell testing, including analysis of fuel cell performance curves to optimize operating conditions.

Introduction

The objective of this work is to develop a low-cost, high-temperature solid-polymer electrolyte membrane (HTSPEM) for use in fuel cells. This advanced membrane is designed to address the present shortcomings of today's Nafion-based solid-polymer electrolyte fuel cells (SPEFCs). The HTSPEM will lower fuel cell cost, improve power density, reduce sensitivity to carbon monoxide, and facilitate thermal water management in the hydrogen fuel stream. The goal of the membrane technology is to provide a clean, efficient, lightweight, and high-density power source that will be useful over a wide range of applications, from next-generation vehicles to stationary power.

Ion-Conducting Polymer Development

The ion-conducting polymer component of the HTSPEM must satisfy a number of criteria simultaneously, the most important of which are as follows:

- Easily synthesized from available, low-cost starting materials
- Highly water-insoluble and film-forming
- Highly ion-conducting (ionic conductivity > 0.1 S/cm)
- Chemically stable to acids/free radicals
- Possessing a thermal/hydrolytic stability temperature > 150 ºC
- Surviving in reformate/air fuel cells for 5,000 hours (automotive applications).

During this project, we have evaluated a large number of sulfonated aromatic polymers produced in our laboratories and elsewhere. Initial evaluation of the polymers' chemical stability (free radical stability, in particular) was conducted with an accelerated peroxide screening test. Although controversial, this test provides some comparative stability data for potential ICPs. By monitoring the mechanical changes and the degradation in ion conductance of a sample in the peroxide test, we can evaluate an ICP's utility without having to develop a composite PEM and corresponding MEA. If the sample passes the peroxide test, it is likely to perform well in long-term, high-current-density single-cell tests. Currently, not much can be said of ultimate ICP performance if the peroxide test performance is less than optimal.

Our testing indicates that select aromatic polymers show promise as fully qualified ICPs for use in fuel cell applications, with continued development. This is one of the objectives for an ongoing Department of Energy (DOE) program for stationary fuel cells (a project in which long-term stability and high-temperature operation are primary goals). For the automotive fuel cell project, we have developed sulfonated poly(phenyl sulfone)-based ICPs, utilizing Amoco's Radel R as a starting point (see Figure 1). To date, we have completed the synthesis and scale-up of this ICP, as well as its incorporation into SPEMs (see discussion of testing, below).

Microporous Substrate Development

The microporous substrate portion of the HTSPEM must provide not only mechanical support for the ICP, but also a porous network, in-plane dimensional stability, and outstanding barrier properties. The greater part of this effort has centered on the development of poly(phenylene benzobisoxazole) microporous substrates. At Foster-Miller, we have previously produced biaxially oriented films of PBO via a proprietary extrusion process. In the fully dense state, these films possess:

- Exceptionally high strength and dimensional stability,
- Superior barrier (gaseous) properties,
- Excellent crease/crack resistance and tear strength, and
- Superior thermal and hydrolytic temperature stability (300ºC).

We have developed a casting process that yields microporous PBO substrates with very high porosity. We have demonstrated that ICPs can be incorporated into these substrates to provide SPEMs with outstanding dimensional stability and proton conductivity equal to or better than that of standard Nafion films. Samples of these membranes have been evaluated at Giner, Inc., and at LANL.

In an effort to develop substrates of higher ultimate strength, allowing for thinner composite membranes and improvements in long-term stability, we continue to investigate the extrusion process. Initial substrates produced via extrusion did not have a pore volume high enough to allow incorporation of sufficient ICP. Although proton conduction could be measured, it was not sufficient for fuel cell requirements. Several experiments have been performed to date to establish the feasibility of extruding the PBO substrate with higher total porosity. Ultimately, the extrusion process should provide continuous substrates with both orientation and sufficient porosity.

Composite Solid-Polymer Electrolyte Membranes

Composite membranes have been made from cast substrates and sulfonated poly(phenyl sulfone) ICP via a solution imbibition process. Control of the

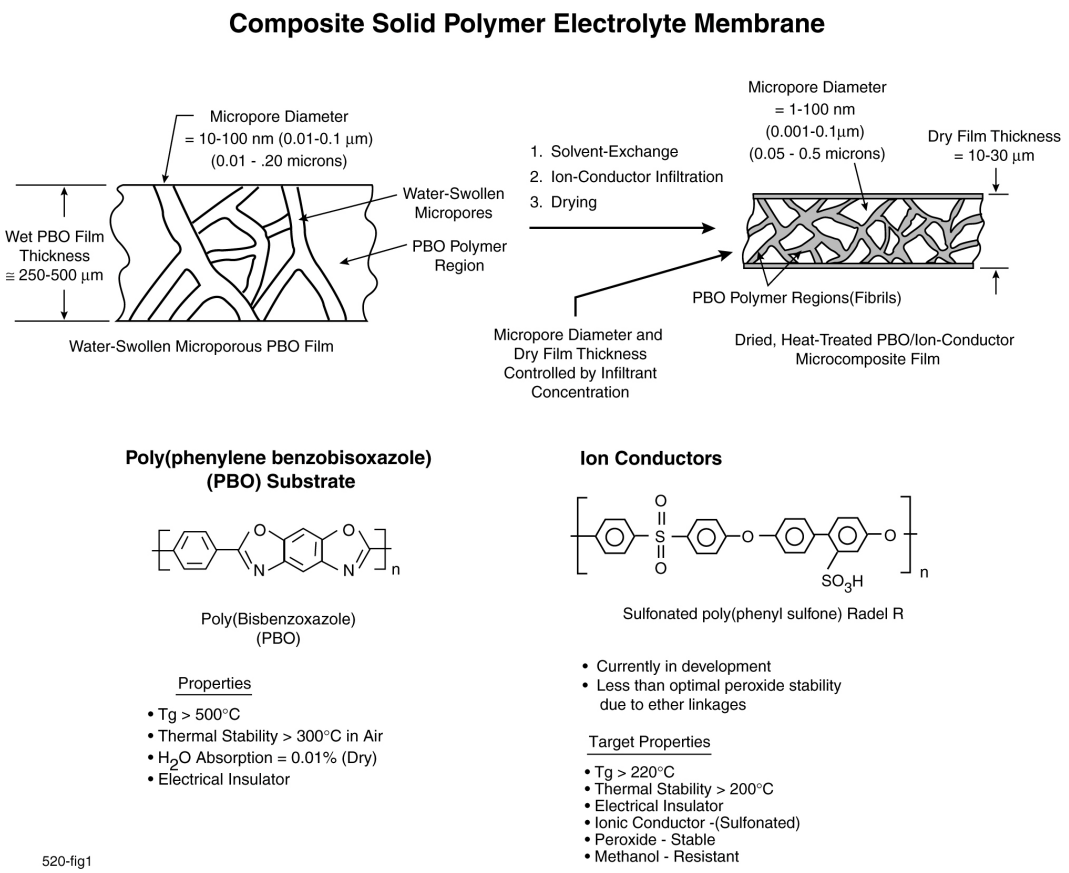

Figure 1. Foster-Miller's composite SPEM consists of a microporous substrate infused with an ion-conducting polymer. The substrate provides mechanical support, mitigating the properties required of the ion-conducting portion and controlling the dimensional change of the membrane during hydration. Each of the components employed in our current version is shown.

substrate porosity and the solution concentration of the ICP allows us to control the final composition. Ideally, the minimum ICP content would be used to achieve sufficient proton conduction, thereby further limiting fuel crossover and water management issues. Membranes are characterized for ion-exchange capacity, ion conductance, gas permeability (nitrogen), and dimensional stability. Some variation occurs in the membrane properties produced via the batch processing approach employed to date; in general, however, our membranes compare favorably with those available commercially. Significant improvements are seen specifically in the gas transmission and dimensional stability (virtually unchanged on hydration).

Membrane Electrode Assembly and Single-Cell Testing

Initial evaluations of the composite SPEMs were performed in an iterative fashion with Giner, Inc., to allow the refinement of the composite fabrication techniques and the components. This work proves the feasibility of the composite concept (see Figure 2). Giner was able to surpass the performance of Nafion 112 with several of the Foster-Miller membranes, using their proprietary electrode and catalyst attachment methods.

Recently, we have been working with LANL in an effort to better understand the performance of our membranes and the techniques needed to attach

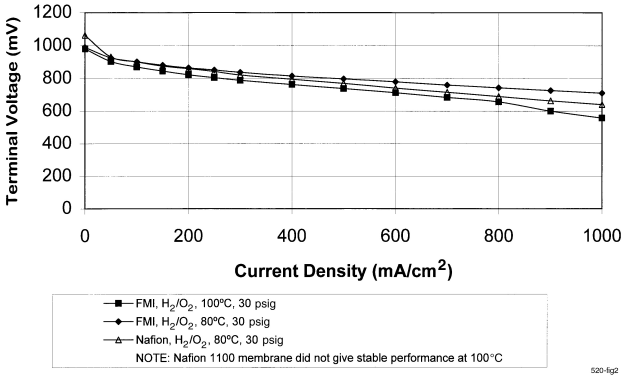

Figure 2. Comparative single-cell performance of Foster-Miller's composite polymer electrolyte membrane (T_{cell} = 80ºC, 100ºC).

catalyst and electrodes. LANL researchers have been able to make MEAs via modifications of standard techniques and test them in single-cell fixtures. Several issues have come to light during their work:

- The composite PEMs developed show very good conductivity when electrodes are properly bonded to the surface.
- Aromatic ionomers behave very differently than commonly used perfluorinated ionomers. Optimization of catalyst and electrode attachment methods will require further efforts with these ionomers.
- The composite membranes of PBO and sulfonated poly(phenyl sulfone) initially fabricated (via cast substrates) may require post-processing to improve their long-term stability.

This project has demonstrated that FMI's composite polymer electrolyte membrane (PEM) is a potentially viable solution for high-temperature SPEFCs. Although further materials development is needed for commercial success, we believe this concept will lead to dramatic advances over current PEM technology – advances that are necessary to make fuel cells a viable power source in the future.

Publications and References

1. R. Formato, R. Kovar, P. Osenar, N. Landrau, and L. Rubin, "Composite Solid Polymer Electrolyte Membranes," PCT Application WO 00/22684.
2. J.E. McGrath, J. Mecham, W. Harrison, S. Mecham, R. Kovar, and R. Formato, "Sulfonated Poly(arylene ether)s as Potential Proton-Exchange Membranes," Abstracts of Papers of the American Chemical Society 1999, Vol. 217, Part 2, p. 342.
3. R. Formato, P. Osenar, R. Kovar, N. Landrau, and L. Rubin, "Novel Ion Conducting Materials Suitable for Use in Electrochemical Applications and Methods Related Thereto," PCT Application WO 00/24796.

D. Development and Optimization of Porous Carbon Papers Suitable for Gas Diffusion Electrodes

Gerald J. Fleming, Principal Investigator
Spectracorp Ltd.
599 Canal St.
Lawrence, MA 01840
(978) 682-1232, fax: (978) 682-3253, e-mail: spectragif@aol.com

DOE Program Manager: Donna Lee Ho
(202) 586-2480, fax: (202) 586-9811, e-mail: donna.ho@ee.doe.gov

DOE Program Support: Larry Blair
(202) 586-0626, fax: (202) 586-9811, e-mail: larry.blair@ee.doe.gov

ANL Technical Advisor: James Miller
(630) 252-4537, fax: (630) 252-4176, e-mail: millerj@cmt.anl.gov

Contractor: Spectracorp Ltd., Lawrence, Massachusetts
Prime Contract No. DE-FC02-97EE50474, September 1997-July 2000
Subcontractors: PSI, Andover, MA; Energy Partners, West Palm Beach, FL; and HPower, Clifton, NJ

Objectives

- Reduce cost of polymer electrolyte membrane (PEM) fuel cell stack by optimizing (through cost reduction and/or improved performance) carbonaceous gas diffusion electrode (GDE).
- Perform manufacturing feasibility analysis on optimized GDE, exploring both optimized batch processing and continuous processing to reduce costs.
- Manufacture small run of optimized GDEs on production equipment and distribute to Department of Energy (DOE) partners for commercial evaluation.

OAAT R&D Plan: Task 13; Barrier B

Approach

- Design and manufacture a matrix of carbonaceous GDEs, utilizing varying compositions and manufacturing techniques (more than 30 variants, including thickness, density, fiber type and length, pore size and distribution, electrical conductivity).
- Test GDE variants in fuel cells to establish performance with respect to industry standard materials.
- Using fuel cell test results, perform manufacturing cost/benefit analysis to determine optimal GDE material.
- On the basis of cost/benefit analysis, manufacture a small production run of optimized GDEs.

Accomplishments

- GDE matrix was designed and all variants of the GDE were manufactured and tested for physical and electrical properties, as well as pore size, pore size distributions, and gas flow. These properties were then correlated (e.g., air flow vs. density, resin content, thickness, and pore size).

- Numerous fuel cell testing parameters (stoichiometries, temperatures, humidification levels, pressures, membranes, electrode treatments) were investigated to obtain a high-performance baseline cell using current state-of-the-art papers.
- Initial cell screening demonstrated very strong performance by several low-cost variants; nonperforming variants were eliminated.
- Combinations of the most promising material variants were produced to explore the limits of potential cost reduction while maintaining excellent cell performance.
- The most promising materials from initial cell screening were retested in short stacks and longer-term single cells to establish reproducibility.
- The lowest-cost, best-performing GDE variant was manufactured on production equipment and is available for evaluation by DOE partners.
- Optimized batch and continuous manufacturing processes are being examined, and proof-of-concept samples have already been produced for several manufacturing steps.

Future Directions

- Distribute optimized GDE to DOE partners for commercial stack evaluation.
- Complete large-volume manufacturing analysis.
- Explore possibility of manufacturing GDE material by means of optimized manufacturing equipment and processes.

Introduction

This program seeks to optimize the physical structure of porous carbon papers for use as gas diffusion electrodes in membrane electrode assemblies (MEAs) for fuel cells. This optimization is directed toward maximizing cell and stack performance with regard to such characteristics as mass transport (H_2O removal) and appropriate electrical conductivity, while reducing costs (e.g., with current state-of-the-art materials).

Our work in the current fiscal year (FY2000) has focused on completing fuel cell screening tests of the GDE matrix, retesting the most promising GDE variants to demonstrate reproducibility, analyzing large-volume GDE manufacturing processes, and manufacturing the optimized GDE for distribution to DOE partners for commercial stack testing.

Approach

The initial fuel cell screenings conducted in FY1999 produced promising results with low-cost materials that were well suited to high-volume and/or continuous production. In FY2000, we sought to establish more robust test conditions that would provide reproducible results on industry standard materials so that subsequent tests on GDE matrix materials would be viable. Once the baseline was established and reproducible results were produced, we would analyze the data, incorporate them into a production analysis for the leading GDE variants, and manufacture a batch of the lowest-cost, best-performing GDE variant on existing production equipment. The possibility of continuously manufacturing the optimized GDE would then be explored.

Results

In FY2000, we worked with several fuel cell manufacturers to ensure stable performance on industry standard baseline materials. During the course of this work, we determined that we would have to sacrifice some raw fuel cell performance in order to obtain reproducible results across the broad range of GDE variants. As a result, the polarization curves presented this year display a 5-10% voltage reduction at a given current with respect to some of the curves presented in FY1999. Raw performance was sacrificed solely to achieve the program's purpose of evaluating variations in the GDE under similar cell conditions; the results do not reflect the GDE's potential in an optimized cell. After several cell test modifications, we reproduced the results with low-cost materials and with some of the more promising GDE variants. The curves demonstrate

comparable performance for lower-cost and industry standard GDE materials.

Figure 1 shows cell voltages at discrete amperages for several materials that were tested in a 13-cell short stack. The low-cost Spectracorp variant is equal to or better than the industry standard material at the high voltages that many companies are utilizing for high efficiencies, and it comes close to matching the industry standard material at lower voltages. Figure 2 shows the performance of the low-cost Spectracorp material versus that of industry standard materials across the full polarization curve. A polarization curve obtained with the low-cost material from a previous screening using an optimized cell is also shown to demonstrate the potential performance of the low-cost material. These figures demonstrate that the low-cost Spectracorp material can match the performance of current state-of-the-art GDE materials.

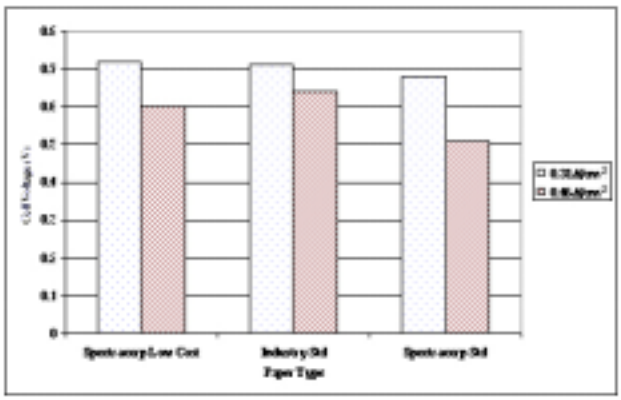

Figure 1. Representative gas diffusion electrode performance at discrete amperages.

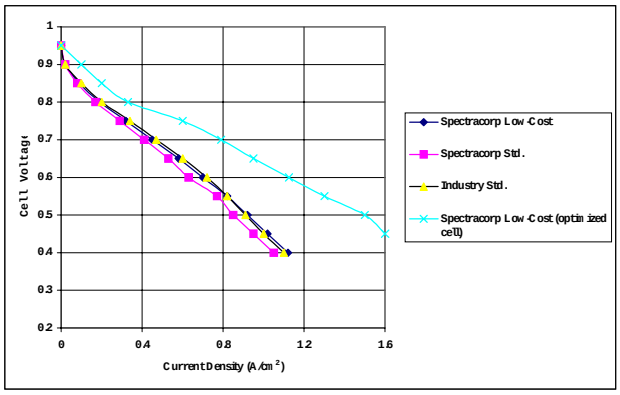

Figure 2. Comparative polarization curves for low-cost gas diffusion electrode.

On the basis of these results, we were able to begin a manufacturing feasibility analysis, including some preliminary processing trials, on a large-volume, continuous manufacturing process for low-cost GDE. We also completed a manufacturing run on the low-cost GDE material, utilizing a batch process on production equipment.

Conclusions

We have demonstrated that it is possible to manufacture a high-performance, carbon-paper-based GDE material at a much lower cost than that of existing materials. Our initial projections indicate that commercial pricing for the new material should be less than $\$10/m^2$, compared with $\$20/m^2$ or higher for existing materials. In addition, the GDE developed in this program is well suited to continuous production leading to a roll product, which is essential for large-volume production of multilayer MEAs. Following initial evaluation of the batch-manufactured GDE resulting from this program, we will continue to work with DOE fuel cell stack partners in order to accelerate the transition to continuous commercial-scale production.

E. Electrodes for PEM Operation on Reformate/Air

Thomas A. Zawodzinski (primary contact), Francisco Uribe, Jayson Bauman, Tommy Rockward, Paul Mombourquette, Markus Vogt, Thomas Springer, Judith Valerio, David Verson, and Shimshon Gottesfeld
Los Alamos National Laboratory
Electronic and Electrochemical Materials and Device Research Group
Los Alamos, New Mexico 87545
(505) 667-0925; fax: (505) 665-4292; e-mail: zawod@lanl.gov

DOE Program Manager: JoAnn Milliken
(202) 586-2480, fax: (202) 586-9811, e-mail: joann.milliken@ee.doe.gov

---

Objectives

To achieve maximum performance in polymer electrolyte fuel cells (PEFCs) under conditions appropriate for reformate/air operation and with methods that allow cost and efficiency targets to be met for transportation.

OAAT R&D Plan: Task 13; Barrier A

Approach

We seek to develop an understanding of electrocatalysis and transport issues related to cathode performance and to use this understanding to guide the development, testing, and demonstration of improved electrodes. To approach requirements for anode performance, we test single cells under conditions of steady-state and transient exposure to various levels of CO, focusing especially on conditions appropriate for off-design conditions of the fuel processor (such as during system start-up). This latter work exploits the ever-increasing levels of CO tolerance achieved. Through applied R&D, we seek to achieve the following cell characteristics simultaneously:

- Highest possible performance at 0.8 V.
- Minimal air injection for CO cleanup.
- Minimal catalyst loading.
- Minimal losses due to dilution at high fuel utilization.

Accomplishments

- *Cathode Performance:* The cell performance at 0.8 V was studied. Improvements, relative to performance obtained at steady state in cells using Pt, were obtained with different alloy catalysts and using low-duty-cycle pulsing of the cell voltage to lower voltages.
  - Demonstrated stable operation of cell yielding 0.4 A/cm^2 @ 0.8 V (on H_2).
  - Dependence of performance on catalyst loading indicates utilization problem.
  - Implementing studies of radically different electrode structures.
  - Completed studies of a series of alloy catalysts, including stability assessment.
- *CO Tolerance:* Achieved reduction in both precious-metal loading (to 0.1 mg/cm^2) and in air bleed (none for 100 ppm) since last review (different cells).
  - New, reconfigured membrane electrode assembly (MEA) allows us to tolerate 100 ppm in reformate with only 0.1 mg/cm^2 of catalyst (with air bleed).
  - New catalysts with reconfigured anode allow full tolerance to 500 ppm in reformate with <5% air bleed, using 0.3 mg/cm^2 anode catalyst (tested for 100 hours), and improved transient behavior for system start-up conditions; 50 ppm in reformate, sometimes higher, was tolerated without air bleeding.
  - Completed combined poisoning/dilution model.

- *System Start-up:* Tests exploiting improved catalysts to assess effects of severe poisoning.

Future Directions

- *Cathode Work:* Overall goal of increasing achievable current density at 0.8 V.
  - Improve cathode catalysts.
  - Vary catalyst layer and backing compositions to improve hydration.
  - Experiment with elevated-temperature operation/alternative hydration methods.
  - Investigate catalyst layer with controlled nanostructures.
- *Anode Work:* Overall goal of minimizing effects of dilution and CO.
  - Improve anode catalysts, reconfigure anodes and effectiveness of air injection for ever higher CO tolerance.
  - Improve catalyst layer composition to further minimize dilution effects, increase fuel utilization.
  - Improve start-up.
- *New Activity on High-Temperature Membranes.*
- *Practical Studies of Critical Impact*
  - MEA durability issues: accelerated life test protocols, "brute force" testing, materials evolution modeling.
  - Break-in effects.
  - New MEA fabrication approaches.
- *Diagnostics*
  - Complete segmented cell development; make design/specs available to companies; implement additional probes for local temperature etc.
  - Devote increased attention to diagnosing long-term performance limitations.
- *Industrial Interactions*
  - Extensive, direct interaction with industrial partners to implement best strategies in stacks.
  - Continue MEA development with outside parties.
  - Implement Web site to allow rapid updating of DOE partners on current work, receive "instant feedback."

Introduction

The requirements for overall PEFC performance include operation under conditions of maximum fuel utilization efficiency, as well as the best possible performance using gasoline-derived reformate. These requirements are tightly coupled; the former entails higher cell voltages, and thus some focus on the PEFC cathode, while higher cell voltages may also provide some "relief" in the context of the stringency of the CO tolerance requirements. As the targets for CO tolerance have been met or exceeded, the focus of this project has shifted to increased emphasis on achieving improved cathode performance at high cell voltages.

Cathode Performance

To meet efficiency requirements for operation with reformed gasoline, the cathode performance must be improved at high cell voltages. Our investigation of this problem has included several studies.

We began with a study of the relative oxygen reduction reaction (ORR) activity of various alloy catalysts in the cell (see Figure 1). So far, PtNi and

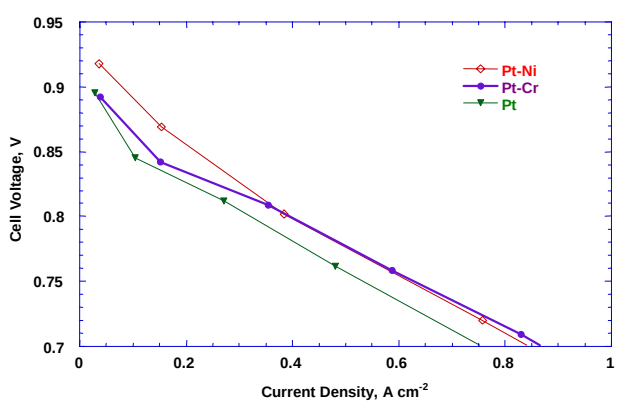

Figure 1. Polarization curves for a series of different cathode catalysts.

PtCr cathode catalysts have been the most active. We were able to achieve our target of 0.4 A/cm^2 @ 0.8 V on hydrogen. These experiments were carried out in 5-cm^2 cells. Scaling up such results is often difficult. We employed the highly active PtCr alloy catalyst in 50-cm^2 cells; Figure 2 shows a typical polarization curve obtained with such a cell.

Operation at high cell voltages necessarily implies operating with little water production at the cathode. We had previously shown that dry conditions lead to poorer ORR kinetics. Figure 3 shows the decline in steady-state current with time after changing the cell voltage from 0.6 to 0.8 V. We tried to overcome this problem by "pulsing" the cell to lower voltages, thus generating more water. The results of such an operation mode, with a 1% duty cycle at the lower cell voltage, are also shown in Figure 3. Clearly, the application of such a pulse provided improved steady-state performance. The nature of the improvement is under investigation. Our ability to achieve 100 hours of stable cell operation with neat H_2 at 0.8 V, 0.4 A/cm^2 at 80°C meets the target for our fiscal year (FY) 2000 (June) milestone. By September of FY 2000, we seek to extend that targeted operation to a cell employing reformate feed to the anode.

Further work was carried out to assess, on a more fundamental level, the utilization of the cathode catalyst. The key finding of this work was that, given our catalyst layer preparation method, there appears to be a limit to how much catalyst is actually accessed; our current estimate is that this amount is less than 40%.

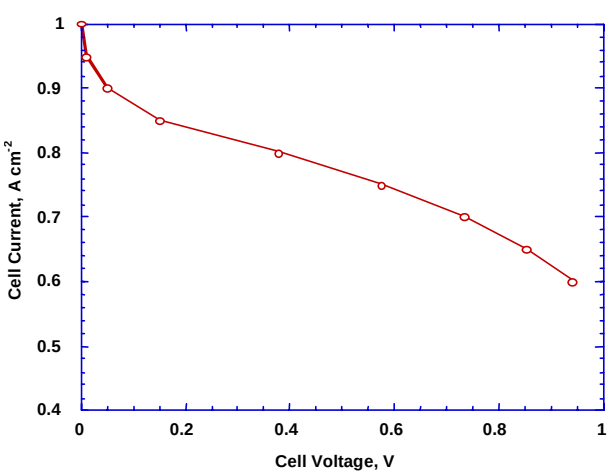

Figure 2. Polarization curve for a 50-cm^2 cell, using a PtCr alloy catalyst on the cathode.

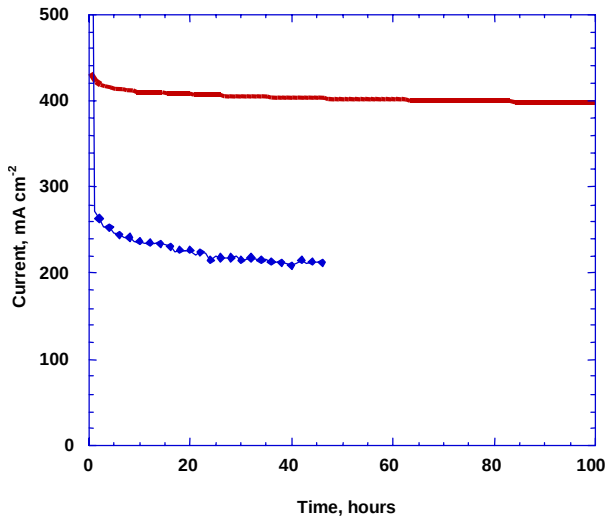

Figure 3. Bottom curve: response of the cell with time after changing the cell voltage from 0.6 to 0.8 V; top curve: effect of pulsing the cell voltage between 0.8 V (99% of the time) and a lower voltage (1%).

CO Tolerance

In Figure 4, we show results from a 500-hour life test of a 50-cm^2 cell, demonstrating tolerance to 100 ppm CO in simulated reformate (meeting our February 2000 milestone). We also met our July 2000 goal of 100 hours of stable performance at 500 ppm CO in reformate with an advanced PtRu catalyst.

We continued to progress toward the simultaneous goals of enhanced CO tolerance with minimal air injection and catalyst loading. We showed that certain new catalysts allowed us to approach a high level of tolerance to 500 ppm CO (see Figure 5). In short-term tests, we can simultaneously lower the catalyst loading to 0.1 mg/cm^2 and achieve complete tolerance to 100 ppm CO with <4% air bleed.

In another set of tests, we have continued our work on the effects of transient excursions in CO levels, which are typical of nonsteady-state reformer operation. Perhaps the most technologically significant result is our finding that injection of air can dramatically improve the recovery from large excursions in CO level. Recovery under such conditions was sluggish without air injection.

We capitalized on the high level of CO tolerance to begin simulating start-up conditions. As shown in Figure 6, even small amounts of air injection can yield tolerance to high levels of CO. Without air

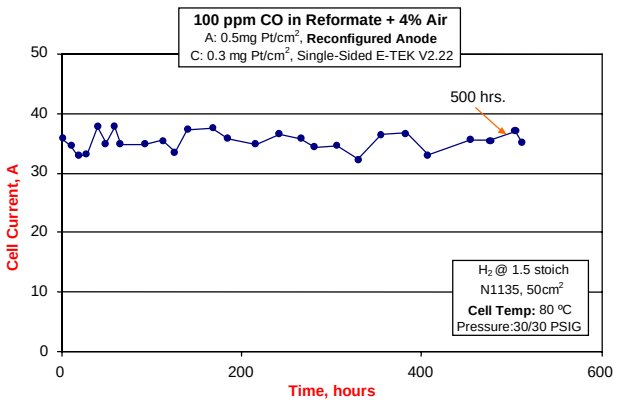

Figure 4. Life test of cell with reconfigured anode, exposed continuously to 100 ppm CO in simulated reformate. (Air bleeding [4%] was used in this cell to achieve complete CO tolerance during the life of the test.)

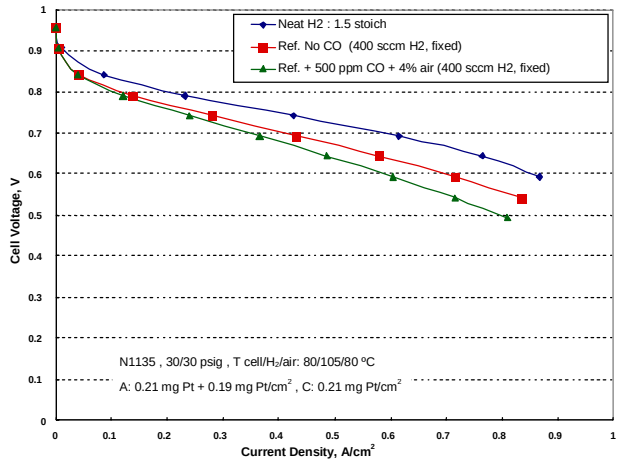

Figure 5. Polarization curves showing combined effects on new catalyst and reconfigured anode, providing near-complete tolerance to 500 ppm CO in reformate.

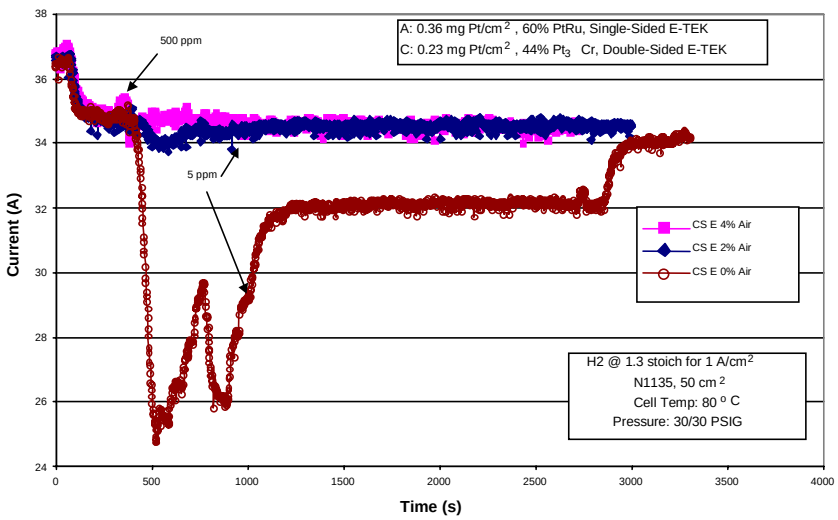

Figure 6. Response of cell to a simulated start-up; the CO level in reformate was systematically decreased from 500 ppm to 50 ppm (75 ppm per minute), then to 5 ppm (15 ppm per minute).

bleeding, it is difficult to achieve full recovery of the cell, even with as little as 5 ppm CO left in the feed stream.

Summary

During FY 2000, we made significant progress toward our R&D goal of improved performance at high cell voltages while operating on reformate/air feeds. We demonstrated that we could achieve stable performance of 0.4 A/cm^2 at 0.8 V with neat hydrogen as a fuel. Although we need to lower the required catalyst loading and operate on reformate, this does represent a substantial first step on the road to simultaneously achieving acceptable performance and high-voltage efficiency. We have also advanced our understanding of limiting factors in cathode performance.

We took advantage of newly available, highly CO-tolerant catalysts to demonstrate a substantial increase in the level of CO that we could accept in reformate. We also capitalized on that high level of tolerance and started to investigate how we could make the system performance more robust in the face of increased CO levels during start-up or

transient phases of operation. Also, we further advanced fundamental understanding of the anode performance by completing and submitting for publication a paper describing combined experimental and modeling studies of the anode.

Finally, we are adopting a more proactive approach to interacting with industry and universities to transfer technology from this program as efficiently as possible.

F. New Electrocatalysts for Fuel Cells

P.N. Ross, N.M. Markovic, T.J. Schmidt, and V. Stamenkovic
Materials Sciences Division, Lawrence Berkeley National Laboratory
University of California, Berkeley, CA 94720
(510) 486-6226, fax: (510) 486-5530, e-mail: pnross@lbl.gov

DOE Program Manager: JoAnn Milliken
(202) 586-2480, fax: (202) 586-9811, e-mail: joann.milliken@ee.doe.gov

---

Objectives

Understand the kinetics and mechanism of electrode reactions in low-temperature fuel cells. Develop new electrocatalysts, using materials-by-design approach.

OAAT R&D Plan: Task 13; Barrier A

Approach

- Study the kinetics of fuel cell electrode reactions on well-characterized model electrodes and high-surface-area fuel cell electrocatalysts, using modern electroanalytical methods.
- Study the mechanisms of the reactions, using state-of-the art in-situ spectroscopes.
- Use ultra-high vacuum (UHV) methods of surface preparation and surface analyses to form tailored surfaces. Synthesize nanoclusters to have the tailored surface.
- Characterize the microstructure of the nanoclusters by high-resolution electron microscopy.
- Transfer technology to catalyst developers/vendors.

Accomplishments

- Development of Pd-based (Pd-Au) CO-tolerant anode electrocatalysts that are three times more active for electrooxidation of CO/H_2 mixtures than is Pt-Ru.
- Elucidation of the reaction mechanism for the “cleansing” of CO adsorbed on Pt and platinum-based alloy surfaces by air bleeding.
- Establishment of the oxygen reduction activity/stability on Pt_3Ni and Pt_3Co bulk alloys and high-surface-area catalysts.

Future Directions

Anode side:

- Determine the optimal surface composition of Pd-Au catalysts for CO tolerance.

- Determine CO tolerance of tailored electrodes consisting of thin films, 1-10 monolayers (ML) in thickness, of Pd on the close-packed single-crystal surfaces of Ta, Re, and W.

Cathode side:

- Optimize PtNi and PtCo catalysts for the oxygen reduction reaction (ORR).
- Pursue Pt-skin structures as novel air cathode electrocatalysts and determine the stability of alloying elements.
- Develop new class of Pt-free catalysts for the ORR.

LBNL's activities during the past fiscal year are described here in terms of two main task areas.

CO-Tolerant Anode Electrocatalysts Based on Bulk Pd Alloys

Using a materials-by-design approach, we found that it is possible to replace one of the best CO-tolerant Pt-based catalysts (Pt-Ru) with new, Pd-based bimetallic catalysts (Pd-Au). We chose to test Pd catalysts because Pd has catalytic properties very similar to those of Pt with respect to the hydrogen oxidation reaction (HOR), but it is more oxophilic than Pt. The latter property may facilitate the oxidative removal of CO at lower potentials than on Pt. Although the HOR kinetics of Pt and Pd are similar, the extraordinary ability of a pure Pd electrode to absorb large amounts of hydrogen into the bulk necessitates restricting the negative limit of Pd to ≈ 0.3 V with respect to the reversible hydrogen electrode (RHE) (see upper panel of Figure 1). Consequently, the bulk Pd electrode cannot be used as anode material for the HOR at potentials relevant for fuel cell applications.

Recently, we have explored the possibility of creating Pd electrocatalysts with the ability to suppress the absorption of hydrogen into the Pd lattice, while keeping Pd activity for the HOR and CO electro-oxidation at relatively low potentials. In the hope that combining Pd with different metals would yield superior activity and stability relative to the pure Pd metal, we studied the electro-oxidation of potential fuels for fuel cells on different Pd bimetallic alloys and thin metal films of Pd deposited on early-period transition metals. Of the various systems examined, we found bimetallic Pd-Au alloys of particular interest because these systems exhibited both high resistance toward the absorption of hydrogen and significant catalytic enhancement for the electro-oxidation of hydrogen in the presence of CO. The upper panel of Figure 1 shows that hydrogen absorption is suppressed on the

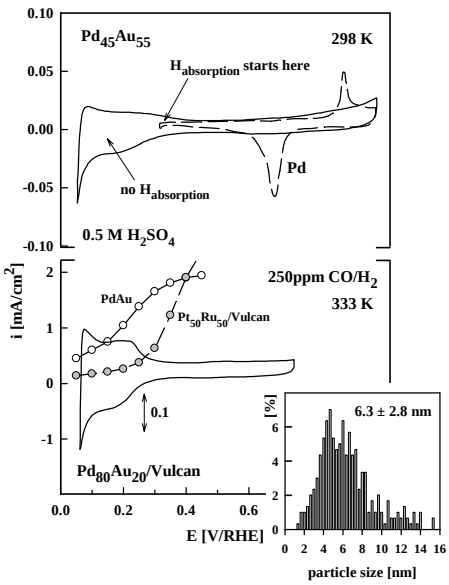

Figure 1. Upper panel: Base CV for $Pd_{45}Au_{55}$ and pure Pd bulk electrodes. **Lower panel:** Base CV for $Pd_{80}Au_{20}$/Vulcan electrode and polarization curves for oxidation of 250-ppm CO/H_2 on $Pd_{80}Au_{50}$/Vulcan and $Pt_{50}Ru_{50}$/Vulcan at 333 K. **Inset:** Particle size distribution of the $Pd_{80}Au_{20}$/Vulcan catalyst via HRTEM.

Pd-Au alloy with surface composition of 55 at% Au, presumably because the electronic properties of Pd are modified by Au.

The electrocatalytic properties of a Vulcan-supported Pd-Au electrocatalyst with bulk stoichiometry of Pd80:Au20 were investigated by means of the thin-film rotating disk electrode (RDE) method. In the base cyclic voltammetry (dotted curve), two potential regions can be distinguished: The potential region of hydrogen adsorption (0.1<E<0.35) is followed by the double-layer region, up to 0.75 V. The similarity of the voltammetry for the bulk electrode and a high-surface-area catalyst is striking and important, because the cyclic voltammetry (CV) of the bulk alloys (see above) has established an "alloy fingerprint" for the Pd-Au

system. The polarization of the anode with a 250-ppm CO/H_2 mixture (open circles) at 60°C is used to measure the CO tolerance of Pd-Au alloy at a particle size of ca. 6 nm (see inset). The findings are compared with previous results for Pt-Ru alloy (closed circles). Interestingly, high current densities can be reached at low potentials on the Pd-Au alloy (e.g., 73 and 206 mA/mg metal at 0.05 and 0.2 V, respectively). Compared with Pt-Ru, the Pd-Au alloy exhibits three times higher catalytic activity, a very promising result for the practical application.

The *mechanism* of action of the Pd-Au electrode during electrooxidation of the H_2/CO mixture may be ascribed to *electronic effects*, where inactive Au atoms alter the electronic properties of the catalytically active Pd atoms. To summarize, the Pd-Au system is a *new class* of CO-tolerant catalysts, where the adsorption energy of CO on Pd-Au is reduced with respect to pure Pd. Oxidative removal of CO *from* Pd sites is thus enhanced, allowing hydrogen oxidation to take place *on* freed Pd sites.

Testing of Prototype Pt Alloy Air Cathode Electrocatalysts

For phosphoric acid fuel cells (PAFCs), Pt-alloy cathode catalysts (e.g., PtNi and PtCo) were found to improve the gas diffusion electrode's performance. Recent work on polymer electrolyte membrane fuel cell (PEMFC) cathode catalysts has indicated similar effects, but the magnitude of this effect is still unclear. It is not yet known whether these materials are stable under PEMFC conditions or whether the leaching of alloy components may lead to ionomer contamination. For the unambiguous determination of the intrinsic catalytic activity of Pt_3Ni and Pt_3Co, we use the rotating ring-disk method (RRDE) with model bulk alloys and the thin-film RRDE method for the carbon-supported fuel cell catalysts. Using these techniques, the intrinsic catalytic activity of electrocatalysts can be assessed in the absence of mass transport resistance, which occurs in membrane electrode assemblies (MEAs). Figure 2 summarizes our preliminary results for the ORR on UHV prepared and characterized bulk Pt_3Ni and Pt_3Co alloy catalysts. Pure Pt is also shown as a reference. The figure also shows that the activity increases at 333 K in the order $Pt_3Ni > Pt_3Co > Pt$, the catalytic activity of Pt_3Ni alloy being *ca.* 25 mV improved with respect to the ORR on pure Pt. We found that Pt alloys were stable

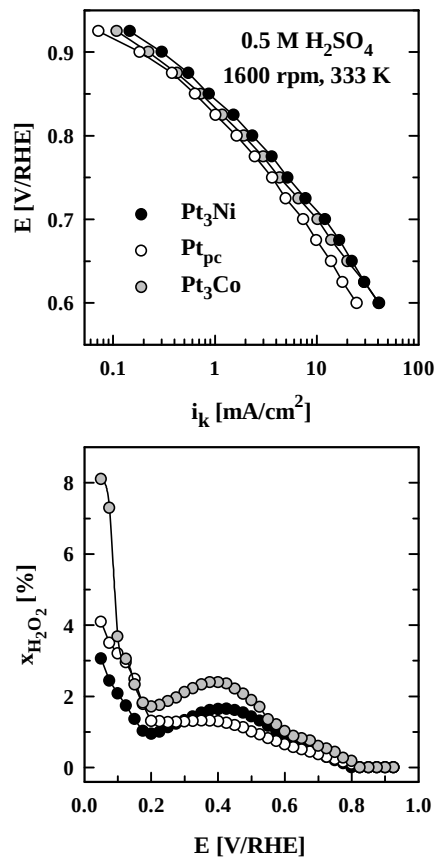

Figure 2. **Upper panel:** Tafel plots for the ORR on polycrystalline Pt, Pt_3Ni, and Pt_3Co bulk electrodes, respectively. **Lower panel:** Fraction of peroxide produced during the ORR on these electrodes.

under our experimental conditions. Figure 2 also shows that similar small amounts of peroxide are detected on the ring electrode on all three surfaces. This may imply that the reaction mechanism on Pt_3Ni and Pt_3Co alloy surfaces is the *same* as one proposed for pure Pt. The kinetics of the ORR on high-surface-area Pt_3Ni and Pt_3Co catalysts prepared by ETEK is very similar to that observed on the bulk electrodes. Although the difference in activity between pure Pt and Pt_3Ni-supported catalysts is rather small (*ca*. 20 mV), confirmation of the high activity of Pt_3Ni catalysts may offer the possibility of decreasing the amount of Pt in air cathode fuel cell catalysts.

In research directed toward improved air electrodes for fuel cells, we had sought to utilize what we termed a "skin effect" to produce a more active state of Pt for the ORR. The skin effect arises from strong Pt surface segregation in Pt_3Ni and

Pt_3Co alloys (i.e., a monolayer "skin" of Pt, the second layer being nearly pure Co and Ni). Preliminary studies of the oxygen reduction activity and stability of the skin structure on Pt_3Co and Pt_3Ni bulk alloys indicate that the Pt "skin" is not stable at relatively high potentials (E > 0.6 V vs RHE). Consequently, the skin structure of Pt_3Co and Pt_3Ni cannot be used as a cathode material for the ORR at potentials relevant for fuel cell applications. Studies of other possible "skin effect" bimetallic systems are in progress.

Publications

1. N.M. Markovic, B.N. Grgur, C.A. Lucas, and P.N. Ross, "Surface Chemistry of CO on Pt(100)-Bimetallic Surfaces: Displacement Effects," *Langmuir*, **16**:1998 (2000).
2. N.M. Markovic, C.A. Lucas, B.N. Grgur, and P.N. Ross, "Surface Electrochemistry of CO and H_2/CO Mixture at Pt(100) Interface: Electrode Kinetics and Interfacial Structures," *J. Phys. Chem.*,**103**:9616 (1999).
3. N.M. Markovic, T.J. Schmidt, B.N. Grgur, H.A. Gasteiger, R.J. Behm, and P.N. Ross, "The Effect of Temperature on Surface Process at the Pt(111)-Liquid Interface: Hydrogen Adsorption, Oxide Formation, and CO Oxidation," *J. Phys. Chem.*, **103**:8568 (1999).
4. C.A. Lucas, B.N. Grgur, N.M. Markovic, and P.N. Ross, "Structural Effects during CO Adsorption on Pt-Bimetallic Surfaces: The Pt(100) Electrode," *Surf. Sci.*, **448**:77 (2000).
5. C.A. Lucas, N.M. Markovic, and P.N. Ross, "Structural Effects during CO Adsorption on Pt-Bimetallic Surfaces: The Pt(111) Electrode," *Surf. Sci.*, **448**:65 (2000).
6. S. Baldelli, N. Markovic, P. Ross, Y-R Shen, and G. Somorjai, "Sum Frequency Generation of CO on (111) and Polycrystalline Platinum Electrode Surfaces: Evidence for SFG Invisible Surface CO," *J. Phys. Chem.*, **103**:8920 (1999).
7. V. Climent, N.M. Markovic, and P.N. Ross, "Kinetics of Oxygen Reduction on an Epitaxial Film of Palladium on Pt(111)," *J. Chem Phys.* **104**:3116 (2000).
8. N.M. Markovic and P.N. Ross, "Electrocatalysis by Design: From the Tailored Surface to a Commercial Catalyst," review article, *Electrochim. Acta*, in press.
9. N.M. Markovic and P.N. Ross, "New Electrocatalysts for Fuel Cells: From Model Surfaces to Commercial Catalysts," review article, *Cattech*, in press.

Book Chapter

1. N.M. Markovic and P.N. Ross., "Electrocatalysis at Well-Defined Surfaces," in *Interfacial Electrochemistry, Theory, Experiment, and Applications*. A. Wieckowski, Ed., Marcel Dekker, Inc., New York, Chapter 46 (1999), p. 821.

Other Publications

1. "Fuel Cell Reactions on Well-Characterized Catalysts," *3rd International Symposium on New Materials for Electrochemical Systems*, Montreal, Canada, July 1999. Extended abstract, pp. 64-67.
2. "Electrocatalysis by Design: From Atomic Level Structures to High Surface Area Catalysts," *3rd International Symposium on Electrocatalysis*, Portoroz, Slovenia, September 1999. Extended Abstract, pp. 49-51.
3. "Electrocatalysis on Well-Characterized Bimetallic Catalysts," *Workshop on Direct Methanol Fuel Cells*, Portoroz, Slovenia, September 1999. Extended Abstract, pp. 63-65.

G. Development of a $10/kW Bipolar Separator Plate

Leonard G. Marianowski (primary contact)
Institute of Gas Technology (IGT)
1700 South Mount Prospect Road
Des Plaines, IL 60018
(847) 768-0559, fax: (847) 768-0916, e-mail: marianow@igt.org

DOE Program Manager: Donna Lee Ho
(202) 586-8000, fax: (202) 586-9811, e-mail: donna.ho@ee.doe.gov

DOE Program Support: Larry Blair
(202) 586-0626, fax: (202) 586-9811, e-mail: larry.blair@ee.doe.gov

ANL Technical Advisor: Walter Podolski
(630) 252-7558, fax: (630) 972-4430, e-mail: podolski@cmt.anl.gov

DOE Contractor: Institute of Gas Technology, Des Plaines, Illinois
Prime Contract No. DE-FC02-97EE50477, November 1998-June 2001
Subcontractors: PEM Plates, LLC, Elk Grove Village, IL 60007; Stimsonite Corporation, Niles, IL 60714; Superior Graphite Corporation, Chicago, IL 60638; and Honeywell, Inc., Torrance, CA 90504

Objectives

- Develop a low-cost molded graphite bipolar separator plate for polymer electrolyte membrane (PEM) fuel cells.
- Evaluate the IGT-molded graphite bipolar separator plate's performance and endurance in fuel cell stacks.
- Build a pilot production molding line with capacity of five plates per hour at PEM Plates, LLC, to evaluate mass production of molded plates.

OAAT R&D Plan: Task 13; Barrier B

Approach

- Select, blend, and optimize inexpensive raw materials for necessary electrical, chemical, and physical properties of bipolar separator plates for a $10/kW manufactured target cost.
- Design, build, and operate the five-plate-per-hour (5-plate/hr) pilot production molding line at PEM Plates, LLC.
- Produce molded bipolar plates from the pilot line for the IGT and Honeywell fuel cell stack tests.
- Assemble fuel cell stacks at IGT to establish the functional performance and endurance of molded plates in stack environments.
- Honeywell, Inc., will assemble and test molded plates from PEM Plates in a fuel cell stack and compare performance against a machined graphite stack.

Accomplishments

- Electrical, chemical, and physical property targets were met or exceeded with an optimized blend of components, in laboratory tests and single-cell tests.
- Fuel cell performance was within 5% of that of state-of-the-art, machined graphite fuel cells in side-by-side tests.

- A 5-plate/hr pilot molding production line facility (with equipment) was built and produced plates for testing at IGT and Honeywell, plus samples for several fuel cell stack developers.
- IGT tested performance of molded bipolar plates produced by PEM Plates in multiple fuel cell stacks of 4, 7, 20, and 52 cells, in both continuous and intermittent operation modes.
- The first 20-cell IGT fuel cell stack using plates produced by PEM Plates operated over 2,300 hours, with excellent plate performance. Extended life testing of the molded plates was accomplished by reuse in subsequent fuel cell stacks; some plates exceeded 5,000 hours of operation.
- Operational functionality of the molded plates was determined in multi-cell fuel cell stacks for heat management, sealing, stacking stability, and water management.
- Several fuel cell developers confirmed the excellent properties of PEM Plates' samples.
- $10/kW cost target is within reach with a separator plate materials cost of $4/kW; however, manufacturing costs at $6/kW are dependent upon details and complexity of the bipolar plate design.

Future Directions

- Design and build the higher-capacity, pre-commercial molding line, incorporating process improvements.
- Continue discussions with commercial fuel cell stack developers to supply molded separator plates.

Introduction

The U.S. Department of Energy (DOE) sponsored a program with the Institute of Gas Technology to develop a molded composite graphite bipolar plate that would be inexpensive and perform as well as state-of-the-art, machined graphitized bipolar plates. IGT and its subcontractors, Superior Graphite Corporation and Stimsonite Corporation, identified moldable blends of graphites, resins, and additives and produced a molded composite graphite bipolar separator plate that is equivalent in function and performance to state-of-the-art, machined graphite plates.

Applications for patents for the blended components and the process have been submitted. PEM Plates, LLC, was formed to commercialize the production of the molded graphite bipolar separator plates. Material and production costs for commercial quantities of the plates are estimated to be on the order of $10/kW; however, manufacturing cost depends on the complexity of the design of the bipolar plate and fuel cell stack.

A variety of different designs of anode and cathode gas flow channels, with water cooling channels, have been molded (i.e., molded directly to net shapes, with no post-molding finishing or machining steps). No reasonable geometric or shape limitations have been encountered, so most cell design configurations are possible. Also, because the molded plates exhibit some degree of inherent flexibility combined with sufficient strength, thinner plates are possible (compared with the plates machined from graphitized carbon).

Results

Molded Bipolar Plate Tests

The molded graphite plates have been tested over the past two years at IGT and also evaluated by other fuel cell stack developers. Numerous out-of-cell tests have measured electrical, chemical, and physical properties. Extensive single-cell tests of the plates have shown consistent performance in excess of 5,000 hours. The molded plates have been successfully scaled up from lab-size 60-cm^2 active area to the full-size DOE vehicular specification of 300-cm^2 active area. Figure 1 compares the hydrogen-air performance at atmospheric pressure of a single cell with molded graphite flow field plates to that of a cell with an identically machined flow field in POCO graphite plates. The performance with the molded plates is within 5% of that with the POCO plates at a typical current density of 400 mA/cm^2. However, at higher currents, the performance is better because the hydrophilic nature of the IGT composition aids the removal of product water.

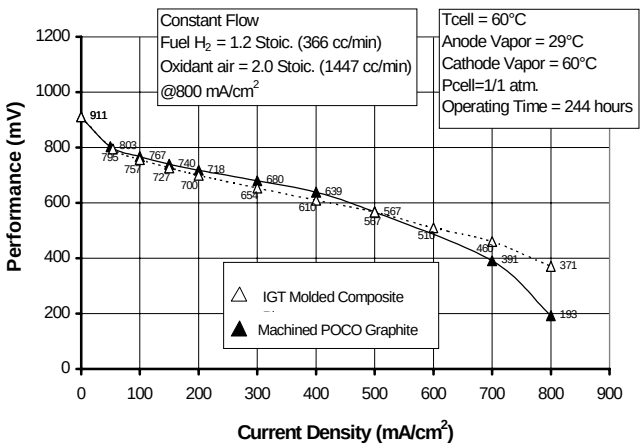

Figure 1. Comparison of molded graphite cell to machined graphite cell.

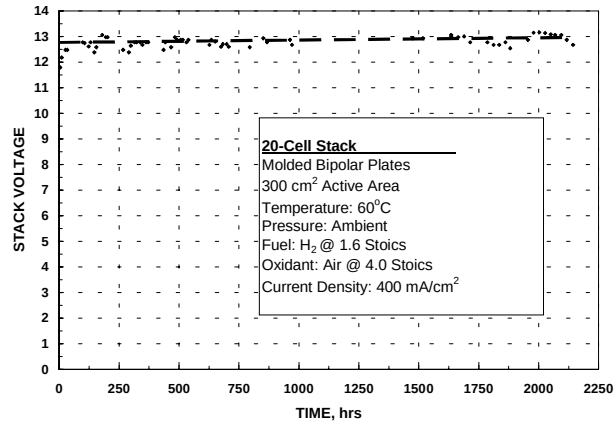

Figure 2. Life test of IGT 20-cell molded bipolar plate fuel cell stack.

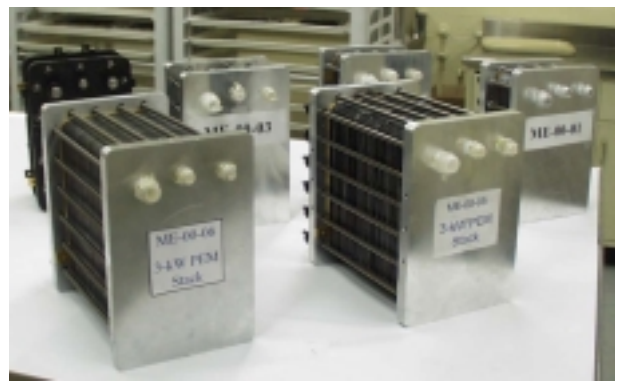

Figure 3. Fuel cell stacks of 7, 20, and 52 cells.

Tests of the molded plates in a well-instrumented, 300-m^2, 20-cell water-cooled stack were conducted for over 2,300 continuous hours (see Figure 2). This demonstrated the endurance of the plates with active thermal management in the 300-cm^2-size stacks with the use of water cooling. Stack testing was conducted mostly in a continuous operation mode of 24 hr/day and 7 days/week, but some tests were also conducted in daily cycles of 8 hours on and 16 hours off, allowing the stack plates to cool and then be reheated each day. In both test modes, the molded plates maintained their integrity, and the fuel cell stack performance was equivalent to that of stacks made with machined graphite plates. Post-test chemical analysis and physical measurements indicated a stable plate composition, with no change in measured properties.

Results of tests of the molded plates operating in fuel cells at various pressures from one to three atmospheres showed that gas sealing and water cooling were accomplished. Figure 3 shows a variety of multi-cell stacks tested, from 7 to 52 cells.

Measurements of Specific Plate Properties

The DOE-specified requirements for conductivity, corrosion, and permeability have been met or exceeded, as indicated in Table 1. In addition, other property assessments of the molded plates that are important in the operation and structure of a fuel cell stack were made by IGT. These included measurements and investigations of crush strength, strength within stacks and during handling, and elastic and permanent creep; water uptake; chemical leachability; cyclic immersion in boiling water

Table 1. Molded plate properties: DOE target values plus IGT measurements.

Plate Property	Measured Value
DOE Specified Properties	
Conductivity	300+ S/cm, about 80% of POCO™ graphite value
DOE Target: > 100 S/cm	
Corrosion	< 5 μA/cm^2
DOE Target: < 16μA/cm^2	
H_2 Permeability	<< 2 x10^{-6} cm^3/cm^2-sec (dry, nonporous plates)
DOE Target: < 2 x10^{-6} cm^3/cm^2-sec	
Additional Properties Measured by IGT	
H_2 Bubble Pressure	> 15 psig (wet, porous plates)
Crush Strength	> 3000 psi
Flexibility	3 – 6% deflection at midspan
Total Creep	~1% elastic deformation at 200 psi and 100 °C
Flexural Strength	6420 psi (820 std. dev.)
Combustibility	Zero (in propane flame)

followed by freezing; noncombustibility; recyclability of components; and potential reuse of components in new plates or other products.

The values of conductivity were measured using the American Society for Testing and Materials (ASTM) C-661 method, and the values were typically exceeded by a factor of three to eight, depending on plate density. Conductivity and surface resistance measurements were always compared with measurements of POCO graphite plates, used as a standard.

The corrosion rate target of less than 16 $\mu A/cm^2$ was also satisfied. This was done in hydrogen, air, and oxygen atmospheres in a dilute sulfuric acid solution with 2 ppm fluoride, using the ASTM G5 method at 90°C and pH ~ 4. The IGT molded composite blend had total corrosion rates below 5 $\mu A/cm^2$. Hydrogen permeability was measured as a function of plate density, related to molding pressure. Plates can be molded either more or less dense than POCO graphite, thereby controlling the porosity. The hydrogen permeability rate measured for the dense, nonporous plates, at 90°C and 207 kPa (30 psig), was always well below the DOE-specified value of 2×10^{-6} cm^3/cm^2-s.

Additional measurements were made of the plate crush strength, flexural strength, mid-span flexibility, and creep characteristics. The molded plates are expected to survive an anticipated holding force exerting 200-psi pressure in the fuel cell stack, including stacking dimensional nonuniformities induced by gasketing or assembly methods, plus a myriad of handling and packaging actions from the production line to stack assembly. The measured strength values shown in Table 1 yield a good safety margin. The strength and slight flexibility of the molded composite plates give the stacks the advantage of greater durability. The plates have retained their electrical and physical properties after being subjected to immersion in boiling water followed by freeze-thaw cycles. Maximum loss of weight in any of the tests has been on the order of 0.5%.

Molded Plate Production and Cost Estimates

IGT and Stimsonite formed a joint venture company called PEM Plates, LLC, with the purpose of producing molded composite bipolar separator plates for fuel cell stack developers. The various steps in the process were explored, and modifications were developed for mass production of the plates. With the knowledge gained from molding the composite plates in the 5-plate/hr pilot line, plus corporate experience with rapid molding machines and inexpensive molds, machine production rates of hundreds of plates per hour are possible. In carload quantities, raw material costs will be $4/kW or less. Production costs are expected to be about $6/kW; however, this cost depends upon the production quantity and the complexity of the plate designs.

Capital and operating costs were analyzed for the custom machines to produce hundreds of plates per hour. To attain production costs below $6/kW, annual production quantities of 100 MW of fuel cells are needed. This is equivalent to about 2,000 cars per year with 50-kW fuel cell engines. As the demand for plates increases, the number of production machines can be increased.

Conclusions

After identifying a unique blend of component materials for a molded graphite bipolar separator plate for PEM fuel cells, development of a rapid molding process began with a pilot production line. Thousands of plates have been molded and thousands of hours of fuel cell stack tests have been conducted, yielding performance practically equivalent to state-of-the-art, machined graphite plates. In commercial production quantities, the manufactured cost of PEM Plates' molded separator plates is estimated to be about $10/kW.

More needs to be done to reach commercial production:

- The new molding process needs to be validated at the pre-commercial manufacturing level.
- Successful molding trials using stack developer designs must be demonstrated.
- Additional stack endurance and verification testing is needed.
- Additional orders from developers are needed in order to increase production volumes to the levels needed to achieve cost reductions.

H. Layered PEM Stack Development

Michael Pien (Project Director)
ElectroChem, Inc.
400 W. Cummings Park
Woburn, MA 01801
(781) 938-5300, fax: (781) 935-6966, e-mail: fuelcell@fuelcell.com

DOE Program Manager: Donna Lee Ho
(202) 586-8000, fax: (202) 586-9811, e-mail: donna.ho@ee.doe.gov

DOE Program Support: Larry Blair (LANL)
(202) 586-0626, fax: (202) 586-9811, e-mail: larry.blair@ee.doe.gov

ANL Technical Advisor: James Miller
(630) 252-4537, fax: (630) 972-4537, e-mail: millerj@cmt.anl.gov

Contractor: ElectroChem, Inc., Woburn, Massachusetts
Prime Contract No. DE-FC02-97EE50475, October 1, 1997-December 31, 2000

Objective

- ElectroChem will validate the suitability of its low-cost, layered separator plate design for light vehicle applications. This novel design will be tested in two stack design versions for reliability and performance under the harsh conditions associated with light vehicle use, and it will also be life-tested.

OAAT R&D Plan: Task 13; Barrier B

Approach

- A 5-kW polymer electrolyte membrane (PEM) fuel cell stack will be designed, assembled, and tested. The design will include water cooling and will be based on a 232-cm^2 (6 in. × 6 in.) active area cell.
- The 5-kW fuel cell will be initially tested under high-energy-density hydrogen/oxygen (H_2/O_2) conditions.
- The 5-kW fuel cell will be integrated into a prototype hydrogen/air system that provides the necessary support for efficient hydrogen/air operation. Dynamic testing will be performed in an attempt to simulate stressful light vehicle operating conditions.
- Simultaneously, a smaller-cell (50-cm^2), 200-W stack will be constructed and life-tested under harsh H_2/O_2 conditions for a minimum of 3,000 hours to validate the survivability of the materials used in the layered plate design.
- The resulting performance data from both stacks will be analyzed. In particular, a detailed external and internal inspection of the 200-W stack for potential signs of degradation and corrosion will be carried out.

Accomplishments

- Both stacks have been designed and are under construction.
- The support system for the 5-kW test system has been initially designed, and component selection is in progress.
- Plans for the stepwise integration of the 5-kW stack are proceeding.

Future Directions

- Conduct dynamic testing of 5-kW stack to simulate light-duty vehicle operation.
- Conduct life-testing of 200-W stack for 3,000 hours.
- Analyze performance data from 5-kW and 200-W stacks.

Introduction

The principal hardware element in a PEM fuel cell is the bipolar separator plate, which in conventional designs is a major cost item in a fuel cell system. The bipolar separator plate must perform a number of important tasks simultaneously, while remaining lightweight and low-cost. It must provide excellent electrical conductivity, keep the gaseous reactants separated, be leak-free, support intricate gas flow patterns to uniformly distribute reactants and water vapor and remove waste products from the membrane electrode assembly (MEA), permit stack cooling, and be fabricated to relatively high tolerances in volume production. Finding a single material for use in inexpensively producing monolithic separator plates remains a challenge. Long experience has shown that graphite has the chemical stability to survive the fuel cell environment, but producing nonporous graphite is a long and expensive industrial process.

Approach

Our approach has been to fabricate separator plates from several materials, thereby relaxing the performance requirements for any one material. Our basic design approach is shown in Figure 1, where a single monolithic plate design (a) is compared with the layered design (b). The principal components of the new design are porous graphite, polycarbonate plastic, and stainless steel.

Previous work had shown that this design provides high performance at low cost while enabling a leak-free stack design that yielded no signs of corrosion or degradation under the harsh test conditions examined. This program is explicitly aimed at extending the testing range to include longer life testing under harsh conditions, as well as a larger-scale (5-kW) stack design. The overall goal is to extend the range of confidence in this plate design for commercial light vehicle mass production applications.

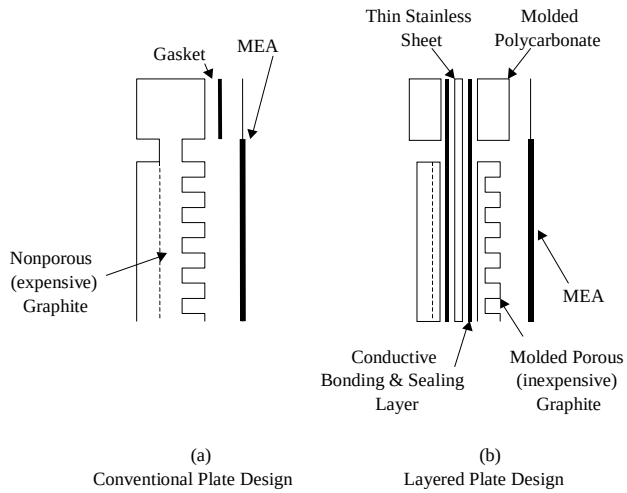

Figure 1. Schematic comparison of a conventional fuel cell separator plate with ElectroChem's layered structure. The typical monolithic plate is usually composed of expensive nonporous graphite or graphite composite. ElectroChem's design uses three primary materials selected for low cost, high performance, and ready availability.

Technical Challenges

A particular feature of the layered separator plate design is its facility for the flexible application of manufacturing technology. The fabrication process for these layered bipolar plates lends itself to low-cost mass production by means of techniques, equipment, and processes used across several industries. Each step, though it comprises several pieces that require individual fabrication and handling, is quite low-cost and rapidly executed. A cost analysis has been carried out specifically for volume production associated with the auto industry.

Some of the results of this analysis are shown in Figures 2 and 3. Of primary interest to the vehicle manufacturer is that the fuel cell separator and cooling plates (one cooling plate for every two active cells) meet the simultaneous requirements of low weight and low cost. The layered separator plate design readily meets both of these requirements,

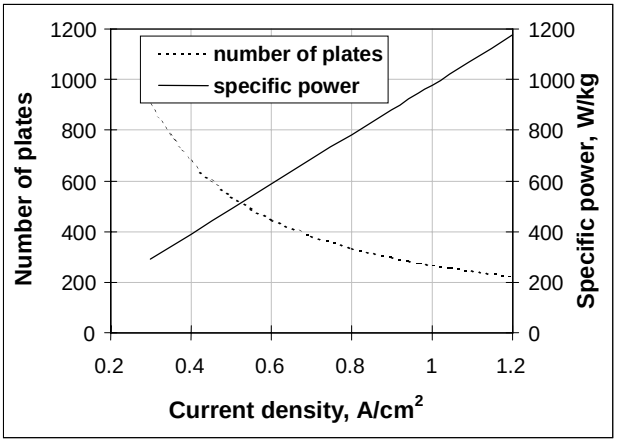

Figure 2. Specific power analysis of layered separator plus cooling plates for a 50-kW stack operating at 0.8 V/cell.

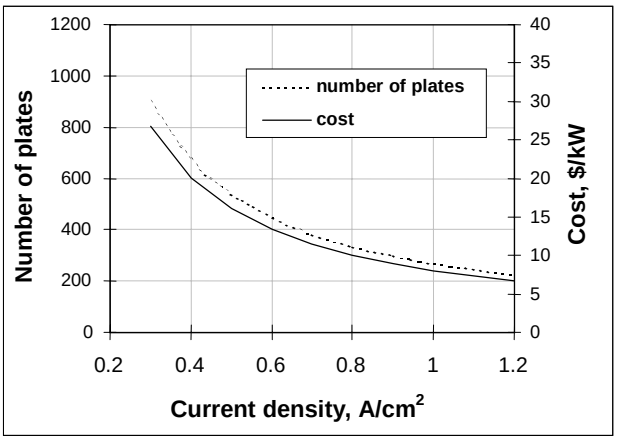

Figure 3. Cost analysis results of layered separator plates plus cooling plates for a 50-kW stack operating at 0.8 V/cell.

using commercially available materials, on the basis of reasonable assumptions about cost savings obtained from volume production techniques.

Our next stage in the validation of this novel plate design comprises extensive testing in (a) subscale stacks, which can examine potential materials degradation scenarios (200 W); and in (b) a 5-kW stack, which operates at a scale and power density comparable with light vehicle applications. Toward this end, two stacks are being developed, and an extensive testing process is planned. A schematic drawing of the 5-kW test system is shown in Figure 4.

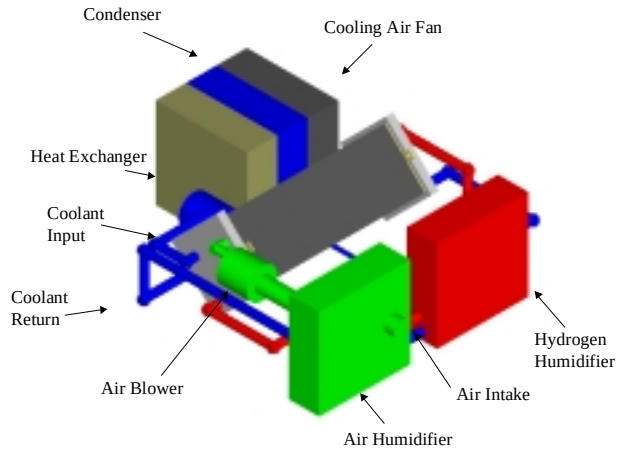

Figure 4. Schematic drawing of the laboratory-scale 5-kW fuel cell system for dynamic testing of the full-scale separator plate design.

Future Challenges

Our design has been developed with an eye toward the progressive commercialization of fuel cells. The approach taken permits us to adapt these materials to a wide range of designs that may vary between fuel cell manufacturers. This successful separator plate design is quite generic and can be adapted to a wide range of flow field patterns. These materials are already produced in bulk, are well engineered, and offer economies of scale that can be attained rapidly with minimal investment.

Meanwhile, this material combination can also be obtained in small volumes at modest cost and inexpensively machined to provide parts that already cost less than their nonporous graphite equivalents. This leads us to anticipate the introduction of these less expensive parts into fuel cells while manufacturing volumes are still small, providing substantial cost savings at every level of production volume.

VI. AIR MANAGEMENT SUBSYSTEMS[1]

A. Turbocompressor for PEM Fuel Cells

Mark K. Gee
Honeywell Engines & Systems
2525 W. 190th Street, MS-36-2-93084
Torrance, CA 90504
(310) 512-3606, fax: (310) 512-4998, e-mail: mark.gee@honeywell.com

DOE Program Manager: Patrick Davis
(202) 586-8061, fax: (202) 586-9811, e-mail: patrick.davis@ee.doe.gov

ANL Technical Advisor: Robert Sutton
(630) 252-4321, fax: (630) 252-4176, e-mail: sutton@cmt.anl.gov

Contractor: Honeywell Engines & Systems, Torrance, California
Prime Contract No. DE-FC02-97EE50479, October 1997-July 2000
DE-FC02-99EE50579, October 1999-June 2001

Objectives

An optimal turbocompressor configuration will be developed, working with fuel cell system manufacturers and carrying on the work currently being performed. A vehicle-ready motor controller will be developed. The turbocompressor/motor controller will be made available for integration in a fuel cell system.

OAAT R&D Plan: Task 13; Barrier D

Approach

Honeywell's approach makes use of

- Automotive and aerospace turbomachinery technology for low cost and low weight/volume ratio.
- Variable nozzle turbine (VNT®) inlet geometry for improved performance across the flow range.
- A mixed-flow-type compressor for improved low-flow performance.
- Contamination/oil-free and zero-maintenance-compliant foil air bearings.
- A high-efficiency, low-cost two-pole toothless motor.
- Low-cost, sensorless variable-speed motor controller topology design.

Accomplishments

- Numerous start/stop cycles with no appreciable wear.
- Stable operation at full turbine temperature (150°C).
- Performance of compressor and turbine mapping close to that predicted.
- Completion of power consumption evaluation.

---

[1] The DOE technical targets for fuel cell system compressor/expanders can be found in Table 5, Appendix B. These targets will be reviewed and possibly revised at a workshop being held early in FY 2001.

- Completion of modification and testing of the turbocompressor with increased turbine inlet temperature (315°C) capability for the Honeywell fuel cell brassboard system.
- Assembly and testing of an aerospace-quality variable-speed brassboard motor controller used to drive the turbocompressor with increased turbine inlet temperature.
- Completion of trade study of the turbocompressor and other compressor/expander designs, with the turbocompressor approach recommended.
- Analysis and design of the turbocompressor with a mixed flow compressor and VNT under way.
- Analysis and design of the vehicle-ready motor controller under way.

Future Directions

- Complete testing of the turbocompressor with increased turbine inlet temperature in the Honeywell fuel cell brassboard system.
- Complete analysis, design, and fabrication of the latest turbocompressor design with the mixed-flow compressor and VNT.
- Complete analysis, design, and fabrication of the vehicle-ready motor controller.
- Complete testing of the turbocompressor and vehicle-ready motor controller.

Introduction

The objective of this work is to develop an air pressurization system to pressurize a fuel cell system for a light-duty vehicle. The turbocompressor is a motor-driven compressor/expander that pressurizes the fuel cell system and recovers energy from the high-pressure exhaust streams. Under contract to the Department of Energy (DOE), Honeywell has designed and developed the motor-driven compressor/expander and evaluated data on its performance, weight, and projected cost. Compared to positive displacement technology, the turbocompressor approach offers the potential for high efficiency and low cost in a compact and lightweight package.

Approach

The turbocompressor, shown in Figures 1 and 2, consists of a compressor impeller, an expander/ turbine wheel, and a motor magnet rotor incorporated onto a common shaft that is operated at speeds of up to 110 thousand revolutions per minute (krpm) on compliant foil air bearings. A motor controller drives the motor, which is capable of driving the turbocompressor to the maximum design speed. The air bearings are lubrication-free, in addition to being lightweight, compact, and self-sustaining (i.e., no pressurized air is required for their operation). The turbocompressor works by drawing in ambient air through the motor/bearing

Figure 1. Honeywell fuel cell turbocompressor.

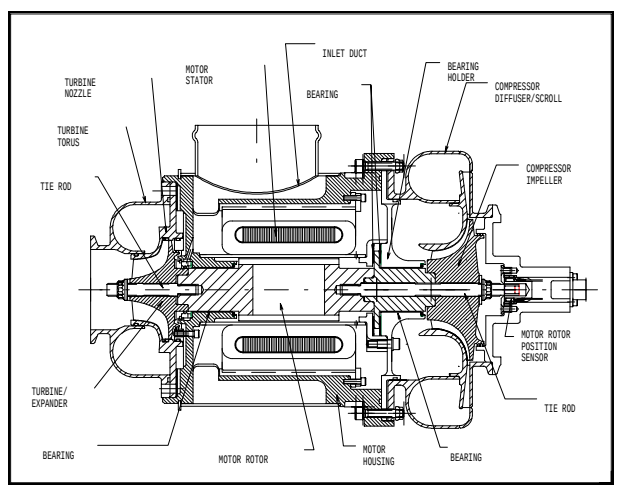

Figure 2. Fuel cell turbocompressor details.

cavities, where it is pressurized by the compressor, delivered to the fuel cell stack, and then expanded through the turbine to enhance the overall turbocompressor/fuel cell system efficiency.

Results

The turbocompressor has operated for more than 300 hours under varying conditions, with and without motor operation. To date, the motor has reached a maximum speed of 110 krpm.

The current Phase II Turbocompressor occupies 10 liters of volume (including the motor) and weighs 8.1 kg mass. It is the only machine that incorporates the motor within both its volume and mass. Even so the machine is still larger than the DOE goals of 4 liters (without motor) and mass of 3 kg (without motor). The power consumption testing of the turbocompressor has also been completed (see Figure 3). To support testing of the Honeywell fuel cell brassboard system, the turbocompressor was modified to handle increased turbine inlet temperatures. In addition, a modified, aerospace-quality controller, intended to replace the commercial unit used previously, has been assembled and tested. Integrated testing prior to delivery to the Honeywell fuel cell brassboard system is scheduled for completion by mid-2000.

As outlined in the Variable Geometry for PEM Fuel Cells program (awarded in March 1999), a trade study to compare the turbocompressor with other compressor/expander devices was completed. The turbocompressor was favored mainly because of its small size, low weight, and increased reliability, as well as for the lack of contamination issues with the air bearings. After reviewing the trade study results with DOE, it was decided to incorporate a mixed flow compressor and a variable nozzle turbine (VNT). The changes will improve the low-flow performance while maintaining efficiency across the flow range. The vehicle-ready motor controller will be of reduced size, incorporate sensorless technology, and have a topology that is configured to reduce production cost. The analysis and design of the turbocompressor with a mixed-flow compressor and VNT and the vehicle-ready motor controller are currently under way.

Conclusions

The turbocompressor concept, using self-sustaining compliant foil air bearings, has demonstrated low power consumption and moderate pressure ratio at low flow rates in a compact, lightweight package. Power consumption can be further lowered if higher expander/turbine

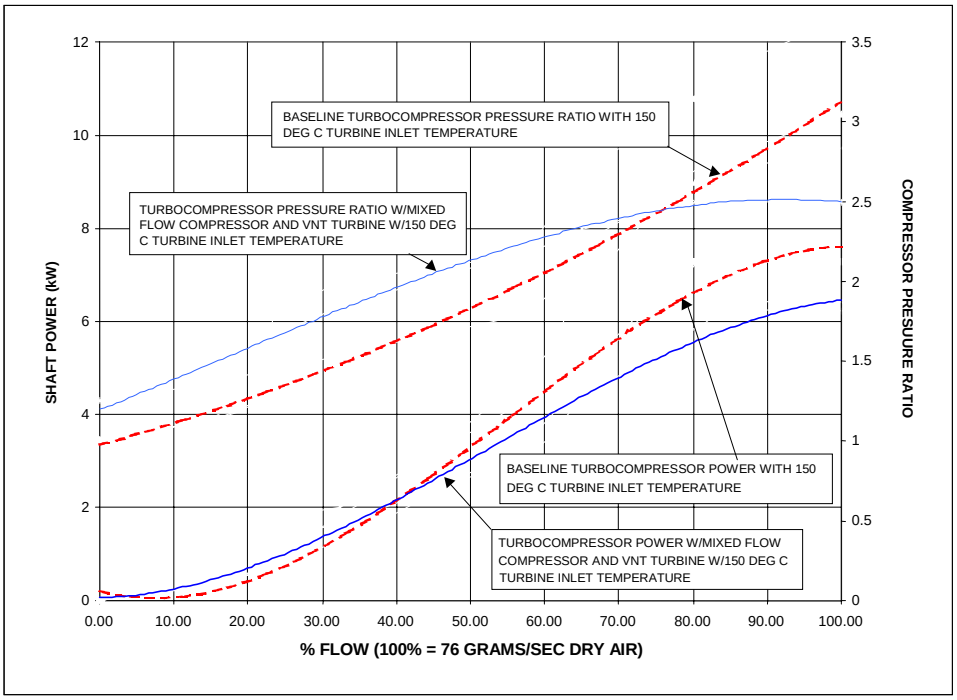

Figure 3. Turbocompressor shaft power/compressor outlet pressure ratio vs. % flow.

temperatures can be provided by the fuel cell system. A turbocompressor capable of increased expander/turbine temperatures will be demonstrated in a Honeywell fuel cell brassboard system by late 2000. The latest turbocompressor/variable-speed motor controller will incorporate a mixed-flow compressor and variable inlet nozzle turbine to improve the pressure ratio at low flows. The variable-speed motor controller's size, weight, and reliability are being addressed with the new sensorless design. The latest design is scheduled to be tested in early 2001.

B. Development of a Scroll Compressor/Expander Module for Pressurization of 50-kW Automotive Fuel Cell Systems

Detlef Westphalen, Ronald Forni, William Murphy, and John Dieckmann
Arthur D. Little, Inc.
20 Acorn Park
Cambridge, MA 02140
(617) 498-5821, fax: (617) 498-7213, e-mail: Westphalen.D@ADLittle.com

John McCullough
Scroll Corporation
Carlisle, MA 01741-1553
(978) 287-4407

DOE Program Manager: Patrick Davis
(202) 586-8061, fax: (202) 586-9811, e-mail: patrick.davis@ee.doe.gov

ANL Technical Advisor: Robert Sutton
(630) 252-4321, fax: (630) 252-4176, e-mail: sutton@cmt.anl.gov

Contractor: Arthur D. Little, Cambridge, Massachusetts
Prime Contract No. DE-FC02-97EE50487, September 30, 1997-December 31, 2000

Objectives

Design, develop, and demonstrate a scroll compressor-expander suitable for pressurization and energy recovery for a 50-kW automotive fuel cell system.

OAAT R&D Plan: Task 13; Barrier D

Approach

- The second-generation design concept was developed through hardware testing of our first-generation compressor/expander module (CEM).
- The second-generation design has increased displacement and higher speed than the first-generation CEM in order to meet the flow requirements for 50-kW fuel cells.
- A second-generation prototype has been fabricated and tested.
- The CEM is being integrated with a fuel cell system as a final step in the development.

Accomplishments

- Designed and demonstrated first-generation CEM and double-ended compressor based on first-generation design.
- Demonstrated key design components of second-generation CEM:
  - Improved, extended-life oil seals.
  - Improved orbiting drive design with better orbiting scroll alignment, less power loss, and no drive belts.
- Designed, fabricated, and successfully tested second-generation CEM at up to 80% of design flow.

Future Directions

- Demonstrate compressor-expander in a fuel cell system.
- Pursue size/weight reduction for hybrid compressor technology while maintaining superior performance characteristics.

Introduction

Nearly all designs for automotive fuel cell systems are based on operation at a pressure up to 3 atm at full load. The viability of these fuel cell systems requires a highly efficient compressor and an efficient expander in order to keep parasitic power demand manageable.

Phase I of the scroll compressor-expander module (CEM) development culminated in the successful demonstration of an efficient scroll CEM capable of pressurization and energy recovery for a 28-kW fuel cell. This first-generation prototype was tested at flow rates up to 42 g/s and compressor discharge pressures up to 32 psig.

The goals of the Phase II work were:

- Increase flow rate,
- Improve oil and cooling systems,
- Eliminate belt drive,
- Demonstrate reliability, and
- Integrate CEM with a fuel cell.

The second-generation prototype compressor is shown in Figure 1. The compressor and expander are mounted on either side of the centrally located orbiting drive. Expander power is transferred to the compressor mechanically through the drive. The orbiting drive is oil-lubricated; oil is prevented from being introduced into the compressor air flow by two sets of oil seals with vented intermediate space.

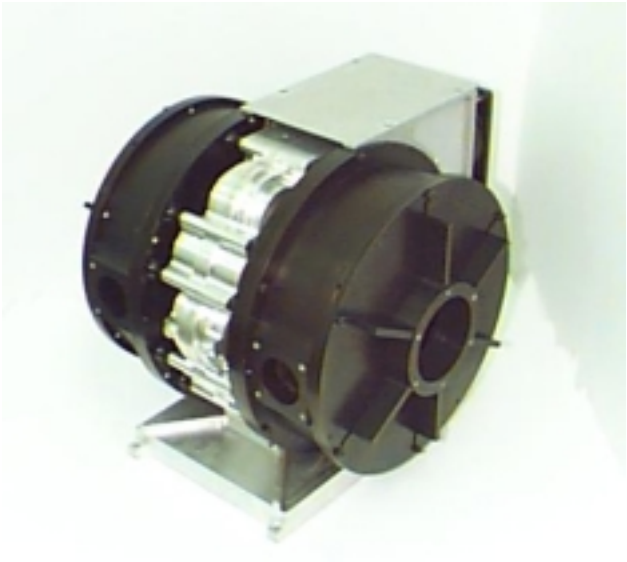

Figure 1. Second-generation scroll CEM.

Approach

The Phase II work included construction of a "back-to-back" (BTB) compressor based on the first-generation design: the expander side was replaced with a second compressor. The BTB unit was used for evaluation of individual CEM component efficiencies and durability testing. It has been operated without incident at flow rates up to 46 g/s and pressures up to 30 psig for a total of 272 hours.

In addition, the first prototype CEM was modified to demonstrate (1) integration of the oil

pump into the orbiting drive and (2) a new orbiting oil-seal system that involves no surface-to-surface contact at the seal point. Both of these modifications have been successfully demonstrated to improve CEM reliability.

Extended reliability testing has been done to verify durability of the first-generation orbiting drive design. About 500 test hours have been accumulated with the BTB compressor and the modified first-generation CEM, without incident, at machine speeds up to 3,450 rpm.

Results

The second-generation CEM has been designed, fabricated, and tested. Design changes (compared with the first generation) are:

- Larger displacement and higher speed in order to achieve 76-g/s flow, suitable for a 50-kW fuel cell.
- Improved thrust bearing to improve scroll alignment.
- Better integration of the oil pump and cooling fans.
- Central-drive design, rather than belt drive, to improve reliability, reduce parasitic losses, and reduce size.
- Additional orbiting drive design changes that will improve reliability and reduce drive losses.
- Magnesium alloy scrolls to reduce weight and reduce bearing loads.

Testing of the second-generation machine was done at up to 80% of design flow. This initial testing has verified the performance projections shown in Figures 2 and 3. Further testing may occur after completion of the fuel cell system testing described below.

Demonstration of the CEM integrated into a fuel cell system is currently in process. This work is being done with Energy Partners. The CEM is shown in the test rig in Figure 4.

Initial testing of the CEM integrated with the permanent-magnet direct-drive motor has been done in conjunction with Energy Partners' humidifier testing. Further work is awaiting final assembly of the fuel cell system. The work will allow testing of system control issues and will show the viability of the scroll compressor for automotive fuel cell applications.

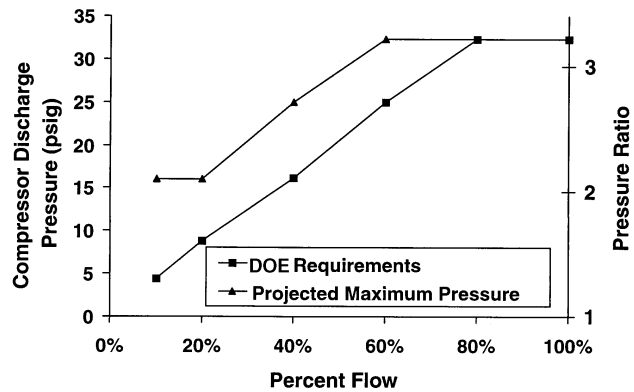

Figure 2. Second-generation scroll CEM operating envelope.

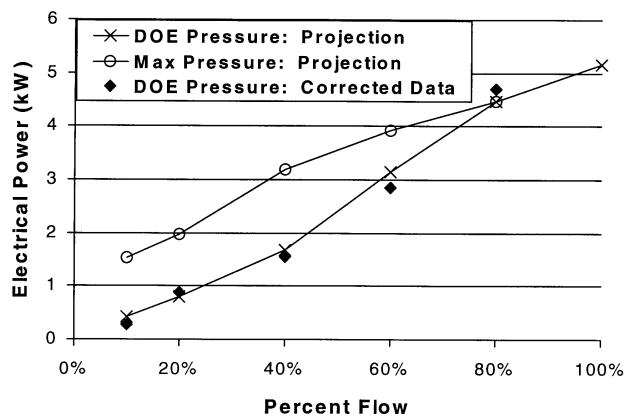

Figure 3. Second-generation scroll CEM projected shaft power.

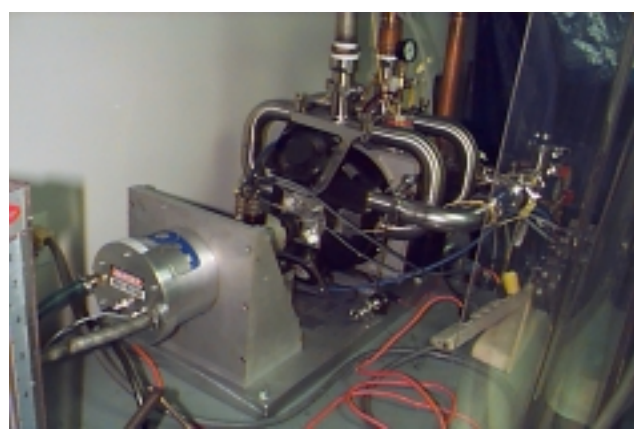

Figure 4. CEM integrated with PM motor in Energy Partners' facilities.

The projected performance envelope of the second-generation scroll CEM is shown in Figure 2. The scroll technology allows for a wide flow range while maintaining system pressure level.

The efficiency benefit of scroll technology for fuel cell pressurization is shown in Figure 3. The figure shows shaft power projections for Department of Energy (DOE) guideline pressures and for the projected maximum pressure curve of Figure 2. The points labeled "Corrected Data" are based on CEM testing at operating conditions nearly identical to the DOE guidelines. The scroll CEM uses a very modest amount of the net fuel cell stack power over the entire flow range. However, the second generation scroll CEM is 27 liters in volume (not including the motor) and has a mass of 36 kg (not including the motor). These parameters are far in excess of the original DOE guidelines of 4 liters volume and 3 kg mass, both without the motor.

C. Variable Delivery Compressor/Expander Development

Ski M. Milburn, Principal Investigator
VAIREX Corporation
3044 Valmont Road
Boulder, CO 80301
(303) 444-4556, fax: (303) 444-6150, e-mail: VAIREX@VAIREX.com

DOE Program Manager: Patrick Davis
(202) 586-8061, fax: (202) 586-9811, e-mail: patrick.davis@ee.doe.gov

ANL Technical Advisor: Robert Sutton
(630) 252-4321, fax: (630) 252-4176, e-mail: sutton@cmt.anl.gov

Contractor: VAIREX Corporation, Boulder, Colorado
Prime Contract No. DE-FCO2-98EE50481, December 19, 1997-June 19, 2000

Objectives

The primary objective for fiscal year (FY) 2000 was to complete development of a second-generation integrated air compressor/expander/motor suitable for installation in 50-kW fuel cell demonstration systems. In particular, we sought to:

- Expand, through research and development, the performance envelope of the *VAIREX* dry piston technology for use as a fuel cell power system air compressor and expander.
- Focus on performance improvements in the areas of operating speed, compressor power consumption, and expander power recovery, as well as on the volume and weight of both devices.
- Define the development pathway to the manufacture of an integrated compressor/expander/motor (iCEM) that will satisfy cost, weight, and volume, as well as performance, requirements for a fuel-cell-powered production vehicle.

OAAT R&D Plan: Task 13; Barrier D

Approach

The current R&D phase moved beyond demonstration of basic capabilities to Department of Energy (DOE) guidelines and projected industry requirements. Specific steps during FY 2000 included:

- Implementation of an improved, simplified mechanism building on the Generation 1 results.

- Design and construction of a Generation 2 integrated, variable-delivery compressor and expander.
- Independent testing of the Generation 2 compressor, expander, and integrated compressor/expander to establish performance envelopes.
- Submission of the final report and the operating manual for the deliverable hardware.

Accomplishments

- Fully demonstrated that the Generation 2 *VAIREX* integrated compressor/expander system meets or exceeds DOE performance guidelines and can be scaled to meet air management system requirements for fuel cell power systems with net power ratings from 2 to 100 kW_e (patents applied for).
- Developed a mechanical design in which major elements of the compressor and expander are identical, with the exception of inlet and outlet valving.
- Developed a unique variable valving system for the expander that allows independent control of inlet timing and duration, as well as pressure regulation independent of air flow or exhaust conditions (patents applied for).
- Integrated a high-efficiency, brushless direct-current (DC) motor and controller suitable for powering by fuel cell stack output voltages.
- Developed and are implementing the development path to the manufactured product; projected cost and durability meet industry requirements.
- Submitted draft of final report and operating manual for this contract phase.

Future Directions

- Continue testing of expander configurations in fuel cell power system environments.
- Continue integration of the air system into the overall fuel cell power system.
- Deliver customer evaluation units in calendar year (CY) 2000.
- Demonstrate a compressor operating envelope that supports net fuel cell power systems in excess of 50 kW_e.
- Continue to reduce power consumption across the operating window.
- Continue to reduce dynamic mass, inertia(s), and overall component weights and costs.
- Continue to implement pathway to manufacture, achieving technical targets within cost constraints acceptable to automotive industry.

Introduction

Automotive fuel cell power systems require pressurized air as a source of oxygen in the fuel cell stack itself, as well as in the fuel reformation process. It has been determined that pressurized air, at a ratio of about 3.2 times the ambient air pressure (3.2 bar), is appropriate for optimal power system performance.

Conventional air systems do not meet the requirements for clean, variable air delivery, independent of pressure, and having power consumption within the available power budget of a fuel cell power system.

VAIREX has used its dry cylinder compressor technology to develop, under DOE auspices, an integrated air system capable of meeting the air requirements for the DOE 50-kW power system guidelines and beyond. An expander, capable of recovering significant energy from the power system exhaust streams and regulating system pressure, is an integrated part of the *VAIREX* system. This integrated air system operates within the parasitic power budget required by the system guidelines.

Approach

Comparison of contact (piston) compressor technology with noncontact (e.g., twin screw or turbine) compressor technology indicated that the piston approach had significant merit in the areas of variable flow control independent of pressure, and of lower power consumption across the operating range, especially at the dominant (20–30%)

operating levels. Also, energy recovery from the power system exhaust gases and system pressure regulation are simplified and are more flexible in the piston approach.

In the first phase of the program, the *VAIREX* technology was demonstrated to be capable of meeting DOE system performance requirements for an automotive fuel cell power system. In the second phase, covered by the referenced contract, the program objectives included improvements in performance; reduction in size, weight, and cost; and definition of a clear path to manufacture.

Results

Mechanical complexity of the air system has been significantly reduced in the current configuration. It should be noted that the compressor and expander in Generation 2 are mechanically identical in every respect except for inlet and outlet valving. Compressor valving is passive, while the expander valving is a unique design permitting dynamic variation of inlet timing and duration, with independent system pressure control. Figure 1 shows the basic mechanical module. Figure 2 is the deliverable configuration of this contract, while Figure 3 shows the customer evaluation version of the iCEM. This latter version is scheduled to be delivered for customer evaluation during CY 2000.

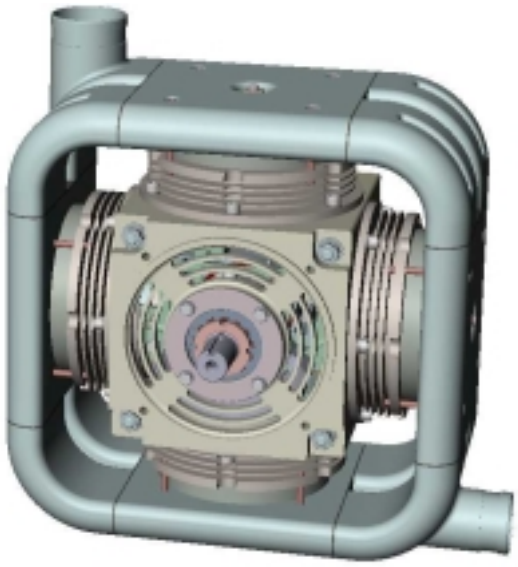

Figure 1. Common compressor/expander module.

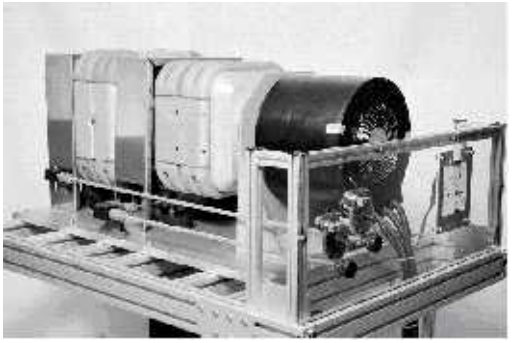

Figure 2. Integrated compressor/expander/motor as delivered.

Figure 3. iCEM, customer evaluation unit.

Modeling, testing, and design efforts on the current configuration have reduced the volume and mass of the compressor and expander hardware by a third with respect to the Generation 1 system. However, the current Generation 2 Vairex compressor occupies a volume greater than 65 liters (not including the motor) and has a mass of more than 27 kg (not including the motor). The new iCEM is expected to have a volume of about 48 liters and a mass below 27 kg, neither of which include the integrated motor. Although this is far above the DOE guidelines of 4 liters volume and 3 kg mass, respectively, the new machine is capable of achieving any desired pressure profile with flow and is capable of pumping more than 125 g/sec. Ongoing development is expected to further reduce the volume and mass of the iCEM by an additional third or more.

Conclusions

The compressor/expander system has demonstrated that pressure ratios well in excess of 3.5 can be generated in one compressor stage, with turn-down ratios (ratio of maximum to minimum air flow) greater than 10:1. The expander section has demonstrated its ability to recover substantial amounts of energy across the system operating range, thus reducing parasitic power consumption. The expander valving system can regulate system pressure independent of air flow rates or exhaust gas conditions. The Generation 2 integrated compressor/expander has significantly reduced power consumption across the operating range.

The net shaft power required to drive the CEM unit as a function of percent compressor flow is presented in Figure 4. Note that Vairex uses an expander inlet temperature of 250°C to present the parasitic loss while most of the other CEM contractors present their data at 150°C. The higher expander inlet temperature allows more power to be extracted from the expander and, thus, reduces the net shaft power to drive the entire unit.

Operating tests indicate the *VAIREX* air system technology is capable of meeting the emerging automotive industry requirements for air flow in the range of 125 grams per second (g/s) at pressure ratios of 4 bar, as compared to the earlier specifications of 76 g/s and 3.2 bar.

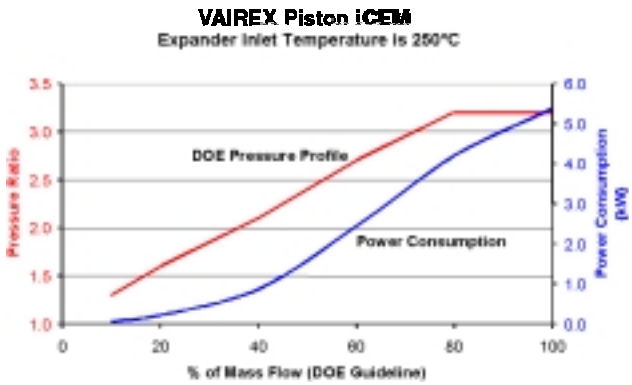

Figure 4. Projected power consumption.

Customer evaluation units in various configurations are being prepared for delivery in CY 2000. These units are designed to assist system integrators in advancing the design and testing of prototype power systems.

References and Publications

J. Cronin and S. Milburn, Report to DOE Blue Ribbon Panel, October 1999.
S. Milburn and W. Butler, Draft Final Report, Program Research and Development Announcement 2A.

D. Turbocompressor for Vehicular Fuel Cell Service

G. Fonda-Bonardi
Meruit, Inc., 1450 23rd St., Santa Monica, CA 90404-2902
(310) 453-3259, fax: (310) 828-5830, e-mail: fbarch@concentric.net

DOE Program Manager: Patrick Davis
(202) 586-8061, fax: (202) 586-9811, e-mail: patrick.davis@ee.doe.gov

ANL Technical Advisor: Robert Sutton
(630) 252-4321, fax: (630) 252-4176, e-mail: sutton@cmt.anl.gov

Contractor: Meruit, Inc.
Prime Contract No. DE-FC02-97EE-50480, October 1997-December 2000
Subcontractor: *FD Contours, Costa Mesa, California*

Objectives

- Validate the design and performance of the gas bearings for the turbocompressor.
- Validate the design and performance of the expander and compressor for fuel cell service.

OAAT R&D Plan: Task 13; Barrier D

Approach

- Design, build, and test a specialized, instrumented test rig for measuring the performance of a new, high-performance gas bearing.
- After completion of the bearing tests, use the test rig to measure the performance of the Department of Energy (DOE)/Argonne National Laboratory near-frictionless carbon (NFC) coating.
- Design, build, and test the prototype of a turbocompressor supplying 76 g/s of air and optimized for service with a 50-kW (net) fuel cell.

Accomplishments

- The gas bearings perform essentially as predicted and are suitable for use in the turbocompressor.
- The test rig is available for further use by DOE for testing the NFC coating.
- The desirable characteristics of a turbocompressor have been quantified, and specialized software for the detailed design has been written.
- Engineering drawings for the fabrication of the prototype turbocompressor have been released.

Future Directions

Build and test the turbocompressor prototype.

Introduction

The design of the turbocompressor is constrained by severe requirements, not all of them purely technical. The compressor supplies air to the fuel cell, and the turbine is driven by the exhaust from the cell, which depends on the type of fuel cell and its mode of operation, as well as on the system components (e.g., reformers, water separators, etc.). Operation of the fuel cell at a higher pressure has the advantages that the efficiency is higher (Hirschenhofer et al. 1994) and the cell volume and weight are smaller, but it has the disadvantage of requiring an air compressor, which requires power to run it.

On the other hand, the exhaust from a high-pressure fuel cell contains recoverable energy, which can be extracted by a turbine and used to offset the parasitic power absorbed by the compressor, but with the added complications (and cost) of a turbine. The amount of energy available depends on many factors, such as

- The pressure and temperature of the exhaust gas from the fuel cell,
- The composition of the exhaust gas,
- The mass flow rate of the exhaust gas, and
- The conditions for which the turbine has been optimized.

Results

Compressor Design

Meruit, Inc., designed a family of compressor wheels (designated by the letters A to Z) with varying characteristics (specific speed, dimensional ratios, etc.) that represent different compromises in providing performance compatible with the DOE specifications. Figures 1 and 2 show the expected performance of two typical wheels, 7016G and 7016T. Both show the pressure vs. mass flow lines required by DOE specifications. Operation of the compressor to the left of the limiting line ("surge line") is impossible because of stall instabilities. Consequently, there is a region in the performance space, between the surge line and the DOE specification, that cannot be reached. This area can be minimized by design, but at some cost elsewhere in the performance plane.

This trade-off is illustrated in a comparison between wheel "G" and wheel "T": the surge line can be moved to the left at the cost of increasing the power consumption at the point of maximum pressure and mass flow. Adding power to the shaft of the turbocompressor by means of an auxiliary motor does not help; it can increase revolutions per minute (RPM) but cannot move the surge line to the left. There seem to be two approaches to solving this problem:

1. Choosing an operating line for the fuel cell that follows the DOE specification from maximum mass flow down to the point where it intersects the surge line, and then following the surge line (or just to the right of it) down to idle.

2. Removing the auxiliary motor from the shaft of the turbocompressor and using it instead to power a separate compressor in series with the turbocompressor. The disadvantage of this approach is the addition of another component to the system.

Expander Design

The basic expander configuration comprises variable inlet vanes (nozzle segments) for the convenient control of back pressure and mass flow for matching the performance of the compressor. Figure 3 schematically shows the geometry of the inlet vanes and their relationship to the blades of the turbine wheel. The gas is injected tangentially through a set of openings, which are adjustable from zero to a maximum by rotating the nozzle segments about their pivots. This rotation is driven by pins engaged in slots (not shown) in a ring surrounding the structure. The gas enters the space at the outer diameter (OD) of the turbine wheel with a velocity that depends on the inlet temperature and the pressure drop across the segments. Meruit, Inc., has designed a family of expander wheels optimized for each of the various types of fuel cell exhaust.

Turbocompressor Performance

The performance of the turbine can be shown in terms of the same variables and units used in the case of the compressor; the graphs can be juxtaposed for immediate visual comparison (Figures 4 and 5).

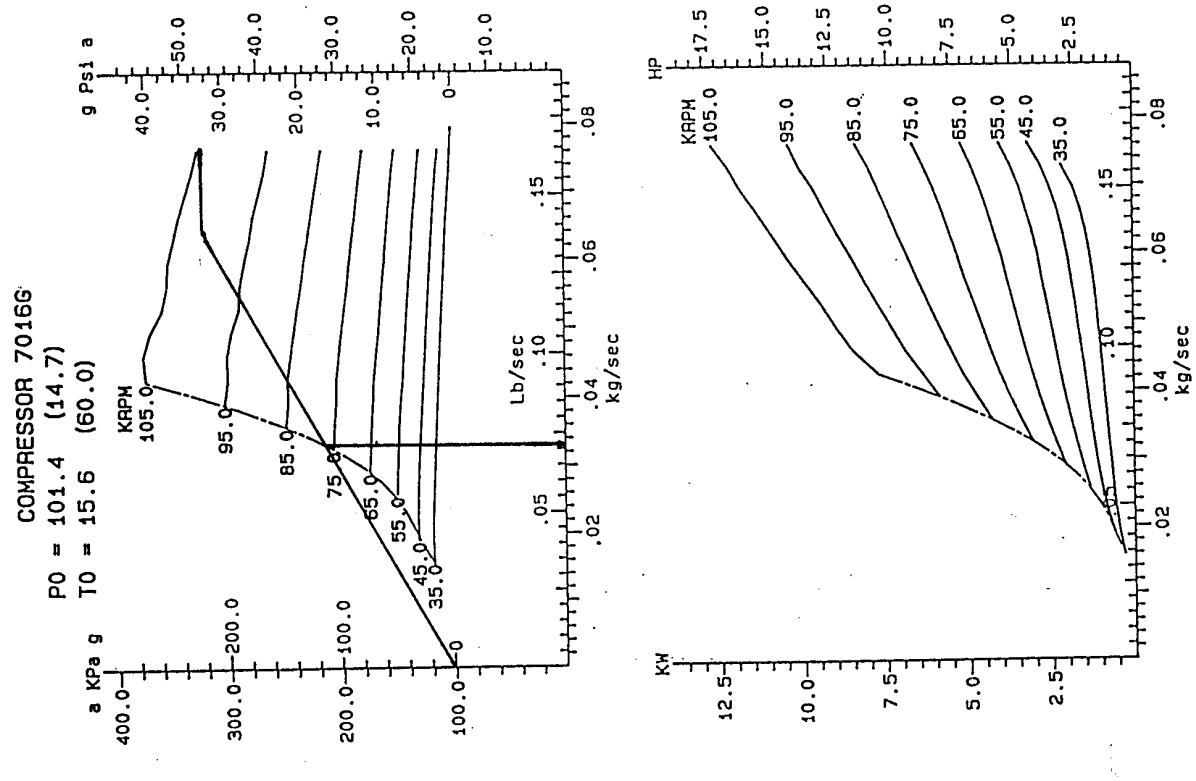

Figure 1. Compressor 7016G

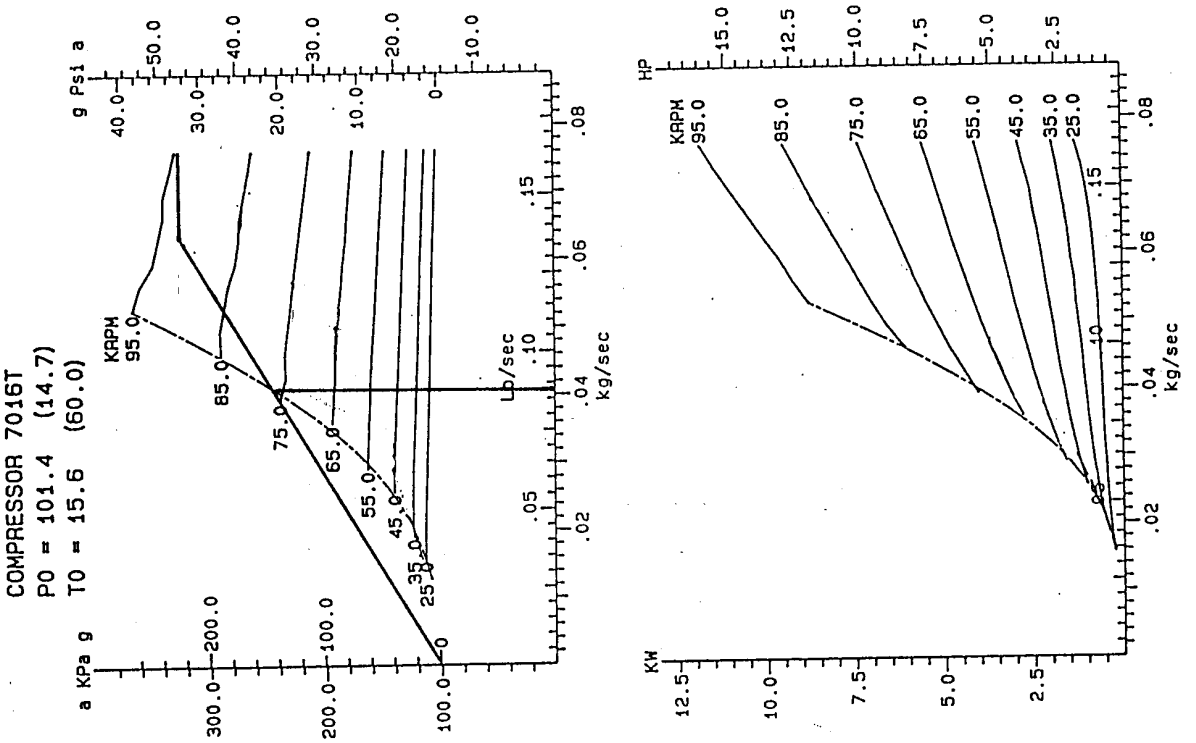

Figure 2. Compressor 7016T

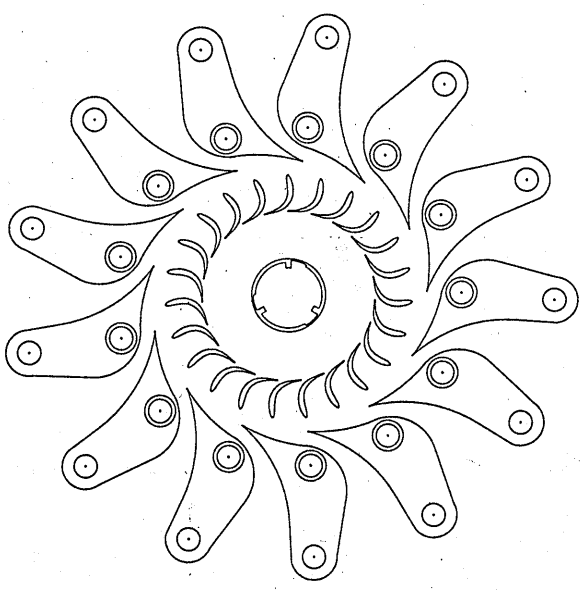

Figure 3. Variable inlet geometry.

The turbine performance graph, showing lines of constant nozzle aperture, is limited to the left by the surge line of the compressor that supplies the air, even though the expander itself has no such limitations: the expander must process what comes from the fuel cell (i.e., the air supplied by the compressor, plus hydrogen and minus water, if such is the case). The compressor graph now shows the line corresponding to 100% open nozzles: no more flow can be demanded than can be processed through the expander. Hence, the operating area for the turbocompressor is constrained by the surge line on one side and the 100% open nozzle line on the other. Within this area, a given point (pressure, mass flow) will correspond to certain well-defined values of RPM and nozzle opening. Conversely, each value of RPM and nozzle opening corresponds to a definite operating point; these are independent variables that can be used in a feedback loop to control the operation of the fuel cell.

Conclusion

Task 1 of the contract (validation of the gas bearings) is completed. The first part of Task 2 (design of a turbocompressor for vehicular fuel cells) is completed, and the expected performance has been quantified and reported. The second part of Task 2 (construction and testing of the turbocompressor) is under way.

Bibliography

J.H. Hirschenhofer et al., *Fuel Cells: A Handbook (Revision 3)*, U.S. Department of Energy, Morgantown Energy Technology Center, DOE/METC-94-1006, 1994.

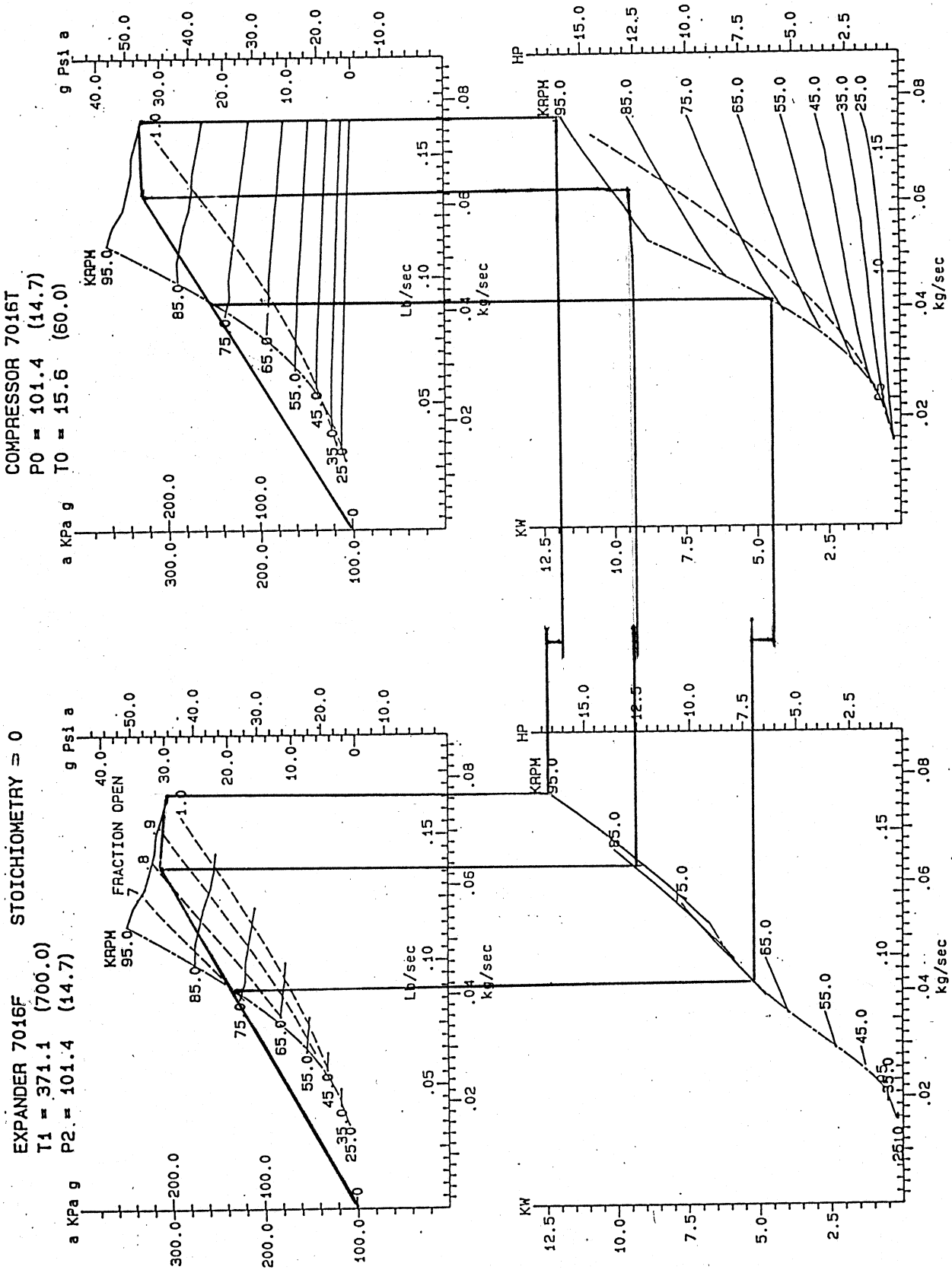

Figure 4. Expander 7016F and Compressor 7016T Performance at 370°C

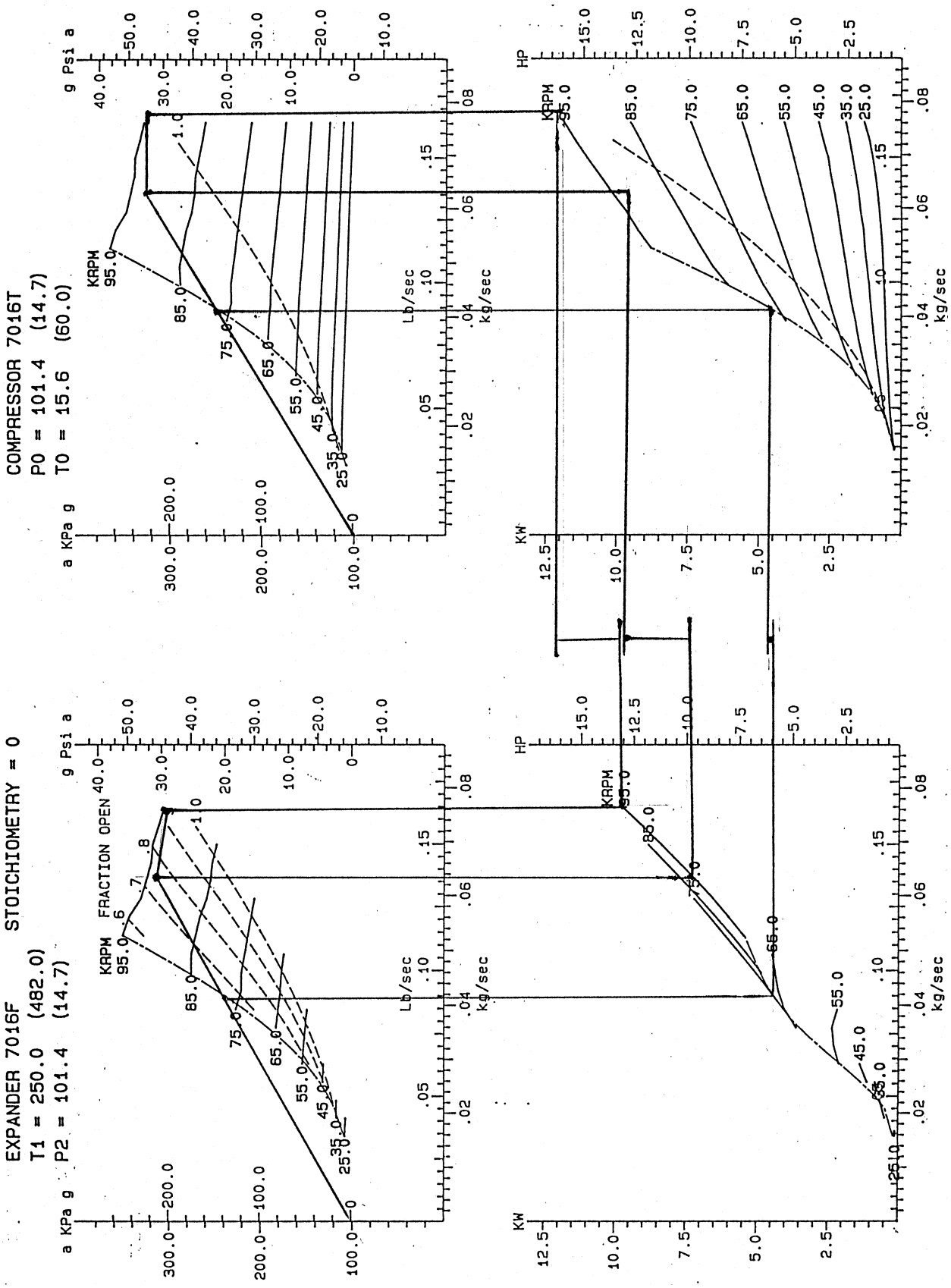

Figure 5. Expander 7016F and Compressor 7016T Performance at 250°C

E. Innovative, High-Efficiency Integrated Compressor/Expander Based on TIVM Geometry

Sterling Bailey, Ph.D., PE (primary contact) and Steve Chomyszak
Mechanology, LLC, 8 North Main Street, Suite 403, Attleboro, MA 02703
(508) 223-1920, fax: (508) 226-3697, e-mail: sterling@mechanology.com, steve@mechanology.com

DOE Program Manager: Patrick Davis
(202) 586-8061, fax: (202) 586-9811, e-mail: patrick.davis@ee.doe.gov

ANL Technical Advisor: George Fenske
(630) 252-5190, fax: (630) 252-4798, e-mail: gfenske@anl.gov

Contractor: Mechanology, LLC, Attleboro, Massachusetts
Prime Contract Nos. 991602401 and OF-00505, June 1999-December 2000

Objectives

- Design an integrated compressor/expander based on the Toroidal Intersecting Vane Machine (TIVM) geometry, following the Department of Energy (DOE) 50-kW_e automotive fuel cell guidelines.
- Predict the performance of the TIVM compressor/expander over the operating range specified in the DOE guidelines.
- Identify the technology developments necessary for this component.
- Fabricate and test a first-generation prototype TIVM compressor/expander.

OAAT R&D Plan: Task 13; Barrier D

Approach

- Modify the geometric design parameters of the TIVM concept to provide a design consistent with the DOE guidelines for a 50-kW_e automotive fuel cell system.
- Develop an engineering simulation model of the design to predict key performance parameters for specified operating conditions and to examine sensitivities to design assumptions.
- Analyze the performance of the design across the DOE-specified operating range.
- Determine the performance impact of variations in friction and leakage characteristics.
- Identify the major uncertainties in achieving the predicted performance and the technology developments necessary to meet the DOE guidelines.
- Design, build, and test a first-generation prototype compressor/expander to confirm the basic operating characteristics of the design and to guide further design refinement.
- Plan and initiate development for the key technology requirements.

Accomplishments

- A TIVM compressor/expander was designed to meet the DOE guidelines.
- A performance prediction model was developed and mathematically validated.
- The design's performance was analyzed across the operating range.

- The predicted parasitic power load is less than that in the DOE guidelines for specified flows and pressures, based on reasonable assumptions for friction and leakage.
- Manufacturing options have been identified that could provide costs near the DOE targets for high-volume production.
- Design features and material properties have been identified to minimize noise.
- Technology needs have been identified and development roadmaps developed.
- Key technology tasks have been initiated in cooperation with national laboratories and commercial vendors.
- A testing facility has been constructed at Mechanology that allows measurement of the TIVM compressor/expander operating characteristics, variation of operating conditions, simulation of fuel stack and other system parameters, and mapping of compressor/expander performance.
- A first-generation TIVM compressor/expander prototype has been designed and is being fabricated. This will be tested in the fourth quarter of 2000.

Future Directions

- The first-generation compressor/expander prototype will be tested over the full range of operating variables, and measured performance will be compared to predictions.
- On the basis of analysis of the experimental data, design features will be refined to optimize performance.
- In parallel with the design evolution, development tasks for materials, manufacturing, cost, and noise minimization will be performed.

Introduction

The Toroidal Intersecting Vane Machine (TIVM) is an innovative mechanical concept, invented and patented by Mechanology, that can be configured as an integrated, positive displacement compressor/expander. Figure 1 illustrates the generic TIVM prototype fabricated by Mechanology to demonstrate the basic operating viability of the concept. In fiscal year (FY) 1999, DOE investigated the TIVM concept for potential application to automotive fuel cell systems and determined that the inherent efficiency, compactness, and thermodynamic attributes of this concept might be of significant benefit. Mechanology was asked to develop a design specifically for the 50-kW_e automotive system and to evaluate its potential performance. On the basis of the encouraging results obtained, a prototype compressor/expander is being fabricated and will be tested in the fourth quarter of 2000.

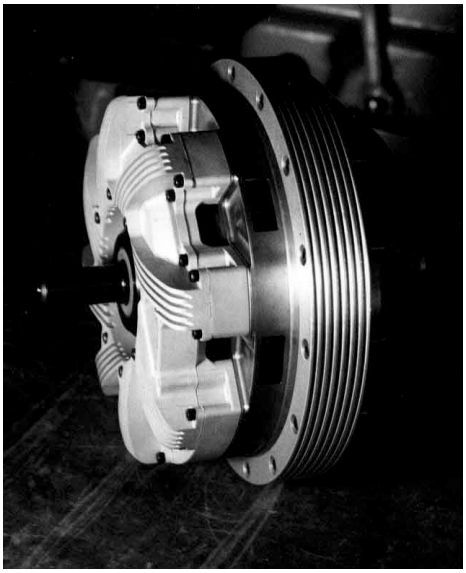

Figure 1. Generic TIVM prototype fabricated by Mechanology.

Approach

In the TIVM geometry, the four functions of intake, compression, expansion, and exhaust occur simultaneously around an intersection that is dynamically created by the intersecting vanes and their housings. With appropriate porting, this produces an integrated, positive displacement compressor/expander. From this basic concept, a design was developed in accordance with the DOE "Supplemental Air-System Guidelines." The TIVM geometry allows considerable flexibility, and the compression and expansion cycles can be individually optimized to the system thermodynamic

requirements. A wide range of designs was found to be capable of meeting the flow and pressure requirements for the compressor and for the expander. A representative design was selected that provides a good balance between operating speed, size, and efficiency. A dynamic engineering simulation model of this design was developed to analyze the performance at specified operating conditions. This model was validated as much as possible with the generic prototype. Where possible, data from the generic prototype were used for the compressor/expander analysis. Incorporating operating conditions from the DOE guidelines, the pressure, flow, and driver power required were predicted from 10% flow to 120% flow. The sensitivity of performance to design assumptions was examined through a series of parametric analyses, which were used to determine material and technology requirements. This design also provides the basis for the full-scale compressor/expander prototype that is being fabricated and will be tested in the fourth quarter of 2000. Future development of the concept will involve iterative prototypes and concurrent technology and manufacturing tasks to satisfy performance, cost, and noise requirements. At this stage of development the projected volume of the TIVM unit is 5.5 liters without the motor and the projected mass is 12 kg, also without the motor. If the development continues as projected this will potentially be the smallest CEM unit, and nearly the lightest in mass, developed under the DOE contracts.

Results

Analysis of the baseline compressor/expander design indicates that it can develop the required compressor outlet pressure of 3.2 atm and flow of 76 g/s at a speed of 4500 rpm. This pressure could be provided at the lower flow operating points; however, it was decreased according to the DOE guidelines. The parasitic electric power required to drive the compressor/expander was calculated, assuming that the motor/controller would have a combined efficiency of 85% (see Figure 2). The predicted power requirements are based on conservative assumptions for friction and leakage; the development tasks are aimed at achieving considerably better values.

Conclusions

The design study has shown that the TIVM compressor/expander can meet the DOE flow and pressure requirements with many specific design points that involve different balances between speed, material requirements, size, and efficiency. The predicted parasitic driver power is quite low compared to the DOE guidelines, even when using conservative assumptions. The technology and manufacturing development needed to achieve or exceed the predicted performance appear to be practical within reasonable time and funding constraints. It is anticipated that the prototype compressor/expander tests in the fourth quarter of 2000 will demonstrate performance that benefits the overall system performance significantly.

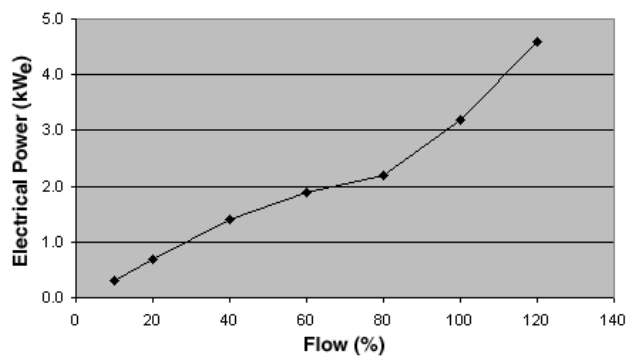

Figure 2. Predicted driver power vs. flow for the TIVM compressor/expander.

VII. HYDROGEN STORAGE[1,2]

A. High-Pressure Conformable Hydrogen Storage for Fuel Cell Vehicles

Andy Haaland
Thiokol Propulsion
P.O. Box 707, M/S 230
Brigham City, UT 84302-0707
(435) 863-6373, fax: (435) 863-8782, e-mail: haalaac@thiokol.com

DOE Program Managers: Sigmund Gronich and JoAnn Milliken
(202) 586-1623, fax: (202) 586-5127, e-mail: sigmund.gronich@ee.doe.gov
(202) 586-2480, fax: (202) 586-9811, e-mail: joann.milliken@ee.doe.gov

LLNL Technical Advisor: Andrew Weisberg
(925) 422-7293, fax: (925) 424-3731, e-mail: weisberg1@llnl.gov

ANL Technical Advisor: Walter Podolski
(630) 252-7558, fax: (630) 972-4430, e-mail: podolski@cmt.anl.gov

Contractor: Thiokol Propulsion, Brigham City, Utah
Prime Contract No. DE-FC02-97EE-50484, May 1997-May 2000
Subcontractors: Aero Tec Laboratories, Inc., Ramsey, NJ; Rotational Molding of Utah, Brigham City, UT; and Powertech Testing Labs, Surrey, B.C., Canada

---

Objectives

- Demonstrate ability to fabricate lightweight, noncylindrical pressure vessels capable of storing hydrogen gas at 5,000 psig. These vessels have been termed "conformable tanks" because they provide the option of configuring the tank geometry to conform to a given fuel storage envelope on a vehicle.
- Demonstrate ability of conformable tanks to meet an industry design standard for gaseous fuel storage. In the absence of an industry-accepted specification for hydrogen gas storage, the NGV2-1998 ANSI standard [modified for 5,000 pounds per square inch, gauge (psig)] was chosen as the design standard for this effort.

OAAT R&D Plan: Task 1; Barrier I

Approach

- Develop technology necessary to produce a plastic-lined, composite-overwrap Type IV tank, using subscale tanks and simple cylindrical geometries.
- Incorporate technology advancements into a subscale, two-cell Type IV conformable tank that will be tested for structural integrity.
- Demonstrate the structural integrity of conformable tank technology on a full-scale tank designed to fit within a storage envelope of 12.8 in. × 21.2 in. × 27.9 in., with a capacity of 3.4 lb of hydrogen. This tank envelope is consistent with space constraints on Ford's P2000 fuel cell vehicle.

---

[1] The Hydrogen Storage System Development Projects are cofunded by the DOE Office of Transporation Technologies and the Office of Power Technologies Hydrogen Program.

[2] The new draft DOE technical targets for on-board hydrogen storage can be found in Table 6, Appendix B.

- Subject full-scale tanks to tests defined in the NGV2-1998 standard (modified for 5,000 psig) that best identify and address critical safety and durability issues for the tank design.

Accomplishments

- Subscale tank development allowed key technologies to be identified for conformable tank manufacture.
- Subscale conformable tank testing demonstrated structural integrity of the tank and validated the design approach.
- Full-scale tank testing demonstrated the tank's ability to operate at 5,000 psig, with a burst safety factor greater than 2.25.
- Full-scale testing of tanks to the drop, penetration, accelerated stress rupture, environmental, and temperature cycling criteria outlined did not reveal any design issues with the current conformable tank design. All tests were successfully passed according to the criteria outlined in the standard (modified for 5,000 psig).

Future Directions

This contract has been completed. An additional proposal has been submitted for a follow-on effort. Future tasks will be completed either on the follow-on contract or using Thiokol discretionary funding. Additional future efforts are defined below:

- Complete the remaining tests on the full-scale tank, outlined in the NGV2-1998 standard.
- Extend the conformable tank design to operate at 10,000 psig.
- Incorporate component and manufacturing cost improvements into the existing tank design.

Introduction

On-board high-pressure storage of hydrogen for fuel-cell-powered vehicles presents a number of technical and economic challenges. Because the energy density of hydrogen is significantly less than that of conventional fuels, larger tanks are required for equivalent range. Furthermore, the geometry of traditional high-pressure cylinders generally does not conform to the available space on the vehicle, thereby raising tank packaging issues. Tank cost and weight also significantly influence the amount of fuel that can be carried.

Thiokol is addressing these issues through the development of high-pressure conformable tanks for on-board hydrogen storage. The lightest-weight approach uses high-strength, filament-wound carbon fiber composite for structural efficiency, with plastic liners to act as permeation barriers. Thiokol's conformable storage concept uses multiple cells, with the number and shape of the cells tailored to maximize internal volume within a rectangular envelope while maintaining membrane loading for structural efficiency. Each cell is filament-wound with a combination of hoop and helical layers, followed by a hoop overwrap over the assemblage of cells. Depending on the shape of the envelope, up to 50% more storage is possible with a conformable tank than with cylinders.

Approach

The full-scale tank under development is a two-cell configuration that fits in an envelope 12.8 in. × 21.2 in. × 27.9 in., with a capacity of 3.4 lb of hydrogen. The conformable tank provides 23% more capacity than two cylinders in the same volume envelope. An optional third cell would increase the tank width to 29.6 in. and the capacity to 4.8 lb of hydrogen. Tank envelopes are consistent with space constraints on Ford's P2000 fuel cell vehicle.

The tank is designed for a service pressure of 5,000 psi, with a burst safety factor of 2.25, consistent with existing standards for high-pressure vehicle fuel tanks. Activities completed in fiscal year (FY) 1999 included full-scale tank design, structural capability demonstration, and liner material evaluation and selection.

Successful completion of FY 1999 activities demonstrated the primary functional requirement for a full-scale, high-pressure conformable hydrogen tank: the capability for safely withstanding the

service pressure of 5,000 psi. However, additional requirements must be satisfied to demonstrate safe and reliable operation of the tank within the motor vehicle environment. Over a lifetime of service, the tank will experience cyclic loading due to repeated fills, extremes of temperature, exposure to corrosive fluids, potential damage both during handling and vehicle operation, and possible creep and stress rupture due to sustained high-pressure loading.

The ANSI/AGA NGV2-1998 standard provides a comprehensive set of design and qualification test requirements for compressed natural gas (CNG) vehicle fuel tanks to ensure safe operation over their lifetime. In the absence of a comprehensive standard for hydrogen vehicle fuel tanks, and because of their similarity to CNG tanks, Thiokol will use NGV2-1998 qualification requirements (modified for tank operation at 5,000 psig) as the basis for safety and durability testing and evaluation under the present program.

The primary approach employed in FY 2000 efforts is to subject a total of six tanks produced using the technology developed in FY 1999 to qualification testing based on NGV2-1998 (modified for 5,000 psig tank operation) to identify and address critical safety and durability issues.

Results

A total of six two-cell conformable tanks were fabricated and delivered to Powertech Laboratories in Surrey, British Columbia, Canada, for testing. The tests conducted, defined in the NGV2-1998 standard, included temperature cycling, accelerated stress rupture, drop, environmental, penetration, and permeation data. Test criteria for the complete NGV2-1998 standard and results obtained on the six tanks are summarized in Table 1.

Conclusions

Thiokol has successfully designed and demonstrated a two-cell conformable tank capable of storing hydrogen at 5,000 psig (5.5 wt.% H_2) that will meet the design criteria of the NGV2-1998 standard. Additional testing will be required to certify the design to the NGV2-1998 standard. Additional challenges for this effort include increasing the tank operating pressure to 10,000 psig and incorporation of lower-cost manufacturing components and techniques. Increasing the pressure to 10,000 psig increases the amount of hydrogen stored by about 70%, but because of the increased amount of carbon fiber required, the weight percentage of hydrogen remains about the same.

Table 1. Conformable hydrogen tank test criteria and results.

Test	Criteria for Successful Test[a]	Result
Burst	Safety factor of 2.25 * 5,000 psig = 11,250 psig	Pass
Ambient cycle	15,000 cycles without failure: 45,000 cycles without rupture to 1.25 safety factor * 5,000 psig = 6,250 psig	Pass
Environmental cycling	Subject to fluid exposure, pendulum impact, gravel impact, high/low/ambient temperature cycling, burst above 9,000 psig	Pass
Flaw tolerance	Machined flaws followed by cycling (15,000 cycles to 6,250 psig)	Not tested[b]
Drop	A total of six drops from a height of 6 ft, followed by ambient cycling of 15,000 cycles to 6,250 psig	Pass
Penetration	Bullet penetration of tank pressurized to 5,000 psig with hydrogen. Tank must not fragment.	Pass
Permeation	Specified leak rate for hydrogen	1.2 scc/L·h
Bonfire	Must safely vent	Not tested
Hydrogen gas cycling	1,000 cycles with hydrogen to 5,000 psig, followed by leak test and destructive inspection	Not tested
Accelerated stress rupture	Tank pressurized to 6,250 psig and held at pressure for 1,000 hours at 149ºF. At conclusion, tank must burst above 8,438 psig.	Pass

[a] Requirements for a tank with 5,000-psig service pressure and 20-year service life.
[b] Tank expected to pass this test, based on positive results for a CNG tank of similar design operating at 3,600 psig.

B. Advanced Chemical Hydride Hydrogen-Generation/Storage System for PEM Fuel Cell Vehicles

Andrew W. McClaine (primary contact), Ronald W. Breault, Christopher Larsen, Ravi Konduri, Jonathan Rolfe, and Fred Becker
Thermo Technologies (a Thermo Electron Company)
P.O. Box 9046
45 First Avenue
Waltham, MA 02454-9046
(781) 622-1032, fax: (781) 622-1025, e-mail: amcclaine@tecogen.com

DOE Program Managers: Sigmund Gronich and JoAnn Milliken
(202) 586-1623, fax: (202) 586-5127, e-mail: sigmund.gronich@ee.doe.gov
(202) 586-2480, fax: (202) 586-9811, e-mail: joann.milliken@ee.doe.gov

LLNL Technical Advisor: Andrew Weisberg
(925) 422-7293, fax: (925) 424-3731, e-mail: weisberg1@llnl.gov

ANL Technical Advisor: Walter Podolski
(630) 252-7558, fax: (630) 972-4430, e-mail: podolski@cmt.anl.gov

Contractor: U.S. Department of Energy (DOE)
Prime Contract No. DE-FC02-97EE50483, September 30, 1997-June 30, 2000
Cofunding provided by the California South Coast Air Quality Management District, Contract No. 98111

Objectives

Develop hydrogen storage and delivery system for the transportation sector, based on the use of chemical-hydride slurry technology, and deliver a 50-kW_e-equivalent hydrogen supply.

OAAT R&D Plan: Task 1; Barrier I

Approach

- Complete the design and fabrication of the prototype hydrogen generation system.
- Evaluate the prototype performance.
- Integrate H_2 supply system into operating conditions of simulated fuel cell power source.
- Test and evaluate performance of the final system.

Accomplishments

- Produced pumpable lithium hydride slurry that is safe to handle and stable for several months.
- Demonstrated that the hydride slurry can be reacted to generate hydrogen on demand.
- Demonstrated that lithium-hydride-slurry hydrogen generator can meet the demands of a light vehicle following the California highway and city protocols.
- Operated hydrogen generator pumps and motors with the hydrogen produced.

Future Directions

This program will be completed this year. Future work should address the integration of the lithium-hydride-slurry hydrogen generator with a PEM fuel cell. Additional development will also be required to address some issues not sufficiently developed during the performance of this contract.

Introduction

The objectives of this year's work were to complete the design and fabrication of a prototype hydrogen generator; to test this generator for its ability to meet the program objectives of providing hydrogen at a rate of 3 kg/hr; to identify the components requiring improvement; and to modify the system to better meet the DOE technical targets for on-board hydride storage of 7,000 WAh/kg and 930 WAh/L.

Approach

During this past year, we have completed the design and fabrication of a prototype mobile hydrogen generator system. We have evaluated the performance of this system, and we have modified the system to improve the performance of several of its components. We are currently working on the final performance evaluation of the mobile hydrogen generator.

Discussion

The chemical-hydride hydrogen-storage system developed during this program has achieved all its goals. An advanced system design based on the developed system and recycling water from the fuel cell would have a gravimetric energy density of 3,364 WAh/kg and a volumetric energy density of 1,954 WAh/L. The system has been demonstrated to follow the hydrogen demand rapidly and to produce in excess of the 3-kg/hr hydrogen flow rate target.

The generator is performing well. When the slurry is turned on, the hydrogen pressure ramps rapidly up to its operating level of 50 psig, and hydrogen flows from the device. Hydrogen production also stops rapidly when the hydride slurry is stopped. (This is important because it shows that the hydrogen production from the slurry is completed in the generator portion of the system.) Hydrocarbon and carbon monoxide (CO) levels in the hydrogen have been measured by mass spectroscopy/gas chromatography (MSGC) at less than 1-ppm levels. The thermal management system, using excess water supply to carry away the heat of reaction, has proven to be effective. Generator temperatures have been maintained at about 150°C. Hydrogen flow rates of 2 kg/hr have been achieved for the full test duration, and hydrogen flow rates of 3 kg/hr have been achieved for shorter periods.

Another important accomplishment is the recognition that the hydride slurry resists burning. This is an important safety feature of the chemical-hydride slurry approach.

Slurry Production

Over the past couple of years, we have developed the ability to produce lithium hydride slurries in a nearly continuous operation. Figure 1 shows a three-gallon batch of lithium hydride slurry being poured into a storage vessel. This is 60% lithium hydride in mineral oil, with a dispersant to maintain the slurry properties. The viscosity of the

Figure 1. Lithium hydride slurry.

slurry is about 2000 cp. This slurry is stable for several weeks or more.

Safety Feature

An important feature of the slurry is its ability to protect the lithium hydride from inadvertent exposure to water or water vapor. If allowed to do so, powdered lithium hydride will absorb water vapor from the air. The reaction of the water vapor and the hydride produces hydrogen and heat. If the day is sufficiently humid, the heat can build up until it ignites the hydrogen. Mixed with mineral oil, the hydride cannot absorb moisture rapidly enough to be a hazard. In addition, because mineral oil has such a high vapor pressure, it actually prevents the ignition of the lithium hydride by open flames. Figure 2 is a sequence of photographs of a test performed with a propane torch. A spoonful of lithium hydride slurry was placed in our fume hood. The flame from the torch, brought near, did not light the slurry. Gasoline would have been ignited. When the flame was held on the slurry for a sufficient time, some of the mineral oil evaporated and burned, but the flame went out when the torch was removed.

Hydrogen Generator Design

The hydrogen generator is made up of storage vessels for the lithium hydride slurry and a small amount of water, pumps for both the slurry and the water, a mixing reactor, a heat exchanger, and a hydroxide storage tank (see Figure 3). Figure 4 shows the prototype hydrogen generator after one of its final test sequences. The reactor is a tube with an auger/mixer running through it. Hydride slurry and water are pumped into the reactor at one end. The auger/mixer moves this mixture through the reactor and mixes it at the same time. Excess water is evaporated, absorbing and carrying the heat of reaction out of the reactor with the hydrogen. Hydrogen and water vapor are separated from the hydroxide product in the head of the hydroxide tank. The water vapor is condensed in the heat exchanger and returned to the water circuit, while the hydrogen is delivered to the fuel cell.

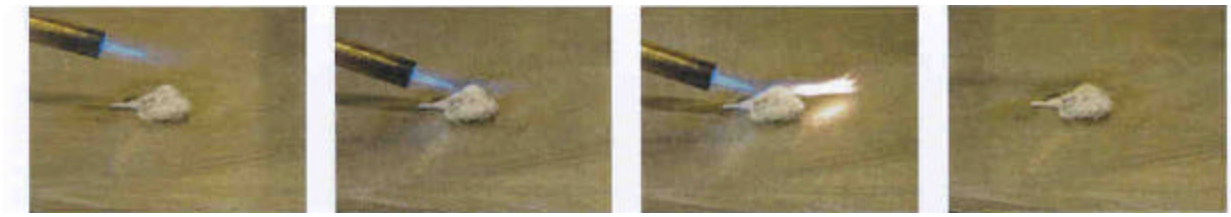

Figure 2. Flame test with LiH slurry.

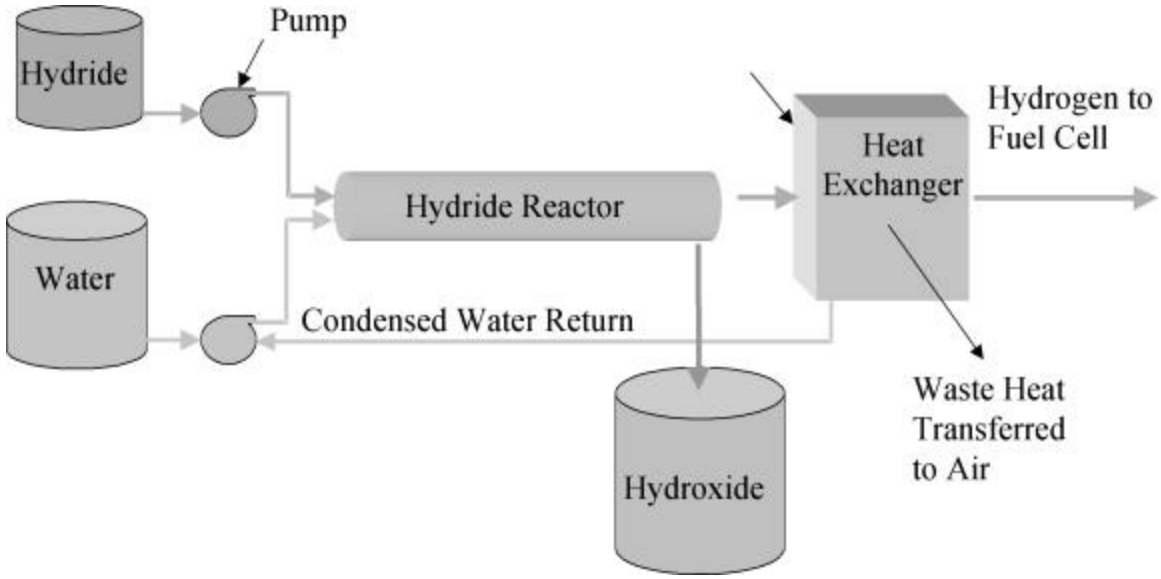

Figure 3. Diagram of the hydrogen generation system.

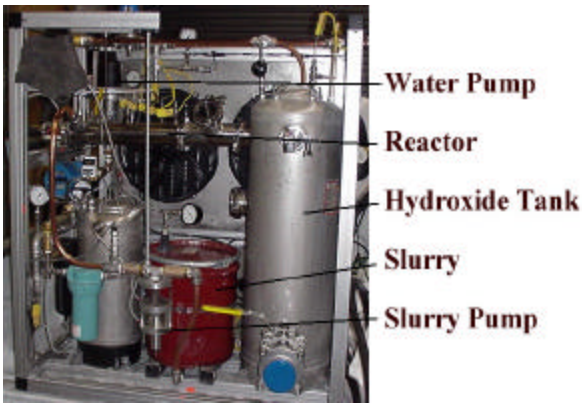

Figure 4. Picture of the prototype hydrogen generator.

Hydrogen Generator Performance

Figure 5 shows the hydrogen and hydride slurry flow rates during a typical test of the system. The maximum flow rate was a little over 2 kg/hr of hydrogen. It is important to note the rapid rise in hydrogen flow rate with increases of the slurry and the rapid drop in the hydrogen flow rate with decreases of the slurry. Because the hydrogen flow stopped when the hydride slurry flow stopped, we were assured that the mixing and reaction in the reactor were complete.

Quality of the Hydrogen

In order to be acceptable in a fuel cell, the hydrogen produced from the lithium-hydride-slurry reactor must have very low CO concentrations (less than 10 ppm).

During one test, measurements were made of the hydrogen leaving the system at points before and after a carbon filter. Table 1 displays the results of these measurements. In both cases, the CO

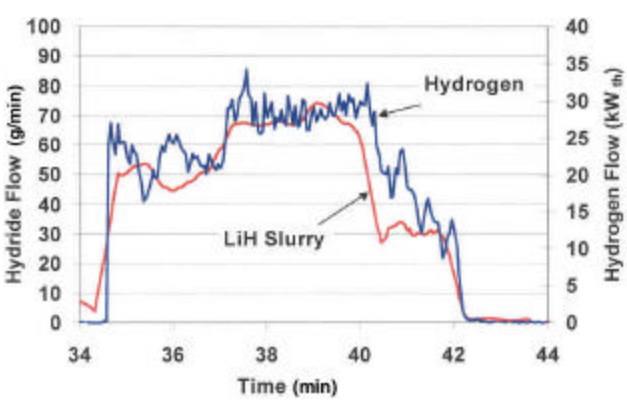

Figure 5. Data showing the slurry and hydrogen flow rates.

Table 1. Measured contaminants in hydrogen.

Mode	Contaminant	ppm
Before Carbon Trap	CO_2	= 2.4
	O_2	= 25
	N_2	= 95
	CO	= 1.5
	Oil	= 0.1
	HC	= 1.2
After Carbon Trap	CO_2	= 0.7
	O_2	= 10
	N_2	= 40
	CO	= 0.1
	Oil	= 0.1
	HC	= 0.8

measurements showed that levels were well below the tolerable levels of a PEM fuel cell. Also measured were concentrations of oxygen, nitrogen, carbon dioxide, mineral oil, and hydrocarbons. The ratio of oxygen to nitrogen was the same as that in air and was different in each measurement, indicating that air contamination may have occurred during the measurement process. Measurements of mineral oil, hydrocarbons, and carbon dioxide were all low. One possible source of the carbon dioxide is from the water used in the system. Untreated tap water was used in all our experiments.

As expected, the CO and hydrocarbon levels were lower after passage through a carbon filter. The results of this test indicate that a carbon filter is probably not necessary for this system.

Economic Analysis

An economic analysis was performed for the regeneration process described above to determine the cost of hydrogen to be expected. Table 2 displays the assumptions used in the economic analysis. The analysis began with a preliminary design of the various components required in the process.

We found this process to be sensitive to the cost of carbon. However, carbon sources appear to be available at costs that will make this process economical. Figure 6 gives the results of our analyses for two plant sizes. The first plant would serve about 250,000 cars per day, whereas the larger plant would serve about 2,000,000 cars per day.

Figure 7 displays the cost of hydrogen from the lithium-hydride-slurry system and from other systems. Given the cost of stored hydrogen from other production methods, the chemical-hydride

Table 2. Assumptions used in economic evaluation.

Capital	$58.8 million
Carbon	Variable
Labor	
Operators	25 at $35,000/yr
Super. & Cleric.	15% of operators
Mainten. & Repairs	5% of capital
Overhead	50% of tot. lab. + mtnc.
Local Tax	2% of capital
Insurance	1% of capital
G&A	25% of overhead
Fed. and State Tax	38% of net profit

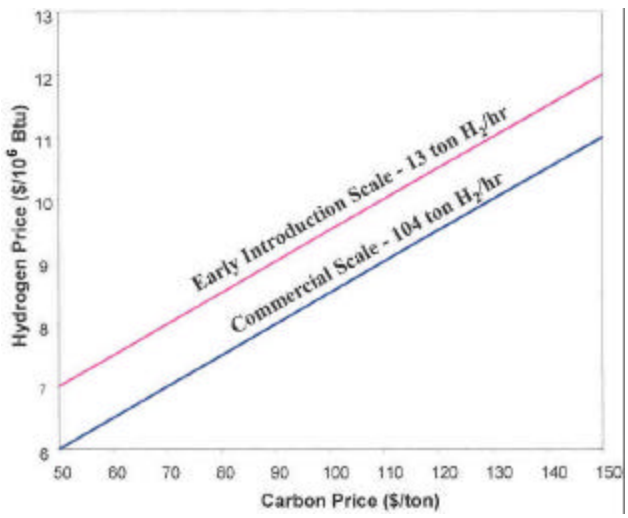

Figure 6. Results of economic analysis.

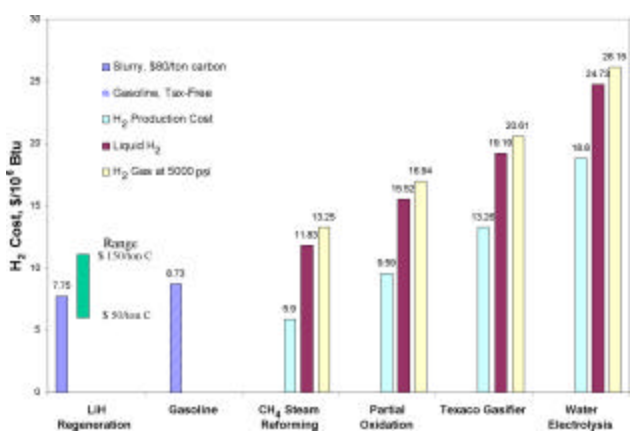

Figure 7. Cost of stored hydrogen as a chemical hydride and by conventional methods.

slurry approach appears very competitive, even against tax-free gasoline.

This analysis began with a preliminary regeneration plant design, which was generated by using ASPEN Plus, version 10.1. Costs determined from this analysis (using methods from Ulrich) ranged from $6.04 to $11.30/10^6 Btu, depending on the cost of the carbon. (A hydrogen cost of $10/10^6 Btu is approximately equivalent to a gasoline cost of $1.14/gal.) This analysis assumes a 15% after-tax rate of return, a carbon cost of $0.025-$0.075/lb ($50-$150/ton), and a high-volume production plant serving 2,000,000 cars per day. The analysis is quite sensitive to the cost of carbon. At $0.04/lb, the carbon is assumed to be obtained from coal at a cost four to eight times the cost of the coal.

This cost compares favorably with that of producing hydrogen from conventional means and storing it as a liquid or compressed gas (Padró and Putsche). Total *stored* hydrogen costs of hydrogen from steam methane reformation (SMR) range from $11.90 to $44.39/10^6 Btu. SMR is about the cheapest source of hydrogen, with costs ranging between $5.97 and $7.46/10^6 Btu. Long-term storage (>30 days) costs range between $7.35 and $36.93/10^6 Btu for compressed hydrogen and between $5.26 and $17.12/10^6 Btu for liquid storage, depending on the size.

Conclusions

In summary, the lithium hydride slurry approach for storing hydrogen provides a viable alternative to storage as liquid hydrogen or highly compressed hydrogen. Storage densities are higher than those for metal hydrides. The gravimetric energy density of 60% lithium hydride slurry is 5,110 WAh/kg, or 15.3% hydrogen. The volumetric energy density is 3,937 WAh/L, or 118 kg H_2/m^3. This is more than twice the volumetric energy density of liquid hydrogen, and it is at ambient pressure and temperature. The slurry is easily pumped and can be reacted with water via mixing to produce hydrogen on demand.

The mobile generator developed for the vehicle program has been shown to produce hydrogen on demand, with complete reaction occurring in the reactor volume. Hydrogen production has been measured up to 3 kg/hr. Based on the prototype generator design, an advanced design is anticipated

to provide a gravimetric energy density of 3,361 Wh/kg and a volumetric energy density of 1,954 Wh/L, assuming that the water from the fuel cell is condensed and used to produce hydrogen in the hydride reactor.

The cost of hydrogen resulting from the carbo-thermal regeneration of lithium hydroxide to lithium hydride is estimated to range from $6.04 for carbon costing $50/ton to $11.30 for carbon costing $150/ton. This is competitive with hydrogen produced by natural gas and stored as a liquid.

The chemical-hydride slurry approach provides other desirable features. The slurry protects the hydride from accidental contact with moisture in the atmosphere (or otherwise). Hydrogen production by reaction of the slurry with water can be performed at elevated pressures, allowing additional power to be generated from the exhaust hydrogen/steam from the reactor and/or allowing the exhaust hydrogen/steam to be used to pressurize air for a more compact fuel cell. Production of hydrogen at elevated pressures also allows the components of the hydrogen generator to be reduced in size.

Acknowledgments

This work is supported by the U.S. Department of Energy (DOE), the California South Coast Air Quality Management District (AQMD Contract No. 98111), and Thermo Power Corporation. The opinions, findings, conclusions, and recommendations are those of the author(s) and do not necessarily represent the views of DOE or AQMD. DOE, AQMD, their officers, employees, contractors, and subcontractors make no warranties, expressed or implied, and assume no legal liability for the information in this report. DOE and AQMD have not approved or disapproved this report, nor have they passed upon the accuracy or adequacy of the information contained herein.

The authors would like to thank DOE, AQMD, and Thermo Power Corporation for the opportunity to demonstrate the chemical-hydride-slurry approach for storing hydrogen. We would also like to thank Ford Motor Company, Air Products, and Morton International for participating in our technical review panel.

References

1. C.E.G. Padró and V. Putsche, *Survey of the Economics of Hydrogen Technologies*, National Renewable Energy Laboratory, NREL/TP-570-27079, Sept. 1999.
2. G.D. Ulrich, *A Guide to Chemical Engineering Process Design and Economics*, John Wiley & Sons, 1984.

FY 2000 Publications and Presentations

- R.W. Breault, C. Larson, and J. Rolfe, "Hydrogen for a PEM Fuel Cell Vehicle Using a Chemical-Hydride Slurry," American Chemical Society Meeting, New Orleans, La., Aug. 24-26, 1999.
- A.W. McClaine, R.W. Breault, J. Rolfe, C. Larsen, R. Konduri, G. Miskolczy, and F. Becker, "Hydrogen Storage Using Slurries of Chemical Hydrides," In *Advances in Hydrogen Energy*, to be published by Kluwer Academic/Plenum Publishers, 2000.

APPENDIX A: ACRONYMS, INITIALISMS, AND ABBREVIATIONS

ACO	adsorption/catalytic oxidation
AGO	anode gas oxidizer
ANL	Argonne National Laboratory
AQMD	California South Coast Air Quality Management District
ASTM	American Society For Testing and Materials
ATR	autothermal reformer
BET	Brunauer-Emmett-Teller
BTB	back-to-back
CARAT	Cooperative Automotive Research for Advanced Technology
CARB	California Air Resources Board
CCM	catalyst-coated membrane
CEM	continuous emission monitor **or** compressor expander module
CFD	computational fluid dynamics
CMEU	compressor/motor/expander unit
CNG	compressed natural gas
CO	carbon monoxide
Cpsi	channels per square inch
CRADA	cooperative research and development agreement
CV	cyclic voltammetry
DC	direct current
DMFC	direct methanol fuel cell
DOE	U.S. Department of Energy
EB	electrode backing
ECO	electrochemical oxidation
EDX	Energy-Dispersive Spectroscopy
EES	Engineering Equation Solver
EXAFS	Extended x-ray absorption fine structure
F^3P	Fuel-flexible, fuel-processing **or** fuel-flexible, fuel-processor
FMI	Foster-Miller, Inc.
FPS	fuel processing system
FUDS	Federal Urban Driving Schedule
FY	Fiscal Year
GC	gas chromatography **or** gas chromatographic
GC/MS	gas chromatography/mass spectrometry
GDE	gas diffusion electrode
GHSV	gas hourly space velocity
GM	General Motors
H_2	Hydrogen
HAZOP	Hazardous Operations
HBT	Hydrogen Burner Technology
HLTS	humidified low-temperature shift
HOR	hydrogen oxidation reaction
HRSG	Heat-recovery steam generator
HRTEM	High-Resolution Transmission Electron Microscopy
HTS	high-temperature shift
HTSPEM	high-temperature solid polymer electrolyte membrane

ICE	Internal Combustion Engine
ICEM	integrated compressor/expander/motor
ICP	Inductively coupled plasma **or** ion-conducting polymer
IFC	International Fuel Cells
IGT	Institute of Gas Technology
krpm	10^3 revolutions per minute
LANL	Los Alamos National Laboratory
LBNL	Lawrence Berkeley National Laboratory
LHV	lower heating value
LTS	low-temperature shift
MEA	membrane electrode assembly **or** membrane/electrode assembly
MSGC	mass spectroscopy/gas chromatography
MTS	medium-temperature shift
NFC	near-frictionless coating
NMOG	nonmethane organic gases
NRC	National Research Council
OAAT	Office of Advanced Automotive Technologies
OD	outer diameter
OEM	original equipment manufacturer
ORR	oxygen reduction reaction
OTT	Office of Transportation Technologies
PAC	process and control
PAFC	phosphoric acid fuel cell
PAH	polycyclic aromatic hydrocarbon
PBO	poly-p-phenylene benzobisoxazole
PEFC	polymer electrolyte fuel cell
PEM	polymer electrolyte membrane
PEMFC	polymer electrolyte membrane fuel cell
PNGV	Partnership for a New Generation of Vehicles
PNNL	Pacific Northwest National Laboratory
POCO	synthetic graphite product from Poco Graphite, Inc. Decatur, Texas
POX	Partial-oxidation reformer **or** partial oxidation reactor
PROX	preferential oxidizer
RDE	rotating disk electrode
RFG	reformulated gasoline
RHE	reversible hydrogen electrode
RPM	revolutions per minute
RRDE	rotating ring disk electrode
scc/L·h	standard cubic centimeters per liter per hour
SEM	Scanning Electron Microscopy
SMR	Steam Methane Reformation
SPEFC	solid polymer electrolyte fuel cell
Stoics	stoichiometry (in some figure labels)
SULEV	super ultralow emissions vehicle
SwRI	Southwest Research Institute
TEM	Transmission Electron Microscopy
THC	total hydrocarbon(s)
TIVM	Toroidal Intersecting Vane Machine
TPD	Temperature-Programmed Desorption
UHV	ultrahigh vacuum
UOB™	Under-Oxidized Burner

VNT®	Variable Nozzle Turbine
WGS	water gas shift
XANES	X-ray Absorption Near-Edge Spectroscopy
XPS	X-ray Photoelectron Spectroscopy
XRD	X-ray Diffraction
XRF	X-ray Fluorescence Spectroscopy
ZEV	zero-emission vehicle

APPENDIX B: DOE TECHNICAL TARGETS FOR FUEL CELL SYSTEMS, SUBSYSTEMS, AND COMPONENTS

Table 1. DOE technical targets for integrated fuel cell power systems operating on gasoline reformate (including fuel processor, stack, and auxiliaries; excluding gasoline tank and DC-DC converter).

Characteristic [a]	Units	Calendar Year		
		1997	2000	2004
Energy efficiency [b] @ 25% of peak power	%	35	40	48
Power density	W/L	200	250	300
Specific power	W/kg	200	250	300
Cost [c]	$/kW	300	150	50
Start-up to full power	min	2	1	0.5
Transient response (time from 10 to 90% power)	sec	30	20	10
Emissions [d]		<Tier 2	<Tier 2	<Tier 2
Durability [e]	hour	1000	2000	5000

[a] Targets pertain to gasoline fuel; all targets will be refined through Systems Analysis and Vehicle Engineering analyses (consistent with those of the PNGV).
[b] Ratio: [dc output energy]/[lower heating value of the input fuel (gasoline)]
[c] Includes projected cost advantage of high volume production and includes cost for assembling/integrating the fuel cell system and fuel processor.
[d] Emission levels will comply with emission regulations projected to be in place when the technology is available for market introduction.
[e] Less than 5% power degradation in the time between catalyst replacement.

Table 2a. DOE technical targets for fuel-flexible fuel processors [a]
(includes controls, shift reactors, CO clean-up, heat exchangers; excludes fuel storage).

Characteristics	Units	Calendar Year		
		1997	2000	2004
Energy efficiency [b]	%	70	75	80
Power density	W/L	400	600	750
Specific power	W/kg	400	600	750
Cost [c]	$/kW	50	30	10
Start-up to full power	min	2	1	0.5
Transient response (time from 10 to 90% power)	sec	30	20	10
Emissions [d]		<Tier 2	<Tier 2	<Tier 2
Durability [e]	hour	1000	2000	5000
CO content steady state [f]	ppm	100	10	10
CO content transient [f]	ppm	5000	500	100
H_2S content in product stream NH_3 content in product stream	ppm	0 <10	0 10	0 <10

[a] Targets pertain to gasoline fuel and are consistent with those of the PNGV.
[b] Fuel processor efficiency = (total fuel cell system efficiency)100%/(fuel cell stack system efficiency), where total fuel cell system efficiency accounts for thermal integration.
[c] High-volume production: 500,000 units per year.
[d] Emission levels will comply with emission regulations projected to be in place when the technology is available for market introduction.
[e] Time between catalyst replacement.
[f] Dependent on stack development (CO tolerance) progress.

Table 2b. Target PROX specifications.

Characteristic	Value
Output CO concentration	< 20 ppm, based on an input reformate composition of 2% CO, 30-75% H_2, balance CO_2 and N_2
Transients	< 20 ppm CO after 1 minute start-up < 20 ppm CO within 2 sec after + 90% electrical load transient
Hydrogen consumption	< 20% of CO removed
Device volume	$\leq 2.0 \times$ catalyst volume
Device cost	< $300 (sized for 50-kW fuel cell system)
Device pressure drop	21 kPa (3.1 psi)
Particulates	Device must be tolerant of soot and debris

Table 2c. Draft technical targets for fuel processor catalysts (gasoline w/30-ppmw sulfur [S])
ATR: Autothermal Reformer / WGS: Water-Gas Shift / PrOx: Preferential Oxidizer.

	ATR	**S Removal**	**WGS**	**PrOx**
GHSV [a,b] (hr^{-1})	200,000	50,000	30,000	150,000
Conversion [c] (%)	> 99	> 97	> 90	> 99.8
H_2 Selectivity [d] (or consumption) (%)	> 80	< 0.1	> 99	< 0.2
Volume [e] (L/kW_e)	< 0.013	< 0.06	< 0.1	< 0.02
Weight [e] (kg/kW_e)	< 0.015	< 0.06	< 0.1	< 0.03
Durability (hr)	5000	5000	5000	5000
Cost ($/$kW_e$)	< 5	< 1	< 1	< 1

[a] Gas Hourly Space Velocity:
[volumetric flow rate of the product gases (25°C, 1atm)]/[bulk volume of the catalyst]

[b] STP equivalents for wet inlet gas; target values are guidelines for single reactor R&D; system/subsystem targets take precedence.

[c] [reactant in (moles) – reactant out (moles)]100%/[reactant in (moles)]

[d] At the ATR: [H_2 in product (moles)]100%/[H_2 "extractable" from ATR feed (moles)]
At the shift reactor: [CO converted to H_2 (moles)]100%/[total CO converted (moles)]

[e] The volume and weight targets include only the catalysts, not the hardware needed to house the catalysts, nor the heat exchangers.

Table 3. DOE technical targets[a] for 50-kW peak power (continuous)[b] fuel cell stack systems running on hydrogen-rich fuel from fuel-flexible fuel processor (includes fuel cell ancillaries: heat, water, air management systems; excludes fuel processing/delivery system).

Characteristic	Unit	Calendar Year		
		1997	2000	2004
Stack system power density [b]	W/L	300	350	500
Stack system specific power	W/kg	300	350	500
Stack system efficiency [c] @ 25% of peak power	%	50	55	60
Stack system efficiency [c] @ peak power	%	40	44	48
Precious metal loading	g/peak kW	2.0	0.9	0.2
Cost [d]	$/kW	200	100	35
Durability (< 5% power degradation)	hour	>1000	>2000	>5000
Transient performance (time from 10 to 90% power)	sec	10	3	1
Cold startup to maximum power at –40°C	min	15	5	2
Cold startup to maximum power at 20°C	min	2	1	0.5
Emissions [e]		<Tier 2	<Tier 2	<Tier 2
CO tolerance (steady state)	ppm	10	100	1000
CO tolerance (transient)	ppm	100	500	5000

[a] Technical targets are consistent with those of the PNGV.
[b] Power refers to net power (i.e. stack power minus auxiliary power requirements).
[c] Ratio: (output dc energy)/(lower heating value of hydrogen-rich fuel stream)
[d] High-volume production: 500,000 units per year.
[e] Emission levels will comply with emission regulations projected to be in place when the technology is available for market introduction.

Table 4a. Draft DOE technical targets for fuel cell stack components [a].

Component	Requirement
Membranes	Cost: $5/kW Stability: < Δ2 mV @ RH 20-100% , < 10% swelling H_2 cross-over: < 1mA/cm^2 Area specific 0.1 ohm-cm2 Gas crossover: < 1%
Electrodes	Cost: $5/kW CO tolerance: 500 ppm steady state, 1000 ppm transient @ 0.2 g Pt/peak kW Durability: 5000 hours Utilization: 85% H_2, 60% O_2
Membrane-electrode assembly	Cost: $10/kW Voltage @ current density: 0.8V @ 0.45 A/cm^2 Power Density: 360 W/cm^2 @ 0.8V
Bipolar plates	Cost: $10/kW (<1kg/kW) H_2 permeation rate: < 2x10^{-6} cm^3/sec-cm^2 @ 80°C, 3atm (<0.1mA/cm^2) Corrosion limit: 16 μA/cm^2 Resistivity: 0.02 ohm-cm

[a] For operation on gasoline reformate: 40% H_2
[b] Targets listed are for conventional membrane technologies (operating temperatures of 60-90°C). High temperature membranes for operation above 100°C might have different characteristics.

Table 4b. Draft DOE technical targets for fuel cell sensors [a].

Sensor	Requirements
Carbon Monoxide	a) <u>1 - 100 ppm reformate pre-stack sensor</u> – Operating temperature: < 150°C – Response time: 0.1 - 1 sec – Gas environment: high humidity reformer/partial oxidation gas: H_2 30-75%, CO_2, CO, N_2, H_2O @ 1-3 atm total pressure – Accuracy: 1 - 10 % full scale b) <u>100 - 1000 ppm CO sensors</u> – Operating temperature: 250°C – Response time: 0.1 - 1 sec – Gas environment: high humidity reformer/partial oxidation gas: H_2 30-75%, CO_2, CO, N_2, H_2O @ 1-3 atm total pressure – Accuracy: 1 - 10 % full scale c) <u>0.1 - 2% CO sensor</u> – Operating temperature: 250°C - 800°C – Response time: 0.1 - 1 sec – Gas environment: high humidity reformer/partial oxidation gas: H_2 30-75%, CO_2, CO, N_2, H_2O @ 1-3 atm total pressure – Accuracy: 1 - 10 % full scale
Hydrogen in fuel processor product gas	– Measurement range: 1 - 100% – Operating temperature: 70 - 150°C – Response time: 0.1 - 1 sec for 90% response of step function – Gas environment: 1-3 atm total pressure, 10-30 mol% water, total H_2 30-75%, CO_2, N_2 – Accuracy: 1 - 10 % full scale
Hydrogen in ambient air (safety sensor)	– Measurement range: 0.1 - 10% – Operating temperature: –30 - 80°C – Response time: <1 sec – Accuracy: 5% – Gas environment: ambient air, RH 10 - 98% – Lifetime: 5 years – Selectivity from interference gases, such as hydrocarbons, is needed.
Sulfur compounds (H_2S, SO_2, organic sulfur)	– Measurement range: 0.05 - 0.5 ppm – Operating temperature: < 400°C – Response time: < 1 min @ 0.05 ppm – Gas environment: H_2, CO, CO_2, hydrocarbons, H_2O
Flow rate of product gas from fuel processor	– Flow rates: 30 - 300 standard L/min – Operating temperature: 80°C – Gas environment: high humidity reformer/partial oxidation gas: H_2 30-75%, CO_2, N_2, H_2O, CO @ 1-3 atm total pressure
Ammonia	– Measurement range: 1 - 10 ppm – Operating temperature: 70 - 150°C – Selectivity: < 1 ppm from matrix gases – Lifetime: 5 - 10 years – Response time: sec – Gas environment: high humidity reformer/partial oxidation gas: H_2 30-75%, CO_2, N_2, H_2O, CO @ 1-3 atm total pressure

Table 4b. Cont.

Sensor	Requirements
Temperature	– Measurement range: –40 - 150°C – Response time: < 0.5 sec with 1.5% accuracy @ –40 - 100°C; < 1 sec with 2 % accuracy @ 100 - 150°C – Gas environment: high humidity reformer/partial oxidation gas: H_2 30-75%, CO_2, N_2, H_2O, CO @ 1-3 atm total pressure – Insensitivity to flow velocity is needed.
Relative humidity for cathode and anode gas streams	– Operating temperature: 30 - 110°C – Measurement range: 20 - 100 % – Accuracy: 1% – Gas environment: high humidity reformer/partial oxidation gas: H_2 30-75%, CO_2, N_2, H_2O, CO @ 1-3 atm
Oxygen concentration in fuel processor and at cathode exit	(a) Oxygen sensors for fuel processor reactor control – Measurement range: 0 - 20% O_2 – Operating temperature: 200 - 800°C – Response time: < 0.5 sec – Accuracy: 2% full scale – Gas environment: high humidity reformer/partial oxidation gas: H_2 30-75%, CO_2, N_2, H_2O, CO @ 1-3 atm b) Oxygen sensors at the cathode exit -- Measurement range: 0 - 50% O_2 – Operating temperature: 30 - 110°C – Response time: < 0.5 sec – Accuracy: 1% full scale – Gas environment: H_2, CO_2, N_2, H_2O @ 1-3 atm total pressure
Differential pressure in fuel cell stack	– Measurement range: 0-1 or 0-10 or 1-3 psig (depending on design of fuel cell system) – Temperature range: 30 - 100°C (–40°C survivability) – Response time: < 1 sec – Accuracy: 1% – Size: ≤ 1in.^{2} – Orientation cannot be a problem. – Must be able to withstand and measure liquid and gas phases.

[a] Sensors must conform to size, weight, and cost constraints required for automotive applications.

Table 5. Current DOE targets for compressors/expanders[a].

Characteristic (units)	Requirement
Input power [b,c] at max flow (kW)	4.3
Efficiency at 100% flow [d]	compressor: 75% @ 3.2 PR expander [c]: 90%
Efficiency at 20% flow [e]	compressor: 65% @ 1.6 PR expander [c]: 80%
Volume [f] (liters)	4
Weight [f] (kg)	3
Cost [f] @100K/yr	$200
Turndown ratio	10
Noise	< 80 dB

[a] A workshop being held early in FY 2001 will review and update the compressor/expander performance targets.
[b] Input power to the controller to power a compressor/expander system producing 76 g/sec (dry) maximum flow. This flow rate roughly corresponds to maximum power for a 50 kW fuel cell system.
[c] Input power and expander efficiency calculated assuming tail gas composition specified by DOE
[d] 100% flow: 82 g/sec (150ºC, 2.8 atm inlet, unless otherwise specified)
[e] 25% flow: 19 g/sec (150ºC, 2.8 atm inlet, unless otherwise specified)
[f] DOE guidelines for volume, weight, and cost do not include the motor/controller or heat rejection (if required).

Table 6. New Draft DOE Targets for On-board Hydrogen Storage Technologies [a,b].

	Units	Physical Storage [c]	Chemical Storage [d]
Storage weight percent [e]	%	6	6
Storage efficiency [f]	%	95	90
Energy density (gas)	$W_{th}h$/liter	1050 [g]	1500 [g]
Specific energy [h]	$W_{th}h$/kg	2000	2000
Cost[i]	$/kW-h	5	5
Cycle life	Cycles	500	500
Operating pressure (gas)	psig	7500 [g]	N/A
Refueling time	min	< 5	< 5
Permeation rate	scc/hr-liter	2.0	N/A

[a] To meet PNGV 380-mile range target; based on LHV of hydrogen.
[b] Work carried out in collaboration with DOE Hydrogen Program.
[c] Includes compressed gas and cryogenic liquid tanks.
[d] Includes materials such as carbon nanostructures, fullerenes, metal hydrides, organometallics, or catalyzed hydrides.
[e] Weight percent H_2 is assumed to be: [weight of H_2]100%/[weight of (H_2 + tank)]
[f] Includes power associated with capturing and releasing hydrogen.
[g] Conceptual designs showed 180 liters (3 tanks) could be packaged without compromising trunk or passenger compartments; assuming 5 kg for +300 mile range in a PNGV-type vehicle yields 0.028 kg/L. Derated by 10% for tank system yields 0.031kg/L. This corresponds to tank pressure of 7500 psig, and 1050 $W_{th}h$/L. Chemical storage target is more aggressive because tanks are marginal in meeting vehicle requirements.
[h] Specific energy is assumed to be: [LHV of H_2 contained]/[weight of (H_2 + tank)]
[i] Based on high volume production of 500,000 units.

This document highlights work sponsored by agencies of the U.S. Government. Neither the U.S. Government nor any agency thereof, nor any of their employees, makes any warranty, express or implied, or assumes any legal liability or responsibility for the accuracy, completeness, or usefulness of any information, apparatus, product, or process disclosed, or represents that its use would not infringe privately owned rights. Reference herein to any specific commercial product, process, or service by trade name, trademark, manufacturer, or otherwise does not necessarily constitute or imply its endorsement, recommendation, or favoring by the U.S. Government or any agency thereof. The views and opinions of authors expressed herein do not necessarily state or reflect those of the U.S. Government or any agency thereof.

Printed on recycled paper

Office of Transportation Technologies Series of 2000 Annual Progress Reports

- Vehicle Propulsion and Ancillary Subsystems
- Automotive Lightweight Materials
- Automotive Propulsion Materials
- Fuels for Advanced CIDI Engines and Fuel Cells
- SIDI Engine R&D
- Combustion and Emission Control for Advanced CIDI Engines
- Transportation Fuel Cell Power Systems
- Vehicle Power Electronics and Electric Machines
- Advanced Technology Development (High-Power Battery)
- Exploratory Technology Research (High-Power Battery)
- Vehicle High-Power Energy Storage
- Electric Vehicle Batteries R&D

and Office of Advanced Automotive Technologies FY2000 Program Highlights

Clean Energy
– for the –
21st Century

www.ott.doe.gov/oaat